UNIVERSIDADE DE LISBOA
Faculdade de Farmácia

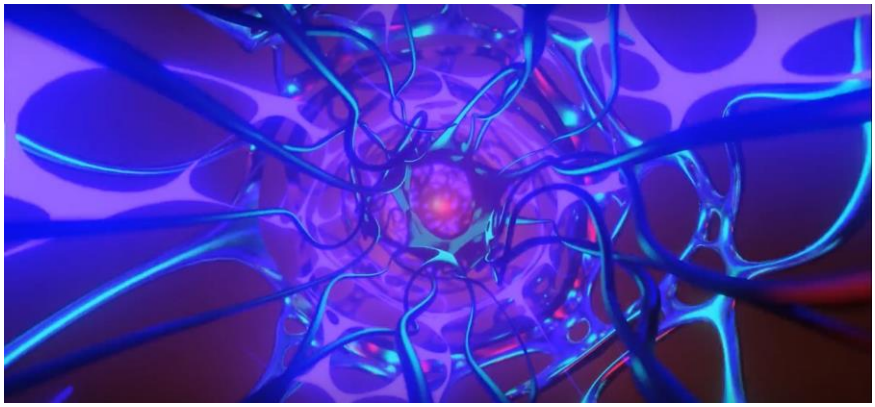

PYRUVATE DEHYDROGENASE COMPLEX DEFICIENCY: MUTATIONAL SPECTRUM IN PORTUGAL, MOLECULAR MECHANISMS UNDERLYING PATHOGENIC VARIANTS AND POTENTIAL THERAPEUTIC EFFECT OF ARGININE

DEFICIÊNCIA DO COMPLEXO DE PIRUVATO DESIDROGENASE: ESPECTRO DAS MUTAÇÕES EM PORTUGAL, MECANISMOS MOLECULARES SUBJACENTES ÀS VARIANTES PATOGÉNICAS E O POTENCIAL EFEITO TERAPÊUTICO DA ARGININA

Hana Pavlů Pereira

Orientadores: Professora Doutora Isabel Antolin Rivera
Doutor João Filipe Bogalho Vicente

Tese especialmente elaborada para obtenção do grau de Doutor em Farmácia, especialidade de Bioquímica

2021

UNIVERSIDADE DE LISBOA
Faculdade de Farmácia

PYRUVATE DEHYDROGENASE COMPLEX DEFICIENCY: MUTATIONAL SPECTRUM IN PORTUGAL, MOLECULAR MECHANISMS UNDERLYING PATHOGENIC VARIANTS AND POTENTIAL THERAPEUTIC EFFECT OF ARGININE

DEFICIÊNCIA DO COMPLEXO DE PIRUVATO DESIDROGENASE: ESPECTRO DAS MUTAÇÕES EM PORTUGAL, MECANISMOS MOLECULARES SUBJACENTES ÀS VARIANTES PATOGÉNICAS E O POTENCIAL EFEITO TERAPÊUTICO DA ARGININA

Hana Pavlů Pereira

Orientadores: Professora Doutora Isabel Antolin Rivera
Doutor João Filipe Bogalho Vicente

Tese especialmente elaborada para obtenção do grau de Doutor em Farmácia, especialidade de Bioquímica

Júri: Presidente:
- Doutor António José Leitão das Neves Almeida, Professor Catedrático e Presidente do Concelho Científico da Faculdade de Farmácia da Universidade de Lisboa;

Vogais:
- Doutor Johannes A. Mayr, Investigador Principal, Paracelsus Medical University Salzburg, Austria;
- Doutora Luísa Maria de Abreu Freire Diogo Matos, Professora Auxiliar, Faculdade de Medicina da Universidade de Coimbra;
- Doutora Diana Andreia Pereira Lousa, Investigadora Auxiliar, Instituto de Tecnologia Química e Biológica António Xavier da Universidade Nova de Lisboa;
- Doutor João Filipe Bogalho Vicente, Orientador, Investigador Auxiliar, Instituto de Tecnologia Química e Biológica António Xavier da Universidade Nova de Lisboa;
- Doutora Maria Isabel Ginestal Tavares de Almeida, Investigadora Principal Aposentada, Faculdade de Farmácia da Universidade de Lisboa;
- Doutora Margarida Maria Fernandes Batista e Silva, Professora Auxiliar, Faculdade de Farmácia da Universidade de Lisboa

Instituções Financiadoras: FCT (SFRH/BD/91729/2012); Instituto de Investigação do Medicamento (iMed.ULisboa) (PEst-OE/SAU/UI4013/2011); iNOVA4Health Research Unit (LISBOA-01-0145-FEDER-007344), which is cofounded by FCT/ Ministério da Ciência e do Ensino Superior, through national funds, and by FEDER under the PT2020 Partnership Agreement

2021

The studies presented in thesis were performed at Research Institute for Medicines (iMed.ULisboa), Faculty of Pharmacy, Universidade de Lisboa, Lisbon, Portugal,under the scientific supervision of Professora Doutora Isabel Antolin Rivera and at Instituto de Tecnologia Química e Biológica António Xavier, Universidade Nova de Lisboa, Oeiras, Portugal, under the scientific supervision of Doutor João Filipe Bogalho Vicente.

This work was supported by Fundação para a Ciência e Tecnologia (FCT), Lisbon, Portugal (grant SFRH/BD/91729/2012 and strategic project UID/DTP/04138/2019) and by iNOVA4Health Research Unit (LISBOA-01-0145-FEDER-007344), which is cofunded by Fundação para a Ciência e Tecnologia/ Ministério da Ciência e do Ensino Superior, through national funds, and by FEDER under the PT2020 Partnership Agreement.

To my family

TABLE OF CONTENTS

ABBREVIATIONS IIX

SUMMARY XI

SUMÁRIO XII

CHAPTER I GENERAL INTRODUCTION 1

I.1. PYRUVATE AND MITOCHONDRIAL ENERGY METABOLISM 2

I.2. PYRUVATE OXIDATION ROUTE, PYRUVATE DEHYDROGENASE COMPLEX 3

I.2.1. Oxidative Decarboxylation of Pyruvate, a Complex Reaction 3

I.2.2. Pyruvate Dehydrogenase, Structural Properties of a Multi-enzyme Complex 5

I.2.2.1. PDC-E1 Subunit 6

I.2.2.2. PDC-E2/E3BP Core 8

I.2.2.3. PDC-E3 Subunit 10

I.2.3. PDC Regulation 10

I.2.4. Nuclear Encoded Mitochondrial Complex 12

I.3. PYRUVATE DEHYDROGENASE DEFICIENCY, A FREQUENT PYRUVATE OXIDATION DEFECT 14

I.3.1. Genotype and Phenotype Variability 15

I.3.2. Available Therapies 16

I.4. INHERITED METABOLIC DISEASES AS CONFORMATIONAL DISORDERS 17

I.4.1. Protein Folding and Quality Control 17

I.4.2. Conformational Disorders 19

I.4.3. Treatment Strategies for Misfolding Disorders 19

I.4.4. A Confirmed Case of PDCD Recovery: Role of Small Molecular Weight Compounds 21

REFERENCES 23

CHAPTER II AIMS AND OUTLINE 33

CHAPTER III PYRUVATE DEHYDROGENASE COMPLEX DEFICIENCY: UPDATING THE CLINICAL, METABOLIC AND MUTATIONAL LANDSCAPES IN A COHORT OF PORTUGUESE PATIENTS 36

III.1. ABSTRACT 37

III.2. BACKGROUND 38

III.3. MATERIALS AND METHODS 39

III.3.1. Cohort of Patients 39

III.3.2. Phenotypic Evaluation 40

III.3.3. Sample Collection and Preparation 40

III.3.4. PDC Activity Assay 40

III.3.5. Preparation of Genomic DNA, RNA and cDNA 41

III.3.6. PCR Amplification of PDC Encoding Genes 41

III.3.7. Sequence Analysis 41

III.3.8. *In silico* Analysis of PDC-E1 Mutations 42

III.4. RESULTS 43

III.4.1. General Information 43

III.4.2. Genetic Findings 46

III.4.3. Biochemical Findings 47

III.4.4. Clinical Features 47

III.4.5. Treatment 49

III.4.6. *In silico* Analysis of Missense Mutations 50

III.5. DISCUSSION 53

SUPPLEMENTARY INFORMATION 57

REFERENCES 60

CHAPTER IV STRUCTURAL AND FUNCTIONAL IMPACT OF CLINICALLY RELEVANT E1 α VARIANTS CAUSING PYRUVATE DEHYDROGENASE COMPLEX DEFICIENCY 64

IV.1. ABSTRACT 65

IV.2. INTRODUCTION 65

IV.3. MATERIALS AND METHODS 68

IV.3.1. Cloning and Mutagenesis 68

IV.3.1.1. Development of a pET-28b-based Bicistronic Expression System 68

IV.3.1.2. Site-Directed Mutagenesis 69

IV.3.2. Expression and Purification of recombinant Human PDC-E1 Variants 69

IV.3.3. Far-UV Circular Dichroism 70

IV.3.4. Differential Scanning Fluorimetry 70

IV.3.5. Dynamic Light Scattering 70

IV.3.6. Limited proteolysis by Trypsin 71

IV.3.7. Activity Assays 71

IV.3.8. *In silico* Analysis 72

IV.4. RESULTS 74

IV.4.1. Production of Recombinant PDC-E1 Variants 74

IV.4.2. Effect of Selected Mutations on PDC-E1 Structure and Stability 75

IV.4.3. Effect of Selected Mutations on Proteolysis by Trypsin 76

IV.4.4. Propensity to Aggregation 78

IV.4.5. Functional Characterization of PDC-E1 Variants 79

IV.4.6. Molecular dynamics simulations of PDC-E1 variants 82

IV.5. DISCUSSION 84

SUPPLEMENTARY INFORMATION 90

REFERENCES 92

CHAPTER V EFFECT OF ARGININE AND THIAMINE ON THE STRUCTURAL AND FUNCTIONAL RECOVERY OF PYRUVATE DEHYDROGENASE COMPLEX PATHOGENIC VARIANTS: *IN VITRO* AND *EX VIVO* STUDIES 97

V.1. INTRODUCTION 98

V.2. MATERIALS AND METHODS 100

V.2.1. Cloning, mutagenesis, expression and purification of recombinant human PDC-E1 variants 100

V.2.2. Effect of arginine: structural and functional studies on recombinant PDC-E1 variants 101

V.2.3. Cell culture 102

V.2.4. Cell incubation 102

V.2.5. Mitochondrial oxygen consumption rate 102

V.2.6. PDC activity 104

V.2.7. Western blot 104

V.2.8. Immunohistochemical analysis 105

V.3. RESULTS AND DISCUSSION 106

V.3.1. Evaluation of arginine effect: structural and functional comparative studies on recombinant human pathogenic PDC-E1 variants 106

V.3.2. Evaluating arginine effect upon patient-derived cell lines 111

V.3.3. Evaluation of arginine and thiamine effects upon PDC activity and mitochondrial function of patient-derived cell lines 114

V.3.4. Mitochondrial Oxygen Consumption Rate 117

V.4. CONCLUSION 120

SUPPLEMENTARY INFORMATION 122

REFERENCES 123

CHAPTER VI GENERAL DISCUSSION AND PERSPECTIVES **127**

REFERENCES 139

LIST OF PUBLICATIONS **145**

ACKNOWLEDGMENTS, AGRADECIMENTOS **146**

FIGURES

Figure I-1	Schematic metabolic route of pyruvate oxidation	4
Figure I-2	PDC assembly and associated reactions	6
Figure I-3	Structure of human PDC-E1 unit	8
Figure I-4	Funnel-shaped free-energy surface conducting the protein folding and aggregation	18
Figure I-5	PDC-E1α protein profile	21
Figure III-1	Magnetic resonance images of brain lesions	48
Figure III-2	Magnetic resonance spectroscopy	49
Figure III-3	*In silico* analysis of PDC-E1 p.R302H variant	51
Figure III-4	*In silico* analysis of PDC-E3 p.P87S variant	52
Figure IV-1	PDC assembly and associated reactions	67
Figure IV-2	Examples of size-exclusion chromatograms	74
Figure IV-3	Far-UV circular dichroism analysis of heterotetrameric WT and PDC-E1 variants	75
Figure IV-4	Thermal stability of heterotetrameric WT and PDC-E1 variants	76
Figure IV-5	Limited proteolysis by trypsin	77
Figure IV-6	Dynamic light scattering, size distribution by intensity	79
Figure IV-7	Aggregation of WT and PDC-E1 variants analysed by dynamic light scattering	80
Figure IV-8	Kinetic analysis of heterotetrameric WT and PDC-E1 variants	81
Figure IV-9	Average root mean square deviation (RMSD) of WT and PDC-E1 variants obtained in MD simulations	83

Figure IV-10 Average inter-subunit contact surface of WT and PDC-E1 variants obtained in MD simulations 83
Figure IV-11 Average root mean square deviation (RMSD) per residue of WT and PDC-E1 variants obtained in MD simulations 85
Figure IV-12 *In silico* analysis of selected PDC-E1 variants 87
Figure IV-S1 Production of the heterologous bicistronic expression vector pET-28b-hPDC-E1 91
Figure V-1 Aggregation of WT and PDC-E1 variants analysed by dynamic light scattering 108
Figure V-2 Functional characterization of clinically relevant PDC-E1 variants 110
Figure V-3 PDC-E1α protein levels assessed by western blot 112
Figure V-4 Immunohistochemical analyses of PDC-E1α deficient fibroblasts 113
Figure V-5 PDC-E1α protein levels assessed by western blot 115
Figure V-6 Functional studies in PDC-E1α deficient patient-derived fibroblasts. 116
Figure V-7 Representation of the fundamental parameters of mitochondrial respiration 117
Figure V-8 Oxygen consumption rates and bioenergetic profile of PDC-E1α deficient patient-derived fibroblasts 119

TABLES

Table I-1	The PDC components	13
Table III-1	List of the analyzed PDC components	42
Table III-2	Genetic, biochemical, clinical and therapeutics data	44
Table III-S1	List of primers used in this study	57
Table IV-1	Thermal and conformational stability and aggregation propensity	78
Table IV-2	Functional impact of PDC-E1 amino acid substitutions in clinically relevant variants	81
Table IV-3	*In silico* analysis of selected PDC-E1 variants	88
Table IV-S1	Oligonucleotides employed in site-directed mutagenesis	90
Table V-1	Schematic presentation of cell incubation times and media.	103
Table V-2	Thermal and conformational stability and aggregation propensity of clinically relevant PDC-E1 variants	109
Table V-3	Functional studies in PDC-E1α deficient patient-derived fibroblasts	116
Table V-S1	Custom-made culture media formulation	122

ABBREVIATIONS

2-OADC	2-oxoacid dehydrogenase complexes
ALDH7A1	aldehyde dehydrogenase 7A1
ATP	adenosine triphosphate
BH_4	tetrahydrobiopterin
BCOADC	branched-chain 2-oxoacid dehydrogenase complex
CD	circular dichroism
CDS	coding sequence
DAPI	4',6-diamidino-2-phenylindole, dihydrochloride
DCA	dichloroacetate
DCPIP	2,6-dichlorophenolindophenol
DLAT	dihydrolipoyllysine-residue acetyltransferase gene
DLD	dihydrolipoyl dehydrogenase gene
DLS	dynamic light scattering
DMEM	Dulbecco's Modified Eagle's Medium
DOL	division-of-labor
DSF	differential scanning fluorimetry
DTT	dithiotreitol
E1	pyruvate dehydrogenase
E2	dihydrolipoyl-lysine-residue acetyltransferase
E3	dihydrolipoyl dehydrogenase
E3BP	E3-binding protein
EMA	European Medicines Agency
EDTA	ethylenediaminetetraacetic acid
FAD	flavin adenine dinucleotide
FCCP	carbonyl cyanide-4-(trifluoromethoxy)phenylhydrazone
IPTG	isopropyl β-D-1-thiogalactopyranoside
IMD	inherited metabolic disorders
LOVD	Leiden Open Variation Database
MD	molecular dynamics
MLS	matrix localization signals

MPC	mitochondrial pyruvate carrier
NAD	nicotine adenine dinucleotide
OCR	oxygen consumption rate
OSCP	subunit of mitochondrial ATP synthase
OGDC	2-oxoglutarate dehydrogenase complex
PAH	phenylalanine hydroxylase
PBMC	peripheral blood mononuclear cells
PC	pharmacological chaperones
PDB	Protein Data Bank
PDC	pyruvate dehydrogenase complex
PDC-E1	component E1 of the pyruvate dehydrogenase complex
PDCD	pyruvate dehydrogenase complex deficiency
PDHA1	pyruvate dehydrogenase alfa gene 1
PDHB	pyruvate dehydrogenase beta gene
PDHX	E3-binding protein (protein X) gene
PDKs	pyruvate dehydrogenase kinases
PDPs	pyruvate dehydrogenase phosphatases
pET-28b-hPDC-E1	plasmid for expression of human heterotetrameric PDC-E1
PKU	phenylketonuria
PMS	phenazine methosulfate
POD	pyruvate oxidation defects
PQC	protein quality control system
PP	pyrophosphate
PR	proteostasis regulators
SBD	subunit binding domain
SIRT	sirtuins
SMW	small molecular weight compounds
SRT	substrate reduction therapy
TCA	tricarboxylic acid cycle
TPP	thiamine pyrophosphate

SUMMARY

Pyruvate dehydrogenase complex (PDC) occupies an essential position in cellular energy production. The oxidative decarboxylation of pyruvate to acetyl-coenzyme A is conducted by a highly organized multienzyme system. Impaired PDC activity leads to a metabolic disorder affecting mainly the tissues with a high demand for ATP.

This work is dedicated to a comprehensive study of PDC and PDC deficiency at diverse levels. We described and discussed the clinical, biochemical and genotypic findings from thirteen Portuguese PDC deficient patients, we submitted the clinically relevant variants to the detailed structural and functional analyses, and we evaluated the ability of arginine and/or thiamine to restore PDC function in patient-derived cell lines.

All patients from our cohort had the clinical onset between the neonatal period and infancy, manifested different degrees of neurological involvement and, interestingly, most of them reached adulthood. The mutational spectrum revealed ten different mutations in the following genes coding for the respective subunits PDHA1 (PDC-E1α), PDHX (PDC-E3BP), and DLD (PDC-E3). The most striking evidence was a relatively high incidence of E3BP deficiency, nevertheless, PDHA1 mutations were predominant.

The selected pathogenic PDC-E1α variants with amino acid substitutions in different structural regions were analyzed by biochemical and biophysical methodologies, combined with molecular dynamics simulations, revealing a limited impact of the mutations on the conformational stability and presenting a significant functional impairment in terms of reduced residual PDC-E1 enzymatic activity and lower affinity for the thiamine pyrophosphate cofactor.

Applying identical methodologies, we evaluated the effect of arginine supplementation on recombinant PDC-E1 variants. Furthermore, we conducted a study assessing the impact of arginine and/or thiamine treatment in patient-derived cell lines. The rescue efficacy of these stabilizing molecules is clearly determined by the mutation per se. Remarkably, the major effect of arginine was observed in p.R253G variant, at all levels of this study. The beneficial effect of arginine upon the recombinant protein and the considerable response to arginine and thiamine supplementation in the patient´s fibroblast, confirmed previous observations demonstrating the efficacy of arginine treatment in improving the clinical phenotype of the patient carrying the p.R253G mutation.

SUMÁRIO

A via metabólica de oxidação do piruvato constitui um processo fundamental no metabolismo energético aeróbico. O complexo piruvato desidrogenase (PDC) há muito que é conhecido como ponto charneira entre o metabolismo glicolítico no citoplasma e o ciclo dos ácidos tricarboxílicos e a fosforilação oxidativa na mitocôndria. A descarboxilação oxidativa do piruvato em acetil-coenzima A é levada a cabo pelo PDC, um sistema multienzimático altamente organizado que coordena vários mecanismos, tais como reações metabólicas acopladas, regeneração de cofatores e regulação precisa da atividade enzimática. A estrutura complexa do PDC envolve múltiplas cópias de três subunidades catalíticas e um componente estrutural, cinco cofatores e várias subunidades com função reguladora.

Uma atividade diminuída do PDC, causada por alterações em qualquer um dos genes codificantes para componentes do complexo, conduz a uma doença metabólica cujos sintomas refletem a sua posição essencial na produção de energia. Efetivamente, a privação energética a nível celular afeta principalmente os tecidos altamente dependentes de ATP, como o sistema nervoso central e periférico, assim como o músculo esquelético. Porém, a manifestação fenotípica do défice em PDC é consideravelmente heterogénea e o diagnóstico preciso, incluindo a identificação da alteração genética, é importante e decisivo para a seleção apropriada da estratégia terapêutica. As terapias disponíveis podem visar: i) a via metabólica através de dieta que estimula uso de fontes energéticas alternativas, ii) o complexo enzimático disfuncional através da inibição do seu sistema regulador com dicloroacetato, ou iii) a sua estimulação por cofatores. Eventualmente, em alternativa, poder-se-á usar uma estratégia inovadora, a estabilização das variantes proteicas por moléculas de baixa massa molecular, atuando como chaperones químicos ou farmacológicos, usada recentemente com sucesso em várias doenças metabólicas (por exemplo na doença de Fabry, na fenilcetonúria, etc.).

Tal como na maior parte das doenças metabólicas hereditárias, também no défice em PDC as mutações missense representam a maioria das substituições ao nível do DNA. A grande maioria das mutações deletérias afetam o gene *PDHA1* que codifica a subunidade α da enzima heterotetramérica PDC-E1 (αα'ββ').

O nosso grupo de investigação reportou anteriormente o estudo de um doente com défice em PDC, causado pela mutação missense p.R253G no gene *PDHA1*, o qual revelou uma melhoria significativa do seu perfil metabólico e clínico após a suplementação com aspartato de arginina. Os dados então obtidos constituíram a base para o trabalho aqui apresentado e que

teve como objetivos: i) atualizar o espetro mutacional da população portuguesa com deficiência de PDC e assim contribuir para o conhecimento global desta patologia rara; ii) elucidar o impacto estrutural e funcional de variantes PDC-E1α clinicamente relevantes; e, com base no conhecimento adquirido dos mecanismos moleculares subjacentes às variantes patogénicas, iii) determinar o potencial efeito terapêutico da arginina e da tiamina. O **capítulo I** é dedicado a uma revisão geral da literatura sobre o défice em PDC, nomeadamente as bases bioquímicas e moleculares, a fisiopatologia e as atuais abordagens terapêuticas; desenvolve-se também o conceito de doenças conformacionais, nas quais o défice em PDC poderá ser incluído, dado a sua importância para o desenvolvimento de novas terapias.

No **capítulo II,** os objetivos deste estudo são delineados e apresenta-se uma visão global do trabalho experimental desenvolvido.

O **capítulo III** é dedicado à caraterização molecular da população Portuguesa com défice em PDC, apresentando-se o espectro mutacional no grupo de treze doentes estudados. Assim, foram detetados sete indivíduos portadores de mutação no gene de *PDHA1* que codifica a subunidade α do componente PDC-E1, cinco doentes com mutações no gene *PDHX* que codifica a subunidade PDC-E3BP e um doente portador de mutações no gene *DLD* que codifica a subunidade PDC-E3. Estes dados correspondem aproximadamente a estudos anteriores que descrevem as mutações *PDHA1* como a causa predominante da deficiência em PDC, mas também revelam um número significativo de doentes com mutações *PDHX* na população portuguesa, sendo a mutação p.R284X, resultante de um efeito fundador, prevalente neste grupo dos doentes. As análises bioquímicas indicaram elevados níveis plasmáticos de lactato e piruvato, enquanto a relação lactato / piruvato estava geralmente abaixo de 16. As atividades enzimáticas, quando comparadas com os valores de controle, revelaram ser independentes do genótipo e variaram entre 8,5% a 30%, sendo este último considerado um valor de corte para deficiência primária em PDC. Relativamente às características clínicas, todos os doentes apresentaram um certo nível de défice psicomotor ou de atraso de desenvolvimento, cuja gravidade parece estar correlacionada com o tipo e localização da mutação e com a subunidade afetada, sugerindo a existência de uma certa correlação entre o genótipo e o fenótipo na população Portuguesa. Surpreendentemente, a maioria dos nossos doentes atingiu a idade adulta, ao contrário do descrito em várias outras publicações, incluindo os doentes portadores das mutações graves no gene *PDHX*, facto que pode eventualmente contribuir para o debate

pertinente sobre a estrutura e estequiometria do núcleo do PDC (constituído pelas sub-unidades E2 e E3BP).

As opções terapêuticas incluem essencialmente a recomendação de dieta cetogénica e suplementação com o cofator tiamina, embora a ingestão de aspartato de arginina juntamente com tiamina tenha revelado um claro efeito benéfico no nosso doente portador da mutação p.R253G no gene *PDHA1*.

O efeito das mutações missense reflete-se principalmente num comprometimento do equilíbrio normal entre folding, tráfico e degradação proteica, podendo hipoteticamente ser corrigido pela recuperação da proteostase normal. Assim, no **capítulo IV** apresenta-se a caracterização bioquímica e biofísica detalhada de variantes da PDH-E1α com relevância clínica, a qual contribuiu de forma decisiva para estabelecer as bases para a descoberta e design de novas terapias farmacológicas para as doenças metabólicas hereditárias. Quatro das variantes identificadas na população portuguesa foram escolhidas para um estudo estrutural e funcional pormenorizado. As variantes p.F205L, p.R253G, p.R378C e p.R378H, correspondem a substituições de aminoácidos em várias regiões da subunidade PDC-E1α. Desenvolvemos uma abordagem experimental que permitiu a produção eficiente do heterotetrâmero PDC-E1 biologicamente ativo (αα'ββ') e a avaliação comparativa da função, da estabilidade térmica e da estabilidade conformacional destas proteínas recombinantes. A análise estrutural demonstrou o impacto limitado destas mutações na estabilidade conformacional, para além de um aumento na propensão para agregar da variante p.R253G em comparação com a PDC-E1 selvagem. No entanto, em comparação com a PDC-E1 selvagem, todas as variantes apresentaram uma diminuição substancial da sua funcionalidade, revelada por uma atividade enzimática residual diminuída e por uma menor afinidade para o cofator pirofosfato de tiamina (TPP). As simulações de dinâmica molecular apontaram nitidamente para uma estabilidade diminuída, traduzida por uma flexibilidade aumentada, de todas as variantes em relação ao heterotetrâmero WT, particularmente na região de ligação ao TPP.

O **capítulo V** é dedicado então ao estudo do potencial efeito de pequenas moléculas atuando na estabilização da estrutura proteica das variantes patogénicas e na recuperação da sua funcionalidade. Com base nos nossos resultados sobre a caraterização estrutural e funcional de variantes recombinantes de PDC-E1, desenvolvemos um estudo comparativo com o objetivo de avaliar o efeito da suplementação de arginina durante a produção das mesmas variantes patogénicas recombinantes (p. F205L, p.R253G, p.R378C e p.R378H). Além disso, realizámos

um estudo para avaliar a capacidade da arginina e/ou tiamina de recuperar a funcionalidade do complexo enzimático em linhas celulares derivadas de doentes hemizigóticos, portadores das variantes p.R88C, p. R253G, p.R263G e p.R378C da PDH-E1α, causadas por mutações no gene *PDHA1*.

Em relação aos estudos *in vitro*, os resultados revelaram que a arginina não induziu qualquer alteração significativa na estrutura das variantes recombinante. Em relação ao impacto moderado a grave na atividade enzimática das variantes, verificou-se que a arginina apenas induziu um resgate parcial da funcionalidade da variante p.R253G.

Os estudos *ex vivo* vieram revelar uma resposta apreciável da linha celular p.R253G ao tratamento com arginina e/ou tiamina, isoladamente ou em conjunto, uma vez que todas as condições de incubação em concentrações terapêuticas induziram um aumento notável tanto no nível de expressão proteica como no nível de atividade enzimática. Estes resultados corroboram, assim, as observações prévias *in vivo* que demonstraram que a suplementação de arginina foi realmente eficaz em melhorar o fenótipo metabólico, enzimático e clínico do doente portador desta variante.

Sendo o défice em PDC uma patologia mitocondrial, pretendemos ainda avaliar o efeito da arginina e/ou tiamina na recuperação da função mitocondrial. Infelizmente, não pudemos confirmar este efeito na linha p.R253G devido a dificuldades experimentais relacionadas com o seu crescimento em cultura. No entanto, os resultados revelaram que todas as linhas celulares estudadas (p.R88C, p.R263G and p.R378C) apresentavam uma respiração basal inferior à da linha controlo, mas que a sua incubação com níveis terapêuticos daqueles compostos resultou num aumento do consumo de oxigénio, e que este era precisamente utilizado para a produção de ATP na linha p.R263G. Este dado traduz uma potencial estabilização desta variante proteica, aumentando a sua funcionalidade e assim permitindo a produção de mais substratos para alimentar a cadeia respiratória.

Globalmente, e conforme observado para outras moléculas estabilizadoras que atuam como chaperones químicos ou farmacológicos, os resultados obtidos destacam que a eficácia de resgate da arginina e da tiamina é claramente determinada pela mutação em si e confirmam a importância de um diagnóstico complexo, combinando aspetos moleculares, bioquímicos e clínicos da deficiência de PDC, fundamental para o estabelecimento da estratégia terapêutica.

Por último, no **capítulo VI** apresenta-se uma discussão geral dos resultados obtidos, incluindo uma análise integrada de todo o trabalho e respetivas conclusões derivadas deste estudo; finalmente, sugerem-se algumas perspetivas de trabalho futuro.

Em suma, este trabalho contribuiu para um melhor conhecimento do défice no complexo piruvato desidrogenase, uma patologia extremamente rara, nomeadamente na elucidação dos mecanismos patogénicos subjacentes às mutações identificadas na população Portuguesa, assim como para a avaliação de novas alternativas terapêuticas que poderão contribuir para uma melhoria da qualidade de vida dos doentes e respetivas famílias.

PALAVRAS-CHAVE

Défice em complexo de piruvato desidrogenase, Análise mutacional, Mutações missense, Folding de proteínas, Correlação genótipo-fenótipo

KEYWORDS

Pyruvate dehydrogenase complex deficiency, Mutational analysis, Missense mutations, Protein misfolding, Genotype–phenotype correlation

Chapter I

General Introduction

I.1. PYRUVATE AND MITOCHONDRIAL ENERGY METABOLISM

Mitochondria exert central bioenergetic functions in the eukaryotic cell, producing up to 95% of energy through oxidative phosphorylation to fuel all cellular processes driven by ATP-dependent pathways (Tzameli 2012). The physiological importance of the mitochondrion has been widely appreciated for a long time, as the platform for energy transduction, signaling and cell death. The disorders of the mitochondrial metabolism are associated not only with metabolic diseases, but dysfunctional mitochondria have also been linked to health problems ranging from heart failure (Huss and Kelly 2005), through cancer (Porporato et al. 2018) to neurodegeneration (Smith and Gallo 2018; Zhou et al. 2018).

The principal biochemical pathway in the matrix of mitochondria is the tricarboxylic acid (TCA) cycle. Dr. Hans Adolf Krebs won the Nobel Prize in Physiology or Medicine in 1953 for its discovery; hence, it is also referred to as the Krebs cycle (Krebs and Johnson 1937). Cytoplasmic metabolites supplying the TCA cycle are divided into two categories: (1) the canonical oxidative pathway and (2) the anaplerotic pathways. The pyruvate oxidation route, representing the canonical pathway, performs a crucial role in feeding the oxidative phosphorylation or ATP production in mitochondria. Bi-directional anaplerotic pathways replenish the pools of metabolic intermediates in the TCA cycle (Kornberg 1966; Owen et al. 2002) and involve many metabolic routes, e.g. the fatty acid synthesis and fatty acids β-oxidation which is involved in energy production especially during fasting.

Pyruvate is the key metabolite for cellular homeostasis and energy metabolism. The pyruvate molecule is the final product of glycolysis, resulting from conversion of phosphoenolpyruvate by pyruvate kinase. Other significant sources include lactate and alanine, converted by lactate dehydrogenase and alanine aminotransferase, respectively (Gray et al. 2014). Inside mitochondria, pyruvate can suffer two irreversible reactions: ATP-dependent carboxylation into oxaloacetate, catalyzed by pyruvate carboxylase, or oxidative decarboxylation to acetyl-coenzyme A (acetyl-CoA), catalyzed by the pyruvate dehydrogenase complex. Both reactions supply the TCA cycle, thus generating reduction equivalents which are directed to the respiratory chain where they are converted into ATP (Linn et al. 1969; Patel and Roche 1990).

The great majority of pyruvate molecules are irreversibly converted by the pyruvate dehydrogenase complex into acetyl-CoA, simultaneously originating reduced nicotinamide

dinucleotide (NADH) and carbon dioxide. Acetyl-CoA is another pivotal molecule since, besides its central role in energy generation, it drives multiple anabolic processes, including cholesterol and acetylcholine biosynthesis. Entering the TCA cycle, acetyl-CoA is engaged in the first step of oxygen-dependent energy production, originating carbon dioxide and energy, conserved in the reduced electron carriers, NADH and flavin adenine nucleotide ($FADH_2$). These carriers are in turn oxidized, supplying electron equivalents and protons, which are transferred to oxygen through the respiratory chain. Finally, the protons pumped across the membrane during electron transfer are used by the ATP synthase to generate ATP (Pithukpakorn 2005; Gray et al. 2014).

I.2. PYRUVATE OXIDATION ROUTE, PYRUVATE DEHYDROGENASE COMPLEX

I.2.1. Oxidative Decarboxylation of Pyruvate, a Complex Reaction

The pyruvate oxidation route constitutes a fundamental pathway in aerobic energy metabolism, serving to bridge glycolytic metabolism in the cytosol with the TCA cycle and oxidative phosphorylation in the mitochondria. The key step, the irreversible conversion of pyruvate to acetyl-CoA with reduction of NAD^+, is conducted by pyruvate dehydrogenase complex (PDC, structure detailed in I.2.2.). Pyruvate oxidation is a multifactorial sequential reaction involving pyruvate transport into the mitochondrial matrix, three enzymatic reactions catalyzed by the functional subunits E1, E2, and E3, the engagement of a structural subunit E3 binding protein (E3BP), initially termed protein X (De Marcucci and Lindsay 1985; Jilka et al. 1986), and regulation by phosphorylation/ dephosphorylation of the PDC-E1α subunit. Pyruvate oxidation involves five cofactors: thiamine pyrophosphate (TPP), lipoic acid (Lip), FAD, coenzyme A (CoA), and NAD (Sperl et al. 2015) (Figures I-1 and I-2). Pyruvate, formed by glycolysis in the cytoplasm, is transported across the inner mitochondrial membrane by the mitochondrial pyruvate carrier (MPC) which is formed by two paralogous subunits (MPC1 and MPC2) (Bricker et al. 2012; Herzig et al. 2012).

Pyruvate dehydrogenase, PDC-E1 subunit (EC 1.2.4.1), catalyzes the first, rate-limiting and irreversible pyruvate decarboxylating step of the whole reaction (Cate et al. 1980; Berg et al. 1998). The reaction takes place in two active sites formed at the interface between the α and β subunits, each requiring the thiamine pyrophosphate cofactor and magnesium ions for

activity. The oxidative decarboxylation of pyruvate is coupled to the reductive acetylation of the lipoamide cofactor. The released acetyl group is subsequently transferred from thiamine pyrophosphate to a lipoate moiety covalently bound to PDC-E2 (Korotchkina and Patel 2001a; Seifert et al. 2007; Gray et al. 2014; Byron and Lindsay 2017).

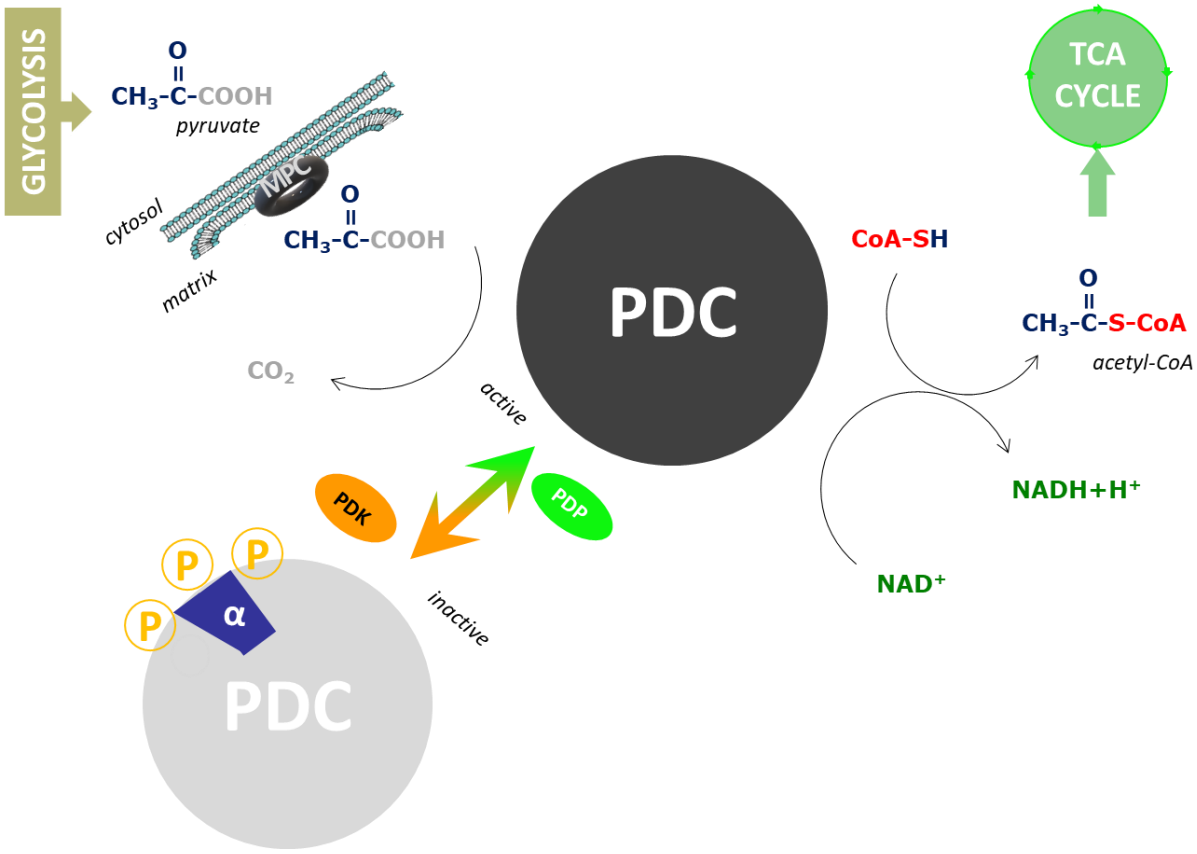

Figure I-1 **Schematic metabolic route of pyruvate oxidation** showing pyruvate transport into the mitochondrial matrix, and the role of the associated kinases (PDK) and phosphatases (PDP) in the regulation of PDC activity.

Dihydrolipoyllysine-residue acetyltransferase, PDC-E2 (EC 2.3.1.12), catalyzes the transfer of the acetyl group from the lipoate moiety to CoA, forming acetyl-CoA and dihydrolipoate. This component is constituted by four domains: the inner domain is endowed with acetyltransferase activity and mediates formation of the complex with E3BP, the subunit binding domain binds PDC-E1, and the two lipoyl domains contain covalently bound lipoate

moieties that are sequentially transferred between the PDC-E1, PDC-E2, and PDC-E3 active sites via a ‘swinging arm’ mechanism (Milne 2002; Smolle et al. 2006; Seifert et al. 2007; Brautigam et al. 2009).

Dihydrolipoyl dehydrogenase, PDC-E3 (EC 1.8.1.4), catalyzes the regeneration of the lipoate group from dihydrolipoate. E3 is a homodimer interacting with the complex core through E3BP. The oxidation of dihydrolipoate results in the reduction of FAD to $FADH_2$ and subsequent reduction of NAD^+ to NADH, which enables regeneration of FAD (Odièvre et al. 2005).

I.2.2. Pyruvate Dehydrogenase, Structural Properties of a Multi-enzyme Complex

In general, the key steps in various mitochondrial pathways are controlled by highly organized enzymatic arrays from the family of 2-oxoacid dehydrogenase complexes (2-OADC). Besides PDC, it is worth to mention the role of 2-oxoglutarate dehydrogenase complex (OGDC) in controlling the TCA cycle flux and of branched-chain 2-oxoacid dehydrogenase complex (BCOADC) in the metabolism of the branched-chain amino acids, leucine, isoleucine and valine (Ciszak et al. 2006; Brautigam et al. 2011; Byron and Lindsay 2017). All members of the 2-oxoacid dehydrogenase complexes family contain in their assembly multiple copies of three distinct enzymes, designated as E1, E2 and E3. Typically, each complex is organized around a core acting as a framework to which multiple dimeric or heterotetrameric E1 and homodimeric E3 enzymes are joined tightly, but noncovalently (Reed and Oliver 1982).

Many investigators have contributed to the understanding of the PDC structure (reviewed by Patel and Roche 1990; Perham 2000; Reed 2001; Byron and Lindsay 2017, with the pioneering contribution from Reed and Oliver 1982). The complex reaction of pyruvate oxidation is catalyzed by a macromolecular machine, possessing properties like high structural stability, coupled and directed metabolic channeling within multi-step reactions by swinging lipoyl arms and regeneration of co-factors. Human PDC is a massive protein complex weighing 8-10 MDa, resulting from the assembly of multiple copies of PDC-E1, PDC-E2, PDC-E3 and E3-binding protein (PDC-E3BP) (Zhou et al. 2001; Milne 2002; Smolle et al. 2006; Yu et al. 2008; Jiang et al. 2018). The morphology of PDC is determined by the 60-meric E2/E3BP core, surrounded by 6-12 E3 dimers and 20-30 E1 heterotetramers (Figure I-2).

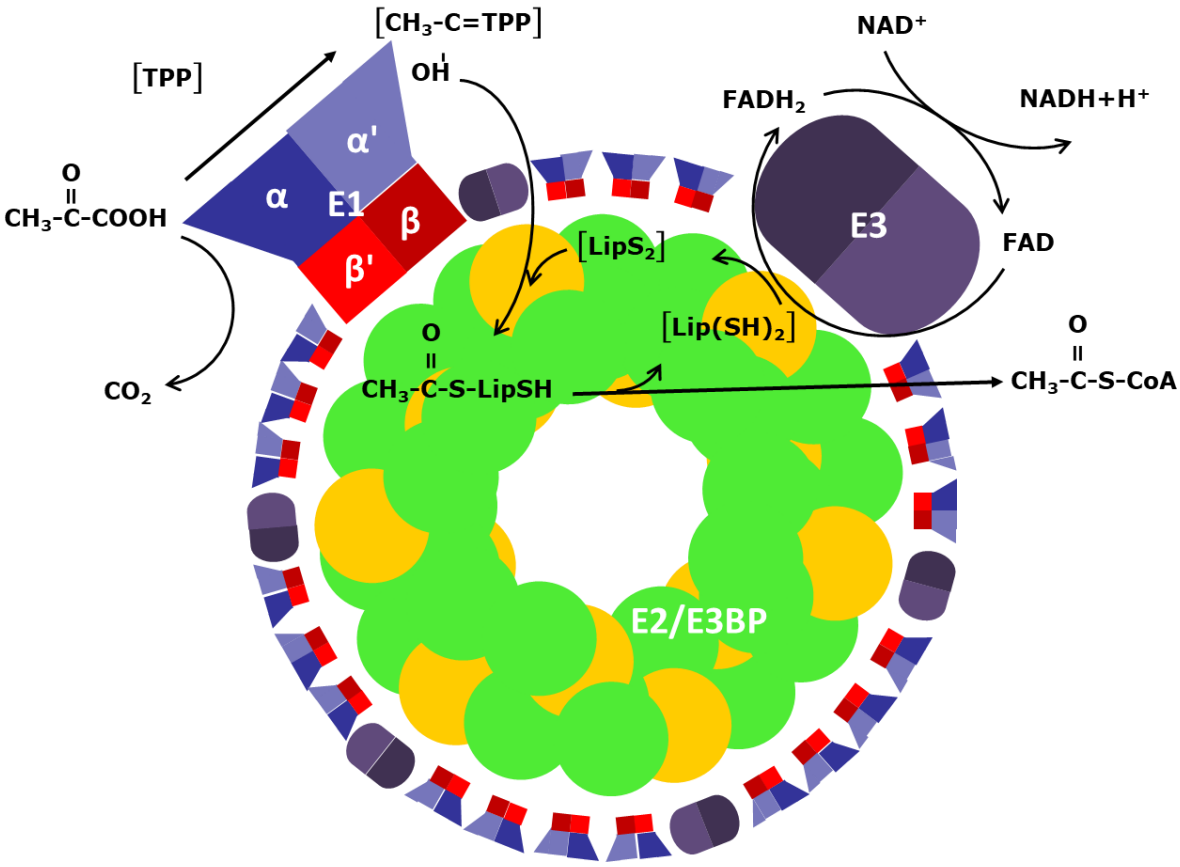

Figure I-2 **PDC assembly and associated reactions.** The PDC-E1 subunit catalyzes the first, rate-limiting and irreversible step. The oxidative decarboxylation of pyruvate is coupled to the reductive acetylation of the lipoamide cofactor and requires thiamine pyrophosphate cofactor. The released acetyl group is transferred from thiamine pyrophosphate to a lipoate moiety covalently bound to PDC-E2, then subsequently to CoA, forming acetyl-CoA and dihydrolipoate. The lipoate moieties are sequentially transferred between the PDC-E1, PDC-E2, and PDC-E3 active sites via a 'swinging arm' mechanism. The lipoate group is regenerated from dihydrolipoate by PDC-E3. The oxidation of dihydrolipoate results in the reduction of FAD to $FADH_2$ and the subsequent reduction of NAD^+ which enables the regeneration of FAD.

I.2.2.1. PDC-E1 Subunit

The crystal structure of human PDC-E1 has been determined by Ciszak and collaborators (Ciszak et al. 2003), with later contributions (Seifert et al. 2007; Kato et al. 2008), including very recent ones (Drakulic et al. 2018; Whitley et al. 2018) and is shown in Figure I-3. The heterotetrameric complex comprises two copies of each subunit E1α and E1β. A two-fold

symmetry axis relates the α with the α' subunit and the β with the β' subunit in a tetrahedral fashion. Hydrophobic α–β contacts and flexible α–β' connections constitute and stabilize the active sites. The funnel-shaped tunnel formed at the α–β interface allows the access to the lipoyl-lysine moiety. Each α subunit has a core region composed of a parallel six stranded β-sheet packed against five helices, involved in binding Mg^{2+} and the pyrophosphate fragment of TPP (PP and PP' domains). Other specific secondary structural elements of the α subunits located at the α–β channel include two loops housing three phosphorylation sites controlling activity regulation, as detailed in section I.2.3 (Korotchkina and Patel 2001a; Imbard et al. 2011; Byron and Lindsay 2017). A recently published analysis of PDC-E1 X-ray crystal structures (Whitley et al. 2018) confirmed the importance of the regulatory phosphorylation loop for the PDC-E1 activation and revealed that altered coenzyme binding can result in phosphorylation loop disorder even in the absence of phosphorylation. Moreover, disordered loops may affect the availability to efficiently bind the lipoyl domain of PDC-E2.

Two domains of the β subunit are of a similar size and correspond to the N- and C- terminal halves of the polypeptide chain. The first domain consists of a parallel six-stranded β-sheet surrounded by seven α-helices. This domain of the β subunits is involved in binding the K^+ ion and the aminopyrimidine ring of TPP (PYR and PYR' domains). The second domain (C and C' domains) has a parallel four-stranded β-sheet with one edge composed of an antiparallel β-strand braced with four helices, two of them on each side of this central β-sheet (Ciszak et al. 2003; Imbard et al. 2011). It has been proposed by several authors that the C and C' domains are involved in anchoring the PDC-E1 to the subunit binding domain of the PDC-E2 subunit (Ævarsson et al. 1999; Ciszak et al. 2003).

The two active sites of the heterotetrameric PDC-E1 enzyme act in a "flip-flop" mechanism, alternating the catalytic phases. Thus, while one active site is involved in the pyruvate decarboxylation, the other is engaged in the reductive acetylation of lipoyl-E2 moiety (Arjunan et al. 2002; Ciszak et al. 2003). Curiously, the generally accepted hypothesis that magnesium is required for PDC-E1 to bind TPP was recently confronted (Whitley et al. 2018), suggesting that the 6-coordinate magnesium binding site is probably necessary to anchor TPP in its canonical bound conformation, but not strictly necessary for PDC-E1 to bind TPP in general.

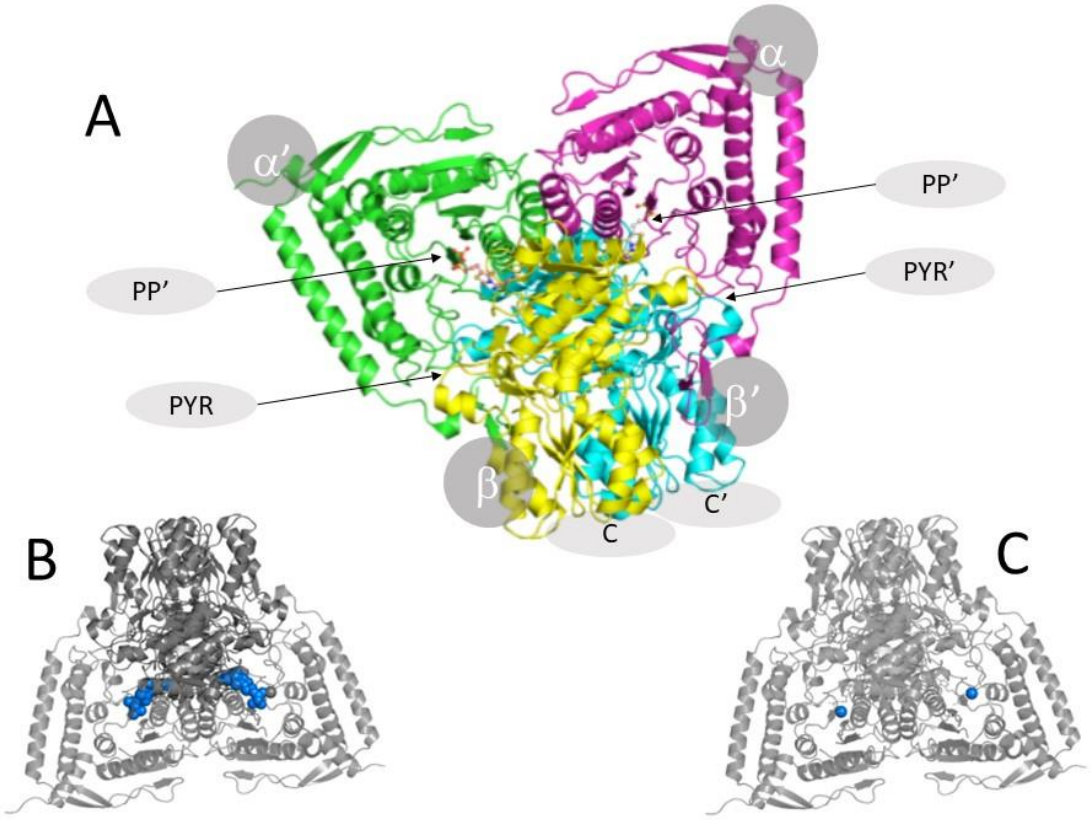

Figure I-3 **Structure of human PDC-E1 unit**. A) Tetrameric assembly colored by chain and viewed from the front, marking the PP, PYR and C domains. Assembly containing two copies of small molecules highlighted in blue: B) TPP and C) Mg^{2+}. Adapted from Protein Data Bank in Europe.

I.2.2.2. PDC-E2/E3BP Core

The members of the family of the 2-OADC share common features in the organization of their structural elements. The enzymatic core occurs, in general, in two different shapes. The basic trimeric units (detailed below) form either eight or twenty vertices, resulting in either a pentagonal dodecahedral 60-meric or a cubic 24-meric assembly, respectively. The 60-meric core is so far found exclusively in PDC from eukaryotic sources and Gram-positive bacteria (Reed 2001; Byron and Lindsay 2017).

The E2 catalytic component has a multi-domain structure, constituted by two tandem lipoyl domains (outer L1 and inner L2 domains), a peripheral subunit binding domain (SBD) and the acetyltransferase/catalytic (C domain), all separated by 25-30 amino acid long flexible linkers

(Guevara et al. 2017). The fundamental building block of the PDC central structure is a basic trimeric unit. The E2 and the E3BP proteins combine to form the icosahedral PDC-E2/E3BP 60-meric core providing the central structural framework and allowing the integration of the multiple copies of PDC-E1 and PDC-E3 components. Initial reports referred to the association of 12 E3BPs to the E2 core, suggesting the so-called "addition model" of the core organization (60 E2 + 12 E3BP) (Maeng et al. 1996; Sanderson et al. 1996). Subsequently, two "substitution" models have been proposed for the E2/E3BP inner core of mammalian PDC: (48 E2 + 12 E3BP) and (40 E2 + 20 E3BP) with 12 or 20 copies of E3BP replacing the equivalent number of E2 proteins in the 60-meric inner core (Hiromasa et al. 2004; Brautigam et al. 2009; Vijayakrishnan et al. 2010, 2011). Variations in both currently accepted models have been attributed to differences between the native and recombinant assemblies (Vijayakrishnan et al. 2011; Byron and Lindsay 2017); however, according to recent studies, there is a considerable potential for variation in both overall E2/E3BP core organization and subunit stoichiometry. Jiang and colleagues strongly suggest that E3BP substitutes for E2 within trimers of the dodecahedron (Jiang et al. 2018). Curiously, this work also provides the hypothesis that, in analogy to human PDC-E2, human PDC-E3BP likely participates in catalysis based on the very similar structure and conservation of residues of E3BP that play a primary substrate binding/enclosing role.

PDC-E1 and PDC-E3 reside close to each other on the complex periphery, however no interactions of catalytic or structural consequence are known to exist between them (Whitley et al. 2018). Despite the high similarity between the primary structures of E3BP and E2, the E3-binding domain of human E3BP is highly specific to human E3, whereas the E1-binding domain of human E2 is highly specific to human E1 (Ciszak et al. 2006).

Remarkably, a trimeric enzyme has been generated by removal of the five C-terminal amino acids of the E2 polypeptide containing a key tyrosine involved in inter-trimer contacts (Marrott et al. 2014). This minimal complex can bind both E1 and E3 components and possesses catalytic activity similar to the native multi-enzyme complex. Recently, Guo and collaborators have reported structurally simplified variants of PDC with high enzymatic activity obtained by targeted modifications of the complex core components (Guo et al. 2017). This raises the question of why all native 2-OADC assemble into such large structures. It seems probable that

the large assembly provides catalytic advantages by its general ability to perform active-site coupling (Marrott et al. 2014; Byron and Lindsay 2017).

I.2.2.3. PDC-E3 Subunit

In mammalians, E3 is a common component to all members of the 2-OADC family, performing a similar catalytic function in all of them. The crystallographic structure of human E3 was first presented in 2006 (Brautigam et al. 2006). E3 is a homodimer with each of the subunits comprising four domains: an FAD domain, an NAD domain, a central domain and an interface domain. The exact stoichiometry of the E3 association with the E3BP remains unclear. The crystal structure of the sub-complex subunit binding domain (E3)SBD:E3BP suggests a 1:1 stoichiometry (Ciszak et al. 2006; Brautigam et al. 2006). However, solution structural studies provided evidence for a 2:1 binding relationship (Smolle et al. 2006; Vijayakrishnan et al. 2011). According to this model, E3 dimers have the potential to form 'cross-bridges' between adjacent E3BPs around the core surface (Vijayakrishnan et al. 2010, 2011). The presence of these crosslinks between the E3BP proteins may facilitate the efficiency of substrate channeling and active-site coupling (Byron and Lindsay 2017).

Compared to the BCOADC, the E3 is more strongly tethered to the PDC core. This difference is attributed to the presence of an arginine residue in the E3BP of the BCOADC, whereas an asparagine is in the PDC. Hypothetically the larger arginine residue causes a steric clash, reducing the binding affinity (Ciszak et al. 2006; Brautigam et al. 2011).

I.2.3. PDC Regulation

Consistent with the pivotal role of PDC in energy metabolism is the tight regulation of its activity, allowing a fine maintenance of cellular homeostasis. Besides the long-term transcriptional regulation, where most PDC transcripts are down-regulated under energetic stress (Zhang et al. 2011), and the metabolite regulation with high levels of NADH and acetyl-CoA inhibiting the complex (Wieland 1983; Yeaman 1989; Strumiło 2005), the precise and rapid regulation of PDC activity is achieved via phosphorylation and dephosphorylation (Linn et al. 1969; Wieland and Jagow-Westermann 1969). Being subject to this short-term regulatory

mechanism, in addition to the end-product inhibition, makes mammalian PDC unusual amongst mitochondrial enzymes/complexes (Byron and Lindsay 2017).

The temporal phosphorylation status provides the appropriate balance between glucose or fatty acid and ketone body production in both the fed and the fasted states. For example, PDC down-regulation during starvation or diabetes secures preserving carbohydrate reserves for tissues that are primarily dependent on glucose for energy. The mitochondrial pyruvate is conserved or diverged to other metabolic pathways, such as gluconeogenesis, in order to maintain blood sugar levels (Gray et al. 2014). PDC up-regulation, e.g., in the fed state, results in the increased acetyl-CoA flux into the TCA cycle, maximizing the energy production as well as carbon supply to biosynthetic pathways.

The reversible phosphorylation of the α subunit of the PDC-E1 component at one or more of the three specific serine residues is achieved by an enzymatic system, involving pyruvate dehydrogenase kinases (PDK) and pyruvate dehydrogenase phosphatases (PDP) (Patel and Roche 1990; Kolobova et al. 2001; Patel and Korotchkina 2006; Kato et al. 2008). The serine residues Ser293 (site 1), Ser300 (site 2) and Ser232 (site 3) are phosphorylated *in vivo* at different rates and with different specificities by four PDK isoforms termed PDK1–PDK4 (Gudi et al. 1995; Rowles et al. 1996). Sites 1 and 2 make part of the phosphorylation loop A, which participates in anchoring the TPP cofactor to the active site, while the phosphorylation loop B, coordinating the magnesium ion, houses site 3 (Ciszak et al. 2003; Kato et al. 2008). Site 1 is preferentially phosphorylated, and sites 2 and 3 are sequentially phosphorylated (Korotchkina and Patel 2001b). PDK1 and 4 are highly expressed in heart, liver and muscle whereas PDK3 is prevalent in kidney, brain and testis (Bowker-Kinley et al. 1998; Sugden and Holness 2003). PDK1 phosphorylates all three serine residues in contrast to PDK2–4 that can modify only sites 1 and 2. Phosphorylation at a single site is sufficient to cause inactivation, apparently by inhibiting substrate and/or TPP (Korotchkina and Patel 2001b). The X-ray structure of a phosphorylated version of human PDC-E1 (site 1, Ser293) indicates that the phosphoryl group prevents TPP-induced ordering of the two loops housing the three phosphorylation sites leading to disruption of substrate channeling (Kato et al. 2008).

In opposition to PDKs, PDPs restore the PDC activity by removing the phosphoryl groups from PDC-E1α. Two distinct PDP isoforms, PDP1 and PDP2, have been identified in humans (Huang et al. 1998). The heterodimeric phosphatases comprise each a catalytic and a regulatory

unit allowing rapid fine response to the actual metabolic condition (Lawson et al. 1997). PDP expression is also tissue-specific: PDP1 is mainly expressed in muscle whereas PDP2 occurs in liver and adipose tissue.

As a gatekeeper between the metabolic pathways of glycolysis and TCA cycle, PDC has been identified as a target for regulating glucose oxidation in cancer cells leading to the Warburg effect (Vander Heiden et al. 2009; Kaplon et al. 2013). Up-regulation of PDK isoforms gene expression is reported in several forms of cancer, while PDKs may be further activated by PDC by binding to the E2/E3BP core. Hence, targeting the PDK:E2/E3BP interaction or a precise selection of the PDK inhibitors could serve as a novel therapeutic approach in oncology (Guevara et al. 2017; Golias et al. 2019). Lysine acetylation of PDC-E1α and PDP1 is common in epidermal growth factor-stimulated cells and diverse human cancer cells. K321 acetylation inhibits PDC-E1α by recruiting PDK1, and K202 acetylation inhibits PDP1 by dissociating its substrate. Both mechanisms promote glycolysis in cancer cells and consequent tumor growth (Fan et al. 2014).

Curiously, a novel model of PDC regulation has been reported, involving SIRT3 (Fan et al. 2014) and SIRT4 (Mathias et al. 2014), from the family of sirtuins, mammalian NAD^+-dependent enzymes that regulate diverse biological processes, including gene expression, stress response, metabolic homeostasis and aging. The lipoamidase activity of SIRT4 controls the lipoylation of the PDC-E2 component and the deacetylase activity of SIRT3 is engaged in the posttranslational modifications involved in the hierarchical regulation of PDP1 and PDC-E1.

I.2.4. Nuclear Encoded Mitochondrial Complex

The mitochondrial proteome consists of over 3,300 proteins and more are being identified constantly (Morgenstern et al. 2017). From those, the mitochondrial DNA (mtDNA) encodes only 13 proteins, all subunits from complexes of the electron transport chain; other proteins, including all PDC components, are nuclear-encoded and synthetized in cytosolic ribosomes. Transport of nuclear-encoded proteins to either the matrix or the intermembrane space requires specific signals. Matrix localization signals (MLS) are situated on the N-terminus of a protein (von Heijne et al. 1989). The constituent PDC subunits are transported in a loosely-folded form to the mitochondria as individual precursor polypeptides (Dudek et al. 2013). A matrix-located

Hsp60/10 chaperone system promotes the maturation and the assembly of the whole complex (Fox et al. 2012).

The catalytic, structural and regulatory elements of the entire assembly, including different isoforms, are listed in Table I-1. In general, the expression of the distinct isoenzymes is tissue-specific. For example, from the two PDC-E1α subunit isoforms, E1α1 is present ubiquitously in somatic tissues, whereas E1α2 is only expressed in human spermatocytes and spermatids (Dahl et al. 1990). Interestingly, our group reported on a young adult female with PDC deficiency associated with *PDHX* mutations, who simultaneously presents the somatic expression of the testis-specific *PDHA2* gene (Pinheiro et al. 2016a, b).

Table I-1 **The PDC components** with the respective subunits and their isoforms, with references to the chromosomal location, HUGO-approved gene symbol and Enzyme Commission (EC) number.

Component	Enzymatic Activity	Enzyme Commission number	Subunit / Isoenzyme	Approved Gene Symbol	HGNC ID	GenBank	Chromosomal Location
PDC-E1	pyruvate dehydrogenase (acetyl-transferring)	EC 1.2.4.1	E1 α1	*PDHA1*	8806	NM_000284	Xp22.12
			E1 β	*PDHB*	8808	NM_000925	3p14.3
			E1 α2	*PDHA2*	8807	NM_005390	4q22.3
PDC-E2	dihydrolipoyllysine-residue acetyltransferase	EC 2.3.1.12		*DLAT*	2896	NM_001931	11q23.1
PDC-3	dihydrolipoyl dehydrogenase	EC 1.8.1.4		*DLD*	2898	NM_000108	7q31.1
PDC-E3BP				*PDHX*	21350	NM_003477	11p13
PDK1	[pyruvate dehydrogenase (acetyl-transferring)] kinase	EC 2.7.11.2		*PDK1*	8809	NM_002610	2q31.1
PDK2				*PDK2*	8810	NM_002611	17q21.33
PDK3				*PDK3*	8811	NM_005391	Xp22.11
PDK4				*PDK4*	8812	NM_002612	7q21.3
PDP1	[pyruvate dehydrogenase (acetyl-transferring)]-phosphatase	EC 3.1.3.43	PDP catalytic subunit 1	*PDP1*	9279	NM_018444	8q22.1
			PDP regulatory subunit	*PDPR*	30264	NM_017990	16q22.1
PDP2			PDP catalytic subunit 2	*PDP2*	30263	NM_020786	16q22.1

Probably, the stoichiometry of the individual components in the mature functional PDC may vary (Byron and Lindsay 2017). This rationale could provide a support to a striking phenomenon described by Sutendra and collaborators in 2014. Although until recently PDC has been considered to be a strictly mitochondrial enzyme, their work clearly revealed detectable

PDC activity in the cell nucleus (de Boer and Houten 2014; Sutendra et al. 2014). Apparently, the intact functional PDC complex, lacking the MLS, can translocate across the mitochondrial membrane from the mitochondria to the nucleus, providing an autonomous source of acetyl-CoA for histone modification. Moreover, due to the absence of PDK in the nucleus, nuclear PDC is not inactivated by phosphorylation. Metabolic regulation of gene transcription, through the so called "moonlighting" of proteins into the nucleus, has been recently described for several cytosolic and mitochondrial enzymes (extensively reviewed by Boukouris et al. 2016).

I.3. PYRUVATE DEHYDROGENASE DEFICIENCY, A FREQUENT PYRUVATE OXIDATION DEFECT

In the group of mitochondrial diseases, clinical manifestations are highly heterogenous, having in common dysfunctions of various organs due to the deficiency in ATP production. Pyruvate oxidation defects (POD) are among the most frequent disorders in the mitochondrial energy metabolism (Sperl et al. 2015). PODs are characterized by insufficient pyruvate turnover in mitochondria and can be caused by various deficiencies in the whole pyruvate oxidation route, including not only the defects of the PDC subunits, but also the misfunctions of the mitochondrial pyruvate import, regulation and metabolism of various cofactors (Sperl et al. 2015).

The first pyruvate oxidation defect has been identified in 1970 by measuring PDC activity and at the time was termed pyruvate decarboxylase deficiency (Blass et al. 1970). Subsequently, genetic defects in all constituent PDC subunits have been described: *PDHA1* (Endo et al. 1989), *DLD* (Liu et al. 1993), *PDHX* (Aral et al. 1997), *PDHB* (Brown et al. 2004) and *DLAT* (Head et al. 2005). Later, a few mutations have been determined in the genes encoding both enzymes of the PDC regulatory system, PDKs and PDPs (Maj et al. 2005) and the mitochondrial pyruvate carrier (Bricker et al. 2012), or genes related to the metabolism of PDC-relevant cofactors (Zeng et al. 2005; Mochel et al. 2008; Cameron et al. 2011; Navarro-Sastre et al. 2011; Mayr et al. 2011b, a, 2014).

I.3.1. Genotype and Phenotype Variability

According to a comprehensive study by Sperl and collaborators, approximately 75% of pyruvate oxidation defects are caused by the deficiency of one of the PDC subunits (Sperl et al. 2015). Symptoms of PDC deficiency (PDCD) correspond to its essential position in energy metabolism. Cellular energy deprivation affects mainly the tissues with a high demand for ATP, such as central and peripheral nervous system and skeletal muscle. Inadequate removal of pyruvate and lactate results in lactic acidemia (Brown et al. 1994; Imbard et al. 2011; Patel et al. 2012; Sperl et al. 2015).

PDCD is a neurologically heterogeneous disorder, and the phenotypic variation is broad. The clinical spectrum ranges from fatal lactic acidosis and progressive neurological and neuromuscular degradation in the neonatal period, to a chronic neurological dysfunction and neurodegenerative condition. Milder forms may present with intermittent ataxia (Imbard et al. 2011). The prevalent clinical phenotype presents during the first year of life, neurological and neuromuscular structural lesions revealed by neuroimaging, and lactic acidosis and a blood lactate:pyruvate ratio ≤20 are the key biomarkers (Patel et al. 2012). Nearly half of the patients with PDC deficiency are diagnosed with Leigh's syndrome (Imbard et al. 2011; Patel et al. 2012). Historically, Leigh's syndrome is characterized as a neurodegenerative disorder caused by deficiencies in the protein complexes associated with oxidative phosphorylation (Mannan et al. 2004).

The severity of the disease is associated with the mutation type and with the subunit affected, even though there is no consensus about the level at which the PDC genotype correlates with the phenotype (Gray et al. 2014; Sperl et al. 2015; Patel et al. 2012). Most PDCD cases result from mutations in *PDHA1*, the X-linked gene encoding the E1α subunit, whereas in few cases mutations reside in genes encoding other subunits: *PDHB* (E1β), *DLAT* (E2), *DLD* (E3), *PDHX* (E3BP).

More than 100 disease-causing mutations are described in *PDHA1*, most frequently missense and nonsense, splicing and frameshift defects affecting the ability of PDC-E1α to bind the thiamine pyrophosphate cofactor, to fold properly and its capacity to be targeted and transported into the mitochondria. Mutations are scattered along the gene, but missense mutations are mainly localized in exons 1-9, whereas most frameshift mutations occur in exons 10 and 11 (Imbard et al. 2011; Patel et al. 2012).

Hemizygous males are generally symptomatic, while in heterozygous females the random-patterns of X-inactivation lead to variable expression of the mutant and normal genes in different tissues. Therefore, the severity of clinical manifestations depends on the proportion of cells expressing the non-affected PDC-E1α subunit (Dahl 1995). Furthermore, the X-inactivation pattern can lead to difficulties in the biochemical determination of the PDCD diagnosis (Sperl et al. 2015).

Notably, mutations in the *DLD* gene coding for the PDC-E3 subunit result in combined deficiencies of the 2-OADC family manifested by lactic acidemias and maple syrup urine disease (Hengeveld and Kok 2002; Odièvre et al. 2005). It is worth to mention that most frequent variants of the *PDHX* gene lead to total absence of the PDC-E3BP. Nevertheless, PDCD patients with non-detectable PDCD-E3BP display 10–20% of PDC activity and appear to retain a residual affinity for PDC-E3 (Marsac et al. 1993; Vijayakrishnan et al. 2010).

I.3.2. Available Therapies

Pyruvate oxidation defects, as most inborn metabolic diseases, remain without effective treatment. The existing therapeutic strategies for pyruvate oxidation defects target either the metabolic pathway or the dysfunctional enzymatic complex. However, their capacity to impro ve and stabilize the clinical course of the disorder is limited.

A ketogenic diet, rich in lipids and poor in carbohydrates, can bypass the energy production by stimulating alternative metabolic pathways, such as β-oxidation and the use of ketone bodies for ATP production (Wexler et al. 1997). A ketogenic diet reduces lactate production and may stimulate mitochondrial biogenesis, having shown to be beneficial for several patients (Head et al. 2005; El-Gharbawy et al. 2011).

The impaired catalytic activity of PDC can be either intervened through the regulatory system or stimulated by cofactors supplementation. Dichloroacetate (DCA), as a xenobiotic inhibitor of PDKs, is used to increase PDC activity by blocking its phosphorylation (Fouque et al. 2003). Phenylbutyrate constrains PDKs by a similar mechanism (Ferriero and Brunetti-Pierri 2013). Moreover, a tight regulation of PDC activity through the control of PDKs is gaining importance not only as a potential oncologic treatment, as mentioned above, but also as a therapeutic approach to Huntington’s disease, where reducing the expression of PDKs through

histone deacetylase inhibitor sodium butyrate may help to increase the PDC activity, thus compensating the transcriptional deregulation and changes in mitochondrial bioenergetics, typical for this disorder (Naia et al. 2017). Hence, a whole new generation of small molecules acting as PDKs inhibitors is under ongoing investigations (Stacpoole 2017).

Supplementation with thiamine, a precursor of thiamine pyrophosphate, may help to overcome the impaired TPP binding to the PDC-E1 active site. Several cases of thiamine-responsive PDC-E1 deficiency have been described, so far (Pastoris et al. 1996; Di Rocco et al. 2000; Naito et al. 2002; Brown 2014; Castiglioni et al. 2015). Nevertheless, there is high variability in the clinical and biochemical response and the distribution of the mutations in the thiamine-responsive variants (Brown 2014). Hence, the exact mechanism of the TPP effect remains unclear, offering a question if beside playing its role as a specific cofactor, TPP could display a stabilizing effect on altered conformation of the PDC-E1 protein.

I.4. Inherited Metabolic Diseases as Conformational Disorders

I.4.1. Protein Folding and Quality Control

The biological and biochemical function of most cellular proteins depends on their unique three-dimensional structure, which is acquired through folding of the newly synthesized polypeptide chain (Gregersen et al. 2006). Native states of proteins almost always correspond to the structures that are thermodynamically more stable under physiological conditions (Dobson 2003). The driving force of protein folding is the search for a conformation with lower free energy than the previous one, making the nascent polypeptide to navigate a complex energy landscape (Figure I-4). The dynamics of the folding process is influenced by the cellular environment and is mainly defined by the interactions between the amino acid residues. The folding of the large multidomain proteins is prompted by macromolecular crowding in the cytosol (Ellis and Minton 2006), which enhances the propensity of folding intermediates and misfolded states to aggregate. A network of chaperones prevents these aberrant interactions and assists in overcoming energetic barriers between the low energy states. In general, a molecular chaperone is defined as any molecule with the capacity of interaction, stabilization or support of another protein in acquiring its functionally active conformation, but without integrating its final structure (Hartl 1996; Gregersen et al. 2006; Balchin et al. 2016).

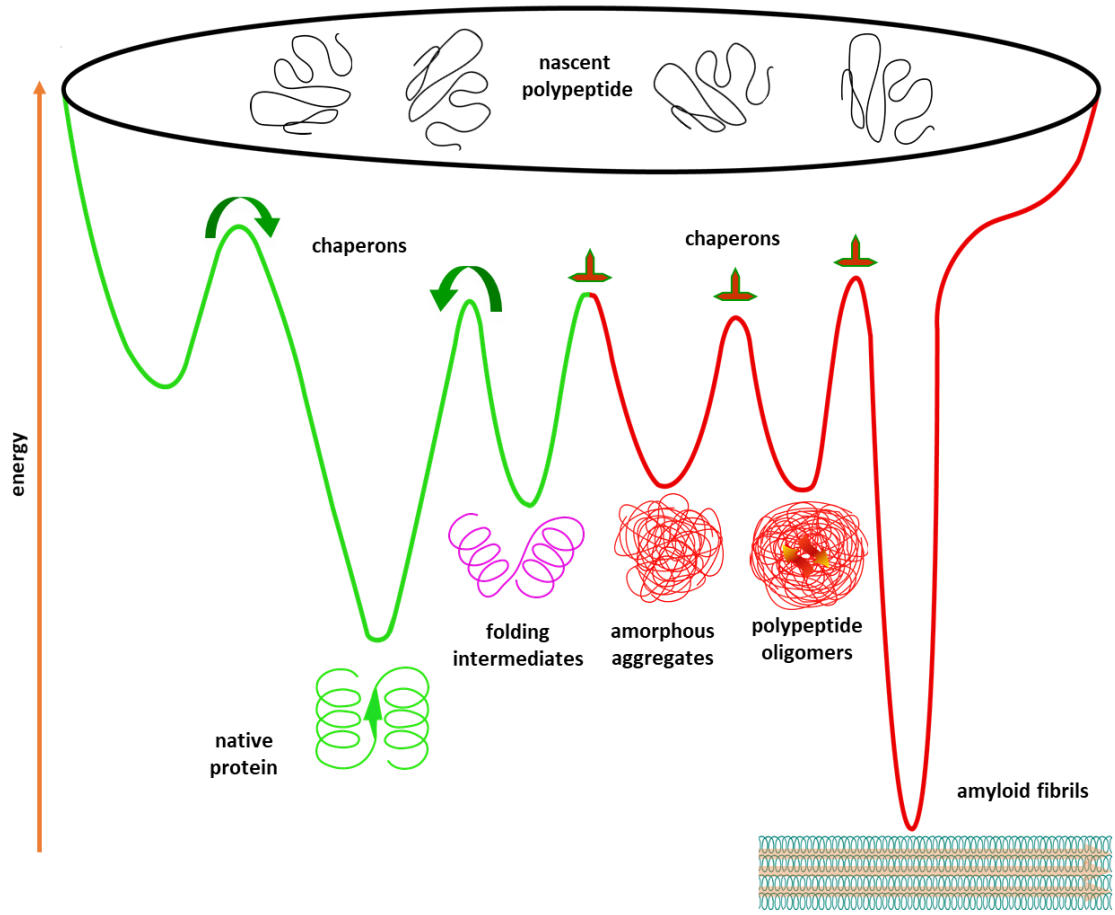

Figure I-4 **Funnel-shaped free-energy surface conducting the protein folding and aggregation.** Proteins fold to the native stave by forming intramolecular interactions (green). Surpassing the kinetically trapped conformations may be accelerated by chaperones. Intermolecular aggregation results in the formation of amorphous aggregates, toxic oligomers or ordered amyloid fibrils (red) and is normally prevented by molecular chaperones. Scheme adapted from Balchin et al. 2016.

An integrated network comprising molecular chaperones and the protein degradation machinery, denominated as protein quality control system (PQC), is responsible for a constant surveillance of protein homeostasis (proteostasis). The PQC controls maintenance of protein structures, prevents aggregation and eliminates misfolded and damaged proteins and polypeptide chains. Accessory factors of the PQC regulate the activity of chaperones and proteases or provide communication between the various components (Dobson 2003; Gregersen et al. 2006; Hartl et al. 2011). The capacity of the proteostasis network deteriorates during aging, facilitating the development of neurodegeneration and other chronic diseases associated with protein aggregation.

I.4.2. Conformational Disorders

Folding is highly dependent on many weak, noncovalent interactions, involving amino acid contacts, both close and distant in sequence (Brockwell and Radford 2007). Hydrophobic forces drive the burial of nonpolar amino acids within the core (Dinner et al. 2000). Thus, the stability of the folded protein structure is rather fragile and subtle changes due to mutation may disturb the balance (Gershenson et al. 2014). Missense mutations resulting in amino acid substitutions may change the folding process leading to the possible formation of new local free energy minima or to the generation of an energetic trap. Partially folded or misfolded proteins expose hydrophobic amino acids, facilitating aggregation. Importantly, gene variations may lead to formation of a new, low global free-energy minimum resulting in a different but stable structure of the protein, which may be prone to aggregation. The fact that protein aggregates can be extremely stable, places them into the deepest valleys of the energy landscape (Dobson 2003; Hartl et al. 2011) (Figure I-4).

Aberrant proteins, which are prematurely eliminated by the PQC, usually give origin to loss-of-function pathogenesis, and result in protein/enzyme activity deficiency, as in many inherited metabolic disorders (IMD) presenting as recessive conditions. In contrast, aberrant proteins which are not eliminated but accumulated and exhibit cellular toxicity result in gain-of-function pathogenesis. The effect of toxic amyloid polypeptides or accumulated and aggregated misfolded proteins often leads to dominant diseases, such as Parkinson, Alzheimer, Huntington and Creutzfeldt-Jakob diseases. Despite a large diversity of protein misfolding effects and a high number of very different defects, the whole group of diseases associated with protein folding can be called conformational disorders (Stefani 2004; Gidalevitz et al. 2010).

I.4.3. Treatment Strategies for Misfolding Disorders

Increasing knowledge on the PQC and proteostasis network led to the general belief that the effect of a missense mutation compromising the normal balance between protein folding, trafficking and degradation should be correctable by restoring proteostasis. New promising therapeutic strategies are lately being developed, based on the capacity of small molecular weight (SMW) compounds to regulate proteostasis (Arakawa et al. 2006; Mu et al. 2008; Powers et al. 2009; Yue 2016).

Chemical chaperones are xenobiotic agents effective in restoring the misfolded unstable aberrant proteins, thereby being able to recover the protein function. The protein stabilization by chemical chaperones is usually non-specific, whereas pharmacological chaperones bind specifically to their target protein. Besides, therapeutically active small molecules can act at different cellular levels, including read-through agents, proteostasis regulators, substrate inhibitors, and autophagy inducers (Matalonga et al. 2017). Several authors suggested a simultaneous use of proteostasis regulators (PR) and pharmacological chaperones (PC) to exploit their synergistic effect (Mu et al. 2008; Wang et al. 2014; Gámez et al. 2018). The PC and PR co-administration may enhance the treatment effectivity by combining the properties of a stress-responsive signalling pathway activator and stabilization of the misfolded protein.

So far, several pharmacological chaperone therapies are already available or in clinical trials for various IMD and have been reviewed by Gámez and collaborators (Gámez et al. 2018). Recently, the first proteostasis modulator compounds were approved as therapeutics that specifically target the folding and trafficking defect of mutant cystic fibrosis transmembrane conductance regulator (Veit et al. 2016), and for transthyretin amyloidosis, a fatal aggregation disease characterized by progressive neuropathy and cardiomyopathy (Baranczak and Kelly 2016).

One of the most remarkable examples is the use of chaperone therapeutics in phenylketonuria (PKU), a disorder caused by deficiency of human phenylalanine hydroxylase (PAH). Curiously, PKU was the first IMD to be partially treatable by early dietary restriction. This matter, in the decade of 1950's, raised polemics and ethical issues concerning the general approach to the treatment of inherited neurodegenerative diseases and apprehensions about preserving and spreading the deleterious mutations through the human gene pool (Sinclair 1962). PKU was also one of the first disorders classified as a misfolding disease (Leandro et al. 2011) and one of the first IMD to obtain an approved oral pharmacological treatment (Muntau et al. 2014). Sapropterin dihydrochloride is a synthetic analog of the natural cofactor of PAH, tetrahydrobiopterin (BH_4). Acting as a pharmacological chaperone, sapropterin dihydrochloride has the capacity to reduce blood phenylalanine concentration in BH_4-responsive patients, and a substantial number of PKU patients can benefit from this treatment. Candidates are carefully selected by sapropterin dihydrochloride response testing. The exact percentual responsiveness is still under prospective studies (Muntau et al. 2019). Finally, yet importantly, the human

medicines committee of the European Medicines Agency (EMA) has newly authorized a formulation of a pegylated recombinant phenylalanine ammonia lyase (pegvaliase) for PAH deficient patients with excessive levels of phenylalanine in the blood (EMA/CHMP/143328/2019, www.ema.europa.eu). By eliminating the accumulated phenylalanine, pegvaliase can partially relieve the symptoms of the disease. However, its inability to produce tyrosine does not solve the pathophysiological consequences of tyrosine depletion in PKU patients. The profound knowledge of the disorder and the detailed comprehension of the protein structure and function, together with the rich offer of distinct prospective therapeutic approaches, either at the level of dietary restrictions, substrate control, protein stabilization, or an interactive combination of several of them makes PKU a model for successful control of inherited metabolic diseases.

I.4.4. A Confirmed Case of PDCD Recovery: Role of Small Molecular Weight Compounds

A particular case of PDC deficiency (PDCD) with mild neurological involvement was reported by our group (Silva et al. 2009). At the time of diagnosis, the six-year-old male patient presented a mild clinical phenotype with ataxia, muscle weakness and global development delay. Biochemical analysis was consistent with a PDCD: patient's lymphocytes exhibited low PDC activity (~11% of control) and the protein levels of PDC-E1α subunit were undetectable by immunoblotting analysis. The result of the molecular genetic analysis was consistent with the diagnosis since the patient carried the c.757A>G transition in *PDHA1* gene, originating the p.R253G PDC-E1α variant.

Following a period of continuous arginine aspartate (Asparten®) intake, clinical signs and symptoms clearly reverted, together with a complete normalization of enzyme activity and immunoblotting profile. Nevertheless, symptomatology quickly returned when interrupting the treatment (Figure I-5). In the following years, the patient proceeded with a regular arginine aspartate administration and currently remains without any clinical signs of PDCD, maintaining normal physical and intellectual activities.

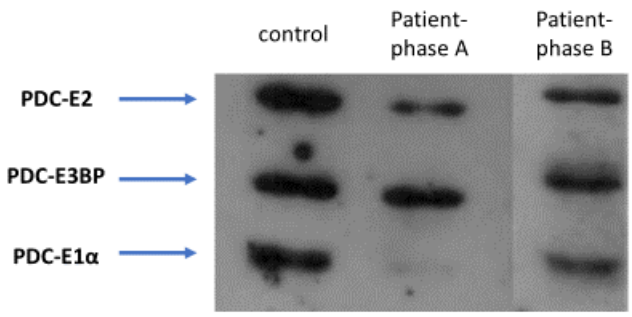

Figure I-5 **PDC-E1α protein profile** comparing lymphocyte homogenates from control, patient at the time of diagnosis (phase A) and one month after starting L-arginine-L-aspartate supplementation (phase B) (Silva et al. 2009)

Successful recovery of a set of clinical and biochemical symptoms in this PDCD patient is raising an intriguing question about the detailed molecular impact of arginine aspartate on PDC. On one hand, studies on patients suffering from peroxisome biogenesis disorder also suggested a beneficial effect of arginine on peroxisomal function (Berendse et al. 2013; Sorlin et al. 2016). On the other, the apparent rescuing effect of arginine upon the cytosolic galactose-1-phosphate uridylyltransferase (GALT) observed *in vitro* for the severe p.Q188R variant (Coelho et al. 2015) did not correspond to the absence of the clinical response to arginine aspartate supplementation in patients homozygous for this mutation (Haskovic et al. 2018). Unravelling the potential effect of arginine as a PDC-E1 stabilizer and putative rescuer of the enzymatic function is one of our aims in this work.

REFERENCES

Ævarsson A, Seger K, Turley S, et al (1999) Crystal structure of 2-oxoisovalerate and dehydrogenase and the architecture of 2-oxo acid dehydrogenase multienzyme complexes. Nat Struct Biol 6:785–792. https://doi.org/10.1038/11563

Arakawa T, Ejima D, Kita Y, Tsumoto K (2006) Small molecule pharmacological chaperones: From thermodynamic stabilization to pharmaceutical drugs. Biochim Biophys Acta 1764:1677–87. https://doi.org/10.1016/j.bbapap.2006.08.012

Aral B, Benelli C, Ait-Ghezala G, et al (1997) Mutations in PDX1, the human lipoyl-containing component X of the pyruvate dehydrogenase-complex gene on chromosome 11p1, in congenital lactic acidosis. Am J Hum Genet 61:1318–1326. https://doi.org/10.1086/301653

Arjunan P, Nemeria N, Brunskill A, et al (2002) Structure of the Pyruvate Dehydrogenase Multienzyme Complex E1 Component from *Escherichia coli* at 1.85 Å Resolution † , ‡. Biochemistry 41:5213–5221. https://doi.org/10.1021/bi0118557

Balchin D, Hayer-Hartl M, Hartl FU (2016) In vivo aspects of protein folding and quality control. Science 353:aac4354. https://doi.org/10.1126/science.aac4354

Baranczak A, Kelly JW (2016) A current pharmacologic agent versus the promise of next generation therapeutics to ameliorate protein misfolding and/or aggregation diseases. Curr. Opin. Chem. Biol. 32:10–21

Berendse K, Ebberink MS, Ijlst L, et al (2013) Arginine improves peroxisome functioning in cells from patients with a mild peroxisome biogenesis disorder. Orphanet J Rare Dis 8:138. https://doi.org/10.1186/1750-1172-8-138

Berg A, Westphal AH, Bosma HJ, De Kok A (1998) Kinetics and specificity of reductive acylation of wild-type and mutated lipoyl domains of 2-oxo-acid dehydrogenase complexes from Azotobacter vinelandii. Eur J Biochem 252:45–50. https://doi.org/10.1046/j.1432-1327.1998.2520045.x

Blass JP, Avigan J, Uhlendorf BW (1970) A defect in pyruvate decarboxylase in a child with an intermittent movement disorder. J Clin Invest 49:423–432. https://doi.org/10.1172/JCI106251

Boukouris AE, Zervopoulos SD, Michelakis ED (2016) Metabolic Enzymes Moonlighting in the Nucleus: Metabolic Regulation of Gene Transcription. Trends Biochem. Sci. 41:712–730

Bowker-Kinley MM, Davis WI, Wu P, et al (1998) Evidence for existence of tissue-specific regulation of the mammalian pyruvate dehydrogenase complex. Biochem J 329 (Pt 1):191–6. https://doi.org/10.1042/bj3290191

Brautigam CA, Wynn RM, Chuang JL, et al (2011) Structural and thermodynamic basis for weak interactions between dihydrolipoamide dehydrogenase and subunit-binding domain of the branched-chain α-ketoacid dehydrogenase complex. J Biol Chem 286:23476–23488. https://doi.org/10.1074/jbc.M110.202960

Brautigam CA, Wynn RM, Chuang JL, et al (2006) Structural insight into interactions between dihydrolipoamide dehydrogenase (E3) and E3 binding protein of human pyruvate dehydrogenase complex. Structure 14:611–621. https://doi.org/10.1016/j.str.2006.01.001

Brautigam CA, Wynn RM, Chuang JL, Chuang DT (2009) Subunit and catalytic component stoichiometries of an in vitro reconstituted human pyruvate dehydrogenase complex. J Biol Chem 284:13086–98. https://doi.org/10.1074/jbc.M806563200

Bricker DK, Taylor EB, Schell JC, et al (2012) A mitochondrial pyruvate carrier required for pyruvate uptake in yeast, Drosophila, and humans. Science 337:96–100. https://doi.org/10.1126/science.1218099

Brockwell DJ, Radford SE (2007) Intermediates: ubiquitous species on folding energy landscapes? Curr. Opin. Struct. Biol. 17:30–37

Brown G (2014) Defects of thiamine transport and metabolism. J Inherit Metab Dis 37:577–585. https://doi.org/10.1007/s10545-014-9712-9

Brown GK, Otero LJ, LeGris M, Brown RM (1994) Pyruvate dehydrogenase deficiency. J Med Genet 31:875–879. https://doi.org/10.1136/jmg.31.11.875

Brown RM, Head RA, Boubriak II, et al (2004) Mutations in the gene for the E1β subunit: A novel cause of pyruvate dehydrogenase deficiency. Hum Genet 115:123–127. https://doi.org/10.1007/s00439-004-1124-8

Byron O, Lindsay JG (2017) The pyruvate dehydrogenase complex and related assemblies in health and disease. In: Sub-Cellular Biochemistry. pp 523–550

Cameron JM, Janer A, Levandovskiy V, et al (2011) Mutations in iron-sulfur cluster scaffold genes NFU1 and BOLA3 cause a fatal deficiency of multiple respiratory chain and 2-oxoacid dehydrogenase enzymes. Am J Hum Genet 89:486–495. https://doi.org/10.1016/j.ajhg.2011.08.011

Castiglioni C, Verrigni D, Okuma C, et al (2015) Pyruvate dehydrogenase deficiency presenting as isolated paroxysmal exercise induced dystonia successfully reversed with thiamine supplementation. Case report and mini-review. Eur. J. Paediatr. Neurol. 19:497–503

Cate RL, Roche TE, Davis LC (1980) Rapid intersite transfer of acetyl groups and movement of pyruvate dehydrogenase component in the kidney pyruvate dehydrogenase complex. J Biol Chem 255:7556–62

Ciszak EM, Korotchkina LG, Dominiak PM, et al (2003) Structural basis for flip-flop action of thiamin pyrophosphate-dependent enzymes revealed by human pyruvate dehydrogenase. J Biol Chem 278:21240–21246. https://doi.org/10.1074/jbc.M300339200

Ciszak EM, Makal A, Hong YS, et al (2006) How dihydrolipoamide dehydrogenase-binding protein binds dihydrolipoamide dehydrogenase in the human pyruvate dehydrogenase complex. J Biol Chem 281:648–655. https://doi.org/10.1074/jbc.M507850200

Coelho AI, Trabuco M, Silva MJ, et al (2015) Arginine functionally improves clinically relevant human galactose-1-phosphate uridylyltransferase (GALT) variants expressed in a prokaryotic model. In: JIMD Reports. Wiley-Blackwell, pp 1–6

Dahl H-HM, Brown RM, Hutchison WM, et al (1990) A testis-specific form of the human pyruvate dehydrogenase E1α subunit is coded for by an intronless gene on chromosome 4. Genomics 8:225–232. https://doi.org/10.1016/0888-7543(90)90275-Y

Dahl HHM (1995) Pyruvate dehydrogenase E1 alpha deficiency: males and females differ yet again. Am J Hum Genet 56:553–7

de Boer VCJ, Houten SM (2014) A Mitochondrial Expatriate: Nuclear Pyruvate Dehydrogenase. Cell 158:9–10. https://doi.org/10.1016/J.CELL.2014.06.018

De Marcucci O, Lindsay JG (1985) Component X: An immunologically distinct polypeptide associated with mammalian pyruvate dehydrogenase multi-enzyme complex. Eur J Biochem 149:641–648. https://doi.org/10.1111/j.1432-1033.1985.tb08972.x

Di Rocco M, Doria Lamba L, Minniti G, et al (2000) Outcome of thiamine treatment in a child with Leigh disease due to thiamine-responsive pyruvate dehydrogenase deficiency. Eur J Paediatr Neurol 4:115–117. https://doi.org/10.1053/ejpn.2000.0278

Dinner AR, Šalib A, Smitha LJ, et al (2000) Understanding protein folding via free-energy surfaces from theory and experiment. Trends Biochem. Sci. 25:331–339

Dobson CM (2003) Protein folding and misfolding. Nature 426:884–90. https://doi.org/10.1038/nature02261

Drakulic S, Rai J, Petersen SV, et al (2018) Folding and assembly defects of pyruvate dehydrogenase deficiency-related variants in the E1α subunit of the pyruvate dehydrogenase complex. Cell Mol Life Sci 75:3009–3026. https://doi.org/10.1007/s00018-018-2775-2

Dudek J, Rehling P, van der Laan M (2013) Mitochondrial protein import: Common principles and physiological networks. Biochim Biophys Acta - Mol Cell Res 1833:274–285. https://doi.org/10.1016/J.BBAMCR.2012.05.028

El-Gharbawy AH, Boney A, Young SP, Kishnani PS (2011) Follow-up of a child with pyruvate dehydrogenase deficiency on a less restrictive ketogenic diet. Mol Genet Metab 102:214–215. https://doi.org/10.1016/j.ymgme.2010.11.001

Ellis RJ, Minton AP (2006) Protein aggregation in crowded environments. Biol Chem 387:. https://doi.org/10.1515/BC.2006.064

Endo H, Hasegawa K, Narisawa K, et al (1989) Defective gene in lactic acidosis: Abnormal pyruvate dehydrogenase E1 α-subunit caused by a frame shift. Am J Hum Genet 44:358–364

Fan J, Shan C, Kang H-B, et al (2014) Tyr Phosphorylation of PDP1 Toggles Recruitment between ACAT1 and SIRT3 to Regulate the Pyruvate Dehydrogenase Complex. Mol Cell 53:534–548. https://doi.org/10.1016/J.MOLCEL.2013.12.026

Ferriero R, Brunetti-Pierri N (2013) Phenylbutyrate increases activity of pyruvate dehydrogenase complex. Oncotarget 4:804–805

Fouque F, Brivet M, Boutron A, et al (2003) Differential effect of DCA treatment on the pyruvate dehydrogenase complex in patients with severe PDHC deficiency. Pediatr Res 53:793–799. https://doi.org/10.1203/01.PDR.0000057987.46622.64

Fox TD, Lukins HB, Nagley P, et al (2012) Mitochondrial protein synthesis, import, and assembly. Genetics 192:1203–34. https://doi.org/10.1534/genetics.112.141267

Gámez A, Yuste-Checa P, Brasil S, et al (2018) Protein misfolding diseases: Prospects of pharmacological treatment. Clin. Genet. 93:450–458

Gershenson A, Gierasch LM, Pastore A, Radford SE (2014) Energy landscapes of functional proteins are inherently risky. Nat. Chem. Biol. 10:884–891

Gidalevitz T, Kikis EA, Morimoto RI (2010) A cellular perspective on conformational disease: the role of genetic background and proteostasis networks. Curr Opin Struct Biol 20:23–32. https://doi.org/10.1016/j.sbi.2009.11.001

Golias T, Kery M, Radenkovic S, Papandreou I (2019) Microenvironmental control of glucose metabolism in tumors by regulation of pyruvate dehydrogenase. Int. J. Cancer 144:674–686

Gray LR, Tompkins SC, Taylor EB (2014) Regulation of pyruvate metabolism and human disease. Cell Mol Life Sci 71:2577–2604. https://doi.org/10.1007/s00018-013-1539-2

Gregersen N, Bross P, Vang S, Christensen JH (2006) Protein misfolding and human disease. Annu Rev Genomics Hum Genet 7:103–24. https://doi.org/10.1146/annurev.genom.7.080505.115737

Gudi R, Melissa MB-K, Kedishvili NY, et al (1995) Diversity of the Pyruvate Dehydrogenase Kinase Gene Family in Humans. J Biol Chem 270:28989–28994

Guevara EL, Yang L, Birkaya B, et al (2017) Global view of cognate kinase activation by the human pyruvate dehydrogenase complex. Sci Rep 7:42760. https://doi.org/10.1038/srep42760

Guo J, Hezaveh S, Tatur J, et al (2017) Reengineering of the human pyruvate dehydrogenase complex: from disintegration to highly active agglomerates. Biochem J 474:865–875. https://doi.org/10.1042/BCJ20160916

Hartl FU (1996) Molecular chaperones in cellular protein folding. Nature 381:571–580

Hartl FU, Bracher A, Hayer-Hartl M (2011) Molecular chaperones in protein folding and proteostasis. Nature 475:324–32. https://doi.org/10.1038/nature10317

Haskovic M, Derks B, Van der Ploeg L, et al (2018) Arginine does not rescue p.Q188R mutation deleterious effect in classic galactosemia. Orphanet J Rare Dis 13:. https://doi.org/10.1186/s13023-018-0954-8

Head RA, Brown RM, Zolkipli Z, et al (2005) Clinical and genetic spectrum of pyruvate dehydrogenase deficiency: Dihydrolipoamide acetyltransferase (E2) deficiency. Ann Neurol 58:234–241. https://doi.org/10.1002/ana.20550

Hengeveld A, Kok A (2002) Structural Basis of the Dysfunctioning of Human 2-Oxo Acid Dehydrogenase Complexes. Curr Med Chem 9:499–520. https://doi.org/10.2174/0929867023370996

Herzig S, Raemy E, Montessuit S, et al (2012) Identification and Functional Expression of the Mitochondrial Pyruvate Carrier. Science 337:93–96. https://doi.org/10.1126/science.1218530

Hiromasa Y, Fujisawa T, Aso Y, Roche TE (2004) Organization of the cores of the mammalian pyruvate dehydrogenase complex formed by E2 and E2 plus the E3-binding protein and their capacities to bind the E1 and E3 components. J Biol Chem 279:6921–33. https://doi.org/10.1074/jbc.M308172200

Huang B, Gudi R, Wu P, et al (1998) Isoenzymes of Pyruvate Dehydrogenase Phosphatase: DNA-derived amino acid sequences, expression, and regulation. J Biol Chem 273:17680–17688

Huss JM, Kelly DP (2005) Mitochondrial energy metabolism in heart failure: a question of balance. J Clin Invest 115:547–55. https://doi.org/10.1172/JCI24405

Imbard A, Boutron A, Vequaud C, et al (2011) Molecular characterization of 82 patients with pyruvate dehydrogenase complex deficiency. Structural implications of novel amino acid substitutions in E1 protein. Mol Genet Metab 104:507–16. https://doi.org/10.1016/j.ymgme.2011.08.008

Jiang J, Baiesc FL, Hiromasa Y, et al (2018) Atomic Structure of the E2 Inner Core of Human Pyruvate Dehydrogenase Complex. Biochemistry 57:2325–2334. https://doi.org/10.1021/acs.biochem.8b00357

Jilka JM, Rahmatullah M, Kazemi M, Roche TE (1986) Properties of a newly characterized protein of the bovine kidney pyruvate dehydrogenase complex. J Biol Chem 261:1858–67

Kaplon J, Zheng L, Meissl K, et al (2013) A key role for mitochondrial gatekeeper pyruvate dehydrogenase in oncogene-induced senescence. Nature 498:109–112. https://doi.org/10.1038/nature12154

Kato M, Wynn RM, Chuang JL, et al (2008) Structural basis for inactivation of the human pyruvate dehydrogenase complex by phosphorylation: role of disordered phosphorylation loops. Structure 16:1849–59. https://doi.org/10.1016/j.str.2008.10.010

Kolobova E, Tuganova A, Boulatnikov I, Popov KM (2001) Regulation of pyruvate dehydrogenase activity through phosphorylation at multiple sites. Biochem J 358:69–77. https://doi.org/10.1042/0264-6021:3580069

Kornberg, L. H (1966) Anaplerotic sequences and their role in metabolism. Essays Biochem 2:1–31

Korotchkina LG, Patel MS (2001a) Probing the Mechanism of Inactivation of Human Pyruvate Dehydrogenase by Phosphorylation of Three Sites. J Biol Chem 276:5731–5738. https://doi.org/10.1074/jbc.M007558200

Korotchkina LG, Patel MS (2001b) Site Specificity of Four Pyruvate Dehydrogenase Kinase Isoenzymes toward the Three Phosphorylation Sites of Human Pyruvate Dehydrogenase. J Biol Chem 276:37223–37229. https://doi.org/10.1074/jbc.M103069200

Krebs HA, Johnson WA (1937) The role of citric acid in intermediate metabolism in animal tissues. Enzymologia 4:148–156

Lawson JE, Park SH, Mattison AR, et al (1997) Cloning, expression, and properties of the regulatory subunit of bovine pyruvate dehydrogenase phosphatase. J Biol Chem 272:31625–31629. https://doi.org/10.1074/jbc.272.50.31625

Leandro J, Simonsen N, Saraste J, et al (2011) Phenylketonuria as a protein misfolding disease: The mutation pG46S in phenylalanine hydroxylase promotes self-association and fibril formation. Biochim Biophys Acta - Mol Basis Dis 1812:106–120. https://doi.org/10.1016/j.bbadis.2010.09.015

Linn TC, Pettit FH, Reed LJ (1969) Alpha-keto acid dehydrogenase complexes. X. Regulation of the activity of the pyruvate dehydrogenase complex from beef kidney mitochondria by

phosphorylation and dephosphorylation. Proc Natl Acad Sci U S A 62:234–41. https://doi.org/10.1073/pnas.62.1.234

Liu TC, Kim H, Arizmendi C, et al (1993) Identification of two missense mutations in a dihydrolipoamide dehydrogenase-deficient patient. In: Proceedings of the National Academy of Sciences of the United States of America. National Academy of Sciences, pp 5186–5190

Maeng CY, Yazdi MA, Reed LJ (1996) Stoichiometry of binding of mature and truncated forms of the dihydrolipoamide dehydrogenase-binding protein to the dihydrolipoamide acetyltransferase core of the pyruvate dehydrogenase complex from Saccharomyces cerevisiae. Biochemistry 35:5879–5882. https://doi.org/10.1021/BI9600254

Maj MC, MacKay N, Levandovskiy V, et al (2005) Pyruvate dehydrogenase phosphatase deficiency: Identification of the first mutation in two brothers and restoration of activity by protein complementation. J Clin Endocrinol Metab 90:4101–4107. https://doi.org/10.1210/jc.2005-0123

Mannan AASR, Sharma MC, Shrivastava P, et al (2004) Leigh's syndrome. Indian J Pediatr 71:1029–33

Marrott NL, Marshall JJT, Svergun DI, et al (2014) Why are the 2-oxoacid dehydrogenase complexes so large? Generation of an active trimeric complex. Biochem J 463:405–412. https://doi.org/10.1042/BJ20140359

Marsac C, Stansbie D, Bonne G, et al (1993) Defect in the lipoyl-bearing protein X subunit of the pyruvate dehydrogenase complex in two patients with encephalomyelopathy. J Pediatr 123:915–920. https://doi.org/10.1016/S0022-3476(05)80387-7

Matalonga L, Gort L, Ribes A (2017) Small molecules as therapeutic agents for inborn errors of metabolism. J. Inherit. Metab. Dis. 40:177–193

Mathias RA, Greco TM, Oberstein A, et al (2014) Sirtuin 4 Is a Lipoamidase Regulating Pyruvate Dehydrogenase Complex Activity. Cell 159:1615–1625. https://doi.org/10.1016/j.cell.2014.11.046

Mayr JA, Feichtinger RG, Tort F, et al (2014) Lipoic acid biosynthesis defects. In: Journal of Inherited Metabolic Disease. John Wiley & Sons, Ltd, pp 553–563

Mayr JA, Freisinger P, Schlachter K, et al (2011a) Thiamine pyrophosphokinase deficiency in encephalopathic children with defects in the pyruvate oxidation pathway. Am J Hum Genet 89:806–812. https://doi.org/10.1016/j.ajhg.2011.11.007

Mayr JA, Zimmermann FA, Fauth C, et al (2011b) Lipoic acid synthetase deficiency causes neonatal-onset epilepsy, defective mitochondrial energy metabolism, and glycine elevation. Am J Hum Genet 89:792–797. https://doi.org/10.1016/j.ajhg.2011.11.011

Milne JLS (2002) Molecular architecture and mechanism of an icosahedral pyruvate dehydrogenase complex: a multifunctional catalytic machine. EMBO J 21:5587–5598. https://doi.org/10.1093/emboj/cdf574

Milne JLS, Shi D, Rosenthal PB, et al (2002) Molecular architecture and mechanism of an icosahedral pyruvate dehydrogenase complex: A multifunctional catalytic machine. EMBO J 21:5587–5598. https://doi.org/10.1093/emboj/cdf574

Mochel F, Knight MA, Tong W-H, et al (2008) Splice mutation in the iron-sulfur cluster scaffold protein ISCU causes myopathy with exercise intolerance. Am J Hum Genet 82:652–60. https://doi.org/10.1016/j.ajhg.2007.12.012

Morgenstern M, Stiller SB, Lübbert P, et al (2017) Definition of a High-Confidence Mitochondrial Proteome at Quantitative Scale. Cell Rep 19:2836–2852. https://doi.org/10.1016/j.celrep.2017.06.014

Mu T-W, Ong DST, Wang Y-J, et al (2008) Chemical and biological approaches synergize to ameliorate protein-folding diseases. Cell 134:769–81. https://doi.org/10.1016/j.cell.2008.06.037

Muntau AC, Adams DJ, Bélanger-Quintana A, et al (2019) International best practice for the evaluation of responsiveness to sapropterin dihydrochloride in patients with phenylketonuria. Mol. Genet. Metab. 127:1–11

Muntau AC, Leandro J, Staudigl M, et al (2014) Innovative strategies to treat protein misfolding in inborn errors of metabolism: pharmacological chaperones and proteostasis regulators. J Inherit Metab Dis. https://doi.org/10.1007/s10545-014-9701-z

Naia L, Cunha-Oliveira T, Rodrigues J, et al (2017) Histone deacetylase inhibitors protect against pyruvate dehydrogenase dysfunction in huntington's disease. J Neurosci 37:2776–2794. https://doi.org/10.1523/JNEUROSCI.2006-14.2016

Naito E, Ito M, Yokota I, et al (2002) Thiamine-responsive pyruvate dehydrogenase deficiency in two patients caused by a point mutation (F205L and L216F) within the thiamine pyrophosphate binding region. Biochim Biophys Acta - Mol Basis Dis 1588:79–84. https://doi.org/10.1016/S0925-4439(02)00142-4

Navarro-Sastre A, Tort F, Stehling O, et al (2011) A Fatal Mitochondrial Disease Is Associated with Defective NFU1 Function in the Maturation of a Subset of Mitochondrial Fe-S Proteins. Am J Hum Genet 89:656. https://doi.org/10.1016/J.AJHG.2011.10.005

Odièvre M-H, Chretien D, Munnich A, et al (2005) A novel mutation in the dihydrolipoamide dehydrogenase E3 subunit gene (DLD) resulting in an atypical form of α-ketoglutarate dehydrogenase deficiency. Hum Mutat 25:323–324. https://doi.org/10.1002/humu.9319

Owen OE, Kalhan SC, Hanson RW (2002) The key role of anaplerosis and cataplerosis for citric acid cycle function. J Biol Chem 277:30409–12. https://doi.org/10.1074/jbc.R200006200

Pastoris O, Savasta S, Foppa P, et al (1996) Pyruvate dehydrogenase deficiency in a child responsive to thiamine treatment. Acta Paediatr Int J Paediatr 85:625–628. https://doi.org/10.1111/j.1651-2227.1996.tb14104.x

Patel KP, O'Brien TW, Subramony SH, et al (2012) The spectrum of pyruvate dehydrogenase complex deficiency: Clinical, biochemical and genetic features in 371 patients. Mol Genet Metab 106:385–394. https://doi.org/10.1016/j.ymgme.2012.03.017

Patel MS, Korotchkina LG (2006) Regulation of the pyruvate dehydrogenase complex. In: Biochemical Society Transactions. pp 217–222

Patel MS, Roche TE (1990) Molecular biology and biochemistry of pyruvate dehydrogenase complexes. FASEB J 4:3224–33. https://doi.org/10.1096/fasebj.4.14.2227213

Perham RN (2000) Swinging Arms and Swinging Domains in Multifunctional Enzymes: Catalytic Machines for Multistep Reactions. Annu Rev Biochem 69:961–1004. https://doi.org/10.1146/annurev.biochem.69.1.961

Pinheiro A, Silva MJ, Pavlu-Pereira H, et al (2016a) Complex genetic findings in a female patient with pyruvate dehydrogenase complex deficiency: Null mutations in the PDHX gene associated with unusual expression of the testis-specific PDHA2 gene in her somatic cells. Gene 591:417–424. https://doi.org/10.1016/j.gene.2016.06.041

Pinheiro A, Silva MJ, Pavlu-Pereira H, et al (2016b) Data supporting the co-expression of PDHA1 gene and of its paralogue PDHA2 in somatic cells of a family. Data in Brief 9:68–77. https://doi.org/10.1016/j.dib.2016.08.029

Pithukpakorn M (2005) Disorders of pyruvate metabolism and the tricarboxylic acid cycle. Mol Genet Metab 85:243–6

Porporato PE, Filigheddu N, Pedro JMB-S, et al (2018) Mitochondrial metabolism and cancer. Cell Res 28:265–280. https://doi.org/10.1038/cr.2017.155

Powers ET, Morimoto RI, Dillin A, et al (2009) Biological and Chemical Approaches to Diseases of Proteostasis Deficiency. Annu Rev Biochem 78:959–991. https://doi.org/10.1146/annurev.biochem.052308.114844

Reed LJ (2001) A trail of research from lipoic acid to alpha-keto acid dehydrogenase complexes. J Biol Chem 276:38329–36. https://doi.org/10.1074/jbc.R100026200

Reed LJ, Oliver RM (1982) Structure-Function Relationships in Pyruvate and α-Ketoglutarate Dehydrogenase Complexes. In: Advances in experimental medicine and biology. pp 231–241

Rowles J, Scherer SW, Xi T, et al (1996) Cloning and Characterization of PDK4 on 7q21.3 Encoding a Fourth Pyruvate Dehydrogenase Kinase Isoenzyme in Human. J Biol Chem 271:22376–22382. https://doi.org/10.1074/jbc.271.37.22376

Sanderson SJ, Miller C, Lindsay JG (1996) Stoichiometry, organisation and catalytic function of protein X of the pyruvate dehydrogenase complex from bovine heart. Eur J Biochem 236:68–77. https://doi.org/10.1111/j.1432-1033.1996.00068.x

Seifert F, Ciszak E, Korotchkina L, et al (2007) Phosphorylation of serine 264 impedes active site accessibility in the E1 component of the human pyruvate dehydrogenase multienzyme complex. Biochemistry 46:6277–6287. https://doi.org/10.1021/bi700083z

Silva MJ, Pinheiro A, Eusébio F, et al (2009) Pyruvate dehydrogenase deficiency: identification of a novel mutation in the PDHA1 gene which responds to amino acid supplementation. Eur J Pediatr 168:17–22. https://doi.org/10.1007/s00431-008-0700-7

Sinclair HM (1962) Historical aspects of inborn errors of metabolism. Proceedings of the Nutrition Society 21: 1-12

Smith GM, Gallo G (2018) The role of mitochondria in axon development and regeneration. Dev Neurobiol 78:221–237. https://doi.org/10.1002/dneu.22546

Smolle M, Prior AE, Brown AE, et al (2006) A new level of architectural complexity in the human pyruvate dehydrogenase complex. J Biol Chem 281:19772–19780. https://doi.org/10.1074/jbc.M601140200

Sorlin A, Briand G, Cheillan D, et al (2016) Effect of l -Arginine in One Patient with Peroxisome Biogenesis Disorder due to PEX12 Deficiency. Neuropediatrics 47:179–181. https://doi.org/10.1055/s-0036-1578798

Sperl W, Fleuren L, Freisinger P, et al (2015) The spectrum of pyruvate oxidation defects in the diagnosis of mitochondrial disorders. J Inherit Metab Dis 38:391–403. https://doi.org/10.1007/s10545-014-9787-3

Stacpoole PW (2017) Therapeutic Targeting of the Pyruvate Dehydrogenase Complex/Pyruvate Dehydrogenase Kinase (PDC/PDK) Axis in Cancer. J Natl Cancer Inst 109:. https://doi.org/10.1093/jnci/djx071

Stefani M (2004) Protein misfolding and aggregation: new examples in medicine and biology of the dark side of the protein world. Biochim Biophys Acta 1739:5–25. https://doi.org/10.1016/j.bbadis.2004.08.004

Strumiło S (2005) Short-term regulation of the mammalian pyruvate dehydrogenase complex. Acta Biochim Pol 52:759–64

Sugden MC, Holness MJ (2003) Recent advances in mechanisms regulating glucose oxidation at the level of the pyruvate dehydrogenase complex by PDKs. Am J Physiol Endocrinol Metab 284:E855-62. https://doi.org/10.1152/ajpendo.00526.2002

Sumegi B, Liposits Z, Inman L, et al (1987) Electron microscopic study on the size of pyruvate dehydrogenase complex in situ. Eur J Biochem 169:223–230. https://doi.org/10.1111/j.1432-1033.1987.tb13601.x

Sutendra G, Kinnaird A, Dromparis P, et al (2014) A nuclear pyruvate dehydrogenase complex is important for the generation of Acetyl-CoA and histone acetylation. Cell 158:84–97. https://doi.org/10.1016/j.cell.2014.04.046

Szabo E, Wilk P, Nagy B, et al (2019) Underlying molecular alterations in human dihydrolipoamide dehydrogenase deficiency revealed by structural analyses of disease-causing enzyme variants. Hum Mol Genet. https://doi.org/10.1093/hmg/ddz177

Tzameli I (2012) The evolving role of mitochondria in metabolism. Trends Endocrinol Metab 23:417–9. https://doi.org/10.1016/j.tem.2012.07.008

Vander Heiden MG, Cantley LC, Thompson CB (2009) Understanding the warburg effect: The metabolic requirements of cell proliferation. Science (80-.). 324:1029–1033

Veit G, Avramescu RG, Chiang AN, et al (2016) From CFTR biology toward combinatorial pharmacotherapy: Expanded classification of cystic fibrosis mutations. Mol Biol Cell 27:424–433. https://doi.org/10.1091/mbc.E14-04-0935

Vijayakrishnan S, Callow P, Nutley MA, et al (2011) Variation in the organization and subunit composition of the mammalian pyruvate dehydrogenase complex E2/E3BP core assembly. Biochem J 437:565–74. https://doi.org/10.1042/BJ20101784

Vijayakrishnan S, Kelly SM, Gilbert RJC, et al (2010) Solution structure and characterisation of the human pyruvate dehydrogenase complex core assembly. J Mol Biol 399:71–93. https://doi.org/10.1016/j.jmb.2010.03.043

von Heijne G, Steppuhn J, Hermann RG (1989) Domain structure of mitochondrial and chloroplast targeting peptides. Eur J Biochem 180:535–545. https://doi.org/10.1111/j.1432-1033.1989.tb14679.x

Wang YJ, Di XJ, Mu TW (2014) Using pharmacological chaperones to restore proteostasis. Pharmacol Res 83:3–9. https://doi.org/10.1016/j.phrs.2014.04.002

Wexler ID, Hemalatha SG, McConnell J, et al (1997) Outcome of pyruvate dehydrogenase deficiency treated with ketogenic diets. Studies in patients with identical mutations. Neurology 49:1655–61. https://doi.org/10.1212/wnl.49.6.1655

Whitley MJ, Arjunan P, Nemeria NS, et al (2018) Pyruvate dehydrogenase complex deficiency is linked to regulatory loop disorder in the αV138M variant of human pyruvate dehydrogenase. J Biol Chem 293:13204–13213. https://doi.org/10.1074/jbc.RA118.003996

Wieland O, Jagow-Westermann B v. (1969) ATP-dependent inactivation of heart muscle pyruvate dehydrogenase and reactivation by Mg++. FEBS Lett 3:271–274. https://doi.org/10.1016/0014-5793(69)80156-0

Wieland OH (1983) The mammalian pyruvate dehydrogenase complex: structure and regulation. Rev. Physiol. Biochem. Pharmacol. 96:123–170

Yeaman SJ (1989) The 2-oxo acid dehydrogenase complex: Recent advances. Biochem. J. 257:625–632

Yu X, Hiromasa Y, Tsen H, et al (2008) Structures of the Human Pyruvate Dehydrogenase Complex Cores: A Highly Conserved Catalytic Center with Flexible N-Terminal Domains. Structure 16:104–114. https://doi.org/10.1016/j.str.2007.10.024

Yue WW (2016) From structural biology to designing therapy for inborn errors of metabolism. J Inherit Metab Dis 39:489–498. https://doi.org/10.1007/s10545-016-9923-3

Zeng WQ, Al-Yamani E, Acierno JS, et al (2005) Biotin-responsive basal ganglia disease maps to 2q36.3 and is due to mutations in SLC19A3. Am J Hum Genet 77:16–26. https://doi.org/10.1086/431216

Zhang F, Xu X, Zhou B, et al (2011) Gene expression profile change and associated physiological and pathological effects in mouse liver induced by fasting and refeeding. PLoS One 6:e27553. https://doi.org/10.1371/journal.pone.0027553

Zhou Z, Austin G, Young L, et al (2018) Mitochondrial Metabolism in Major Neurological Diseases. Cells 7:229. https://doi.org/10.3390/cells7120229

Zhou ZH, McCarthy DB, O'Connor CM, et al (2001) The remarkable structural and functional organization of the eukaryotic pyruvate dehydrogenase complexes. Proc Natl Acad Sci U S A 98:14802–7. https://doi.org/10.1073/pnas.011597698

Chapter II

Aims and Outline

Pyruvate oxidation defects and particularly pyruvate dehydrogenase complex deficiency represent a significant subgroup among mitochondrial diseases. The broad phenotypic spectrum of PDC deficiency, common to many disorders of mitochondrial energy metabolism, often constrains the achievement of a rapid diagnosis. The detailed knowledge, combining molecular, biochemical and clinical aspects of PDC deficiency, is fundamental for a correct stratification, for an establishment of the treatment strategy and for a possible design of new therapeutic avenues.

This work aimed to:
i) characterize the mutational spectrum in the Portuguese PDC deficient population and consequently to contribute to the general landscape of PDC deficiency;
ii) to elucidate the structural and functional impact of clinically relevant PDC-E1α variants;
iii) based on the acquired knowledge of molecular mechanisms underlying the pathogenic variants, to ascertain the potential therapeutic effect of small molecular weight compounds, namely arginine and thiamine.

In chapter III, we focus on the identification of disease-causing mutations in the Portuguese PDC deficient population. We describe and discuss the clinical, biochemical and genotypic data of thirteen PDC deficient patients, seeking to obtain a complete characterization and to establish possible genotype-phenotype correlations.

Chapter IV is dedicated to a comprehensive functional and structural characterization of clinically relevant *PDHA1* missense mutations found in the Portuguese population (p. F205L, p.R253G, p.R378C and p.R378H). Analyzing recombinant heterotetrameric (αα'ββ') PDC-E1 variants produced in a prokaryotic expression system, complementary biophysical methodologies combined with molecular dynamics (MD) simulations allowed the comparative evaluation of the functional properties and of the thermal and conformational stability of the proteins.

In chapter V, we assessed the ability of arginine and thiamine in functionally rescuing E1α variants, either *in vitro* using the same heterologous expression system as in chapter IV, or *ex vivo* using patients-derived cultured cells (fibroblasts).

We ultimately aim to provide relevant experimental evidence for the development of new therapeutic approaches for PDC deficiency, thus contributing to a better clinical outcome of PDC deficient patients and an improvement in their quality of life. Additionally, and importantly, these new therapeutic avenues could be translated to other genetic diseases belonging to the vast group known as conformational disorders.

Chapter

III

Pyruvate Dehydrogenase Complex Deficiency: Updating the Clinical, Metabolic and Mutational Landscapes in a Cohort of Portuguese Patients

Hana Pavlů-Pereira[1], Maria João Silva[1,2], Cristina Florindo[1], Sílvia Sequeira[3], Ana Cristina Ferreira[3], Sofia Duarte[3], Ana Luísa Rodrigues[4], Patrícia Janeiro[4], Anabela Oliveira[5], Daniel Gomes[5], Anabela Bandeira[6], Esmeralda Martins[6], Roseli Gomes[7], Sérgia Soares[7], Isabel Tavares de Almeida[1,2], João B. Vicente[8], Isabel Rivera[1,2]

[1]*Metabolism & Genetics Group, Research Institute for Medicines (iMed.ULisboa), Faculty of Pharmacy, Universidade de Lisboa, Portugal*
[2]*Department of Biochemistry and Human Biology, Faculty of Pharmacy, Universidade de Lisboa, Portugal*
[3]*Department of Pediatrics, Hospital D. Estefânia, Lisbon, Portugal*
[4]*Department of Pediatrics, Hospital Santa Maria, Lisbon, Portugal*
[5]*Department of Medicine, Hospital Santa Maria, Lisbon, Portugal*
[6]*Department of Pediatrics, Hospital Santo António, Porto, Portugal*
[7]*Department of Neuropediatrics, Hospital Pedro Hispano, Matosinhos, Portugal*
[8]*Instituto de Tecnologia Química e Biológica António Xavier, NOVA University of Lisbon, Oeiras, Portugal*

Orphanet Journal of Rare Diseases ***15****, 298 (2020)*

III.1. ABSTRACT

Background: The pyruvate dehydrogenase complex (PDC) catalyzes the irreversible decarboxylation of pyruvate into acetyl-CoA. PDC deficiency can be caused by alterations in any of the genes encoding its several subunits. The resulting phenotype, though very heterogeneous, mainly affects the central nervous system. The aim of this study is to describe and discuss the clinical, biochemical and genotypic information from thirteen PDC deficient patients, thus seeking to establish possible genotype-phenotype correlations.

Results: The mutational spectrum showed that seven patients carry mutations in the *PDHA1* gene encoding the E1α subunit, five patients carry mutations in the *PDHX* gene encoding the E3 binding protein, and the remaining patient carries mutations in the *DLD* gene encoding the E3 subunit. These data corroborate earlier reports describing *PDHA1* mutations as the predominant cause of PDC deficiency but also reveal a notable prevalence of *PDHX* mutations among Portuguese patients, most of them carrying what seems to be a private mutation (p.R284X). The biochemical analyses revealed high lactate and pyruvate plasma levels whereas the lactate/pyruvate ratio was below 16; enzymatic activities, when compared to control values, indicated to be independent from the genotype and ranged from 8.5% to 30%, the latter being considered a cut-off value for primary PDC deficiency. Concerning the clinical features, all patients displayed psychomotor retardation/developmental delay, the severity of which seems to correlate with the type and localization of the mutation carried by the patient. The therapeutic options essentially include the administration of a ketogenic diet and supplementation with thiamine, although arginine aspartate intake revealed to be beneficial in some patients. Moreover, *in silico* analysis of the missense mutations present in this PDC deficient population allowed to envisage the molecular mechanism underlying these pathogenic variants.

Conclusion: The identification of the disease-causing mutations, together with the functional and structural characterization of the mutant protein variants, allow to obtain an insight on the severity of the clinical phenotype and the selection of the most appropriate therapy.

III.2. BACKGROUND

Pyruvate dehydrogenase complex (PDC) deficiency, first described in 1970 by Blass and colleagues (Blass et al. 1970), is an inborn error of mitochondrial energy metabolism. The pyruvate oxidation route, that bridges the cytosolic glycolytic pathway and the mitochondrial tricarboxylic acid cycle (Patel and Harris 1995), involves not only PDC but also pyruvate transport and the ancillary metabolic routes associated with various cofactors. PDC, which irreversibly decarboxylates pyruvate to acetyl coenzyme A, comprises three functional (E1 or pyruvate dehydrogenase, E2 or dihydrolipoamide transacetylase, and E3 or dihydrolipoyl dehydrogenase) and one structural (E3BP or E3 binding protein, formerly designated by protein X) components, and the regulatory PDC kinases and PDC phosphatases, which control the complex activity via phosphorylation/dephosphorylation (Patel and Korotchkina 2006). The E1 subunit catalyzes the first, rate-limiting and irreversible step of the reaction which takes place in two active sites formed at the interface between their two α and two β subunits, each requiring a thiamine pyrophosphate cofactor and magnesium ions for activity (Cate et al. 1980; Berg et al. 1998).

The great majority (≈77%) of patients with PDC deficiency harbor mutations in the X-linked *PDHA1* gene which encodes the E1α subunit. Hemizygous males are usually symptomatic whereas heterozygous females present variable expression due to random patterns of X-inactivation in different tissues, the clinical manifestations depending on the proportion of cells expressing the mutant E1α subunit. The remaining cases are caused by mutations in the genes encoding the remaining subunits: *PDHB* encoding E1β (4.3%), *DLAT* encoding E2 (1.5%), *DLD* encoding E3 (6.2%) and *PDHX* encoding E3BP (10.7%) (Sperl et al. 2015).

The clinical presentation is extremely heterogeneous, ranging from a fatal lactic acidosis and progressive neurological and neuromuscular degradation in the neonatal period to a chronic neurological dysfunction and neurodegenerative condition. Inadequate removal of lactate but mainly of pyruvate (Debray et al. 2007) results in lactic acidemia which, together with the blood lactate/pyruvate ratio ≤20, is recognized as an important biomarker (Imbard et al. 2011; Patel et al. 2012). The primary phenotypic manifestation corresponds to an impairment of neurological and/or developmental functions, leading to a wide range of symptoms and clinical features: hypotonia, seizures, ataxia, respiratory distress (like apnea and hypoventilation), facial dysmorphism, and peripheral neuropathy. Structural and functional brain abnormalities are also

described, including ventriculomegaly and Leigh syndrome. According to their severity, the phenotypes can be divided into three main categories: neonatal, infantile and benign (Brown et al. 1994; Wexler et al. 1997; Robinson et al. 2001).

The therapeutic strategies target: i) the metabolic pathway, bypassing energy production via a ketogenic diet (Wexler et al. 1997; Sofou et al. 2017), ii) the regulatory system of the dysfunctional PDC, using xenobiotic inhibitors (Fouque et al. 2003; Ferriero and Brunetti-Pierri 2013), or iii) stimulation of the residual PDC activity with supplementation of cofactors (Pastoris et al. 1996; Naito et al. 2002). Nevertheless, none of these treatments is sufficiently effective and the responsiveness is markedly individual. Thus, the precise diagnosis, including the identification of the genetic defect and the phenotypic consequences, is becoming increasingly decisive for selecting the appropriate therapeutic strategy. Knowledge on the functional and structural impact of the identified mutations on the resulting PDC component variant provides relevant information for informed decisions on the therapeutic approaches.

In this study, we describe and discuss the profiles of thirteen Portuguese PDC deficient patients with reference to their clinical data, biochemical findings and results of DNA analysis, thus seeking to establish possible genotype-phenotype correlations. This is the first report on phenotypic and genotypic variability in a subset of PDC deficient patients diagnosed in Portugal.

III.3. MATERIALS AND METHODS

III.3.1. Cohort of Patients

This study included all PDC deficient patients whose diagnosis was confirmed at the molecular level: thirteen individuals comprising a pair of monozygous twin siblings, 6 being females and 7 males. Since patients originated from all regions of Portugal, this cohort can be considered representative of the whole population. The diagnosis of patients, suspected due to high lactate and pyruvate plasma levels and respective lactate/pyruvate ratio < 20, was confirmed by reduced PDC activity (*ca* <30 % of laboratory control mean: 1734 ± 455 (range: 1279 – 2189) pmol·min^{-1}·mg protein^{-1}; n = 70) in peripheral lymphocytes and/or cultured fibroblasts originating from skin biopsy, and also by identification of the causative mutation(s).

This study was approved by the local Ethics Committees and informed consents were obtained from the patients or their parents, who were also enrolled in the study, whenever necessary and possible. Declaration of Helsinki was also strictly observed.

III.3.2. Phenotypic Evaluation

The physicians following these patients completed a questionnaire involving a wide range of parameters, namely: general characteristics of the patients, clinical features, brain malformations, biochemical findings, genetic findings, and current therapy.

III.3.3. Sample Collection and Preparation

Blood samples were collected after overnight fasting by venipuncture into EDTA-and perchloric acid-containing tubes for plasma separation and quantification of lactate and pyruvate levels, respectively, and into heparin-containing tubes for peripheral blood mononuclear cells (PBMC) isolation.

PBMC were separated at room temperature on a Ficoll-Paque gradient. Fibroblasts were cultured in Dulbecco's Modified Eagle Medium supplemented with 10% newborn calf serum and 1% antibiotic/antimycotic solution. Pelleted cells were resuspended in homogenization buffer (80 mM KH_2PO_4, pH 7.4, 2 mM EDTA). PBMC suspensions were immediately disrupted by sonication, whereas fibroblast suspensions were treated with 5 mM dichloroacetate for 15 minutes at 37 °C. The reaction was blocked by addition of a stopping solution (25 mM NaF, 25 mM EDTA, 4 mM DTT), and cells were disrupted by three freeze/thaw cycles.

III.3.4. PDC Activity Assay

Enzymatic activity was measured using a radiochemical method based on the release of $^{14}CO_2$ from [1-^{14}C]-pyruvate (Clot et al. 1992) with minor modifications (Johannes Mayr and Wolfgang Sperl, personal communication). Briefly, 100 µL of cell homogenates were incubated at 37 °C for 10 minutes in 100 µL of reaction buffer (32 mM phosphate buffer containing 4 mM $MgCl_2$, 2 mM $CaCl_2$, 0.5 mM NAD^+, 0.5 mM TPP, 0.1 mM CoA and 5 mM carnitine; final concentrations); blanks were obtained by replacing the cell homogenate with homogenizing

buffer. Then, the reaction was started by addition of 50 µL [1-^{14}C]-pyruvate solution (0.5 mM, 0.067 µCi) and allowed to proceed for 30 minutes, after which the reaction was stopped by addition of 80 µL 6N H_2SO_4. The released $^{14}CO_2$ was trapped in filter paper saturated with benzethonium hydroxide, for 15 minutes post-incubation at room temperature and under gentle stirring, and its amount measured in a scintillation counter. All samples were analyzed in triplicates and PDC activity was expressed in pmol·min^{-1}·mg protein^{-1}.

III.3.5. Preparation of Genomic DNA, RNA and cDNA

Genomic DNA and, eventually, total RNA were isolated from peripheral blood leukocytes using the Puregene Cell and Tissue kit (Gentra Systems) and the Trizol method, respectively; 5 µg of total RNA were used for the reverse transcription reaction (Amersham First Strand cDNA Synthesis kit, GE Healthcare Bio-Science Corp.).

III.3.6. PCR Amplification of PDC Encoding Genes

The complete sequence of each gene was obtained by PCR amplification of individual exons, including intronic boundaries, or overlapping fragments of the respective cDNA. The PDC subunits under analysis together with their coding genes, approved symbols and reference sequences are listed in Table III-1, whereas primer sequences designed for each gene amplification are listed in Supplementary table III-S1.

III.3.7. Sequence Analysis

PCR and RT-PCR products were purified from solution or directly from agarose gels, using Isolate II PCR and Gel Kit (Bioline). PCR forward or reverse primers were added to the purified products from each individual sample and submitted to bi-directional Sanger sequencing. All chromatograms corresponding to PCR and RT-PCR fragments were analyzed with BLAST (NCBI).

Table III-1 **List of the analyzed PDC components** showing the type of enzymatic activity, the Enzyme Commission (EC) number, the gene symbol, the HUGO identification, the reference sequences and the chromosomal localization.

Component / subunit	Enzymatic Activity	Enzyme Commission number	Approved Gene Symbol	HGNC ID	GenBank		Chromosomal Location
E1α	pyruvate dehydrogenase (acetyl-transferring)	EC 1.2.4.1	*PDHA1*	8806	NM_000284.4	NG_016781.1	Xp22.12
E1β			*PDHB*	8808	NM_000925.4	NG_016860.1	3p14.3
E2	dihydrolipoyllysine-residue acetyltransferase	EC 2.3.1.12	*DLAT*	2896	NM_001372031.4	NG_013342.1	11q23.1
E3	dihydrolipoyl dehydrogenase	EC 1.8.1.4	*DLD*	2898	NM_000108.5	NG_008145.1	7q31.1
E3BP	-		*PDHX*	21350	NM_001135024.1	NG_013368.1	11p13

III.3.8. *In silico* Analysis of PDC-E1 Mutations

To better establish genotype-phenotype correlations regarding the missense mutations in *PDHA1*, we undertook an *in silico* analyses of protein variants resulting from the described mutations. Besides evaluating the potential pathogenicity of the mutations using the PolyPhen-2 server (Adzhubei et al. 2010), we sought to obtain structural models of the protein variants through two complementary strategies, previously described for the p.R253G, p.R378C, p.R378H, and p.F205L variants (Pavlu-Pereira et al. 2021), and herein extended to p.R302H: i) submitting the sequence of the amino acid substituted variant to the SwissModel server and retrieving the corresponding model; and ii) using the Mutagenesis tool in Pymol (version 1.7) (Waterhouse et al. 2018) employing the structure of WT PDC-E1 (PDB entry 3EXE) as template (Whitley et al. 2018).

III.4. RESULTS

III.4.1. General Information

The broad phenotypic spectrum of PDC deficiency, common to many other genetic mitochondrial disorders, often hampers the achievement of a rapid diagnosis. Patients were suspected to be PDC deficient based on clinical signs /symptoms and biochemical data, namely elevated plasma lactate (L) and pyruvate (P) levels with low L/P ratio and/or impaired PDC activity, but only those with genetic confirmation were considered in this study. Thus, a total of 13 individuals, all of European ancestry, were diagnosed (Table III-2). The prevalence of PDC deficiency in Portugal is therefore estimated to be 1/790,000, comparable to the prevalence of 1/1,000,000 reported by Orphanet, the portal of rare diseases and orphan drugs, and also to the values calculated for the French population (1/827,000 – 1/1,135,000) (Imbard et al. 2011; DeBrosse et al. 2012).

The 13 patients, seven males and six females, were born between 1983 and 2018, their current ages varying from 20 months to 36 years, with a median age of 15.5 years. Consanguinity was reported only in three families harboring PDHX mutations. Among this group of 13 patients, only two were siblings, born from a triplet pregnancy after in vitro fertilization (two affected males and one unaffected female) who carry a PDHA1 mutation. No affected relatives are known in any of these families.

All patients showed the first symptoms either in the neonatal period (five individuals, 38.5 %) or during infancy (eight individuals, 61.6 %) with a median age of 0.5 years. In some cases, however, the diagnosis was only achieved later, mainly among the older patients who presented a less severe clinical picture (five individuals confirmed between 3.3 and 17 years); indeed, the most striking example is the deficiency in E3 (also designated by dihydrolipoamide dehydrogenase, DLD), which was only diagnosed when the patient was 17 years old.

All patients but one are alive; the deceased patient is a boy carrying the c.1132C>T mutation in PDHA1 (generating the p.R378C E1α variant); the death occurred at the age of 3.3 years and was caused by cardiorespiratory arrest.

Table III-2 **Genetic, biochemical, clinical and therapeutics data** concerning the cohort of 13 Portuguese PDC deficient patients

Patient	**1-JCF**	**2-MJG**	**3-DMN**	**4-GCN[a]**	**5-RCN[a]**	**6-JAR**	**7-ARV**	**8-GMR**	**9-MJP**	**10-LCM**	**11-AVB**	**12-MBS**	**13-MMS**
General Information													
Year of birth	1996	2000	2005	2011	2011	2015	1983	2002	2018	2015	1988	2004	2001
Gender	M	M	M	M	M	M	F	M	F	F	F	F	F
Consanguinity	N	N	NA	N	N	N	N	Y	Y	N	N	Y	N
Age of onset (years)	1.9	2	Neonatal period	0.6	Neonatal period	0.5	1	0.5	Neonatal period	0.5	Neonatal period	Neonatal period	0.4
Age of diagnosis (years)	9	5.3	0.4	0.6	0.6	1	6	2	Neonatal period	3.3	Neonatal period	0.5	17
Actual age (years)	23	19	14	8	8	Deceased at 3.3	36	17	1	4	31	15	18
Genetic findings													
Affected gene	*PDHA1*	*PDHA1*	*PDHA1*	*PDHA1*	*PDHA1*	*PDHA1*	*PDHA1*	*PDHX*	*PDHX*	*PDHX*	*PDHX*	*PDHX*	*DLD*
Affected protein componente	E1α	E1α	E1α	E1α	E1α	E1α	E1α	E3BP	E3BP	E3BP	E3BP	E3BP	E3
Nucleotide exchange	c.615C>G	c.757A>G	c.905G>A	c.1132C>T	c.1132C>T	c.1132C>T	c.1133G>A	c.850C>T / c.850C>T	c.850C>T / c.850C>T	c.850C>T / c.850C>T	c.850C>T / c.483delC	c.160+1G>A / c.160+1G>A	c.259C>T / c.803_804delAG
Precursor protein exchange	p.F205L	p.R253G	p.R302H	p.R378C	p.R378C	p.R378C	p.R378H	p.R284X / p.R284X	p.R284X / p.R284X	p.R284X / p.R284X	p.R284X / p.P161Pfs*17	p.G26Vfs*7 / p.G26Vfs*7	p.P87S / p.Q268Rfs*3
Localization of mutation	Exon 7	Exon 7	Exon 10	Exon 11	Exon 11	Exon 11	Exon 11	Exon 7	Exon 7	Exon 7	Exon 7/Exon 4	Intron 1	Exon 4/Exon 9
Mutation type	Missense	Missense	Missense	Missense	Missense	Missense	Missense	Nonsense	Nonsense	Nonsense	Nonsense / Frameshift	Splicing	Missense / Frameshift
Biochemical Findings													
Highest plasma lactate ($mmol \cdot L^{-1}$)	7.9	4	9.1	9.4	6.6	8.9	4.5	3.5	17	3	4.4	12.2	3
Highest plasma pyruvate ($mmol \cdot L^{-1}$)	0.527	0.3	0.398	NA	0.81	0.631	0.274	0.331	0.61	0.27	0.27	0.569	NA
Ratio L/P in same sample	14	12	20	NA	8	14	16	16	14	9	16	16	NA
Enzyme activity in lymphocytes	30	13	25[b]	28	40	8.5	19	30	25	30	21.3 / 16.3[b]	29	29

Table III-2 (continued)

Patient	1-JCF	2-MJG	3-DMN	4-GCN[a]	5-RCN[a]	6-JAR	7-ARV	8-GMR	9-MJP	10-LCM	11-AVB	12-MBS	13-MMS
Clinical Features													
DD/MR/PMR	Moderate	Mild	Severe	Severe	Severe	Moderate	Moderate	Severe	Severe	Severe	Severe	Severe	Moderate
Hypotonia	Y	Y	Y	Y	Y	Y	Y	Y	Y	Y	N	Y	Y
Seizures	N	N	Y	Y	Y	Y	Y	Y	N	N	N	N	Y
Microcephaly	Y	N	Y	N	N	N	Y	N	Y	Y	N	N	N
Dystonia	Y	N	Y	Y	Y	Y	N	Y	N	N	Y	Y	Y
Ataxia	Y	Y	N	Y	Y	N	N	Y	N	N	Y	Y	Y
Peripheral neuropathy	Y	Y	NA	N	N	N	N	N	N	N	N	N	N
Facial dysmorphisms	N	N	N	N	N	N	Y	N	N	N	N	N	N
Spasticity	Y	N	Y	Y	Y	N	N	N	N	N	N	N	N
Respiratory distress	N	N	Y	N	Y	Y	N	N	N	N	N	N	N
Ocular manifestations	N	N	Cortical blindness	N	N	N	N	Strabismus	Nystagmus, loss of visual	Loss of visual acuity	N	Nystagmus, strabism	Astigmatism
Brain Malformations													
Basal ganglia abnormalities	Y	N	Y	Y	Y	Y	N	N	N	N	N	N	N
Cerebral brain atrophy	Y	N	Y	N	N	N	N	Y	Y	Y	N	N	Y
Cerebellar brain atrophy	Y	N	Y	N	N	N	N	N	N	N	N	N	N
Therapy													
Ketogenic diet	N	N	N	Y	Y	Y	N	Y	Y	Y	N	Y	N
Thiamine	N	Y	N	Y	Y	Y	Y	Y	Y	Y	Y	Y	Y
Arginine aspartate	N	Y	N	N	N	N	N	N	Y	Y	N	N	N
Antiepiletic drugs	N	N	Y	Y	Y	Y	Y	N	N	N	N	N	Y

DD/ MR/PMR—development delay, mental retardation, psychomotor retardation

Normal levels of plasma lactate—< 2.2 mmol/L

Normal levels of plasma pyruvate—< 0.180 mmol/L

Normal L/P ratio—< 20

Y—yes; N—no; NA—not available

[a] Twins

[b] Enzyme activity in fibroblasts

III.4.2. Genetic Findings

In this cohort of 13 patients, it was shown that patients carried mutations in three different genes: seven in the PDHA1 gene, five in the PDHX gene, and one in the DLD gene (Table III-2). The mutational spectrum revealed ten different mutations: five in PDHA1, three in PDHX and two in DLD.

As expected for an X-linked disorder, most patients with mutations in PDHA1, are males (6/7) in families with no consanguinity, but it is interesting to notice that, in all these patients, mutations arrived by a de novo mechanism, confirmed by parental sequencing, and that mosaicism was absent. On the other hand, most patients with mutations in PDHX, displaying an autosomal recessive mode of inheritance, are females (4/5) and consanguinity was detected in three cases. Finally, the single patient with mutations in DLD, also displaying an autosomal recessive mode of inheritance, is a compound heterozygous female with no consanguinity reported in her family.

In this patient cohort, all five different *PDHA1* mutations are missense (c.615C>G, c.757A>G, c.905G>A, c.1132C>T, and c.1133G>A), generating respectively the p.F205L, p.R253G, p.R302H, p.R378C and p.R378H E1α variants. The prevalence of missense mutations, in principle the less severe mutation type, strongly correlates with the majority of patients being males. On the contrary, the three mutations detected in *PDHX* gene (c.160+1G>A, c.483delC and c.850C>T), being nonsense (p.R284X) and frameshift (p.G26Vfs*7 and p.P161Pfs*17), usually result in absent protein, hence their highly deleterious consequences. Three out of the five patients are homozygous for the p.R284X variant, whereas one of the remaining patients is a compound heterozygote expressing the p.R284X and p.P161Pfs*17 variants, while the other is homozygous for the mutation generating the p.G26Vfs*7 variant. Regarding the two identified *DLD* mutations, both c.259C>T and c.803_804delAG are novel (Exome Variant, LOVD or ClinVar). The c.259C>T mutation generates the E3 p.P87S variant. Moreover, c.803_804delAG, originating a frameshift variant (p.Q268Rfs*3), is predicted to be very severe.

III.4.3. Biochemical Findings

All patients, regardless of the carried mutation, were suspected of PDC deficiency due to their elevated plasma lactate and pyruvate levels: lactate ranging from 3.0 to 17.0 $mmol \cdot L^{-1}$ (median value 6.6 ± 3.9) and pyruvate from 0.27 to 0.81 $mmol \cdot L^{-1}$ (median value 0.398 ± 0.086). Lactate/pyruvate ratios as expected, with a single exception, were ≤16, i.e., in the normal range. PDC deficiency was confirmed by determination of PDC activity. Enzymatic assays were performed either in circulating lymphocytes (12 patients) or cultured fibroblasts (two patients), both tissues having been analyzed in patient 11. All patients had their enzymatic activities confirmed in a second independent sample and the results always matched. Interestingly, a single false negative result was found in the lymphocytes of a female patient later identified with a *PDHA1* mutation. In our experience, the cut-off value for considering a primary PDC deficiency should be ≤ 30% of control activity and, indeed, all patients but one presented enzymatic activities ranging from 8.5% to 30% (median value 28.0 ± 7.9). The single exception was one of the siblings carrying the p.R378C variant in *PDHA1*, who presented 40 % of normal control activity (Table III-2), surprisingly the one whose symptoms manifested earliest in the neonatal period.

However, when stratifying the values of enzyme activity according to the affected PDC subunit, we observed some differences. Patients carrying *PDHX* mutations displayed higher and more similar values of relative activity (median value 29 ± 3.4 %), whereas patients carrying *PDHA1* mutations displayed a wider range of activity (median value 23.5 ± 10.7 %), with half of them below 20 %.

III.4.4. Clinical Features

The clinical features observed in these patients' cohort are displayed in Table III-2 and, according to the most recently published data (Sperl et al. 2015), can be roughly divided into two categories: one caused by *PDHA1* and *PDHX* mutations, and the other caused by *DLD* mutations. Indeed, the clinical phenotypes manifested by patients carrying *PDHA1* and *PDHX* mutations are quite variable and almost undistinguishable.

Concerning neurological features, all individuals presented development delay/psychomotor retardation, which ranged from severe (eight patients: 61.5 %) to moderate

(four patients: 30.8 %) or very mild (one patient who attended normal school: 7.7 %). Hypotonia was also observed in all individuals, with a single exception (Patient 11) who nevertheless could display it at an earlier age. Seizures were reported in half the individuals, especially those carrying *PDHA1* mutations (5/7 patients: 71 %). On the other hand, ocular manifestations were more frequent in individuals harboring *PDHX* mutations (4/5 patients: 80 %). Microcephaly, dystonia and ataxia were also reported in half the patients of both these gene defects. As expected, facial dysmorphism was only detected in a single female patient carrying a *PDHA1* mutation. The patient with DLD deficiency revealed moderate developmental delay/psychomotor retardation, seizures, hypotonia, dystonia and ataxia. Basal ganglia abnormalities were exclusively observed in patients carrying mutations in *PDHA1*. Cerebral atrophy, but not cerebellar atrophy, was detected mainly in patients carrying *PDHX* mutations. However, in patients carrying *PDHA1* mutations, cerebral atrophy, when present, was always associated with cerebellar atrophy (Figures III-1 and III-2). Patient 13, harboring *DLD* mutations, presented partial agenesis of *corpus callosum*.

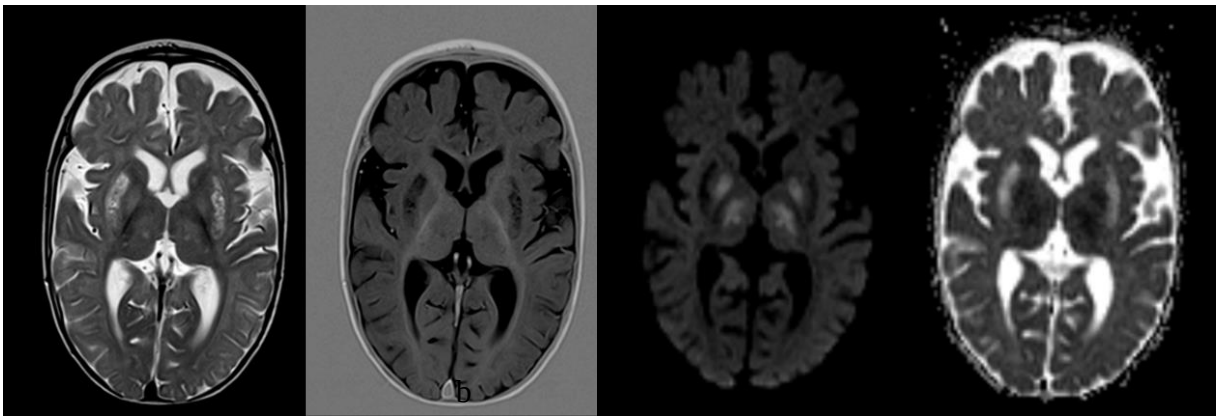

Figure III-1 **Magnetic resonance images of brain lesions** of an 8-month-old patient carrying a PDHA1 mutation. Hyperintense bilateral and symmetrical lesions in the thalami, globus pallidus and putamina, on T2 weighted images, hypointense on T1 and with diffusion restriction suggestive of acute lesions; there is no diffusion restriction suggestive of chronic lesions. **a** axial T2, **b** axial T1 IR, **c** axial DWI, **d** axial ADC.

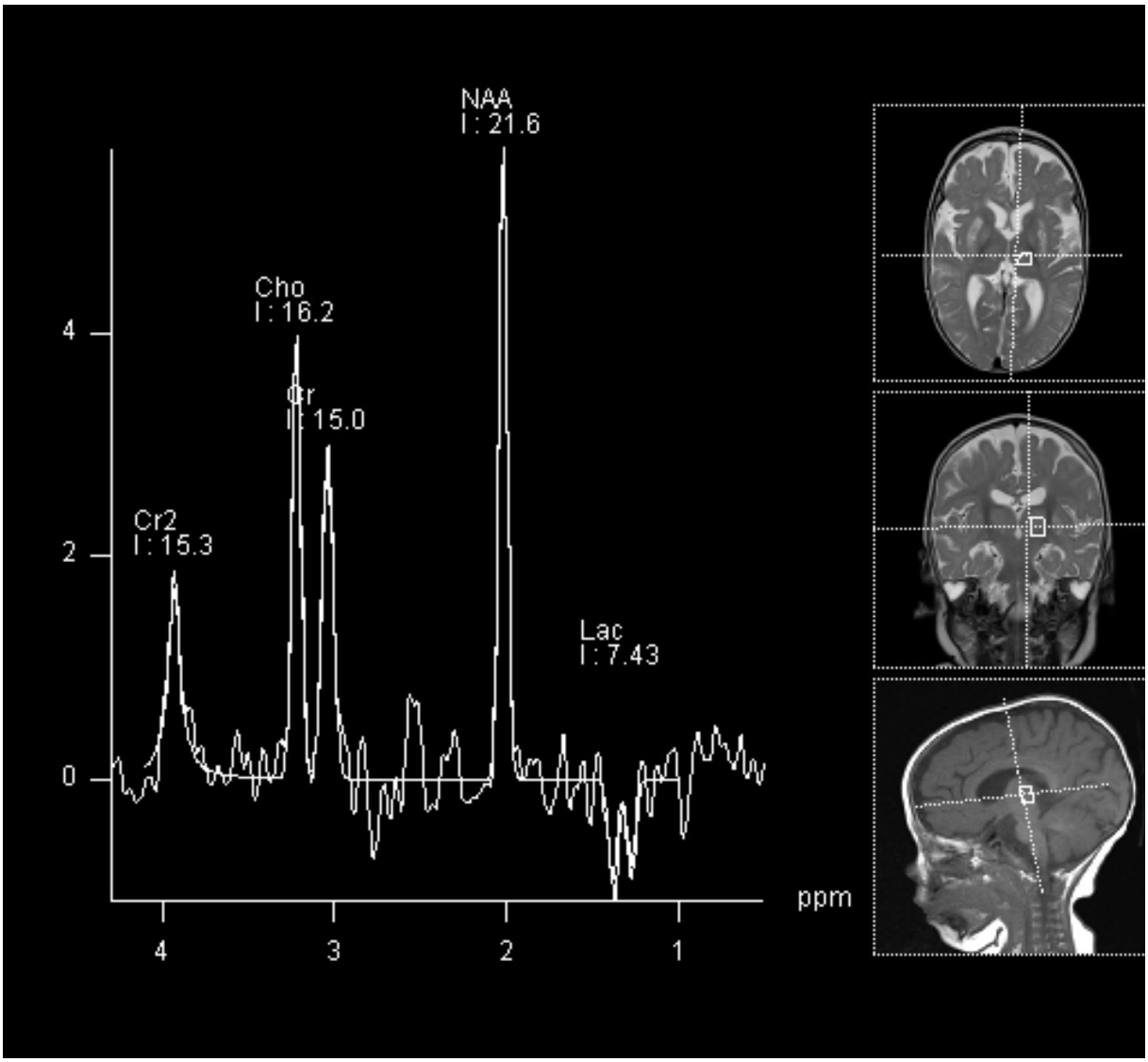

Figure III-2 **Magnetic resonance spectroscopy** of a patient carrying a PDHA1 mutation. Spectroscopy with TE = 135 ms in left thalamus; slight reduction of NAA, increased choline and lactate

III.4.5. Treatment

All the patients are under therapeutic measures which include ketogenic diet, thiamine supplementation and antiepileptic drugs. Three patients with *PDHA1* mutations (3/7: 43 %) and three with *PDHX* mutations (3/5: 60 %) are under ketogenic diet with clearly beneficial effects on childhood-onset epilepsy or paroxysmal dystonia. The rationale for the ketogenic diet is that ketone bodies generated by fatty acid oxidation serve as an alternative energy substrate to

glucose as the glycolytic end product, pyruvate, is not optimally metabolized. The long-term thiamine supplementation, as PDC cofactor, is prescribed in almost all patients (11/13), and antiepileptic drugs only in those presenting seizures (Table III-2). Finally, it is interesting to mention that three of the patients carrying mutations in the *PDHA1* gene were under arginine aspartate supplementation, with beneficial effects at the physical and intellectual levels, especially Patient 2.

III.4.6. *In silico* Analysis of Missense Mutations

Bioinformatic analysis using the PolyPhen-2 server (Adzhubei et al. 2010) suggested that all mutations but one affecting E1α subunit are most probably damaging. The E1α p.R302H, p.R378C and p.R378H variants displayed a score of 1.000 (sensitivity 0.00 and specificity 1.00), p.F205L displayed a score of 0.919 (sensitivity 0.81 and specificity 0.94), and p.R253G displayed a score of 0.007 (sensitivity 0.96 and specificity 0.75) thus being considered benign. As for E3 subunit, the p.P87S variant is predicted to be most probably damaging, with a score of 0.996 (sensitivity 0.55 and specificity 0.98).

To complement the information of the PolyPhen-2 server, which solely bases its predictions on the polypeptide sequence and overlooks other structural and functional details, such as e.g. cofactor binding and interaction with other proteins, we obtained and thoroughly inspected structural models of each E1α variant. The models obtained for the E1α p.R253G, p.R378C, p.R378H and p.F205L variants have been recently described by our group, attempting to understand the molecular mechanisms underlying the pathogenicity of the corresponding mutations (Pavlu-Pereira et al. 2021). All mutations result in putative loss of H-bonds, electrostatic or hydrophobic interactions between the side chains of the substituted amino acids and neighboring residues, with predicted effects on P-loop destabilization, inter-subunit interactions and proper oligomeric assembly, as well as interaction with other PDC components. Herein, we additionally generated a structural model of the E1α p.R302H variant (Figure III-3). R302 is located at one end of the P-loop A, its side chain being within electrostatic and H-bonding distance to the side chain or main chain carbonyl moieties of Y287, R288, Y289, H290 (active site residue) and G298, all residues belonging to the same P-loop. Upon substitution by a histidine residue, most of the possible interactions between its side chain and other residues

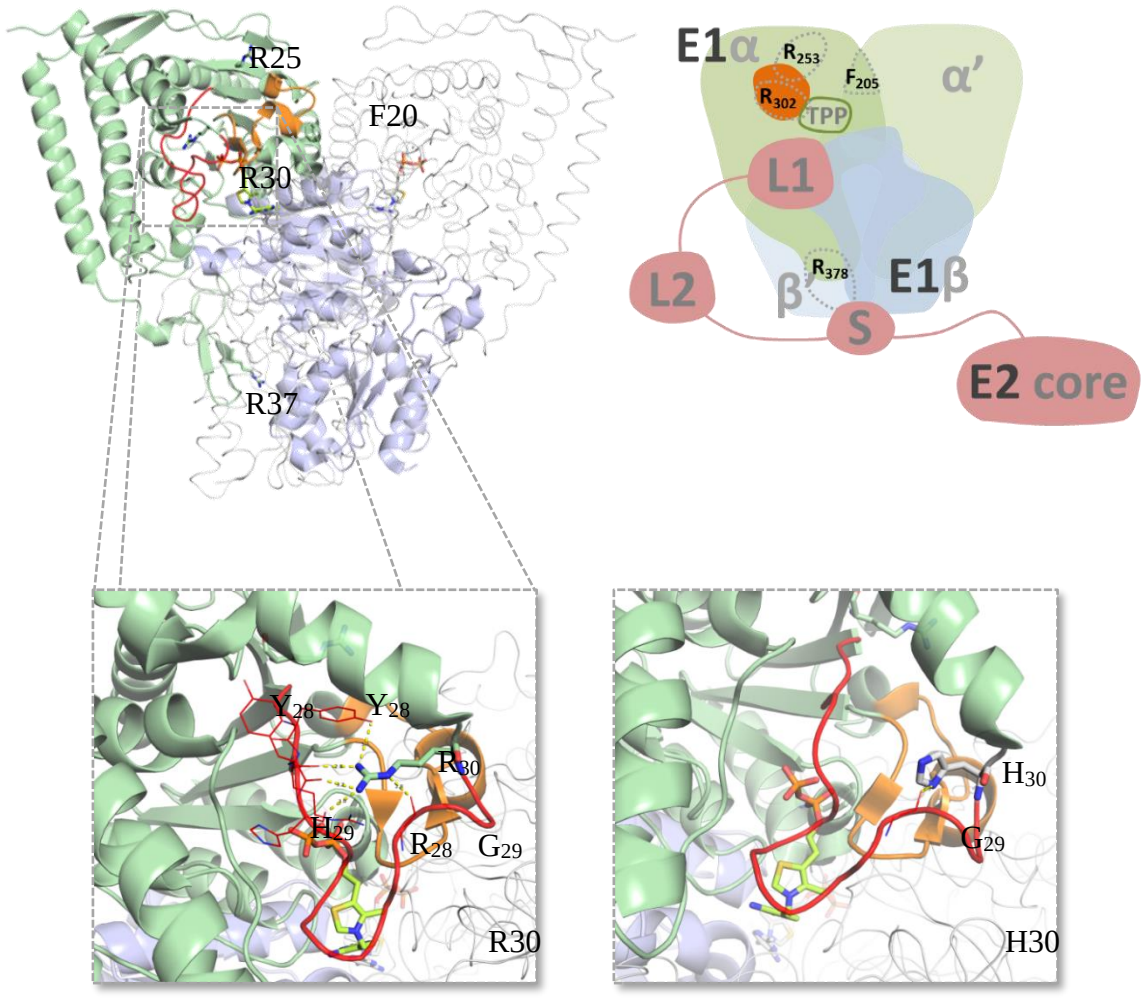

Figure III-3 **In silico analysis of pyruvate dehydrogenase complex E1 p.R302H variant.** Top left panel, cartoon and ribbon representation of the heterotetrameric PDC E1 crystallographic structure (PDB entry 3EXE). E1α subunit represented in green; E1β represented in blue; E1α phosphorylation loop A represented in orange. The corresponding E1α′ and E1β′ subunits are represented as a gray ribbon. Residues that are substituted in variants identified in Portuguese PDC deficient patients with mutations in PDHA1, encoding the PDH E1α subunit, are represented in sticks. Top right panel, scheme representing the possible impact of substituted residues in pathogenic E1α variants: p.R253G substitution located near phosphorylation loop A (orange shape); p.F205L substitution possibly affecting αα′ interface (each E1α subunit represented in different shades of green); p.R302H substitution located in phosphorylation loop A close to the TPP cofactor binding site; p.R378C/H substitutions located close to the αβ interface (each E1β subunit represented in different shades of blue), and possibly affecting the interaction with a domain of the PDC E2 component. Bottom panel, zoom-in on the region surrounding R302 (left), showing its possible interactions with neighboring residues (Y287, R288, Y289, H290 and G298), only the latter being retained upon substitution by H in the p.R302H variant (right). Structural model of PDC-E1 p.R302H variant was obtained by loading the structure of WT PDC-E1 (PDB entry 3EXE) into Pymol and applying the mutagenesis tool to generate all possible rotamers of the substituting amino acid side chain.

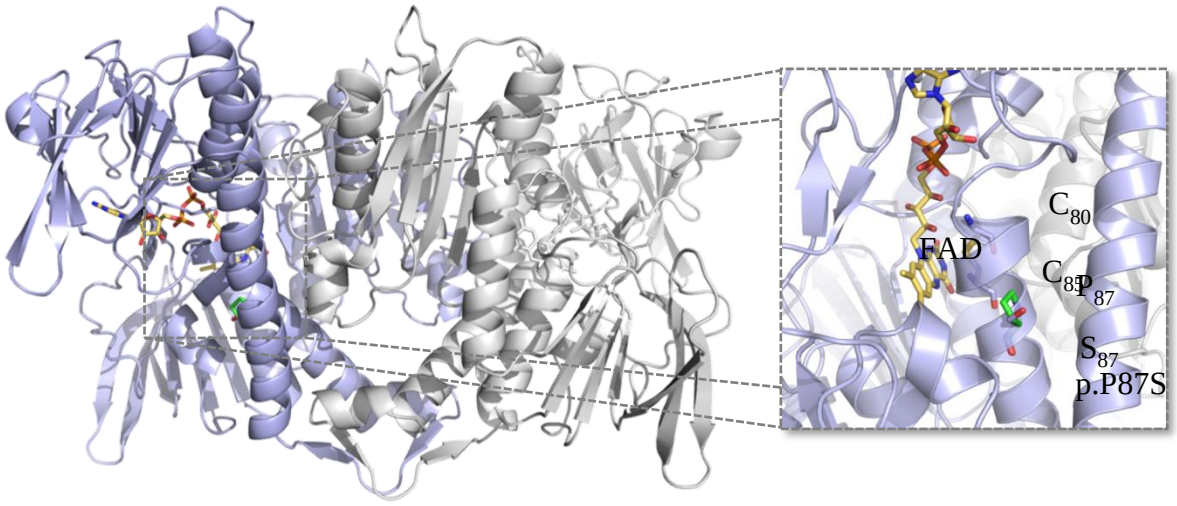

Figure III-4 **In silico analysis of pyruvate dehydrogenase complex E3 p.P87S variant.** Cartoon representation of homodimeric PDC E3 crystallographic structure (PDB entry 6I4T; one monomer represented in blue, the other in grey). Flavin adenine dinucleotide (FAD) cofactor in yellow sticks. Right panel, zoom-in on the location of the P87S substitution. P87 is located at an α-helix which contains the active site cysteine residues C80 and C85. Substitution of P by S will likely affect the helix structure and disturb the proximity between the active site disulphide and the FAD cofactor. Structural model of PDC-E1 p.R302H variant was obtained by loading the structure of WT PDC-E3 (PDB entry 6IT4) into Pymol and applying the mutagenesis tool to generate all possible rotamers of the substituting amino acid side chain.

in the P-loop are lost. The single remaining H bond is that between the side chain imidazole and the main chain carbonyl of G298. Therefore, in the p.R302H E1α variant, the net loss of four possible side chain interactions with other P-loop A residues (Figure III-3) is likely to contribute to a more disordered loop and consequently lower enzymatic activity. Notably, the degree of disorder in P-loop A has been negatively correlated with E1 enzymatic activity, since an ordered loop favors TPP binding, which itself promotes P-loop A order (Whitley et al. 2018).

To further understand the pathogenicity of the *DLD* mutation generating the E3 p.P87S variant, a structural model was obtained (Figure III-4) based on the reported 3D crystallographic structure of another disease-causing E3 variant (PDB entry 6I4T) (Szabo et al. 2019). As observed in Figure III-4, P87 is located at a helix that lines with the flavin adenine dinucleotide isoalloxazine ring and contains the active site disulfide composed of C45 and C50. Substitution of P87 by a serine is likely to alter the flexibility and thus the overall stability of the respective helix, possibly affecting the enzymatic activity.

III.5. DISCUSSION

The diagnosis of PDC deficiency is extremely challenging due to a phenotypic presentation that can be observed in many other neurological disorders, especially those causing abnormal mitochondrial metabolism (Sperl et al. 2015; Ciara et al. 2016; Shin et al. 2017). Indeed, PDC deficiency can be included in the vaster group of pyruvate oxidation defects (POD) which also involves defects in genes coding for proteins participating in the whole pyruvate oxidation route, including cofactors, regulation of PDC and the mitochondrial pyruvate carrier (Sperl et al. 2015). Nevertheless, in this study, we only included patients carrying mutations in the genes encoding the PDC subunits (*PDHA1*, *PDHB*, *PDHX*, *DLAT* and *DLD*). Accordingly, and comparing the prevalence rate we obtained *versus* the previously reported prevalence (respectively 1:790,000 and 1:1,000,000) we may assume that no significant number of patients were missed.

In such context, we aimed to present the first report on a cohort of PDC deficient Portuguese patients combining information on the associated clinical, biochemical, enzymatic and genotypic spectra. The mutational spectrum of PDC deficiency in this group of patients revealed ten different mutations affecting three genes, *PDHA1* (five), *PDHX* (three) and *DLD* (two). Concerning the prevalence of the deficiency of each gene, these data generally agree with literature surveys (Patel et al. 2012; Sperl et al. 2015) and also with several studies focused on different populations (Barnerias et al. 2010; Quintana et al. 2010; Imbard et al. 2011). However, the frequency of mutations in the *PDHA1* gene is lower than the usually reported average of 75–80%, due to a high number of patients harboring the PDHX gene (38% in our cohort versus 10% in the literature).

The most striking evidence is the relatively high incidence of E3BP deficiency, mostly caused by a p.R284X E3BP variant, half the cases originating from the Azores Islands, thus denoting a founder effect. This E3BP variant was first described by our group (Pinheiro et al. 2016) and, until now, only another Portuguese patient has been reported to carry this mutation (Nogueira et al. 2019). Furthermore, the mutational spectrum of E3BP deficiency in Portugal includes very severe mutations, leading to null alleles. Nevertheless, our older patients surprisingly reached adulthood, in line with the high proportion of long-term survival among reported E3BP deficient patients (Marsac et al. 1993; Brown et al. 2007; Imbard et al. 2011). In general, an overwhelming majority of the mutations hitherto identified in the *PDHX* gene

are, as in this work, deletions, nonsense mutations, point mutations at intron-exon boundaries, or even large intra-genic rearrangements, expected to result in a complete absence of E3BP protein (Brown et al. 2007; Imbard et al. 2011; Gray et al. 2014; Byron and Lindsay 2017). Despite this fact, the patients retain considerably significant PDC activity (20-30 %), considering the expected impairment on PDC assembly. On the one hand, as a structural subunit devoid of enzymatic activity, E3BP does not directly contribute to the complex catalytic activity. On the other hand, the significantly truncated E3BP, if present at all in the cell, would likely compromise the structure of the E2/E3BP PDC core and binding of the E3 component. Both E2 and E3BP components have a similar structure and domain organization, despite only E2 being catalytically active (Harris et al. 1997). However, the possibility of the E2 core directly binding to the E3 enzyme may underlie the observed residual PDC activity (Brown et al. 2007; Vijayakrishnan et al. 2011; Gray et al. 2014; Byron and Lindsay 2017). In their recent work, Prajapati and collaborators report a non-uniform stoichiometry of the E2/E3BP PDC core. The imbalanced distribution of E2 and E3BP constituents of the trimeric units results into structurally dynamic E1 and E3 clusters (Prajapati et al. 2019). Moreover, for one of the proposed models of *E. coli*, the PDC core is a fully functional E2 homotrimer operating in a "division-of-labor" mechanism, including binding of the E3 component (Song and Jordan 2012; Prajapati et al. 2019).

Concerning the mutational spectrum of E1α deficiency, five different *PDHA1* mutations were identified, all but a single one (c.1132C>T, encoding the p.R378C variant) from non-consanguineous patients. Almost all mutations affect an arginine codon (Vitkup et al. 2003) and those located in exons 10 and 11 cause a severe phenotype, because the resulting protein variants present very low enzyme activity. On the contrary, the two mutations located in exon 7 originate moderate (c.615C>G, encoding the p.F205L variant) or very mild (c.757A>G, encoding the p.R253G variant) phenotypes. Interestingly, mutations affecting codon 378 are considered particularly lethal (Patel et al. 2012). Indeed, from our male patients carrying the p.R378C mutation, one deceased at three years of age and the twins, presently aged 8 years, display a severe clinical picture. However, a female patient bearing the p.R378H substitution reached the adulthood, probably due to a lyonization effect.

Regarding a possible genotype-dependent phenotypic presentation, our data is roughly suggestive of such a correlation. Effectively, the patients harboring the most deleterious

mutations (c.905G>A and c.1132C>T in *PDHA1* and all the mutations in *PDHX*) present the most severe phenotypes, involving serious psychomotor retardation, hypotonia and seizures, whereas those carrying less severe mutations accordingly display a better clinical outcome. The most puzzling observation concerns the female carrying mutations in *DLD*. Despite being a compound heterozygote bearing two severe mutations, her clinical course was reasonable until 2018 when she suffered an acute metabolic decompensation originating spastic tetraparesis with gait and language loss. Although she partially recovered language, she currently presents a moderate-to-severe psychomotor handicap. Despite the E3 subunit being common to other enzyme complexes such as α-ketoglutarate dehydrogenase and branched-chain amino acid dehydrogenase, this patient did not display the associated biochemical or clinical phenotypes.

Irrespectively of our patients' cohort size, the majority of our PDC deficient patients remarkably reached adulthood, as opposed to several other reports (Barnerias et al. 2010; Quintana et al. 2010; Patel et al. 2012; DeBrosse et al. 2012). Concerning the therapeutic measures to which these individuals are subjected, it is clear they are only palliative, since all patients but one continue presenting clinical features ranging from moderate to severe forms. The single exception is Patient 2 who seems to represent an exceptional case, because his treatment only encompasses thiamine (E1 subunit cofactor) and arginine aspartate supplementation (Silva et al. 2009). Arginine aspartate (Asparten®, Sargenor®) is an anti-asthenic over-the-counter medicine. Aspartate is considered an anaplerotic agent, whereas arginine has the ability to suppress aggregation during protein folding by binding to the folding intermediates through weak interactions, thus being considered a putative chemical chaperone (Arakawa and Tsumoto 2003; Tsumoto et al. 2004; Baynes et al. 2005). This patient carries the *PDHA1* c.757A>G mutation that originates the p.R253G E1α variant, whose *in silico* and *in vitro* analyses with the recombinant protein exhibited lower affinity for TPP and lower residual enzymatic activity, in addition to increased proneness to aggregation, in comparison with WT PDC-E1 (20). The same impairment on the affinity for TPP was observed in various *PDHA1* missense mutations (20). Thiamine supplementation is thus likely to ameliorate the functional impact in terms of TPP affinity for several of these variants (Pavlu-Pereira et al. 2021). Nevertheless, our observation of the serious regress of the clinical symptoms, while the arginine aspartate uptake was interrupted in Patient 2 (Silva et al. 2009), suggests that this patient benefits from both arginine aspartate and thiamine treatments.

In conclusion, the identification of the disease-causing mutations, together with the functional and structural characterization of the respective protein variants, allows getting insight on the severity of the clinical phenotype and the selection of the most appropriate therapy, namely the option for a ketogenic diet.

ACKNOWLEDGMENTS

We acknowledge Dra. Carla Conceição, from the Radiology Department of Hospital D. Estefânia, Lisboa, for her contribution with the MRI images.

SUPPLEMENTARY INFORMATION

Supplementary Table III-S1 List of primers used in this study.

cDNA amplification

***PDHA1* messenger** (2 fragments)

PDHA1-5'-F	5' – GGGCACCTGAAGGAGACTT – 3'
PDHA1-R	5' – CTTTAGTTCTTCCACACTGG – 3'
PDHA1-F	5' – AGTGGATGGAATGGATATCC – 3'
PDHA1-3'-R	5' – GTCTGGTAGCCCCCTGAAGG – 3'

***PDHX* messenger** (2 fragments)

PXF2-F	5' – CTGCTGCGTTATCTTGTGGGCT – 3'
PXW2-R	5' – TGAGTGAATGTGCCCACTGCATTG – 3'
PXP2-F	5' – CAATGCAGTGGGCACATTCACTGA – 3'
PXR2-R	5' – TAACAACTACTGAATCAACTAAGC – 3'

***DLD* messenger** (2 fragments)

E3A-F	5' – AGCGGAGAAAGTATTGGCGGA – 3'
E3D-R	5' – TTTAGTTTGAAATCTGGTATTGAC – 3'
E3D-F	5' – CAGCAGTTGAACGTTTAGGTCATG – 3'
E3F-R	5' – TCTTGGAGCTGTGAGAATATCCT – 3'

Genomic DNA amplification

***PDHA1* gene**

PDHA1-1-F	5' – GCGCAGCGCATGACGTTATTACG – 3'
PDHA1-1-R	5' – CCGGCCAGCCCGGGAGGTCT – 3'
PDHA1-2-F	5' – GCCAAAGCATGGATTCATTT – 3'
PDHA1-2-R	5' – TCTGAACTTCTGATCCTGGACA – 3'
PDHA1-3-F	5' – CCAAGCCCCATCTCATTG – 3'
PDHA1-3-R	5' – ACACAGTTCCACCACAAACC – 3'
PDHA1-4-F	5' – TTATTGCTTCTGGTTTGGGC – 3'
PDHA1-4-R	5' – CCCCTTTCTGTAAATCAACAGC – 3'
PDHA1-5-F	5' – TGGTTGAGCCTCAGAGTACA – 3'
PDHA1-5-R	5' – TGGCTGTACTAGCTTCAGGA – 3'

PDHA1-6-F	5’ – GATTCTGGCCAGGAGTGAAA – 3’
PDHA1-6-R	5’ – GGTGAGCTCCTTCACAGGAA – 3’
PDHA1-7-F	5’ – AGGAGGCCTTTCTGTGCTTT – 3’
PDHA1-7-R	5’ – CGGCCCCACCACAGGGTTCCT – 3’
PDHA1-8-F	5’ – TGTCGCCCCTCCCCTGTTTAT – 3’
PDHA1-8-R	5’ – CTTCCATCTCATGCACCTCA – 3’
PDHA1-9-F	5’ – TGAGCCACCATCCTGGCCTT – 3’
PDHA1-9-R	5’ – GCGTACATGAAGTGAACTGG – 3’
PDHA1-10-F	5’ – ATTTCACTCATTGGGACATCC – 3’
PDHA1-10-R	5’ – TGGTTCACAGTCCACCAAAA – 3’
PDHA1-11-F	5’ – TTTTGGTGGACTGTGAACCA – 3’
PDHA1-11-R	5’ – GTCTGGTAGCCCCCTGAAGG – 3’

***PDHX* gene**

PX1F	5’-AGAGACCTAAAGGCACCGCT-3’
PX1R	5’-AAGCAGGCCCTCAATCATAA-3’
PX2F	5'-TGGGAATCTTTTAGACTTTGGA-3’
PX2R	5’-TGCTGAACCCAGAAAACCTT-3´
PX3F	5’-CAACCCAGAAATAGCTACGGA-3’
PX3R	5’-CACATTAAAAATAAGGAGGCAAAA-3’
PX4F	5’-TGCAGTCATGGGGTTTTACTT-3’
PX4R	5’-ACAGCAACTTCCTACGTGATG-3’
PX5F	5’-GTGACCATCTGTGGGAGTCA-3’
PX5R	5’-TTATTCAGAAAACAACTCTTGCAT-3’
PX6F	5’-TCACCTGCGTTTTCTGAAAGT-3’
PX6R	5’-GTGAGCCAAGATTGTGCCAT-3’
PX7F	5’-TTCCACTTGTGGTTTAACGGA-3’
PX7R	5’-TTTCCTCTAGCACAAATATACCCA-3’
PX8F	5'-ACAAGTTTGAAGTTGTAATGGTCA-3’
PX8R	5’-GAGGGAGATCAAACGATAGGA-3´
PX9F	5’-TTTTTCTGTAACCGCCTTGG-3’
PX9R	5’-TCTCCCCTTCACACACACAA-3’

PX10F 5’-GGTAACAAAATCAAATCAAGGCA-3’

PX10R 5’-TTCAGATAAATGAAAGGCTGACA-3’

PX11F 5’-ACGGAAAGGGGACTTTGATT-3’

PX11R 5’-TTGAGGACTAGGCAAGTCGG-3’

***DLD* gene**

DLD1-F 5’ – CTCCCGGGTGATGACGTA – 3’

DLD1-R 5’ – CTCCCGGGTGATGACGTA – 3’

DLD2-F 5' – TTGATACGTTTGCCCAAAAT – 3’

DLD2-R 5’ – ATTGAAATAGAAAGGAACTGTCAG– 3´

DLD3-F 5’ – TGCTGATTTGTACTGTAAGAGGTT – 3’

DLD3-R 5’ – TGATCAACCCTTCCCAAATTA – 3’

DLD4-F 5’ – CCGAATAGCTTGTTTTGTAGAAG – 3’

DLD4-R 5’ – TTGTCTAATCTAGTCTCAATCCAT – 3’

DLD5-F 5’ – GAACGAAACTCCGTCTCAAAA – 3’

DLD5-R 5’ – TCTTTAGACAGAAGAGCCAAGTCA – 3’

DLD6-F 5’ – TTGGTGAGTGAAAAACACTGC – 3’

DLD6-R 5’ – TCCCCTGTAACCAAGTTCAAA – 3’

DLD7-F 5’ – AAGTAAGGAAGCATTTTGTTTTAG – 3’

DLD7-R 5’ – TCAGTCAGAAATCTCTCAAAGTTC – 3’

DLD8-F 5' – TCTGCAAATTTGGAACCCAT – 3’

DLD8-R 5’ – GGACCTTTAAGTCCCTTCCAA– 3´

DLD9-F 5’ – AAGATGATTTCGTAAACATTTGCT – 3’

DLD9-R 5’ – TTGCTTAAAGAGACAGGGATGA – 3’

DLD10-F 5’ – CTTGAGAAATTGCTGGCCTT – 3’

DLD10-R 5’ – TTCCCCAAAGCCAATACATA – 3’

DLD11-F 5’ – TTTTTGGTGACTTGTTTACTGGAA – 3’

DLD11-R 5’ – TGCTGTTTCTCAACCACCAA – 3’

DLD12-F 5’ –TCCTTCTATGTGCTTTGCGA– 3’

DLD12-R 5’ – TCTTAATGGGATTTCTCTGGTTTT – 3’

DLD13+14-F 5’ – CCCCTCAACAATTGCTATCC – 3’

DLD13+14-R 5’ – TGGAGCTGTGAGAATATCCTGTT – 3’

REFERENCES

Adzhubei IA, Schmidt S, Peshkin L, et al (2010) A method and server for predicting damaging missense mutations. Nat. Methods 7:248–249

Arakawa T, Tsumoto K (2003) The effects of arginine on refolding of aggregated proteins: Not facilitate refolding, but suppress aggregation. Biochem Biophys Res Commun 304:148–152. https://doi.org/10.1016/S0006-291X(03)00578-3

Barnerias C, Saudubray JM, Touati G, et al (2010) Pyruvate dehydrogenase complex deficiency: Four neurological phenotypes with differing pathogenesis. Dev Med Child Neurol 52:e1–e9. https://doi.org/10.1111/j.1469-8749.2009.03541.x

Baynes BM, Wang DIC, Trout BL (2005) Role of arginine in the stabilization of proteins against aggregation. Biochemistry 44:4919–4925. https://doi.org/10.1021/bi047528r

Berg A, Westphal AH, Bosma HJ, De Kok A (1998) Kinetics and specificity of reductive acylation of wild-type and mutated lipoyl domains of 2-oxo-acid dehydrogenase complexes from Azotobacter vinelandii. Eur J Biochem 252:45–50. https://doi.org/10.1046/j.1432-1327.1998.2520045.x

Blass JP, Avigan J, Uhlendorf BW (1970) A defect in pyruvate decarboxylase in a child with an intermittent movement disorder. J Clin Invest 49:423–432. https://doi.org/10.1172/JCI106251

Brown GK, Otero LJ, LeGris M, Brown RM (1994) Pyruvate dehydrogenase deficiency. J Med Genet 31:875–879. https://doi.org/10.1136/jmg.31.11.875

Brown RM, Head RA, M AA, et al (2007) Pyruvate dehydrogenase E3 binding protein (protein X) deficiency. Dev Med Child Neurol 48:756–760. https://doi.org/10.1111/j.1469-8749.2006.tb01362.x

Byron O, Lindsay JG (2017) The pyruvate dehydrogenase complex and related assemblies in health and disease. In: Sub-Cellular Biochemistry. pp 523–550

Cate RL, Roche TE, Davis LC (1980) Rapid intersite transfer of acetyl groups and movement of pyruvate dehydrogenase component in the kidney pyruvate dehydrogenase complex. J Biol Chem 255:7556–62

Ciara E, Rokicki D, Halat P, et al (2016) Difficulties in recognition of pyruvate dehydrogenase complex deficiency on the basis of clinical and biochemical features. The role of next-generation sequencing. Mol Genet Metab reports 7:70–6. https://doi.org/10.1016/j.ymgmr.2016.03.004

Clot JP, Benelli C, Fouque F, et al (1992) Pyruvate dehydrogenase activity is stimulated by growth hormone (GH) in human mononuclear cells: A new tool to measure GH responsiveness in man. J Clin Endocrinol Metab 74:1258–1262. https://doi.org/10.1210/jcem.74.6.1592868

Debray FG, Mitchell GA, Allard P, et al (2007) Diagnostic accuracy of blood lactate-to-pyruvate molar ratio in the differential diagnosis of congenital lactic acidosis. Clin Chem 53:916–921. https://doi.org/10.1373/clinchem.2006.081166

DeBrosse SD, Okajima K, Zhang S, et al (2012) Spectrum of neurological and survival outcomes in pyruvate dehydrogenase complex (PDC) deficiency: Lack of correlation with genotype. Mol Genet Metab 107:394–402. https://doi.org/10.1016/j.ymgme.2012.09.001

Ferriero R, Brunetti-Pierri N (2013) Phenylbutyrate increases activity of pyruvate dehydrogenase complex. Oncotarget 4:804–805

Fouque F, Brivet M, Boutron A, et al (2003) Differential effect of DCA treatment on the pyruvate dehydrogenase complex in patients with severe PDHC deficiency. Pediatr Res 53:793–799. https://doi.org/10.1203/01.PDR.0000057987.46622.64

Gray LR, Tompkins SC, Taylor EB (2014) Regulation of pyruvate metabolism and human disease. Cell Mol Life Sci 71:2577–2604. https://doi.org/10.1007/s00018-013-1539-2

Harris RA, Bowker-Kinley MM, Wu P, et al (1997) Dihydrolipoamide dehydrogenase-binding protein of the human pyruvate dehydrogenase complex. DNA-derived amino acid sequence, expression, and reconstitution of the pyruvate dehydrogenase complex. J Biol Chem 272:19746–19751. https://doi.org/10.1074/jbc.272.32.19746

Imbard A, Boutron A, Vequaud C, et al (2011) Molecular characterization of 82 patients with pyruvate dehydrogenase complex deficiency. Structural implications of novel amino acid substitutions in E1 protein. Mol Genet Metab 104:507–16. https://doi.org/10.1016/j.ymgme.2011.08.008

Marsac C, Stansbie D, Bonne G, et al (1993) Defect in the lipoyl-bearing protein X subunit of the pyruvate dehydrogenase complex in two patients with encephalomyelopathy. J Pediatr 123:915–920. https://doi.org/10.1016/S0022-3476(05)80387-7

Naito E, Ito M, Yokota I, et al (2002) Thiamine-responsive pyruvate dehydrogenase deficiency in two patients caused by a point mutation (F205L and L216F) within the thiamine pyrophosphate binding region. Biochim Biophys Acta - Mol Basis Dis 1588:79–84. https://doi.org/10.1016/S0925-4439(02)00142-4

Nogueira C, Silva L, Pereira C, et al (2019) Targeted next generation sequencing identifies novel pathogenic variants and provides molecular diagnoses in a cohort of pediatric and adult patients with unexplained mitochondrial dysfunction. Mitochondrion 47:309–317. https://doi.org/10.1016/j.mito.2019.02.006

Pastoris O, Savasta S, Foppa P, et al (1996) Pyruvate dehydrogenase deficiency in a child responsive to thiamine treatment. Acta Paediatr Int J Paediatr 85:625–628. https://doi.org/10.1111/j.1651-2227.1996.tb14104.x

Patel KP, O'Brien TW, Subramony SH, et al (2012) The spectrum of pyruvate dehydrogenase complex deficiency: Clinical, biochemical and genetic features in 371 patients. Mol Genet Metab 106:385–394. https://doi.org/10.1016/j.ymgme.2012.03.017

Patel MS, Harris RA (1995) Mammalian alpha-keto acid dehydrogenase complexes: gene regulation and genetic defects. FASEB J 9:1164–72. https://doi.org/10.1096/fasebj.9.12.7672509

Patel MS, Korotchkina LG (2006) Regulation of the pyruvate dehydrogenase complex. In: Biochemical Society Transactions. pp 217–222

Pavlu-Pereira H, Lousa D, Tomé CS, et al (2021) Structural and functional impact of clinically relevant E1α variants causing pyruvate dehydrogenase complex deficiency. Biochimie 183:78–88. https://doi.org/10.1016/j.biochi.2021.02.007

Pinheiro A, Silva MJ, Pavlu-Pereira H, et al (2016) Complex genetic findings in a female patient with pyruvate dehydrogenase complex deficiency: Null mutations in the PDHX gene associated with unusual expression of the testis-specific PDHA2 gene in her somatic cells. Gene 591:417–424. https://doi.org/10.1016/j.gene.2016.06.041

Prajapati S, Haselbach D, Wittig S, et al (2019) Structural and Functional Analyses of the Human PDH Complex Suggest a "Division-of-Labor" Mechanism by Local E1 and E3 Clusters. Structure 27:1124-1136.e4. https://doi.org/10.1016/j.str.2019.04.009

Quintana E, Gort L, Busquets C, et al (2010) Mutational study in the PDHA1 gene of 40 patients suspected of pyruvate dehydrogenase complex deficiency. Clin Genet 77:474–482. https://doi.org/10.1111/j.1399-0004.2009.01313.x

Robinson JN, Norwitz ER, Mulkern R, et al (2001) Prenatal diagnosis of pyruvate dehydrogenase deficiency using magnetic resonance imaging. Prenat Diagn 21:1053–1056. https://doi.org/10.1002/pd.187

Shin HK, Grahame G, McCandless SE, et al (2017) Enzymatic testing sensitivity, variability and practical diagnostic algorithm for pyruvate dehydrogenase complex (PDC) deficiency. Mol Genet Metab 122:61–66. https://doi.org/10.1016/j.ymgme.2017.09.001

Silva MJ, Pinheiro A, Eusébio F, et al (2009) Pyruvate dehydrogenase deficiency: identification of a novel mutation in the PDHA1 gene which responds to amino acid supplementation. Eur J Pediatr 168:17–22. https://doi.org/10.1007/s00431-008-0700-7

Sofou K, Dahlin M, Hallböök T, et al (2017) Ketogenic diet in pyruvate dehydrogenase complex deficiency: short- and long-term outcomes. J Inherit Metab Dis 40:237–245. https://doi.org/10.1007/s10545-016-0011-5

Song J, Jordan F (2012) Interchain acetyl transfer in the E2 component of bacterial pyruvate dehydrogenase suggests a model with different roles for each chain in a trimer of the homooligomeric component. Biochemistry 51:2795–2803. https://doi.org/10.1021/bi201614n

Sperl W, Fleuren L, Freisinger P, et al (2015) The spectrum of pyruvate oxidation defects in the diagnosis of mitochondrial disorders. J Inherit Metab Dis 38:391–403. https://doi.org/10.1007/s10545-014-9787-3

Szabo E, Wilk P, Nagy B, et al (2019) Underlying molecular alterations in human dihydrolipoamide dehydrogenase deficiency revealed by structural analyses of disease-causing enzyme variants. Hum Mol Genet. https://doi.org/10.1093/hmg/ddz177

Tsumoto K, Umetsu M, Kumagai I, et al (2004) Role of arginine in protein refolding, solubilization, and purification. Biotechnol. Prog. 20:1301–1308

Vijayakrishnan S, Callow P, Nutley MA, et al (2011) Variation in the organization and subunit composition of the mammalian pyruvate dehydrogenase complex E2/E3BP core assembly. Biochem J 437:565–74. https://doi.org/10.1042/BJ20101784

Vitkup D, Sander C, Church GM (2003) The amino-acid mutational spectrum of human genetic disease. Genome Biol 4:R72. https://doi.org/10.1186/gb-2003-4-11-r72

Waterhouse A, Bertoni M, Bienert S, et al (2018) SWISS-MODEL: Homology modelling of protein structures and complexes. Nucleic Acids Res 46:W296–W303. https://doi.org/10.1093/nar/gky427

Wexler ID, Hemalatha SG, McConnell J, et al (1997) Outcome of pyruvate dehydrogenase deficiency treated with ketogenic diets. Studies in patients with identical mutations. Neurology 49:1655–61. https://doi.org/10.1212/wnl.49.6.1655

Whitley MJ, Arjunan P, Nemeria NS, et al (2018) Pyruvate dehydrogenase complex deficiency is linked to regulatory loop disorder in the αV138M variant of human pyruvate dehydrogenase. J Biol Chem 293:13204–13213. https://doi.org/10.1074/jbc.RA118.003996

Chapter IV

Structural and Functional Impact of Clinically Relevant E1α Variants Causing Pyruvate Dehydrogenase Complex Deficiency

Hana Pavlů-Pereira[1], Diana Lousa[2], Catarina S. Tomé[1,2], Cristina Florindo[1], Maria João Silva[1], Isabel Tavares de Almeida[1], Paula Leandro[1], Isabel Rivera[1], João B. Vicente[2]

[1] *Research Institute for Medicines (iMed.ULisboa) and Department of Biochemistry and Human Biology, Faculty of Pharmacy, Universidade de Lisboa, Lisbon, Portugal*

[2] *Instituto de Tecnologia Química e Biológica António Xavier, Universidade Nova de Lisboa, Oeiras, Portugal*

Biochimie ***183****, 78-88 (2021)*

IV.1. ABSTRACT

Pyruvate dehydrogenase complex (PDC) catalyzes the oxidative decarboxylation of pyruvate to acetyl-coenzyme A, hinging glycolysis and the tricarboxylic acid cycle. PDC deficiency, an inborn error of metabolism, has a broad phenotypic spectrum. Symptoms range from fatal lactic acidosis or progressive neuromuscular impairment in the neonatal period, to chronic neurodegeneration. Most disease-causing mutations in PDC deficiency affect the PDHA1 gene, encoding the α subunit of the PDC-E1 component. Detailed biophysical analysis of pathogenic protein variants is a challenging approach to support the design of therapies based on improving and correcting protein structure and function. Herein, we report the characterization of clinically relevant PDC-E1a variants identified in Portuguese PDC deficient patients. These variants bear amino acid substitutions in different structural regions of PDC-E1a. The structural and functional analyses of recombinant heterotetrameric (αα'ββ') PDC-E1 variants, combined with molecular dynamics (MD) simulations, show a limited impact of the amino acid changes on the conformational stability, apart from the increased propensity for aggregation of the p.R253G variant as compared to wild-type PDC-E1. However, all variants presented a functional impairment in terms of lower residual PDC-E1 enzymatic activity and ≈3-100× lower affinity for the thiamine pyrophosphate (TPP) cofactor, in comparison with wild-type PDC-E1. MD simulations neatly showed generally decreased stability (increased flexibility) of all variants with respect to the WT heterotetramer, particularly in the TPP binding region. These results are discussed in light of disease severity of the patients bearing such mutations and highlight the difficulty of developing chaperone-based therapies for PDC deficiency.

IV.2. INTRODUCTION

Pyruvate oxidation constitutes a fundamental pathway in aerobic energy metabolism. The key step in this route is catalyzed by the mitochondrial pyruvate dehydrogenase complex (PDC) that irreversibly converts pyruvate to acetyl-coenzyme A with concomitant reduction of nicotine adenine dinucleotide (NAD^+) (Figure IV-1). This highly organized enzyme complex comprises multiple copies of three catalytic subunits and one structural component: pyruvate dehydrogenase (E1), dihydrolipoyl-lysine-residue acetyltransferase (E2), dihydrolipoyl

dehydrogenase (E3) and E3 binding protein (E3BP) (Zhou et al. 2001; Patel and Korotchkina 2006; Yu et al. 2008; Jiang et al. 2018). Human PDC employs five cofactors/co-substrates, namely thiamine pyrophosphate (TPP), lipoic acid, coenzyme A, flavin adenine dinucleotide (FAD) and NAD^+, and is tightly regulated by pyruvate dehydrogenase kinases (PDKs) and pyruvate dehydrogenase phosphatases (PDPs), both acting on the PDC-E1 component.

PDC deficiency can result from mutations in the genes encoding the different subunits of the complex. Its broad phenotypic spectrum ranges from fatal lactic acidosis or progressive neurological and neuromuscular degradation in the neonatal period, to a chronic neurodegenerative condition. Current therapies are limited to ketogenic diet which stimulates alternative pathways for energy production (Wexler et al. 1997), vitamin supplementation (Pastoris et al. 1996) and administration of dichloroacetate or phenylbutyrate to block PDC phosphorylation, thus activating the complex (Fouque et al. 2003; Ferriero et al. 2013). The ketogenic diet, which may be useful to control childhood-onset epilepsy or paroxysmal dystonia if not started too late, may otherwise prove inefficient.

The PDC-E1 component (EC 1.2.4.1) assembles as a heterotetramer comprising two α and two β subunits (αα'ββ') and nearly 75% of disease-causing mutations in PDC deficiency affect the α subunit of PDC-E1 (E1α) encoded by *PDHA1* (HGNC ID 8806) mapping to region Xp22.12. Its 1173-bp coding sequence (CDS) encodes a precursor protein which includes an N-terminal 29-amino acids mitochondria-targeting signal peptide (Ho et al. 1989). The funnel-shaped tunnels formed at each α/β interface of the αα'ββ' tetrahedral arrangement accommodate two active sites and grant access to the lipoyl-lysine moiety of the PDC-E2 component during the catalytic reaction. Correct incorporation of the TPP cofactor necessary for the catalytic reaction involves interactions between α and β subunits of both heterodimers in each heterotetramer. TPP is used to cleave the Cα-C(=O) bond of pyruvate followed by reductive acetyl transfer to lipoyl-dihydrolipoamide acetyltransferase. The α/β channel contains two phosphorylation loops (A and B) harboring the E1α phosphorylation sites 1, 2 and 3 (respectively, S293, S300 and S232) that regulate enzymatic activity (Korotchkina and Patel 2001a; Ciszak et al. 2003; Kato et al. 2008; Byron and Lindsay 2017).

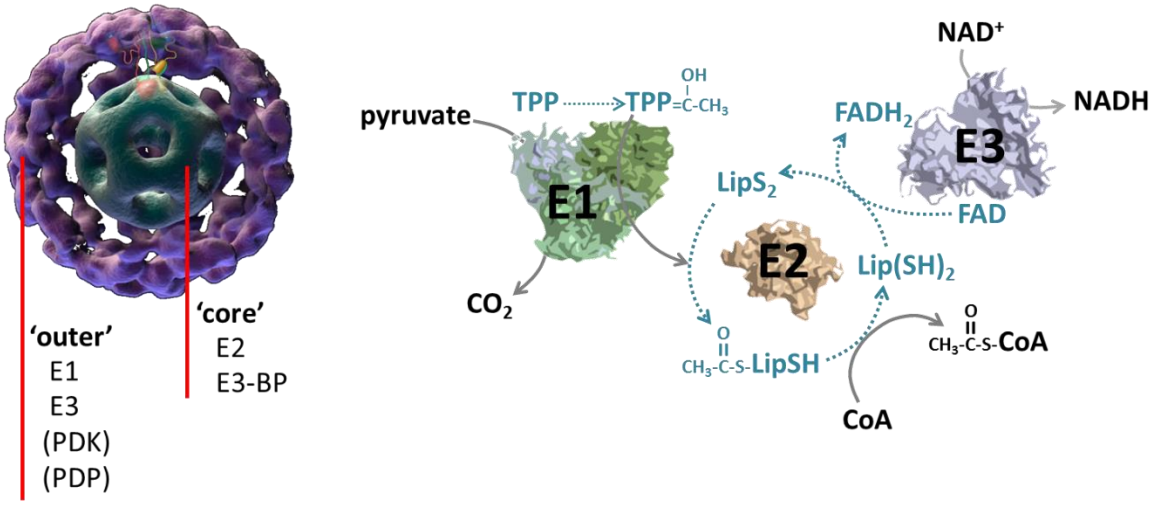

Figure IV-1 **Pyruvate dehydrogenase complex assembly and associated reactions.** Human pyruvate dehydrogenase complex is a ≤11-MDa assembly comprising multiple subunits in a variable stoichiometry: the 60-meric pentagonal E2/E3BP dodecahedron is surrounded by a flexible shell comprising 20-30 E1 heterotetramers and 6-12 E3 homodimers with addition of multiple copies of regulatory PDKs and PDPs units (Sumegi et al. 1987; Zhou et al. 2001; Byron and Lindsay 2017; Golias et al. 2019). PDC-E1 catalyzes the first, rate-limiting and irreversible oxidative decarboxylation of pyruvate, which requires a thiamine pyrophosphate (TPP) cofactor and is coupled to the reductive acetylation of the lipoamide cofactor ($LipS_2$). The released acetyl group is transferred from TPP to a lipoate moiety covalently bound to PDC-E2, then subsequently to CoA, forming acetyl-CoA and dihydrolipoate. The lipoate moieties are sequentially transferred between the PDC-E1, PDC-E2, and PDC-E3 active sites via a 'swinging arm' mechanism. The lipoate group is regenerated from dihydrolipoate by PDC-E3. The oxidation of dihydrolipoate results in the reduction of FAD to $FADH_2$ and a subsequent reduction of NAD^+ which enables FAD regeneration (Cate et al. 1980; Berg et al. 1998; Milne 2002; Odièvre et al. 2005; Smolle et al. 2006; Seifert et al. 2007; Brautigam et al. 2009). PDC structure by Sriram Subramaniam, available through National Cancer Institute (NCI), Research in NIH Labs and Clinics. Structures of PDC-E1, PDC-E2 and PDC-E3 generated with Pymol (DeLano Scientific, San Carlos, USA), using the PDB codes 3EXE (Whitley et al. 2018), 6ZLO (Forsberg et al. 2020) and 6I4T (Szabo et al. 2019), respectively.

Considering the high prevalence of missense mutations usually leading to protein misfolding, inborn errors of metabolism are recognized as conformational disorders (Gregersen et al. 2006). Detailed structural and functional analyses of misfolded protein variants is opening avenues for designing new therapies based on the rescue of protein structure and function (Yue 2016). In PDC-E1α deficiency (ORPHAN 79243; OMIM 312170) missense mutations account for ≥ 60 % of the identified DNA changes (Patel et al. 2012). Yet, the impact of these missense mutations has thus far been mainly predicted *in silico* (Imbard et al. 2011), only a limited

number of E1α variants having been functionally and structurally characterized *in vitro* (Tripatara et al. 1999; Jacobia et al. 2001; Drakulic et al. 2018; Whitley et al. 2018).

In the present work, we investigated the structural and functional properties of PDC-E1α variant proteins p.F205L, p.R253G, p.R378C and p.R378H identified in Portuguese PDC deficient patients and resulting from *PDHA1* missense mutations. While the mutations generating the p.F205L, p.R378C and p.R378H variants have been reported in different patient populations at variable frequencies (respectively, 4.5-7.7 %, 1.5-23.1%, and 6.1-9.4%) (Lissens et al. 2000; Imbard et al. 2011; Patel et al. 2012; Pavlu-Pereira et al. 2020), the p.R253G is thus far unique to the Portuguese population. Using the biologically active recombinant heterotetrameric PDC-E1 form produced in *Escherichia* (*E.*) *coli*, we observed overall subtle perturbations in protein folding and stability, except for the aggregation prone p.R253G variant, whereas the mutations significantly affected enzymatic activity and the affinity for the TPP cofactor.

IV.3. MATERIALS AND METHODS

IV.3.1. Cloning and Mutagenesis

IV.3.1.1. Development of a pET-28b-based Bicistronic Expression System

The plasmids with cloned human PDC E1α cDNA (*PDHA1*, GenBank ID5160, NM_000284.3) and PDC E1β cDNA (*PDHB*, GenBank ID5162, NM_000925.3), respectively starting from positions 233 and 134, lacking the sequences encoding the signaling peptides, were a kind gift from Prof. M.S. Patel, State University of New York at Buffalo, NY (USA). To produce the heterotetrameric PDC-E1 (αα'ββ') proteins in *E. coli*, a pET28b based bicistronic expression system was obtained (pET-28b-hPDC-E1) where each cDNA was under the control of a T7 promoter. A sequence encoding a hexa-histidine tag was present 5' to the E1α subunit cDNA and the T7 terminator was localized 3' to the E1β subunit-encoding cDNA (Supplementary figure IV-S1).

IV.3.1.2. Site-Directed Mutagenesis

The studied mutations were introduced into the wild-type (WT) pET-28b-hPDC-E1 bicistronic expression vector using QuikChange II XL Site-Directed Mutagenesis Kit (Agilent Technologies, USA) and the primers in Supplementary Table 1. The complete sequences encoding both E1α and E1β subunits in every variant-expressing construct were verified by bi-directional Sanger´s sequencing (list of sequencing primers in Supplementary Table 1).

IV.3.2. Expression and Purification of recombinant Human PDC-E1 Variants

For optimization of protein production, cell growth conditions were screened regarding: *E. coli* host strain (BL21(DE3) vs BL21(DE3) Rosetta), growth media (Luria-Bertani Broth vs M9 Minimal Medium (Maniatis et al. 1982), supplemented with 1 mM $MgSO_4$, 100 µM $CaCl_2$ and 0.4% glucose), isopropyl β-D-1-thiogalactopyranoside (IPTG) concentration (1 mM vs 400 µM), thiamine hydrochloride concentration (600 µM vs 300 µM), protein expression temperature (37 vs 30 °C) and induction period (4 h vs over-night). Expression conditions were selected based on SDS-PAGE analysis. Accordingly, transformed *E. coli* BL21 (DE3) Rosetta cells were cultured at 37 °C in M9 medium. After cell density reached $A_{600nm}\approx0.3$, protein expression was induced by 400 µM IPTG, together with 600 µM thiamine hydrochloride. Following induction, cells were transferred to 30 °C and harvested after 4 h incubation.

Bacterial cells were resuspended in buffer A (50 mM potassium phosphate buffer; 300 mM KCl; 10% glycerol; pH 7.5) containing 1 $mg \cdot mL^{-1}$ lysozyme, 1 mM phenylmethanesulfonyl fluoride and 1 $mg \cdot L^{-1}$ DNaseI and disrupted by sonication as described in Ref. (Mendes et al. 2014). The cellular lysate was clarified by centrifugation (8,000 ×g, 8 min, 4 °C), and the His-tagged recombinant proteins were purified by immobilized metal affinity chromatography using a 1-mL HisTrap™ High-Performance column (GE Healthcare, USA) and eluted with increasing imidazole concentrations up to 500 mM in buffer A. The purified His-tagged proteins were then loaded into a 16/600 HiLoad Superdex S200 column (GE Healthcare) on an ÅKTA-Prime system (GE Healthcare) at 4 °C equilibrated and eluted at 0.6–0.7 $mL \cdot min^{-1}$ with Buffer A, to isolate the PDC-E1 heterotetramer. Protein purity was analyzed by SDS-PAGE and the protein concentration determined by the Bradford assay (Bradford 1976). Pure PDC-E1 protein batches were aliquoted and stored at -80 °C until further usage.

IV.3.3. Far-UV Circular Dichroism

Far-UV circular dichroism (CD) spectra and thermal denaturation profiles were recorded in a Jasco J-815 spectropolarimeter (Easton, MD, USA) equipped with a Jasco CDF-426S Peltier temperature controller, in a 0.1 cm path quartz cuvette. Samples were diluted to 0.15 $mg \cdot mL^{-1}$ in buffer A. Spectra were acquired at 20 °C as follows: eight accumulations; 50 $nm \cdot min^{-1}$ scan rate; data pitch 0.5 nm; data integration time (DIT) 1 s; bandwidth 1 nm; N_2 flow 8 $L \cdot min^{-1}$. The experimental setup for thermal denaturation profiles was: λ=222 nm; temperature range 20-90 °C; 1 $°C \cdot min^{-1}$ gradient; data pitch 0.5 °C; DIT 1 s; bandwidth 1 nm; N_2 flow 4 $L \cdot min^{-1}$. Thermal denaturation curves were analyzed with Graphpad Prism (Graphpad Software Inc., CA, USA), fitting the data to a monophasic sigmoidal curve. Melting temperatures (T_m) were determined as the inflexion points from the fitted sigmoidal thermal denaturation curves.

IV.3.4. Differential Scanning Fluorimetry

Differential scanning fluorimetry (DSF) assays were performed in a C1000 Touch thermal cycler equipped with a CFX96 optical reaction module (Bio-Rad, Hercules, CA, USA). Wild-type and PDC-E1 variants at 0.1 $mg \cdot mL^{-1}$ (≈0.66 μM in tetramer) in buffer A were mixed with SYPRO orange (Invitrogen Corporation, Carlsbad, CA, USA) at a 5× working concentration (Niesen et al. 2007), in a 50 μL total reaction volume. Data were acquired using the system setup described in Ref. (Coelho et al. 2014) and analyzed with Graphpad Prism. Thermal denaturation curves were fitted to a monophasic sigmoidal function, the T_m values representing the inflexion points of each transition.

IV.3.5. Dynamic Light Scattering

Dynamic light scattering (DLS) data were acquired in a ZetaSizer Nano-S (Malvern Instruments, Malvern, UK) particle size analyzer, coupled to a Peltier temperature control unit, using a He–Ne laser as light source (633 nm). Samples were diluted in buffer A to 0.15 $mg \cdot mL^{-1}$ and centrifuged at 10,000 ×g for 4 min at 4 °C to remove large aggregates. Thermal aggregation profiles were obtained between 25 and 70 °C at 1 $°C \cdot min^{-1}$, recording particle size average,

distribution, and total scattering intensity. Data were processed using Zetasizer Nano DTS software v 7.12 (Malvern Instruments). From the software output, we analyzed separately the percentage of each oligomeric species employing the following size constraints: >20 nm, higher order oligomers or aggregates; 5-20 nm, tetramer; <5 nm, glycerol and other small molecules. Thermal aggregation data were fitted with a sigmoidal function, the aggregation temperature (T_{agg}) being defined as the midpoint of the transition. The aggregation kinetics was monitored at 37 °C for approximately 40 min. Data were fitted to a plateau followed by one phase decay (tetramers) or association (aggregates) equation, yielding the observed aggregation rates k_{agg}.

IV.3.6. Limited proteolysis by Trypsin

PDC-E1 samples were diluted in buffer A to 0.2 $mg \cdot mL^{-1}$ and incubated with trypsin (Sigma-Aldrich, MO, USA) at a 1:200 ratio (mass:mass) at 37 °C for 1h. At time intervals, the proteolysis was stopped by addition of soybean trypsin inhibitor (Sigma-Aldrich) (1:1.5 protease to inhibitor, mass ratio). Samples were analyzed by SDS-PAGE. The intensity of the gel bands was determined by densitometric analysis using ImageJ. The E1α band was normalized for that of E1β and data were fitted to a mono-exponential decay curve to obtain the observed proteolytic rate constant k_{obs}.

IV.3.7. Activity Assays

The PDC-E1 specific activity was determined according to a previously described spectrophotometric method (Korotchkina and Patel 2001b), with minor modifications. Briefly, pyruvate oxidative decarboxylation by PDC-E1 is monitored by the decrease in Abs_{600nm} caused by the phenazine methosulfate (PMS)-mediated reduction of the artificial two electron acceptor 2,6-dichlorophenolindophenol (DCPIP, ε_{600nm} = 20.7 $mM^{-1} \cdot cm^{-1}$). Assays were carried out at 37 °C, starting with a 4-min pre-incubation of a mixture containing PDC-E1 (100 µg) in buffer A, TPP (at different concentrations, up to 2 mM), 4 mM $MgCl_2$, 48 µM DCPIP, 1.5 mM PMS and 20% of Buffer B (100 mM potassium phosphate buffer, 10% glycerol, pH 7.0). The reaction was started by adding pyruvate (at different concentrations, up to 0.5 mM) to the pre-incubated mixture. DCPIP reduction was monitored on a Shimadzu UV1800 UV-Vis spectrophotometer (Shimadzu Corporation, Japan) equipped with a Shimadzu TCC-100 temperature-controlled

cell holder and a Starna 'Spinette' electronic cell stirrer. PDC-E1 specific activity was measured against a blank reaction containing thermally denatured WT PDC-E1 devoid of detectable enzymatic activity. One unit (U) of enzyme activity is defined as 1 nmol of reduced DCPIP (corresponding to 1 nmol of pyruvate becoming oxidized) formed per min per mg of protein. Kinetic parameters for pyruvate and TPP were obtained using variable concentrations of pyruvate (0-0.5 mM) or TPP (0-2 mM), at fixed concentrations of TPP (0.2 mM) and pyruvate (0.5 mM), respectively. Data were either fitted with the Michaelis-Menten equation, or with a sigmoidal equation accounting for allosteric cooperativity:

$$\mathrm{V} = V_{\max} \times \frac{[\mathrm{S}]^{\mathrm{h}}}{[S_{0.5}]^{\mathrm{h}} + [\mathrm{S}]^{\mathrm{h}}} \qquad \text{(equation 1)}$$

IV.3.8. *In silico* Analysis

The coordinates of human PDC-E1 (PDB ID: 3EXE) were loaded into PyMOL (DeLano Scientific, San Carlos, USA) and the mutagenesis tool was used to generate each amino acid substitution. All possible rotamers of the substituting residues and the resulting steric hindrances were analyzed. Complementary to this approach, the sequences of each variant were submitted to Swiss Model (Waterhouse et al. 2018) to obtain the corresponding structural models.

Molecular dynamics (MD) simulations were performed for the WT and the four PDC-E1 variants (p.R253G, p.R378C, p.R378H and p.F205L). The WT simulations used the X-ray structure of PDC-E1 bound to TPP as a starting point (PDB code 3EXE) (Kato et al. 2008) and the variants' simulations started from the structures generated with PyMOL's mutagenesis tool. Each system comprised the complex formed by the four PDC-E1 subunits (α, α', β and β') with two bound TPP molecules (one in each α subunit), two Mg^{2+} and two crystallographic K^+ ions. These systems were placed in a box with a distance of 10 Å between the protein and the box walls, solvated by water molecules and neutralized by the addition of K^+ ions. Three replicates were simulated for each system by assigning different starting velocities.

MD simulations were performed with the GROMACS (Berendsen et al. 1995) package version 2020.3 with an integration timestep of 2 fs and using periodic boundary conditions. The AMBER 14SB (Maier et al. 2015) force field was used to model the peptide and the TIP3P

model was used for water (Jorgensen et al. 1983). The TPP parameters were calculated with the Antechamber module (Wang et al. 2006) using the general Amber force field (GAFF) (Wang et al. 2004). A set of restrained electrostatic potential (RESP) (Bayly et al. 1993) atomic charges for TPP were calculated at the RHF/6-31+G(d) level using Gaussian 09 (M. J. Frisch, G. W. Trucks, H. B. Schlegel, G. E. Scuseria, M. A. Robb, J. R. Cheeseman, G. Scalmani, V. Barone, B. Mennucci, G. A. Petersson, H. Nakatsuji, M. Caricato, X. Li, H. P. Hratchian, A. F. Izmaylov, J. Bloino, G. Zheng, J. L. Sonnenberg, M. Had). A cutoff of 8 Å was used for nonbonded interactions. Long-range electrostatic interactions were treated with the Particle-mesh Ewald method (Darden et al. 1993), and a continuum model correction for energy and pressure was applied to long-range van der Waals interactions. Temperature coupling was applied separately to the protein+TPP+Mg^{2+} and solvent+K^{+} atoms, using the v-rescale algorithm (Bussi et al. 2007), setting the reference temperature to 300 K and using a temperature coupling constant of 0.1 ps. The pressure was kept at 1 bar using the Parrinelo-Rahman coupling scheme (Parrinello and Rahman 1981) with a coupling constant of 5 ps and an isothermal compressibility of 4.6×10^{-5} bar. Bonds formed by hydrogen atoms were constrained using the LINCS algorithm (Hess et al. 1997), and water molecules were constrained using the SETTLE algorithm (Miyamoto and Kollman 1992).

Three energy minimization steps were performed using the steepest descent algorithm. In the first step, all atoms were restrained with a force constant of 1000 kJ/mol $Å^2$ except the hydrogen atoms. In the second step, only C-α atoms were restrained with the same force constant and in the last step no restrains were used. The simulations were initialized using a four-step procedure. In the first 100 ps, velocities were generated from a Boltzmann distribution at 300 K, all the heavy atoms were restrained, and the simulation was performed in the NVT ensemble with a temperature coupling constant of 0.01 ps^{-1}. This was followed by 100 ps of simulation in the NVT ensemble, with a temperature coupling constant of 0.1 ps^{-1}, maintaining the restraints on the heavy atoms. In the following 100 ps of simulation, the pressure coupling was turned on using a coupling constant of 5 ps^{-1}, while keeping all the other parameters unchanged. In the final step, the restraints were applied only to the protein Cα atoms system was simulated for 100 ps in the same conditions used in the previous step. This initialization was followed by a production run, where the systems were simulated for 200 ns without any position restraints.

IV.4. RESULTS

IV.4.1. Production of Recombinant PDC-E1 Variants

Employing a bicistronic vector encoding both the E1α (WT and variants) and E1β (WT) subunits, all recombinant variants of human mature PDC-E1 were successfully purified with yields in the range of 1-2 mg of pure PDC-E1 heterotetramer per liter of culture, irrespectively of the mutation. Oligomeric profiles, monitored by size exclusion chromatography, exhibited three peaks corresponding to aggregates, heterotetramers, and dimers (mostly αα', rarely ββ'). The predominant oligomeric form corresponded to the αα'ββ' heterotetramer for the WT and studied PDC-E1α variants, except for p.F205L which was isolated mostly in the αα' dimeric form (Figure IV-2). Further analyses were performed using exclusively the purified, biologically active heterotetramers.

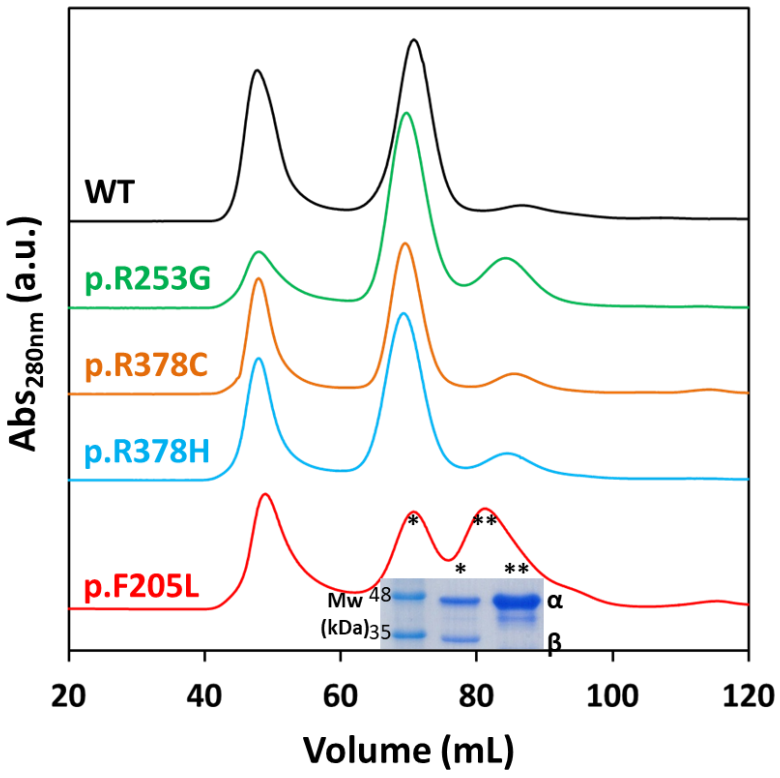

Figure IV-2 **Examples of size-exclusion chromatograms.** First peak corresponds to higher oligomers or aggregates, eluted near after the void volume; second peak, eluted at ≈70 mL, corresponds to the fraction of αα'ββ' heterotetramers; third peak, eluted at V≥81 mL, corresponding to homodimeric PDC-E1α and low molecular weight contaminants. Inset, SDS-PAGE analysis of eluted fractions corresponding to heterotetrameric (*) and αα' homodimeric (**) p.F205L variant.

IV.4.2. Effect of Selected Mutations on PDC-E1 Structure and Stability

WT PDC-E1 and all studied variants exhibited similar Far-UV CD spectra, exhibiting two broad bands with local minima at ≈210 nm and ≈222 nm (Figure IV-3A). Thermal denaturation profiles obtained by monitoring at 222 nm the unfolding of α-helical regions yielded a single transition for all proteins (Figure IV-3B). The corresponding T_m values (Table 1) only differed significantly from the WT protein for the variants with substitutions in R378 (ΔT_m = +2.4 °C for p.R378C; ΔT_m = +1.5 °C for p.R378H).

Resistance to thermal denaturation was also analyzed by DSF. Denaturation profiles of all studied proteins presented a single apparent transition (Figure IV-4). Data for WT PDC-E1 were best fitted with T_m = 40.4 ± 0.4 °C and all protein variants displayed T_m values quite similar to WT PDC-E1 (Table IV-1). Moreover, the fitted slopes and consequently the onset of denaturation temperatures were also nearly identical for all variants.

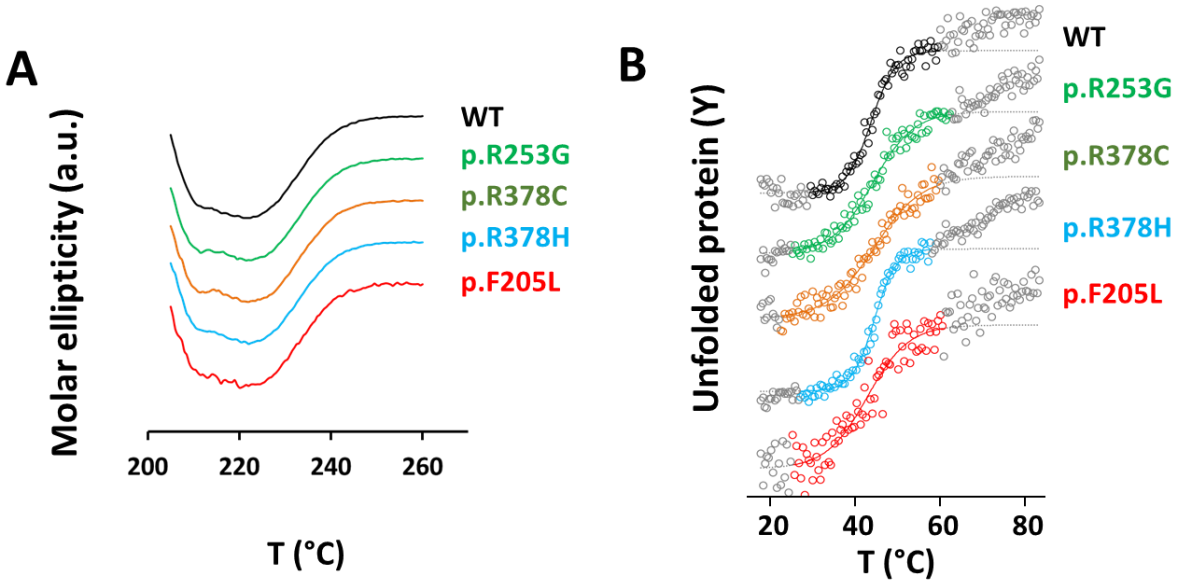

Figure IV-3 **Far-UV circular dichroism (CD) analysis of heterotetrameric WT and PDC-E1 variants.** (**a**) far-UV CD spectra of purified heterotetramers of WT and PDC-E1 variants. Similar spectra were obtained for all variants, indicating no significant changes in the content of secondary structure elements. Spectra resulting from 8 accumulations at 20 °C, at a 50 nm·min^{-1} scan rate, in a 0.1 cm light path cuvette; (**b**) thermal denaturation of purified heterotetramers of WT and PDC-E1 variants obtained by monitoring molar ellipticity at 222 nm with a linear temperature increase from 20 to 90 °C at 1 °C·min^{-1}, sampling 0.5 °C in a 0.1 cm light path cuvette. All proteins at 0.15 mg·mL^{-1} in buffer A.

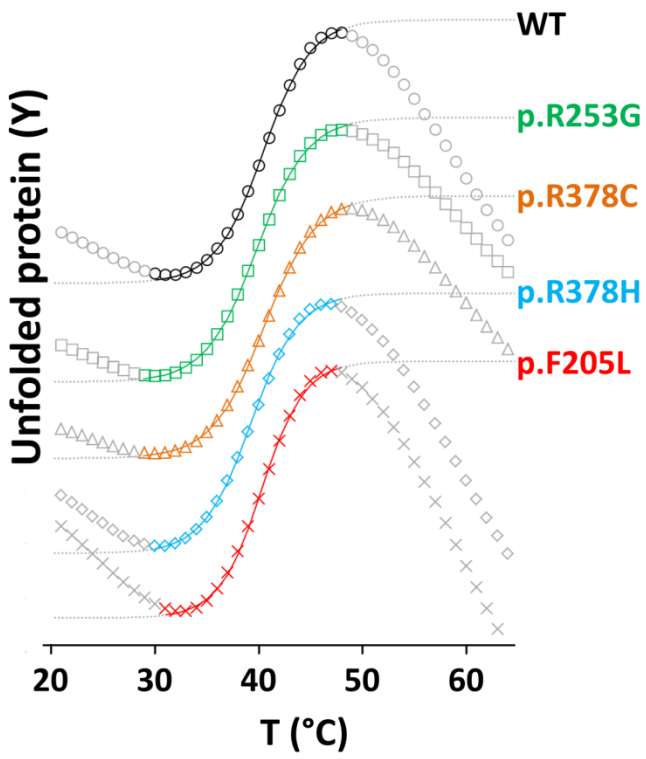

Figure IV-4 **Thermal stability of heterotetrameric WT and PDC-E1 variants.** Thermal denaturation profiles of WT and PDC-E1 variants obtained by differential scanning fluorimetry (DSF). DSF was performed in a 50 µL final volume containing 0.1 mg·mL^{-1} of protein in buffer A and 5× SYPRO Orange. After a 10-min incubation at 20 °C, temperature was linearly increased from 20 to 90 °C at 1 °C·min^{-1}. Fluorescence changes were recorded in the FRET channel. Data were best fitted with a monophasic sigmoidal function within the colored part of the curves.

IV.4.3. Effect of Selected Mutations on Proteolysis by Trypsin

Limited proteolysis by trypsin was employed to assess the impact of the mutations on the global conformational flexibility. Undigested PDC-E1 exhibited two bands corresponding to the α and β subunits (respectively, ≈43 and ≈35 kDa). While partial digestion of E1α was observed already at time 1 min, the E1β subunit appeared resistant to proteolysis at t≥20 min, when E1α already appeared considerably degraded (Figure IV-5A). Densitometric data corresponding to WT PDC-E1α proteolysis as a function of time (Figure IV-5B) were best fitted with a single exponential decay curve, yielding a proteolytic rate of 0.161 ± 0.035 min^{-1} (Table IV-1). The p.R253G and p.R378C variants were trypsin digested at slightly higher apparent

proteolytic rates (Table IV-1). The remaining variants exhibited a similar behavior to the WT protein (Figure IV-5B).

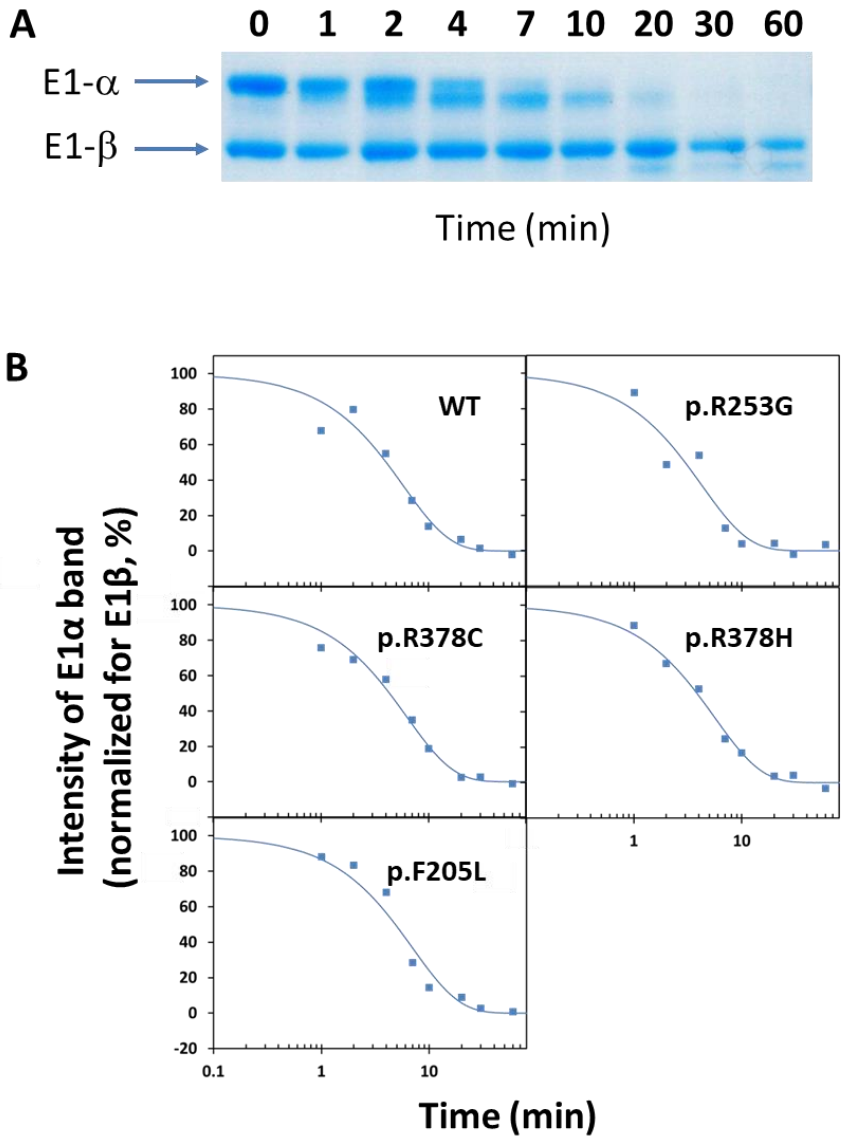

Figure IV-5 **Limited proteolysis by trypsin.** *Panel A*, example of SDS-PAGE (WT) demonstrates that partial digestion of E1α was observed immediately from the starting point, whereas E1β subunit appeared resistant to proteolysis at least up to 20 min, when E1α is already considerably degraded. *Panel B*, Global conformational changes of purified heterotetramers of WT and PDC-E1 variants, followed by limited proteolysis by trypsin. WT and PDC-E1 variants at a concentration of 0.2 mg.mL^{-1} in buffer A were incubated with trypsin at a ratio 1:200, at 37 °C, during 1h. Data best fitted to a single exponential decay curve.

IV.4.4. Propensity to Aggregation

Dynamic light scattering was employed to compare the propensity of the studied variants for aggregation. Three optically active species were detected in different particle size ranges (Figure IV-6) and assigned to different oligomeric arrangements or solution components, namely glycerol. Data were analyzed in terms of the relative fractions of tetramers and aggregates (or higher oligomers) as a function of temperature or time. Thermal aggregation profiles (Figure IV-7A) showed that for each variant the decrease in tetrameric species was accompanied by the increase in larger sized oligomers/aggregates, resulting in nearly identical estimated T_{agg} (Table IV-1). From the tested variants, only the p.R253G exhibited a lower T_{agg} value, when compared with the WT PDC-E1. Just like the thermal aggregation profiles, the kinetics of tetrameric species disappearance neatly coincided with that of higher oligomers/aggregates formation (Figure IV-7B; Table IV-1). Consistently with the thermal aggregation profiles, the p.R253G variant exhibited a higher susceptibility to isothermal aggregation than the WT enzyme. Moreover, the p.R378H variant also exhibited a slightly higher propensity to aggregation (Table IV-1).

Table IV-1 **Thermal and conformational stability and aggregation propensity** of clinically relevant PDC-E1 heterotetrameric variants.

	CD	DSF	DLS				
	Thermal denaturation		Thermal aggregation		Aggregation kinetics		Limited Proteolysis
			tetramer	aggregates	tetramer	aggregates	
	T_m (°C)	T_m (°C)	T_{agg} (°C)	T_{agg} (°C)	k_{agg} (min^{-1})	k_{agg} (min^{-1})	k_{obs} (min^{-1})
WT	46.8 ± 0.9	40.4 ± 0.4	40.0 ± 0.5	39.9 ± 0.5	0.145 ± 0.022	0.144 ± 0.028	0.161 ± 0.035
p.R253G	47.7 ± 0.9	39.9 ± 0.4	38.2 ± 0.4[a]	38.2 ± 0.5[a]	0.442 ± 0.120	0.485 ± 0.001	0.277 ± 0.025[aa]
p.R378C	49.2 ± 0.6[a]	40.5 ± 0.3	40.6 ± 0.1	40.6 ± 0.3	0.129 ± 0.048	0.126 ± 0.038	0.222 ± 0.030
p.R378H	48.3 ± 0.2[aa]	39.3 ± 0.2	39.0 ± 0.8	39.1 ± 0.9	0.217 ± 0.067	0.311 ± 0.001	0.122 ± 0.012[aa]
p.F205L	46.7 ± 0.1	40.4 ± 0.2	39.9 ± 0.6	39.7 ± 0.4	0.179 ± 0.035	0.186 ± 0.046	0.183 ± 0.028

CD, Far-UV circular dichroism (replicates from three independent protein batches, except for p.F205L, for which replicates were from two independent protein batches); DSF, differential scanning fluorimetry (replicates from two independent protein batches); DLS, dynamic light scattering (replicates from two independent protein batches).
Statistically significant difference between WT and variant; [a] $p < 0.0001$; [aa] $p < 0.005$
Statistical significance (p value) was determined using the Student's t test.

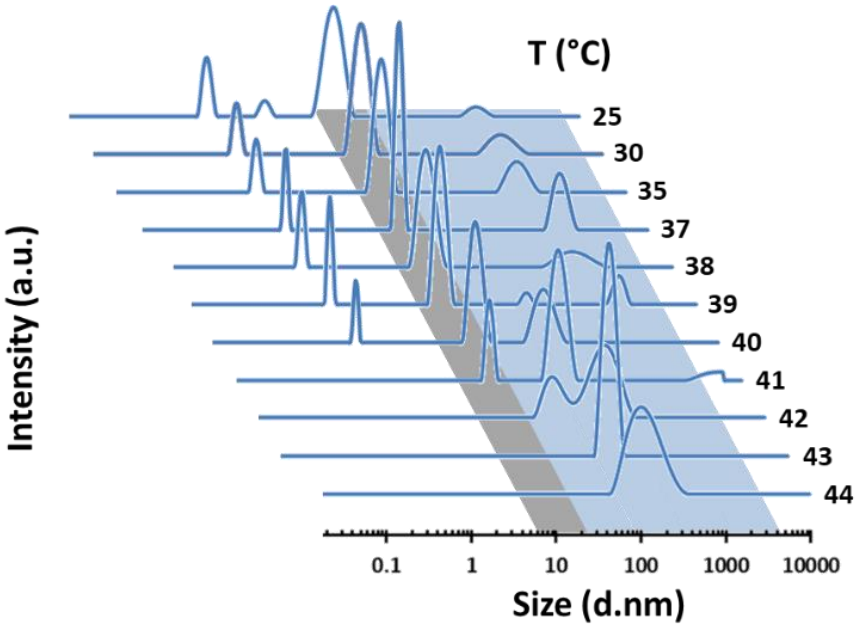

Figure IV-6 **Dynamic light scattering, size distribution by intensity.** Evolution of oligomeric species corresponding to different points of thermal aggregation curve (SMW solutes (e.g. glycerol) ≤ 1; heterotetramers = 5-20; higher oligomers / aggregates ≥ 50 d.nm).

IV.4.5. Functional Characterization of PDC-E1 Variants

The recombinant WT human PDC-E1 heterotetramer and the studied variants were functionally characterized employing the DCPIP assay, yielding kinetic parameters for the pyruvate substrate and the TPP cofactor (Table IV-2). As a control, we tested the homodimeric (αα') forms of PDC-E1α WT and variants and observed null enzymatic activity (*not shown*). The dependence of reaction velocity on pyruvate concentration, tentatively fitted with equation 1, displayed Michaelis-Menten-like saturation kinetics behavior (Figure IV-8), which was confirmed by the fitted *h* values close to 1 (*not shown*). Therefore, the data were refitted with Michaelis-Menten curves, yielding K_m values in the 40-50 μM range for the WT and all PDC-E1 variants, except for p.R378H, with a K_m of ≈20 μM. While the p.R253G variant exhibits a V_{max} for pyruvate ≈60 % of that measured for WT PDC-E1, the remaining variants have >10× lower V_{max} values. Perhaps the most interesting functional impairment regards the affinity for the TPP cofactor. Dependence of initial velocity on TPP concentration exhibited an obvious sigmoidal profile indicative of allosteric cooperativity (Figure IV-8B), in accordance with the fitted *h* values (Table IV-2).

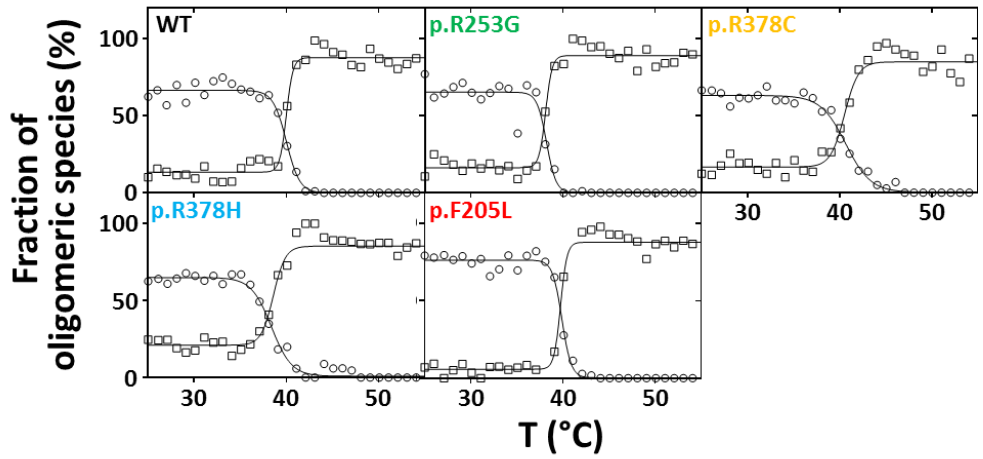

(a)

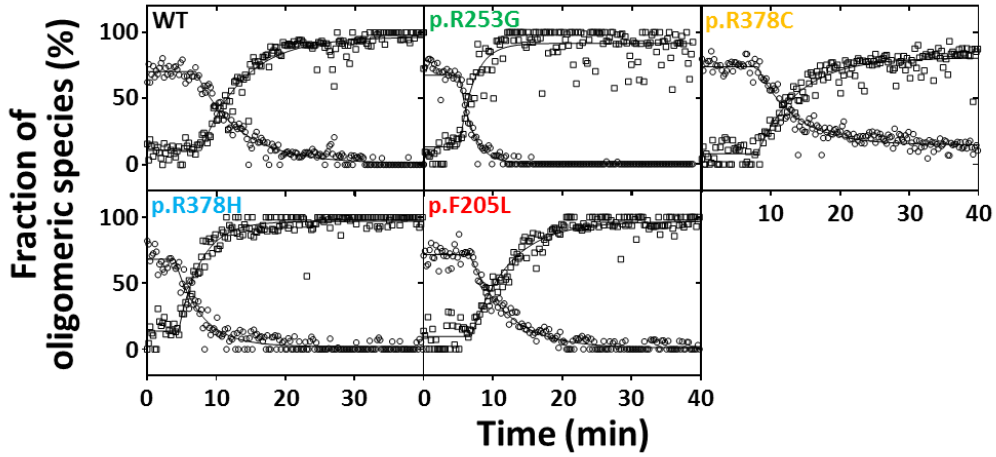

(b)

Figure IV-7 **Aggregation of WT and PDC-E1 variants analysed by dynamic light scattering.** Thermal aggregation (a) and kinetics of isothermal aggregation (b) of purified heterotetramers of WT and PDC-E1 variants monitored by dynamic light scattering. (a), thermal aggregation profile was assessed by a linear temperature increase from 25 to 70 °C at 1 °C·min^{-1}. Distribution of scattering intensity data was adapted to the progression of each oligomeric species (circles, heterotetramers; squares, higher oligomers/aggregates) fraction and normalized and fitted to a plateau followed by one phase association equation, the aggregation temperature (T_{agg}) being defined as the temperature of the starting point of the scattering intensity change belonging to each respective profile. (b), thermal aggregation kinetics followed at 37 °C during 40 min. Light scattering intensity data were assigned to each fraction of oligomeric species (circles, heterotetramers; squares, higher oligomers/aggregates), the aggregation coefficient k_{agg} being defined as the observed rate constant best fitting the formation (higher oligomers/aggregates) or disappearance (heterotetramers) of each oligomeric form. All protein samples were tested at 0.15 mg·mL^{-1} in buffer A.

Table IV-2 **Functional impact of PDC-E1 amino acid substitutions** in clinically relevant variants.

	Pyruvate[a]		TPP[b]			Residual activity (%)	
	V_{max} (U*)	K_M (µM)	V_{max} (U*)	*h*	$S_{0.5}$ (µM)	250 µM pyruvate 200 µM TPP [c]	500 µM pyruvate 50 µM TPP [d]
WT	306.5 ± 5.5	43.0 ± 2.6	257.0 ± 4.8	1.5 ± 0.1	4.9 ± 0.3	100	100
p.R253G	176.7 ± 2.3	42.3 ± 1.9	151.1 ± 5.3	2.2 ± 0.2	55.6 ± 3.0	58	24.8
p.R378C	24.0 ± 1.0	47.7 ± 6.7	21.7 ± 0.8	1.3 ± 0.1	15.4 ± 1.6	7.9	7
p.R378H	14.1 ± 0.8	19.9 ± 4.6	13.8 ± 0.7	1.4 ± 0.2	21.4 ± 2.8	4.9	4.4
p.F205L	24.1 ± 0.6	47.2 ± 4.0	153.0 ± 2.2	4.2 ± 0.3	475.5 ± 9.5	7.3	0

[a] Kinetic parameters for pyruvate obtained at a TPP fixed concentration of 0.2 mM
[b] Kinetic parameters for TPP obtained at a pyruvate fixed concentration of 0.5 mM
* 1 U = 1 nmol of reduced DCPIP (oxidized pyruvate) formed per min per mg of protein
[c] Enzymatic activity determined with 0.25 mM pyruvate, near saturation for WT PDC-E1 (Figure 5), at saturating TPP (0.2 mM)
[d] Enzymatic activity determined with 50 µM TPP, near saturation for WT PDC-E1 (Figure 5), at saturating pyruvate (0.5 mM)

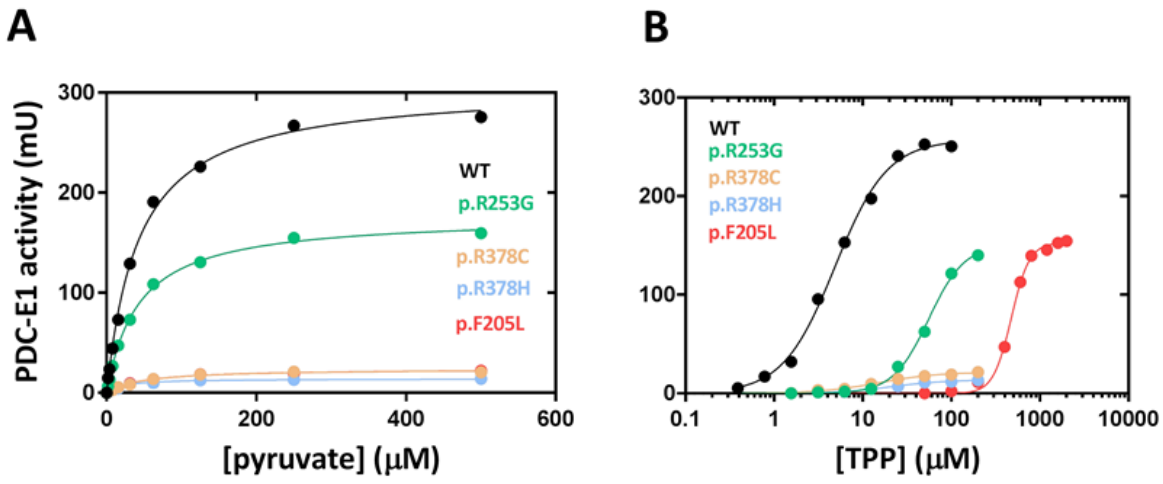

Figure IV-8 **Kinetic analysis of heterotetrameric WT and PDC-E1 variants.** PDC-E1-catalyzed pyruvate oxidative decarboxylation was measured in a spectrophotometer by monitoring the decrease in Abs_{600nm} resulting from DCPIP reduction. Assays were carried out at 37 °C. After a 4-min pre-incubation of WT or PDC-E1 variants (100 µg) in buffer A, TPP (*Panel A*, 0.2 mM; *Panel B*, 0-2 mM), 4 mM $MgCl_2$, 48 µM DCPIP, 1.5 mM PMS and 20% of Buffer B (100 mM potassium phosphate buffer, 10% glycerol, pH 7.0), the reaction was started by pyruvate addition (*Panel A*, 0-0.5 mM; *Panel B*, 0.5 mM). PDC-E1 specific activity was measured against a blank reaction containing thermally denatured WT PDC-E1 devoid of detectable enzymatic activity. One unit (U) of enzyme activity is defined as 1 nmol of oxidized pyruvate formed per min per mg of protein. Kinetic parameters were obtained by fitting the data with the Michaelis-Menten equation for pyruvate (*Panel A*) or with equation 1 for TPP, yielding sigmoidal curves accounting for allosteric cooperativity (*Panel B*).

While the p.R253G, p.R378C and p.R378H presented *h* values similar to the WT PDC-E1, the p.F205L displayed a much stronger apparent cooperativity. Importantly, all variants are characterized by a markedly lower affinity for the TPP cofactor, exhibiting 3-100× higher $S_{0.5}$ values. In terms of maximal velocity, both the p.R253G and the p.F205L variants exhibit V_{max} values for TPP ≈60 % of that measured for WT PDC-E1, while the p.R378C and p.R378H variants have >10× lower V_{max} values.

To better appreciate the functional impairment of each variant, we determined the residual activity of each variant at pyruvate or TPP concentrations near saturation for the WT PDC-E1 (Figure IV-8; Table IV-2). When compared with the WT PDC-E1 protein, all variants but the p.R253G exhibited near null residual PDC-E1 activity. While the p.R253G PDC-E1 may appear to be kinetically competent (58% of WT activity at near-saturation pyruvate concentrations), its reduced affinity for TPP makes its residual activity drop to ≈25 % of WT PDC-E1 activity.

IV.4.6. Molecular dynamics simulations of PDC-E1 variants

Molecular dynamics simulations were performed to obtain molecular insights into the effect of each mutation on the enzyme structure and dynamics. Three replicates of 200 ns were simulated for the WT and the different variants with bound TPP and the analysis focused on the last 100 ns, where the simulations are reasonably equilibrated. The average root mean square deviation (RMSD) of the protein Cα atoms shows that the WT structure is more stable than all the variants' structures, with p.F205L displaying the highest deviation from the X-ray structure (Figure IV-9A). The same trend is observed when focusing on the residues that interact with TPP in the X-ray structure, indicating that this region is destabilized by all the mutations (Figure IV-9B).

The inter-subunit contact surface shows that the WT has a larger contact surface, which is reduced in all the variants, particularly in p.F205L (Figure IV-10).

Mapping the RMSD of each residue on the protein structure revealed that both in the WT and in all the variants the most unstable region corresponds to loop A (Figure IV-11). In the variants, this region has a higher RMSD than in the WT, indicating that the mutations accentuate the instability of this region.

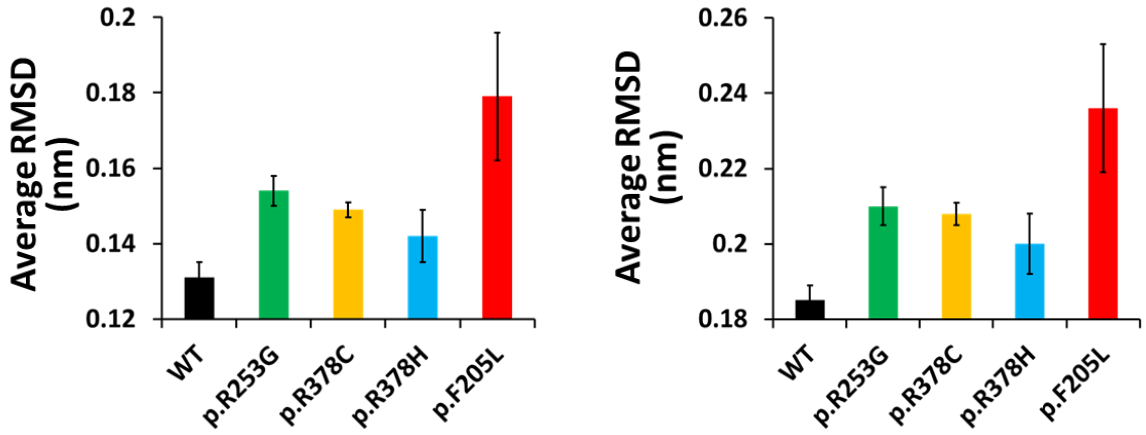

(a) (b)

Figure IV-9 **Average root mean square deviation (RMSD) of WT and PDC-E1 variants obtained in MD simulations.** The RMSD was calculated using the X-ray structure 3EXE as a reference and averaged over the last 100 ns of simulation across all the replicates for each variant. The error bars were calculated using a bootstrap method: for each variant, three new values were resampled with replacement from the original set of three replicates and their mean value was computed. This process was repeated 1000 times and the error was calculated as the standard deviation of these 1000 mean values. The RMSD was calculated over all the protein Cα atoms (Panel A) and over all the atoms of the residues which are within 4 Å from TPP in the X-ray structure (Panel B).

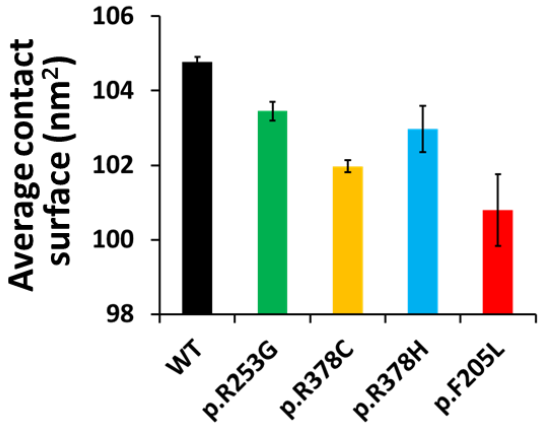

Figure IV-10 **Average inter-subunit contact surface of WT and PDC-E1 variants obtained in MD simulations.** The contact surface was computed by summing the solvent accessible surface area (SASA) for each individual subunit (as if they were not in contact with one another) and then subtracting the SASA obtained for the whole complex and dividing by 2. The average contact surface was obtained over the last 100 ns of simulation across all the replicates for each variant. The error bars were computed as described in Figure IV-9.

IV.5. DISCUSSION

Available approaches to PDC deficiency treatment are still scarce, and for most of them the therapeutic efficiency is limited. Detailed knowledge of the protein structure and function and comprehensive biochemical and biophysical characterization of clinically relevant protein variants set the bases for drug discovery and design of new pharmacological therapies for inherited metabolic disorders (Yue 2016). To investigate the molecular mechanisms underlying the pathogenic effect of *PDHA1* mutations present in Portuguese PDC deficient patients, we analyzed the recombinant p.F205L, p.R253G, p.R378C and p.R378H PDC-E1 variants.

The use of a heterologous bicistronic expression system and size-exclusion chromatography as the last purification step enabled the efficient production and isolation of the biologically active heterotetrameric PDC-E1 component from the inactive dimeric PDC-E1αα' and higher oligomers/ aggregates. Complementary biophysical methodologies allowed the comparative evaluation of the thermal and conformational stability of the recombinant proteins.

Far-UV CD spectra of WT PDC-E1 and variants revealed practically identical features consistent with predominantly α-helical globular proteins. The nearly identical spectra are in accordance with none of the amino acid substitutions seemingly affecting secondary structure elements (Figure IV-12). Accordingly, protein thermal denaturation monitored by far-UV CD revealed similar T_m values between WT PDC-E1 and the studied variants. Yet, the p.R378C and p.R378H variants exhibited slightly higher T_m values than WT, which is unusual in clinically relevant missense variants, since misfolding is typically accompanied by a decrease in resistance to thermal denaturation. DSF thermal denaturation profiles were quite similar among all studied proteins, overall characterized by 6-9 °C lower melting temperatures than those determined by far-UV CD. This difference is likely related to the structural elements analyzed by each methodology. Interestingly, both yielded thermal denaturation profiles with a single transition when two structurally different PDC-E1 subunits (α and β) become denatured, despite the sensitivity of both methods to detect even the independent denaturation of domains within single subunits (e.g. in Refs (Tomé et al. 2019; Zuhra et al. 2019)). This indicates that both subunits have identical melting temperatures and/or that they exhibit cooperative unfolding.

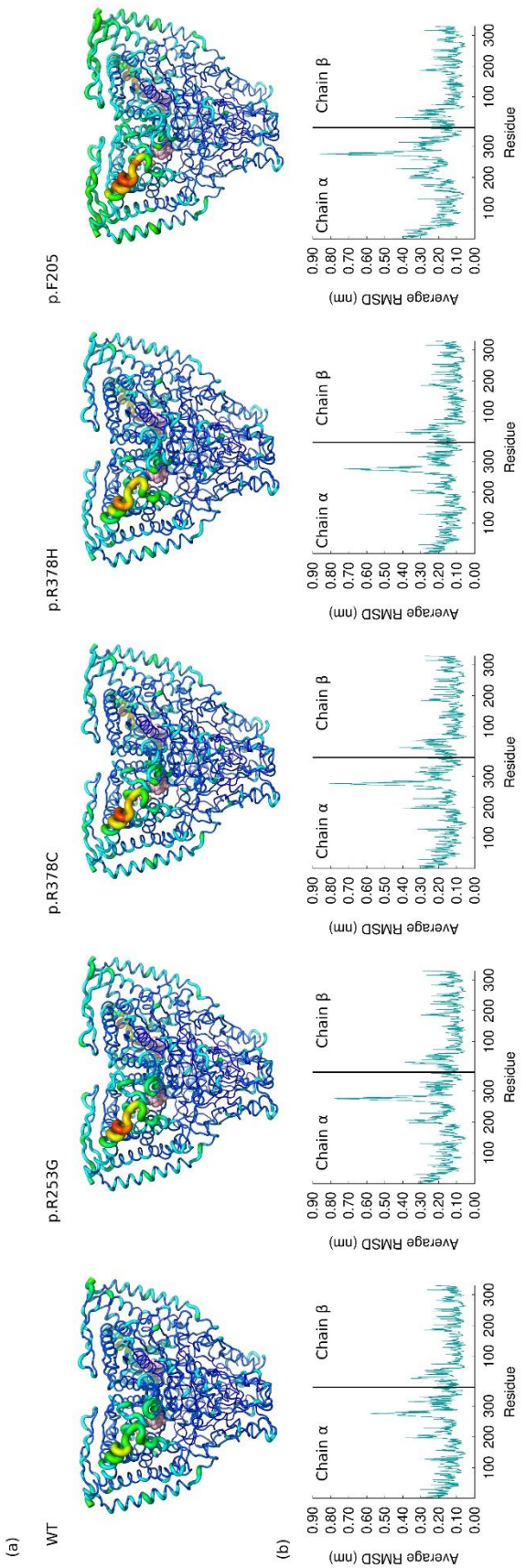

Figure IV-11 **Average root mean square deviation (RMSD) per residue of WT and PDC-E1 variants obtained in MD simulations.** The RMSD was calculated using the X-ray structure 3EXE as a reference and averaged over the last 100 ns of simulation across all the replicates for each variant. All the atoms of each residue were included in the calculation and the values were averaged over each pair of identical subunits (αα' and ββ'). The average RMSD values are mapped onto the protein structure using a color and cartoon-thickness gradient (thicker, red regions correspond to high RMSD values and thin dark blue regions correspond to low RMSD values), highlighting the TPP residue using pink spheres (*Panel A*). The average RMSD values per residue are plotted to enable a quantitative comparison (*Panel B*)

Despite the similar overall thermal stability of the p.R253G and p.R378C PDC-E1 variants when compared to the WT protein, these variants presented slightly higher proteolytic rates (k_{obs}) as determined by limited proteolysis. This is suggestive of a less compact structure (or more flexible conformation) of these variants, consistent with the respective amino acid substitutions being located at unstructured loops and the possible interactions disrupted by the amino acid substitutions.

Finally, the structural impact of the studied amino acid changes was also evaluated at the level of aggregation propensity. DLS allowed distinguishing and monitoring (as a function of linearly increasing temperature or as a function of time at a physiological temperature) the thermally induced conversion of active heterotetrameric PDC-E1 into inactive higher oligomers and/or aggregates. The most notable difference with respect to WT PDC-E1 was that of the p.R253G variant, which initiated aggregation at a lower temperature and aggregated ~3× faster (at 37 °C) than the WT protein. Disturbed aggregation associated with protein misfolding resulting from amino acid substitutions is a common feature in conformational disorders. A small change in a local environment may expose relatively unstable regions of a protein, thus contributing to its aggregation. The increased propensity for aggregation of the p.R253G variant is consistent with the observation that fibroblasts of a patient with a mutation encoding this variant exhibited nearly null expression of PDC-E1α and ≈10% PDC enzymatic activity of control cells (Silva et al. 2009). This suggests that p.R253G aggregation may result in protein degradation by the cellular protein quality control machinery.

At the functional level, while WT PDC-E1 displayed K_M and $S_{0.5}$ values, respectively for pyruvate and TPP, in the range of K_d values reported in the literature for pyruvate analogues (Seifert et al. 2007) and TPP (Roche and Reed 1972; Seifert et al. 2006; Kato et al. 2008), the clinically relevant recombinant PDC-E1 variants were functionally impaired. Indeed, the observed *in vitro* residual enzyme activities (determined at near saturation pyruvate and TPP concentrations for WT PDC-E1) neatly correlated with some of the patients' phenotypes, in what concerns disease severity. Indeed, the p.R378C and p.R378H variants presented nearly undetectable enzymatic activities, being associated with severe forms of disease (Patel et al. 2012). The p.R253G variant, exhibiting detectable activity, was identified in a patient with a mild phenotype (Dahl and Brown 1994; Naito et al. 2002; Silva et al. 2009). Cultured fibroblasts from patients expressing the p.F205L PDC-E1α variant exhibited very low PDC-E1 enzymatic

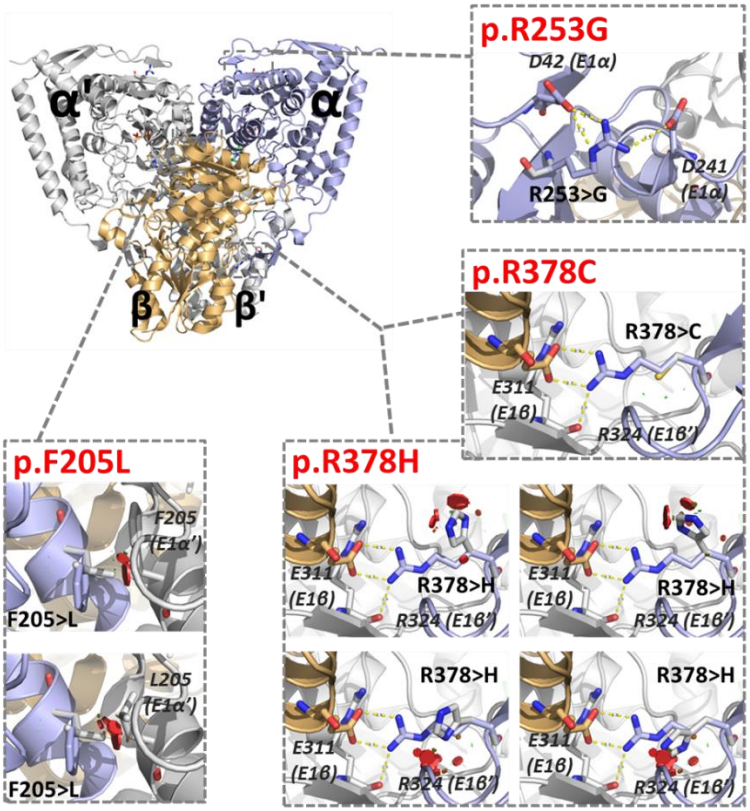

Figure IV-12 ***In silico*** **analysis of selected PDC-E1 variants.** Zoom-in on local effects of the selected amino acid substitutions in each PDC-E1 variant. Structural models of PDC-E1 variants were obtained by loading the structure of WT PDC-E1 (PDB entry 3EXE) into Pymol and applying the mutagenesis tool to generate all possible rotamers of the substituting amino acid side chains.

activity and responded positively to TPP (Dahl and Brown 1994; Naito et al. 2002), in full accordance to the results herein described. Notably, patients' phenotypes decreased in severity upon thiamine therapy (Naito et al. 2002), which neatly fits with the observed V_{max} for TPP of the p.F205L variant reaching ≈60 % of the WT value (Table IV-2). Besides the negative impact on the enzymatic activity, while the affinity for pyruvate remained essentially identical between the WT and PDC-E1 variants, a strong impact was observed on the affinity for the TPP cofactor. Indeed, while the p.R253G and p.F205L variants display the highest V_{max} for TPP among the studied variants, they also exhibit the lowest apparent affinity (respectively, ≈10× and ≈100× lower, estimated from the $S_{0.5}$ values) for TPP as compared to WT PDC-E1. The residual enzymatic activity of the R378 variants at near-saturation pyruvate and TPP concentrations (for WT PDC-E1), together with their lower affinity for TPP, render these variants kinetically

incompetent in a physiological context. Likewise, the p.F205L has practically null activity at near-saturation TPP concentrations for WT PDC-E1 due to the extremely low affinity of this variant for TPP.

To further understand and rationalize the impact of the studied amino acid changes on protein structure and function, we performed molecular dynamics simulations of WT PDC-E1 and the pathogenic variants herein studied, using the WT PDC-E1 structure as a template (PDB entry 3EXE). We sought to complement the information on stability/flexibility by MD simulations with a zoomed-in view to each amino acid substitution (Figure IV-12 and Table IV-3).

Table IV-3 ***In silico*** **analysis of selected PDC-E1 variants.**

Amino acid residue (in WT PDC-E1)	**Position/Interactions (in WT PDC-E1)**	**Variant**	**Effect of amino acid substitution**
R253	- located in a disordered loop; - side chain within electrostatic contact distance with side chains of E1α D42 and D241 (phosphorylation loop B)	p.R253G	- loss of electrostatic interactions with E1α D42 and E1α D241.
R378	- located in a disordered loop far (≈26 Å) from the enzyme active site; - side chain in close electrostatic contact distance with side chain of E1β E311 (end of a disordered loop containing E1β E319, assigned as a key residue controlling the interaction between E1 and E2) and the backbone carbonyl of E1β' R324;	p.R378C p.R378H	- loss of electrostatic interactions with E1β E311 and E1β' R324.
F205L	- located in an α-helix at the interface between the two α subunits within the thiamine binding motif; - phenyl ring of E1α F205 in close proximity to the phenyl ring of E1α' F205, indicating possible π-stacking hydrophobic interaction	p.F205L	- substitution within the thiamine binding motif, a 30-33 amino acid sequence presenting the GDG and NN residues at N- and C-terminus, respectively, and common to all TPP enzymes (PDC-E1α: G195 to N225); - loss of E1α-F205/E1α'-F205 interaction.

Despite the disparate locations of the different affected residues in the protein structure, MD simulations revealed that the generally observed decreased stability of all variants with respect to WT PDC-E1 particularly affects the active site near the TPP binding region. While all amino acid substitutions in these pathogenic variants lead to loss of electrostatic and van der Waals interactions with neighboring residues (Figure IV-12 and Table IV-3), it is noteworthy that even remote mutations such as those affecting R378 seem to propagate through the protein to affect the stability of the TPP binding region and to compromise the inter-subunit interactions (which are also required for TPP incorporation). These observations neatly correlated with the most obvious impact of the mutations in functional terms, which concerned the affinity for the TPP cofactor. As particularly evident for the p.F205L and p.R253G variants, the extent to which the mutations affected TPP affinity (Table IV-2) is fully matched by the degree of destabilization of the TPP binding region (Figures IV-9 and IV-11). Indeed, the location of F205 in the thiamine binding motif, a 30-33 amino acid sequence presenting the GDG and NN residues at N- and C-terminus, respectively, and common to all TPP enzymes (PDC-E1α: G195 to N225) (Brown 2014), fully justifies the 100-times lower affinity for TPP observed for this variant in comparison with WT PDC-E1. Importantly, a PDC deficient patient expressing the p.F205L was described as being responsive to thiamine supplementation (Naito et al. 2002).

In addition to the effects observed for the E1 component variants, we cannot exclude an effect of these mutations on the interaction with other PDC components. For example, the PDC-E1α C-terminal region (residues Y369-S390) has a putative role in stabilizing helix A190-N195 holding the K^+ on the PYR domain of the neighboring β' subunit (Ciszak et al. 2003). So, while the R378 substitutions clearly impair the αβ interactions within PDC-E1 and affect E1α TPP binding, this structural perturbation may also propagate to the E1-E2 interaction, underlining the severe phenotypes observed in patients bearing the corresponding mutations (Patel et al. 2012).

The combination of biophysical methodologies, functional studies and *in silico* analysis of clinically relevant PDC-E1 variants clearly indicate that apparently discrete local structural effects of amino acid substitutions in PDC-E1α variants are strongly amplified to impact on protein aggregation, heterotetramer assembly and cofactor binding. Indeed, using a yeast model to study protein variants equivalent to those generated by clinically relevant mutations in human PDC-E1α (p.A169V, p.M210V, and p.R302C), Drakulic et al. interestingly demonstrated

similar global effects of discrete amino acid substitutions *a priori* seeming structurally 'innocuous' (Drakulic et al. 2018) affecting not only PDC function but also subunit structure and complex assembly. However, the variants herein studied exhibit the strongest negative effect in terms of affinity for the TPP cofactor and residual enzymatic activity, which underlies their functional impairment and the respective patients' phenotypes. Moreover, these studies suggest that TPP supplementation seems like a viable option to ameliorate the functional impairment of these variants, while chemical or pharmacological chaperones could help to prevent aggregation (p.R253G) or stabilize tetrameric (p.F205L) PDC-E1. This highlights the requirement for PDC-E1α variants to be structurally and functionally characterized to better envisage the correct therapeutic approach.

ACKNOWLEDGMENTS

We are thankful to Prof. Cláudio M. Soares for helpful discussions regarding the parameterization of TPP for MD simulations.

SUPPLEMENTARY INFORMATION

Supplementary Table IV-S1 **Oligonucleotides employed in site-directed mutagenesis** to generate PDC-E1α variants.

Primer ID	Sequence (5'-3'; mutated base underlined)
SalI-F	ATCTTCCCCATCGGTGATGTCG**A**CGATATAGGCGCCAGCAACCGCACCTG
SalI-R	GTCCACGCCAACGACCGCGGATATAGC**A**GCTGTAGTGGCTACCCCTTCTA
F205L_F	ACCAGGGCCAGATATT**G**GAAGCTTACAACATGGC
F205L_R	CCATGTTGTAAGCTTC**C**AATATCTGGCCCTGGTT
R253G_F	CGATTTCATTCCTGGGCTG**G**GAGTGGATGGAATGG
R253G_R	CATTCCATCCACTC**C**CAGCCCAGGAATGAAATCGC
R378C_F	CGACCCACCTTTTGAAGTT**T**GTGGTGCCAATCAGTG
R378C_R	CACTGATTGGCACCACAAACTTCAAAAGGTGGGTCG
R378H_F	CCACCTTTTGAAGTTCATGGTGCCAATCAGTGG
R378H_R	CACTGATTGGCACCATGAACTTCAAAAGGTGGG

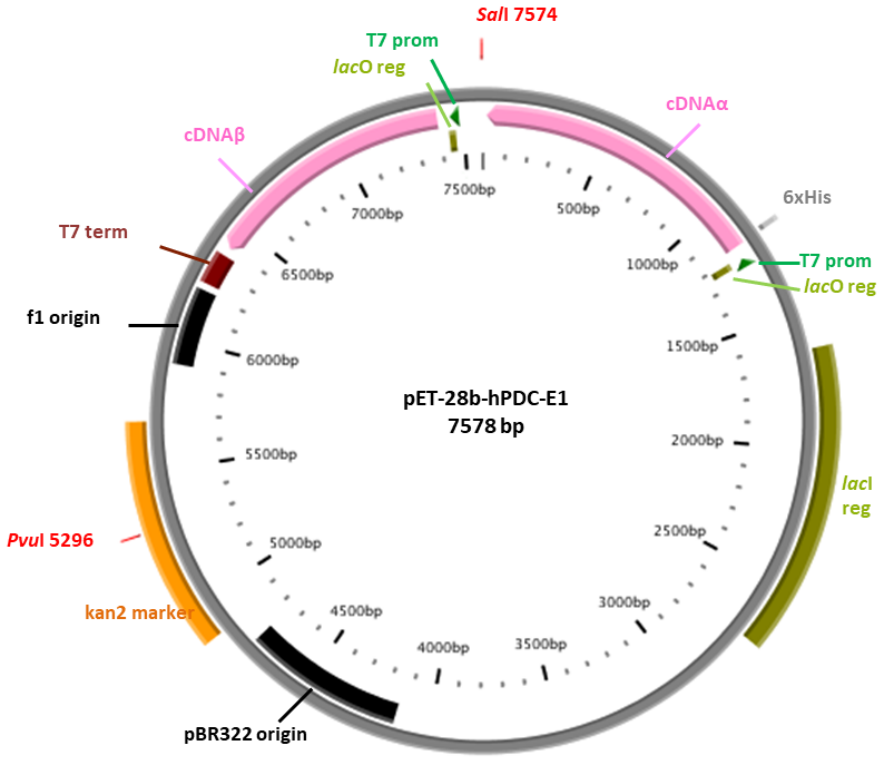

Supplementary Figure IV-S1 **Production of the heterologous bicistronic expression vector pET-28b-hPDC-E1.** The human pyruvate dehydrogenase E1α subunit (*hPDHA1*) and human pyruvate dehydrogenase E1β subunit (*hPDHB*) cDNAs cloned into the *Nhe*I/*Eco*RI and *Nco*I /*Xho*I sites of the pET-28b MCS, respectively (pET-28b-hE1α and pET-28b-E1β) were supplied by Prof. Patel. By site directed mutagenesis and using primers SalI-F and SalI-R (Table S1) a SalI restriction site was introduced ≈ 90 bp 5' to the T7 promotor of the pET-28b-E1β expression construct (p.941G>A) thus obtaining the pET-28b-E1β(+SalI). Both constructs were then digested with PvuI and SalI and the achieved 5290 bp fragment from pET-28b-hE1α and 2269 bp from pET-28b-E1β(+SalI) were ligated, thus obtaining the bicistronic expression system pET-28b-hPDC-E1.

REFERENCES

Bayly CI, Cieplak P, Cornell WD, Kollman PA (1993) A well-behaved electrostatic potential based method using charge restraints for deriving atomic charges: The RESP model. J Phys Chem 97:10269–10280. https://doi.org/10.1021/j100142a004

Berendsen HJC, van der Spoel D, van Drunen R (1995) GROMACS: A message-passing parallel molecular dynamics implementation. Comput Phys Commun 91:43–56. https://doi.org/10.1016/0010-4655(95)00042-E

Berg A, Westphal AH, Bosma HJ, De Kok A (1998) Kinetics and specificity of reductive acylation of wild-type and mutated lipoyl domains of 2-oxo-acid dehydrogenase complexes from Azotobacter vinelandii. Eur J Biochem 252:45–50. https://doi.org/10.1046/j.1432-1327.1998.2520045.x

Bradford MM (1976) A rapid and sensitive method for the quantitation of microgram quantities of protein utilizing the principle of protein-dye binding. Anal Biochem 72:248–254. https://doi.org/10.1016/0003-2697(76)90527-3

Brautigam CA, Wynn RM, Chuang JL, Chuang DT (2009) Subunit and catalytic component stoichiometries of an in vitro reconstituted human pyruvate dehydrogenase complex. J Biol Chem 284:13086–98. https://doi.org/10.1074/jbc.M806563200

Brown G (2014) Defects of thiamine transport and metabolism. J Inherit Metab Dis 37:577–585. https://doi.org/10.1007/s10545-014-9712-9

Bussi G, Donadio D, Parrinello M (2007) Canonical sampling through velocity rescaling. J Chem Phys 126:014101. https://doi.org/10.1063/1.2408420

Byron O, Lindsay JG (2017) The pyruvate dehydrogenase complex and related assemblies in health and disease. In: Sub-Cellular Biochemistry. pp 523–550

Cate RL, Roche TE, Davis LC (1980) Rapid intersite transfer of acetyl groups and movement of pyruvate dehydrogenase component in the kidney pyruvate dehydrogenase complex. J Biol Chem 255:7556–62

Ciszak EM, Korotchkina LG, Dominiak PM, et al (2003) Structural basis for flip-flop action of thiamin pyrophosphate-dependent enzymes revealed by human pyruvate dehydrogenase. J Biol Chem 278:21240–21246. https://doi.org/10.1074/jbc.M300339200

Coelho AI, Trabuco M, Ramos R, et al (2014) Functional and structural impact of the most prevalent missense mutations in classic galactosemia. Mol Genet genomic Med 2:484–96. https://doi.org/10.1002/mgg3.94

Dahl H-HM, Brown GK (1994) Pyruvate dehydrogenase deficiency in a male caused by a point mutation (F205L) in the E1α subunit. Hum Mutat 3:152–155. https://doi.org/10.1002/humu.1380030210

Darden T, York D, Pedersen L (1993) Particle mesh Ewald: An N·log(N) method for Ewald sums in large systems. J Chem Phys 98:10089–10092. https://doi.org/10.1063/1.464397

Drakulic S, Rai J, Petersen SV, et al (2018) Folding and assembly defects of pyruvate dehydrogenase deficiency-related variants in the E1α subunit of the pyruvate dehydrogenase complex. Cell Mol

Life Sci 75:3009–3026. https://doi.org/10.1007/s00018-018-2775-2

Ferriero R, Manco G, Lamantea E, et al (2013) Phenylbutyrate therapy for pyruvate dehydrogenase complex deficiency and lactic acidosis. Sci Transl Med 5:. https://doi.org/10.1126/scitranslmed.3004986

Forsberg BO, Aibara S, Howard RJ, et al (2020) Arrangement and symmetry of the fungal E3BP-containing core of the pyruvate dehydrogenase complex. Nat Commun 11:1–10. https://doi.org/10.1038/s41467-020-18401-z

Fouque F, Brivet M, Boutron A, et al (2003) Differential effect of DCA treatment on the pyruvate dehydrogenase complex in patients with severe PDHC deficiency. Pediatr Res 53:793–799. https://doi.org/10.1203/01.PDR.0000057987.46622.64

Golias T, Kery M, Radenkovic S, Papandreou I (2019) Microenvironmental control of glucose metabolism in tumors by regulation of pyruvate dehydrogenase. Int. J. Cancer 144:674–686

Gregersen N, Bross P, Vang S, Christensen JH (2006) Protein misfolding and human disease. Annu Rev Genomics Hum Genet 7:103–24. https://doi.org/10.1146/annurev.genom.7.080505.115737

Hess B, Bekker H, Berendsen HJC, Fraaije JGEM (1997) LINCS: A linear constraint solver for molecular simulations. J Comput Chem 18:1463–1472. https://doi.org/10.1002/(SICI)1096-987X(199709)18:12<1463::AID-JCC4>3.0.CO;2-H

Ho L, Wexler ID, Liu TC, et al (1989) Characterization of cDNAs encoding human pyruvate dehydrogenase alpha subunit. Proc Natl Acad Sci U S A 86:5330–4. https://doi.org/10.1073/pnas.86.14.5330

Imbard A, Boutron A, Vequaud C, et al (2011) Molecular characterization of 82 patients with pyruvate dehydrogenase complex deficiency. Structural implications of novel amino acid substitutions in E1 protein. Mol Genet Metab 104:507–16. https://doi.org/10.1016/j.ymgme.2011.08.008

Jacobia SJ, Korotchkina LG, Patel MS (2001) Differential effects of two mutations at arginine-234 in the α subunit of human pyruvate dehydrogenase. Arch Biochem Biophys 395:121–128. https://doi.org/10.1006/abbi.2001.2576

Jiang J, Baiesc FL, Hiromasa Y, et al (2018) Atomic Structure of the E2 Inner Core of Human Pyruvate Dehydrogenase Complex. Biochemistry 57:2325–2334. https://doi.org/10.1021/acs.biochem.8b00357

Jorgensen WL, Chandrasekhar J, Madura JD, et al (1983) Comparison of simple potential functions for simulating liquid water. J Chem Phys 79:926–935. https://doi.org/10.1063/1.445869

Kato M, Wynn RM, Chuang JL, et al (2008) Structural basis for inactivation of the human pyruvate dehydrogenase complex by phosphorylation: role of disordered phosphorylation loops. Structure 16:1849–59. https://doi.org/10.1016/j.str.2008.10.010

Korotchkina LG, Patel MS (2001a) Probing the Mechanism of Inactivation of Human Pyruvate Dehydrogenase by Phosphorylation of Three Sites. J Biol Chem 276:5731–5738. https://doi.org/10.1074/jbc.M007558200

Korotchkina LG, Patel MS (2001b) Site Specificity of Four Pyruvate Dehydrogenase Kinase Isoenzymes toward the Three Phosphorylation Sites of Human Pyruvate Dehydrogenase. J Biol

Chem 276:37223–37229. https://doi.org/10.1074/jbc.M103069200

Lissens W, De Meirleir L, Seneca S, et al (2000) Mutations in the X-linked pyruvate dehydrogenase (E1) α subunit gene (PDHA1) in patients with a pyruvate dehydrogenase complex deficiency. Hum. Mutat. 15:209–219

M. J. Frisch, G. W. Trucks, H. B. Schlegel, G. E. Scuseria, M. A. Robb, J. R. Cheeseman, G. Scalmani, V. Barone, B. Mennucci, G. A. Petersson, H. Nakatsuji, M. Caricato, X. Li, H. P. Hratchian, A. F. Izmaylov, J. Bloino, G. Zheng, J. L. Sonnenberg, M. Had and DJF Gaussian 09 Revision A.1. Gaussian, Inc, Wallingford CT, 2009

Maier JA, Martinez C, Kasavajhala K, et al (2015) ff14SB: Improving the Accuracy of Protein Side Chain and Backbone Parameters from ff99SB. J Chem Theory Comput 11:3696–3713. https://doi.org/10.1021/acs.jctc.5b00255

Maniatis T, Fritsch EF, Sambrook J (1982) Molecular Cloning : a Laboratory Manual. Cold Spring Harbor Laboratory Press

Mendes MIS, Colaço HG, Smith DEC, et al (2014) Reduced response of Cystathionine Beta-Synthase (CBS) to S-Adenosylmethionine (SAM): Identification and functional analysis of CBS gene mutations in Homocystinuria patients. J Inherit Metab Dis 37:245–254. https://doi.org/10.1007/s10545-013-9647-6

Milne JLS (2002) Molecular architecture and mechanism of an icosahedral pyruvate dehydrogenase complex: a multifunctional catalytic machine. EMBO J 21:5587–5598. https://doi.org/10.1093/emboj/cdf574

Miyamoto S, Kollman PA (1992) Settle: An analytical version of the SHAKE and RATTLE algorithm for rigid water models. J Comput Chem 13:952–962. https://doi.org/10.1002/jcc.540130805

Naito E, Ito M, Yokota I, et al (2002) Thiamine-responsive pyruvate dehydrogenase deficiency in two patients caused by a point mutation (F205L and L216F) within the thiamine pyrophosphate binding region. Biochim Biophys Acta - Mol Basis Dis 1588:79–84. https://doi.org/10.1016/S0925-4439(02)00142-4

Niesen FH, Berglund H, Vedadi M (2007) The use of differential scanning fluorimetry to detect ligand interactions that promote protein stability. Nat Protoc 2:2212–21. https://doi.org/10.1038/nprot.2007.321

Odièvre M-H, Chretien D, Munnich A, et al (2005) A novel mutation in the dihydrolipoamide dehydrogenase E3 subunit gene (DLD) resulting in an atypical form of α-ketoglutarate dehydrogenase deficiency. Hum Mutat 25:323–324. https://doi.org/10.1002/humu.9319

Parrinello M, Rahman A (1981) Polymorphic transitions in single crystals: A new molecular dynamics method. J Appl Phys 52:7182–7190. https://doi.org/10.1063/1.328693

Pastoris O, Savasta S, Foppa P, et al (1996) Pyruvate dehydrogenase deficiency in a child responsive to thiamine treatment. Acta Paediatr Int J Paediatr 85:625–628. https://doi.org/10.1111/j.1651-2227.1996.tb14104.x

Patel KP, O'Brien TW, Subramony SH, et al (2012) The spectrum of pyruvate dehydrogenase complex deficiency: Clinical, biochemical and genetic features in 371 patients. Mol Genet Metab

106:385–394. https://doi.org/10.1016/j.ymgme.2012.03.017

Patel MS, Korotchkina LG (2006) Regulation of the pyruvate dehydrogenase complex. In: Biochemical Society Transactions. pp 217–222

Pavlu-Pereira H, Silva MJ, Florindo C, et al (2020) Pyruvate dehydrogenase complex deficiency: updating the clinical, metabolic and mutational landscapes in a cohort of Portuguese patients. Orphanet J Rare Dis 15:. https://doi.org/10.1186/s13023-020-01586-3

Roche TE, Reed LJ (1972) Function of the nonidentical subunits of mammalian pyruvate dehydrogenase. Biochem Biophys Res Commun 48:840–846. https://doi.org/10.1016/0006-291X(72)90684-5

Seifert F, Ciszak E, Korotchkina L, et al (2007) Phosphorylation of serine 264 impedes active site accessibility in the E1 component of the human pyruvate dehydrogenase multienzyme complex. Biochemistry 46:6277–6287. https://doi.org/10.1021/bi700083z

Seifert F, Golbik R, Brauer J, et al (2006) Direct kinetic evidence for half-of-the-sites reactivity in the E1 component of the human pyruvate dehydrogenase multienzyme complex through alternating sites cofactor activation. Biochemistry 45:12775–12785. https://doi.org/10.1021/bi061582l

Silva MJ, Pinheiro A, Eusébio F, et al (2009) Pyruvate dehydrogenase deficiency: identification of a novel mutation in the PDHA1 gene which responds to amino acid supplementation. Eur J Pediatr 168:17–22. https://doi.org/10.1007/s00431-008-0700-7

Smolle M, Prior AE, Brown AE, et al (2006) A new level of architectural complexity in the human pyruvate dehydrogenase complex. J Biol Chem 281:19772–19780. https://doi.org/10.1074/jbc.M601140200

Sumegi B, Liposits Z, Inman L, et al (1987) Electron microscopic study on the size of pyruvate dehydrogenase complex in situ. Eur J Biochem 169:223–230. https://doi.org/10.1111/j.1432-1033.1987.tb13601.x

Szabo E, Wilk P, Nagy B, et al (2019) Underlying molecular alterations in human dihydrolipoamide dehydrogenase deficiency revealed by structural analyses of disease-causing enzyme variants. Hum Mol Genet. https://doi.org/10.1093/hmg/ddz177

Tomé CS, Lopes RR, Sousa PMF, et al (2019) Structure of full-length wild-type human phenylalanine hydroxylase by small angle X-ray scattering reveals substrate-induced conformational stability. Sci Rep 9:13615. https://doi.org/10.1038/s41598-019-49944-x

Tripatara A, Korotchkina LG, Patel MS (1999) Characterization of point mutations in patients with pyruvate dehydrogenase deficiency: Role of methionine- 181, proline-188, and arginine- 349 in the α subunit. Arch Biochem Biophys 367:39–50. https://doi.org/10.1006/abbi.1999.1231

Wang J, Wang W, Kollman PA, Case DA (2006) Automatic atom type and bond type perception in molecular mechanical calculations. J Mol Graph Model 25:247–260. https://doi.org/10.1016/j.jmgm.2005.12.005

Wang J, Wolf RM, Caldwell JW, et al (2004) Development and testing of a general amber force field. J Comput Chem 25:1157–1174. https://doi.org/10.1002/jcc.20035

Waterhouse A, Bertoni M, Bienert S, et al (2018) SWISS-MODEL: Homology modelling of protein structures and complexes. Nucleic Acids Res 46:W296–W303. https://doi.org/10.1093/nar/gky427

Wexler ID, Hemalatha SG, McConnell J, et al (1997) Outcome of pyruvate dehydrogenase deficiency treated with ketogenic diets. Studies in patients with identical mutations. Neurology 49:1655–61. https://doi.org/10.1212/wnl.49.6.1655

Whitley MJ, Arjunan P, Nemeria NS, et al (2018) Pyruvate dehydrogenase complex deficiency is linked to regulatory loop disorder in the αV138M variant of human pyruvate dehydrogenase. J Biol Chem 293:13204–13213. https://doi.org/10.1074/jbc.RA118.003996

Yu X, Hiromasa Y, Tsen H, et al (2008) Structures of the Human Pyruvate Dehydrogenase Complex Cores: A Highly Conserved Catalytic Center with Flexible N-Terminal Domains. Structure 16:104–114. https://doi.org/10.1016/j.str.2007.10.024

Yue WW (2016) From structural biology to designing therapy for inborn errors of metabolism. J Inherit Metab Dis 39:489–498. https://doi.org/10.1007/s10545-016-9923-3

Zhou ZH, McCarthy DB, O'Connor CM, et al (2001) The remarkable structural and functional organization of the eukaryotic pyruvate dehydrogenase complexes. Proc Natl Acad Sci U S A 98:14802–7. https://doi.org/10.1073/pnas.011597698

Zuhra K, Sousa PMF, Paulini G, et al (2019) Screening Pyridine Derivatives against Human Hydrogen Sulfide-synthesizing Enzymes by Orthogonal Methods. Sci Rep 9:684. https://doi.org/10.1038/s41598-018-36994-w

Chapter

V

Effect of Arginine and Thiamine on the Structural and Functional Recovery of Pyruvate Dehydrogenase Complex Pathogenic Variants: *In Vitro* and *Ex Vivo* Studies

Hana Pavlů-Pereira[1], Cristina Florindo[1], Maria João Silva[1], Johannes A. Mayr[2], Wolfgang Sperl[2], Filipa S. Carvalho[3], Vanessa A. Morais[3], Isabel Tavares de Almeida[1,4], João B. Vicente[5], Isabel Rivera[1,4]

[1] *iMed.ULisboa – Instituto de Investigação do Medicamento, Faculdade de Farmácia, Universidade de Lisboa, Lisboa, Portugal*
[2] *Department of Paediatrics, Paracelsus Medical University, SALK Salzburg, Austria*
[3] *iMM Instituto de Medicina Molecular João Lobo Antunes, Faculdade de Medicina, Universidade de Lisboa, Lisboa, Portugal*
[4] *Department of Biochemistry and Human Biology, Faculdade de Farmácia, Universidade de Lisboa, Lisboa, Portugal*
[5] *Instituto de Tecnologia Química e Biológica António Xavier, Universidade Nova de Lisboa, Oeiras, Portugal*

Manuscript in preparation

V.1. INTRODUCTION

Pyruvate, as a key compound in aerobic energy metabolism, is fundamental for maintenance of cellular homeostasis. The irreversible oxidative decarboxylation of pyruvate to acetyl-coenzyme A, with the simultaneous reduction of NAD^+, is conducted by the pyruvate dehydrogenase complex (PDC). The importance of this multi-component enzyme complex as a gatekeeper between the glycolytic metabolism in the cytosol and the tricarboxylic acid cycle in the mitochondria has been recently reinforced by PDC becoming a target for regulating glucose oxidation in cancer cells (Vander Heiden et al. 2009; Kaplon et al. 2013).

The multifactorial sequential reaction of pyruvate oxidation (Figures I-1 and I-2, Chapter I) comprises several steps, starting by pyruvate transport into the mitochondrial matrix, involving the participation of various cofactors: thiamine pyrophosphate (TPP), lipoic acid, flavin adenine dinucleotide, coenzyme A (CoA) and nicotinamide adenine dinucleotide (NAD), along with different catalyzing mechanisms, as coupled metabolic channeling, swinging lipoyl arms and regeneration of cofactors (Cate et al. 1980; Berg et al. 1998; Sperl et al. 2015; Guo et al. 2017). Moreover, the accurate and rapid regulation of PDC activity via phosphorylation and dephosphorylation contributes to the fine maintenance of cellular homeostasis (Linn et al. 1969; Patel and Korotchkina 2006; Seifert et al. 2007).

Human PDC is a massive protein complex weighing 8-10 MDa, resulting from an assembly of multiple copies of catalytic and structural components: pyruvate dehydrogenase (E1, EC 1.2.4.1), dihydrolipoyllysine-residue acetyltransferase (E2, EC 2.3.1.12), dihydrolipoyl dehydrogenase (E3, EC 1.8.1.4) and E3 binding protein (E3BP) (Figure I-2, Chapter I). The PDC morphology is determined by a 60-meric E2/E3BP core surrounded by 6-12 E3 dimers and 20-30 E1 heterotetramers (Zhou et al. 2001; Milne 2002; Ciszak et al. 2003; Smolle et al. 2006; Yu et al. 2008; Jiang et al. 2018), as well as by different copies of PDKs and PDPs.

Impaired PDC activity leads to metabolic disorder with symptoms corresponding to its essential position in energy production; indeed, cellular energy deprivation affects the tissues with a high demand for ATP such as central and peripheral nervous systems and skeletal muscle. Additionally, inadequate removal of pyruvate and lactate results in lactic acidemia (Brown et al. 1994; Imbard et al. 2011; Patel et al. 2012; Sperl et al. 2015).

The existing therapeutic strategies target either the metabolic pathway or the dysfunctional enzymatic complex. A ketogenic diet can bypass the energy production by stimulating

alternative metabolic pathways (Wexler et al. 1997) and clinical benefits have been demonstrated in several patients (Head et al. 2005; El-Gharbawy et al. 2011), namely upon childhood-onset epilepsy or paroxysmal dystonia. The impaired catalytic activity of PDC can be either intervened through the regulatory system or stimulated by cofactor supplementation. Dichloroacetate or phenylbutyrate are used to increase PDC activity by blocking its phosphorylation (Fouque et al. 2003; Ferriero and Brunetti-Pierri 2013) and supplementation with thiamine, a precursor of thiamine pyrophosphate, may help to overcome the defective TPP binding to the PDC-E1 active site. Several cases of thiamine-responsive PDC-E1 deficient patients have been described, so far (Pastoris et al. 1996; Di Rocco et al. 2000; Naito et al. 2002; Brown 2014; Castiglioni et al. 2015); nevertheless, there is a high variability in the clinical and biochemical response and also in the distribution of the mutations leading to thiamine-responsive variants (Brown 2014). Hence, the exact mechanism underlying the TPP effect remains unclear, offering a question if besides playing its role as a specific cofactor, TPP could display a stabilizing effect on altered conformation of the PDC-E1 protein. Stabilization of misfolded proteins by small weight molecular compounds is a challenging approach to the design of novel therapies aiming at the improvement and correction of protein structure and function (Yue 2016).

Our group identified a Portuguese patient carrying the p.R253G PDC-E1α variant which revealed to be remarkably responsive to arginine supplementation (Silva et al. 2009). This observation, together with our recent results from biophysical and functional studies on several PDC-E1 recombinant proteins (Pavlu-Pereira et al. 2021) prompted us to evaluate the potential effect of arginine as a PDC-E1 stabilizer and putative rescuer of its enzymatic function. Accordingly, we designed a comparative study aiming to evaluate the effect of arginine supplementation during production of the recombinant pathogenic variants p.F205L, p.R253G, p.R378C and p.R378H, identified in the Portuguese PDC deficient population (Pavlu-Pereira et al. 2020). In addition, we undertook a study to evaluate the ability of arginine and/or thiamine to restore PDC function and mitochondrial bioenergetics in cell lines derived from hemizygous patients bearing the p.R88C, p. R253G, p.R263G and p.R378C PDC-E1α variants caused by mutations in the *PDHA1* gene.

V.2. MATERIALS AND METHODS

All procedures followed standard ethical regulations and were approved by the local Ethics Committees. Informed consent for participation in the study was obtained from all patients or their parents.

V.2.1. Cloning, mutagenesis, expression and purification of recombinant human PDC-E1 variants

The heterotetrameric PDC-E1 (αα'ββ') proteins were produced and purified as described previously (Pavlu-Pereira et al. 2021). Briefly, to generate the PDC-E1α variants p.F205L, p.R253G, p.R378C and p.R378H, the mutations underlying them were introduced into the developed wild-type (WT) pET-28b-hPDC-E1 bicistronic expression vector containing both PDC E1α subunit cDNA (*hPDHA1*, GenBank ID 5160, NM_000284.3) and E1β subunit cDNA (*hPDHB*, GenBank ID 5162, NM_000925.3).

After optimization, proteins were produced under the following condition: transformed *E. coli* BL21 (DE3) Rosetta cells were cultured at 37 °C in M9 medium and, when cell density reached A_{600nm}≈0.3, protein expression was induced by adding 400 μM isopropyl β-D-1-thiogalactopyranoside (IPTG), together with 600 μM thiamine hydrochloride. Following induction, cells were transferred to 30 °C for 4 h and harvested by centrifugation. To study the potential effect of arginine as a chemical chaperone, after IPTG induction bacterial cultures were split in two batches, one of them being supplemented with 25 mM L-arginine hydrochloride. This concentration was selected as a result of an initial screen using 5, 25 and 50 mM arginine hydrochloride, a range chosen taking into consideration that the arginine aspartate intake by the reported patient was estimated to correspond to a ≈ 4 mM of circulating arginine load (Silva et al. 2009) and also based on our group experience regarding studies on the effect of low molecular weight compounds on the stabilization of other human proteins (Nascimento et al. 2008).

Bacterial cells were resuspended in buffer A (50 mM potassium phosphate buffer; 300 mM KCl; 10% glycerol; pH 7.5) containing 1 $mg \cdot mL^{-1}$ lysozyme, 1 mM phenylmethylsulfonyl fluoride and 1 $mg \cdot L^{-1}$ DNaseI and disrupted by sonication. After the first purification step by immobilized metal affinity chromatography (detailed in Chapter IV), the His-tagged

recombinant proteins were loaded into a HiLoad Superdex 200 column (GE Healthcare) to assess the oligomeric profile and to further isolate the PDC-E1 αα'ββ' heterotetramer.

V.2.2. Effect of arginine: structural and functional studies on recombinant PDC-E1 variants

Far-UV circular dichroism (CD) spectra and thermal denaturation profiles were recorded in a Jasco J-815 spectropolarimeter (Easton, MD, USA) as described in Chapter IV (section IV.3.3.). Thermal denaturation curves were analyzed with Graphpad Prism (Graphpad Software Inc., CA, USA), fitting the data to a monophasic sigmoidal curve. Thermal denaturation was also monitored by differential scanning fluorimetry (DSF), performed in a C1000 Touch thermal cycler equipped with a CFX96 optical reaction module (Bio-Rad, Hercules, CA, USA) as described in section IV.3.4. Variations in T_m values were considered significant when $|\Delta T_m| \geq 2$ °C (above the standard deviation) (Senisterra and Finerty 2009). Dynamic light scattering (DLS) data were acquired in a ZetaSizer Nano-S (Malvern Instrument, Malvern, UK) particle size analyser as in section IV.3.5. Thermal aggregation profiles were assessed in the range between 25 °C and 70 °C and thermal aggregation kinetics was monitored at 37 °C. Data were processed using Zetasizer Nano DTS software v 7.12 (Malvern Instrument), regarding the evolution of each oligomeric species. Proteolytic rates were evaluated by limited proteolysis by trypsin at 37 °C with and a 1:200 ratio (mass:mass) as described in section IV.3.6.

The PDC-E1 specific activity was determined according to a previously described spectrophotometric method (Korotchkina and Patel 2001), monitoring the oxidative decarboxylation of pyruvate by PDC-E1 by a decrease in absorbance at 600 nm resulting from reduction of 2,6-dichlorophenolindophenol mediated by phenazine methosulfate. Assays were carried out at 37 °C; the reaction was started by adding 2 mM pyruvate to the mixture containing PDC-E1 (100 μg) in buffer A, 0.2 mM TPP, 4 mM $MgCl_2$, 48 μM DCPIP, 1.5 mM PMS and 20% of Buffer B (100 mM potassium phosphate buffer, 10% glycerol, pH 7.0) after a 4-min pre-incubation.

V.2.3. Cell culture

Skin biopsies obtained from a control individual (wild-type genotype or WT) and from four hemizygous PDC-E1α deficient patients (p.R88C, p.R253G, p.R263G and p.R378C genotypes) were used to prepare primary fibroblast cultures. Human skin fibroblasts were routinely cultivated in Dulbecco's Modified Eagle's Medium (DMEM, low glucose, with sodium bicarbonate; Sigma-Aldrich, Inc., St. Louis, USA), supplemented with 10% (v/v) fetal bovine serum (Sigma-Aldrich) and with penicillin-streptomycin solution (Sigma-Aldrich; 100 U / 0.1 mg/mL, respectively). All cultures were maintained at 37 °C in a humidified atmospheric environment with 5 % CO_2. Fibroblasts were commonly washed with Dulbecco's Phosphate Buffered Saline (DPBS, Sigma-Aldrich), detached and harvested using 0.5 % trypsin (trypsin-EDTA solution, Sigma-Aldrich), and sub-cultured several times in the ratio 1:3 in order to obtain an adequate amount of material for analysis.

V.2.4. Cell incubation

During 48 h, cells were preincubated in an adapted custom-made DMEM with concentrations of arginine and thiamine reduced to the corresponding plasmatic physiological levels, 80 μM and 15 nM respectively (DMEM-low-A/low-T); detailed media formulation is presented in Supplementary Table V-1. Afterwards, a fresh DMEM-low-A/low-T was added, and fibroblasts were cultured during a period of 24 h, supplemented with arginine and/or thiamine at physiological vs. therapeutical levels, according to the scheme shown in Table V-1. Based on the experience with thiamine and arginine treatment in PDC deficient patients acquired by our physician collaborators, we established the therapeutic concentrations of arginine at 4 mM (high-A) and thiamine at 100 μM (high-T) for the cell cultures.

V.2.5. Mitochondrial oxygen consumption rate

Mitochondrial function was evaluated by measuring the oxygen consumption rate (OCR) in the XF24 Extracellular Flux Analyzer (Seahorse Bioscience, Agilent, Santa Clara, CA, USA), according to the standard protocol (Agilent Seahorse XF Cell Mito Stress Test Kit User Guide), using the method described previously (De Matos et al. 2019). Briefly, after 48 h pre-

incubation in DMEM-low-A/low-T, fibroblasts were seeded in 24-well XF plates at a density of 5×10^5 cell/well, cultured for 8 h in DMEM-low-A/low-T at 37°C in a humidified atmospheric environment with 5 % CO_2 and then incubated during a period of 12 h with/without addition of arginine and/or thiamine at therapeutic levels (high-A / high-T), according to the scheme shown in Table V-1. Prior to the assay, cells were incubated at 37 °C in the absence of CO_2 for 1 h to allow temperature and pH equilibration, in a custom-made SH-DMEM medium appropriate for use in Seahorse XF instruments (medium formulation in Supplementary Table V-1) with the respective concentrations of arginine and thiamine for every batch.

Table V-1 **Schematic presentation of cell incubation times and media.** After a routine cultivation in the common DMEM and a period of pre-incubation in the custom-made medium with physiological concentrations of arginine and thiamine (80 µM and 15 nM, respectively), the cells were supplemented with arginine and/or thiamine at therapeutical levels (4 mM and 100 µM, respectively).

Routine cultivation	**Pre-incubation 48 h**	**Incubation 24 h**	
		12 h	**12 h**
DMEM complete	DMEM-low-A/low-T	high-A/low-T	-
		low-A/high-T	-
		high-A/high-T	-
		low-A/low-T	
		high-A/low-T	
		low-A/high-T	
		high-A/high-T	

OCR was assessed in a time course set-up where the specific compounds were sequentially injected in the following order and concentrations: oligomycin (1 µM), carbonyl cyanide-4-(trifluoromethoxy)phenylhydrazone (FCCP) (1.5 µM and 1 µM), and rotenone plus antimycin A (1 µM). A titration with FCCP was performed to determine the optimal FCCP concentration. The results were normalized to the protein concentration assayed according to the standard Bradford method (Bradford 1976). Five wells from each sample were measured in a total of n = 3 experimental assays. The analysis was performed simultaneously in the same plate for the control and compound treated cells. For data analysis, the following formulas were applied: Non-mitochondrial Oxygen Consumption, Minimum rate measurement after Rotenone/antimycin A injection; Basal Respiration, (Last rate measurement before first

injection)-(Non-Mitochondrial Respiration Rate); Maximal Respiration, (Maximum rate measurement after FCCP injection)-(Non-Mitochondrial Respiration), H^+ (Proton) Leak, (Minimum rate measurement after Oligomycin injection)-(Non-Mitochondrial Respiration); ATP Production, (Last rate measurement before Oligomycin injection)-(Minimum rate measurement after Oligomycin injection); Spare Respiratory Capacity, (Maximal Respiration)-(Basal Respiration).

V.2.6. PDC activity

Pelleted cells were resuspended in homogenization buffer (80 mM KH_2PO_4, pH 7.4, 2 mM EDTA) and treated with 5 mM dichloroacetate (DCA) for 15 minutes at 37 °C. The reaction was blocked by addition of a stopping solution (25 mM NaF, 25 mM EDTA, 4 mM DTT), and cells were disrupted by three freezing/thawing cycles.

PDC enzymatic activity was determined using a radiochemical method based on the release of $^{14}CO_2$ from [1-^{14}C]-pyruvate (Clot et al. 1992) with minor modifications (Johannes Mayr and Wolfgang Sperl, personal communication). Briefly, 100 µL of cell homogenates were pre-incubated at 37 °C for 10 minutes in 100 µL of reaction buffer (32 mM phosphate buffer containing 4 mM $MgCl_2$, 2 mM $CaCl_2$, 0.5 mM NAD^+, 0.5 mM thiamine pyrophosphate, 0.1 mM CoA and 5 mM carnitine; final concentrations). Subsequently, the reaction was started by addition of 50 µL [1-^{14}C]-pyruvate solution (0.5 mM, 0.067 µCi). After 30 minutes, the reaction was stopped by addition of 80 µL 6N H_2SO_4. The released $^{14}CO_2$ was trapped in paper filter saturated with benzethonium hydroxide, during a 15 min post-incubation period at room temperature, and its amount measured in a scintillation counter. Protein concentration was determined by the Bradford assay (Bradford 1976). All samples were analyzed in triplicates and PDC activity was measured against blank with homogenizing buffer replacing the cell homogenate and expressed in pmol·min^{-1}mg protein^{-1}.

V.2.7. Western blot

Cultured fibroblasts were resuspended in homogenization buffer (80 mM KH_2PO_4, pH 7.4, 2 mM EDTA) and cell disruption was achieved by sonication. Total protein extracts (50 µg) were mixed with Laemli loading buffer, resolved in a 12 % sodium dodecyl sulfate-

polyacrylamide gel electrophoresis (SDS-PAGE) and transferred onto polyvinylidene difluoride membranes (GE Healthcare Life Sciences, Amersham Hybond) at 300 mA for 100 minutes at 4 °C. Membranes were blocked with 5 % bovine serum albumin in Tris-buffered saline with 0.1 % Tween® 20 (TBS-T) for one hour at room temperature, followed by incubation with MitoProfile® Pyruvate dehydrogenase (PDH) WB Antibody Cocktail (MSP07/ab110416, Abcam) or anti-PDHA1 antibody (MSP03/ab110330, Abcam). Membranes were probed with horseradish peroxidase-conjugated goat anti-mouse IgG, followed by chemiluminescent detection with SuperSignal West Femto Maximum Sensitivity Substrate (Thermo Fisher Scientific).

V.2.8. Immunohistochemical analysis

Immunohistochemical detection of the proteins was performed in the initial phase of this work; thus, only the effect of arginine was studied, and the scheme of cell incubation differed slightly from the procedure mentioned above. Briefly, after a 48 h preincubation in DMEM-low-A medium (Supplementary Table V-1) followed by 48 h incubation with or without the supplementation of arginine at 4 mM, fibroblasts were seeded onto eight-chamber culture slides (Falcon™, USA) and cultivated during an additional period of 24 h with arginine at physiological vs. therapeutical levels. Then, the chambers were separated, and the cells stabilized onto the slides by fixation solution (formaldehyde 4%; buffered pH 6.9). After the heat-induced epitope retrieval in TE-T buffer (10 mM Tris pH 9.0, 1 mM EDTA, 0.05% Tween 20) for 40 min at 95 °C, the immunohistochemical staining was carried out using the Envision Detection System (Dako, Glostrup, Denmark) according to the manufacturer's instructions and to the procedure previously described (Zimmermann et al. 2009).

The immunodetection set included anti-PDC-E1α mouse monoclonal antibody (Abcam) and anti-actin rabbit monoclonal antibody (Abcam), diluted in Dako-antibody diluent with background reduction and Alexa Fluor™ 488 anti-mouse and Alexa Fluor™ 594 anti-rabbit secondary antibodies (Thermo Fisher Scientific). Nuclear and chromosome counterstain with DAPI (4',6-diamidino-2-phenylindole, dihydrochloride) was used to detect the nucleus.

V.3. RESULTS AND DISCUSSION

V.3.1. Evaluation of arginine effect: structural and functional comparative studies on recombinant human pathogenic PDC-E1 variants

These *in vitro* experiments were designed to evaluate the ability of arginine to stabilize the conformational structure and to rescue the enzymatic activity of recombinant human PDC-E1 variants identified in Portuguese patients, namely p.F205L, p.R253G, p.R378C and p.R378H.

All recombinant human PDC-E1 variants were successfully produced and purified, yielding 1-2 mg of pure PDC-E1 protein per liter of culture, a range which was not altered by the presence of arginine (25 mM) during the protein expression induction. Biologically active αα'ββ' heterotetramers were isolated using size exclusion chromatography and comparatively analyzed.

Regardless of all studied variants being expressed in the presence of arginine or not, they all exhibited similar Far-UV CD spectra, characteristic of a protein with a high content of α-helical secondary structure elements, demonstrated by the prominent minimum at 222 nm. Thermal denaturation profiles obtained either by far-UV CD or DSF did not display any significant T_m changes for any of the protein variants expressed in the presence of arginine.

The effect of arginine on the global conformational stability was assessed by limited proteolysis by trypsin, with no apparent effect on the proteolytic rates. In order to evaluate the impact of arginine on propensity to aggregation, dynamic light scattering was employed. Data analysis focused on the optically active species corresponding to tetramers and aggregates (or higher oligomers), as described in section IV, Figure IV-6. Thermal aggregation profiles revealed similar estimated T_{agg} (Table V-2, Figure V-1) for all the tested variants, only p.R253G exhibiting a lower T_{agg} value which however remained unaffected by arginine. Correspondingly, the isothermal kinetics of tetrameric species disappearance and of aggregates formation (Figure V- 1) revealed a higher susceptibility of the p.R253G variant to aggregation which was not improved by arginine. Moreover, the p.R378H variant also exhibited a slightly higher propensity to aggregation which was sparsely improved by arginine (Table V-2, Figure V-1).

Table V-2 associates the summarized results of the structural studies described in the previous work (Pavlu-Pereira et al. 2021) to the results achieved with the same variants

produced with and without arginine supplementation. Regardless of their properties concerning the thermal and conformational stabilities or aggregation propensity, none of the variants exhibited any significant improvement when expressed in the presence of arginine.

To further test the hypothetical rescue by arginine of the deleterious consequences induced by the studied mutations, a functional comparative analysis of the recombinant PDC-E1α variants was undertaken. The recombinant WT human PDC-E1 displayed a specific catalytic activity of 370 ± 27 U which was not altered by arginine (Figure V-2) and was used as a reference for expressing the residual activity of the protein variants.

The two variants with substitutions in R378 revealed the lowest activities, close to undetectable for p.R378H, which precludes establishing whether arginine afforded any functional rescue. Notably, a statistically significant result was observed for the p.R253G variant expressed in the presence of arginine, since PDC-E1 activity increased from 21 ± 4 to 37 ± 4 % (p=0.0002). Conversely, the p.F205L variant activity apparently decreased from 54 ± 8 to 32 ± 4 %; ($p < 0.0001$) when arginine was present in the expression media. This effect together with the relatively high basal activity of the p.F205L variant may be associated with two experimental conditions. Firstly, the experiment was designed aiming at the positive selection of heterotetrameric PDC-E1, which in the case of this variant was a minor fraction of the total protein (Pavlu-Pereira et al. 2021). Secondly, the PDC-E1 activity assay methodology was set to saturating concentrations of TPP cofactor (0.2 mM). According to published reports and to our findings (Naito et al. 2002; Pavlu-Pereira et al. 2021), the severe impairment on the affinity to the TPP cofactor typically displayed by the p.F205L variant can be notably compensated by TPP saturating concentrations. Thus, neither the relatively high basal activity, nor the negligible impact of arginine regarding the p.F205L variant shown here, may resemble the real circumstances. On the other hand, the increase on the activity of the p.R253G variant induced by arginine is consistent with the trend brought about by arginine intake in the reported patient (Silva et al. 2009). These data strongly support the notion that increasing the patients' enzymatic activity to minimal threshold level is sufficient to reverse or at least ameliorate the phenotype (Yue 2016).

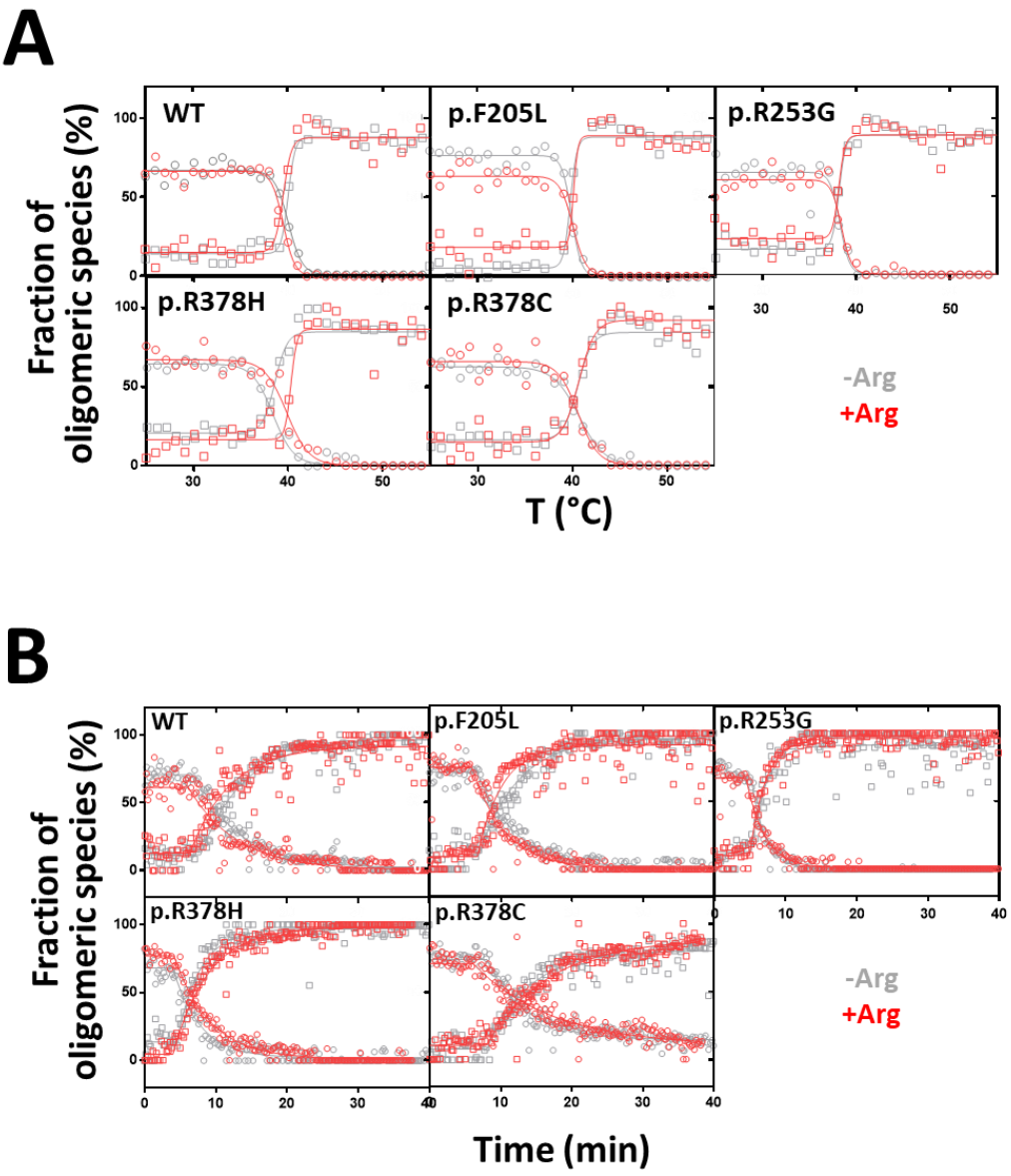

Figure V-1 **Aggregation of WT and PDC-E1 variants analysed by dynamic light scattering.** Thermal aggregation (A) and kinetics of aggregation (B) of purified heterotetramers of WT and PDC-E1 variants, produced in the absence (gray symbols) and presence (red symbols) of 25 mM arginine, monitored by dynamic light scattering. *Panel A*, thermal aggregation profile was assessed by a linear temperature increase from 25 to 70 °C at 1 °C.min^{-1}. Distribution of scattering intensity data was adapted to the evolution of each oligomeric species (circles, heterotetramers; squares, higher oligomers/aggregates) fraction and normalized and fitted to a plateau followed by one phase association equation, the aggregation temperature (T_{agg}) being defined as the temperature of the starting point of the scattering intensity change belonging to each respective profile. *Panel B*, thermal aggregation kinetics followed at 37 °C. The aggregation coefficient k_{agg} was defined as the observed rate constant best fitting the formation (higher oligomers/aggregates) or disappearance (heterotetramers) of each oligomeric form.

Table V-2 **Thermal and conformational stability and aggregation propensity of clinically relevant PDC-E1 variants** produced in the absence (-Arg) or presence of arginine (+Arg).

Variant	CD		DSF		DLS								Limited Proteolysis	
	Thermal denaturation				Thermal aggregation				Aggregation kinetics					
					tetramer		aggregates		tetramer		aggregates			
	T_m (°C)		T_m (°C)		T_{agg} (°C)		T_{agg} (°C)		k_{agg} (min^{-1})		k_{agg} (min^{-1})		k_{obs} (min^{-1})	
	-Arg	+Arg	-Arg	+Arg	-Arg	+Arg	-Arg	+Arg	-Arg	+Arg	-Arg	+Arg	-Arg	+Arg
WT	46.8 ± 0.9	47.2 ± 0.7	40.4 ± 0.4	40.6 ± 0.9	40 ± 0.5	39.6 ± 0.2	39.9 ± 0.5	39.6 ± 0.3	0.145 ± 0.022	0.175 ± 0.038	0.144 ± 0.028	0.203 ± 0.036	0.161 ± 0.035	0.189 ± 0.032
p.F205L	46.7 ± 0.1	47.4 ± 0.6	40.4 ± 0.2	40.2 ± 0.2	39.9 ± 0.6	39.8 ± 0.9	39.7 ± 0.4	40.2 ± 0.5	0.179 ± 0.035	0.22 ± 0.028	0.186 ± 0.046	0.261 ± 0.059	0.183 ± 0.028	0.181 ± 0.043
p.R253G	47.7 ± 0.9	47.9 ± 0.4	39.9[a] ± 0.4	38.7[a] ± 0.4	38.2 ± 0.4	38.4 ± 0.5	38.2 ± 0.5	38.6 ± 0.4	0.442 ± 0.120	0.378 ± 0.110	0.485 ± 0.001	0.421 ± 0.161	0.277 ± 0.025	0.249 ± 0.040
p.R378C	49.2 ± 0.6	49.2 ± 0.2	40.5 ± 0.3	40.7 ± 0.3	40.6 ± 0.1	40.6 ± 0.1	40.6 ± 0.3	40.6 ± 0.3	0.129 ± 0.048	0.13 ± 0.053	0.126 ± 0.038	0.126 ± 0.040	0.222 ± 0.030	0.159 ± 0.042
p.R378H	48.3 ± 0.2	48.6 ± 0.1	39.3 ± 0.2	40.1 ± 0.1	39 ± 0.8	39.9 ± 0.1	39.1[aa] ± 0.9	40.1[aa] ± 0.5	0.217 ± 0.067	0.195 ± 0.004	0.311 ± 0.001	0.219 ± 0.025	0.122 ± 0.012	0.099 ± 0.016

CD, Far-UV circular dichroism (replicates from three independent protein batches, except for p.F205L,for which replicates were from two independent protein batches); DSF, differential scanning fluorimetry (replicates from two independent protein batches); DLS, dynamic light scattering (replicates from two independent protein batches).

[a] Statistically significant difference between expression with (+Arg) and without arginine (-Arg); p = 0.0012;

[aa] p = 0.0018; Statistical significance (p value) was determined using the Student's t test.

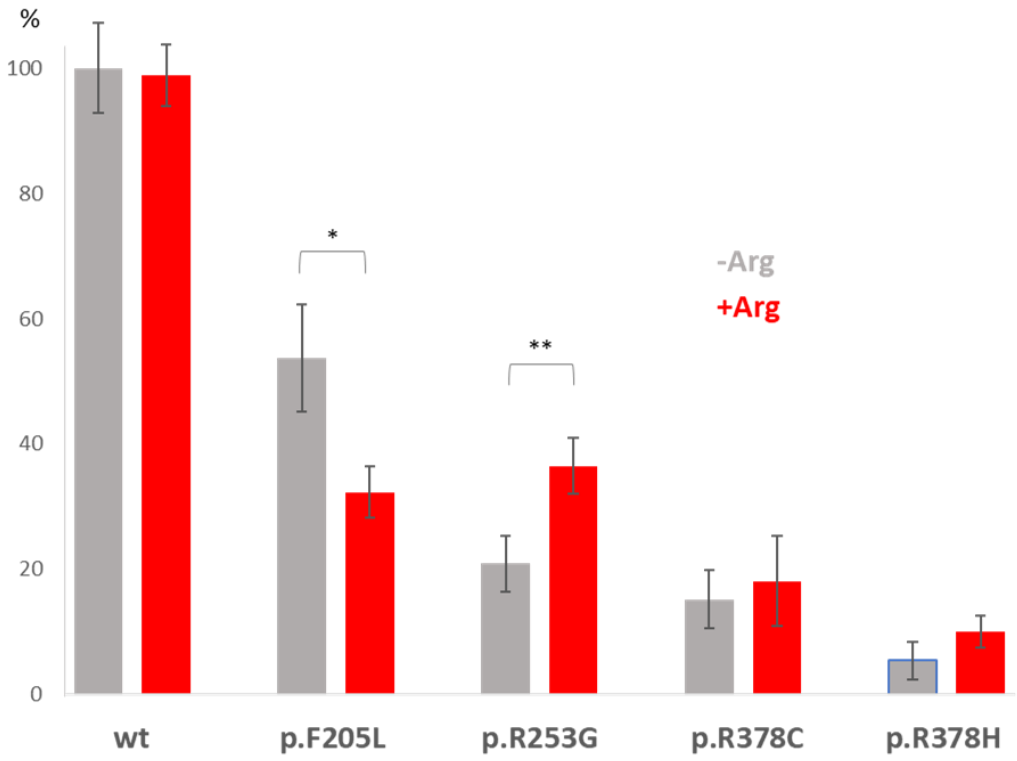

Figure V-2 **Functional characterization of clinically relevant PDC-E1 variants** produced in the absence (-Arg) or presence of arginine (+Arg). PDC-E1 specific catalytic activity determined with 2 mM pyruvate and 0.2 mM TPP and normalized to the WT (-Arg) condition. *Statistically significant difference between expressions with and without Arg; $p < 0.0001$; ** $p = 0.0002$. Statistical significance (p value) was determined using the Student's t test. Four replicates from four independent protein batches, except for WT (-Arg e +Arg) and p.R253G (-Arg) for which five replicates were from four independent protein batches, and for p.F205L for which five replicates were from three independent protein batches.

In summary, since the analyzed protein variants displayed a marginal effect regarding the stability and the propensity towards aggregation (Pavlu-Pereira et al. 2021), arginine did not induce any significant shift in any of these evaluated parameters. Regarding the severe to moderate impact on the enzymatic activity, the molecular mechanism underlying the limited functional rescue of the p.R253G variant is still to be fully understood. Presumably, the chemical chaperone nature of arginine may help stabilizing the otherwise disordered phosphorylation loop B, thus enabling transient TPP stabilization at the active site. In this context, however, the null or negligible effect of arginine on the other variants, also presenting

a considerable degree of destabilization of the TPP binding region (Pavlu-Pereira et al. 2021), remains to be interpreted.

V.3.2. Evaluating arginine effect upon patient-derived cell lines

We further evaluated the potential effect of arginine on improving PDC activity in PDCD patient-derived cell lines, thus aiming to confirm the *in vivo* effect observed in the patient harboring the p.R253G variant (Silva et al. 2009). However, it is well recognized that many PDC deficient cell lines are quite difficult to grow in culture due to lactate accumulation leading to medium acidification, and also to poor energy production. Indeed, this was the case of the fibroblast cell line carrying the p.R253G variant which revealed an extremely slow growth.

So, the pilot *ex vivo* experiments for evaluation of arginine ability to rescue PDC function were achieved with well-established cell lines available at the laboratory, namely fibroblasts derived from skin biopsies obtained from a control individual and from patients harboring the hemizygous mutations p.R88C, p.R263G and p.R378C in the *PDHA1* gene.

Cells were cultured in an adapted custom-made DMEM with concentration of arginine reduced to the corresponding plasmatic physiological level until reaching 80% of confluence. Then, fibroblasts were cultured during a period of 48 h with new medium supplemented with arginine at physiological (80 μM) vs. therapeutical levels (4 mM). Whole cell extracts were prepared to further analyses.

Immunochemical analysis by western blot and respective densitometric analysis revealed that the normalized PDC-E1α levels were moderately (p.R88C and p.R263G) or severely (p.R378C) impaired, as compared to the control cell line. After 48 h of culture in medium supplemented with arginine at therapeutic concentration, the lower (p.R88C and p.R263G) or almost absent (p.R378C) levels of PDC-E1α protein detected in these three PDC-deficient cell lines were not increased (Figure V-3A and V-3B). Moreover, the cell lines were also analyzed by immunohistochemical staining which corroborated the results obtained by immunoblotting (Figure V-4).

During this pilot experiment, PDC enzymatic activity was determined in whole cell lysates as well as in isolated mitochondria; however, no significant effect of arginine was observed upon the catalytic activity determined in any of the studied cell lines (results not shown).

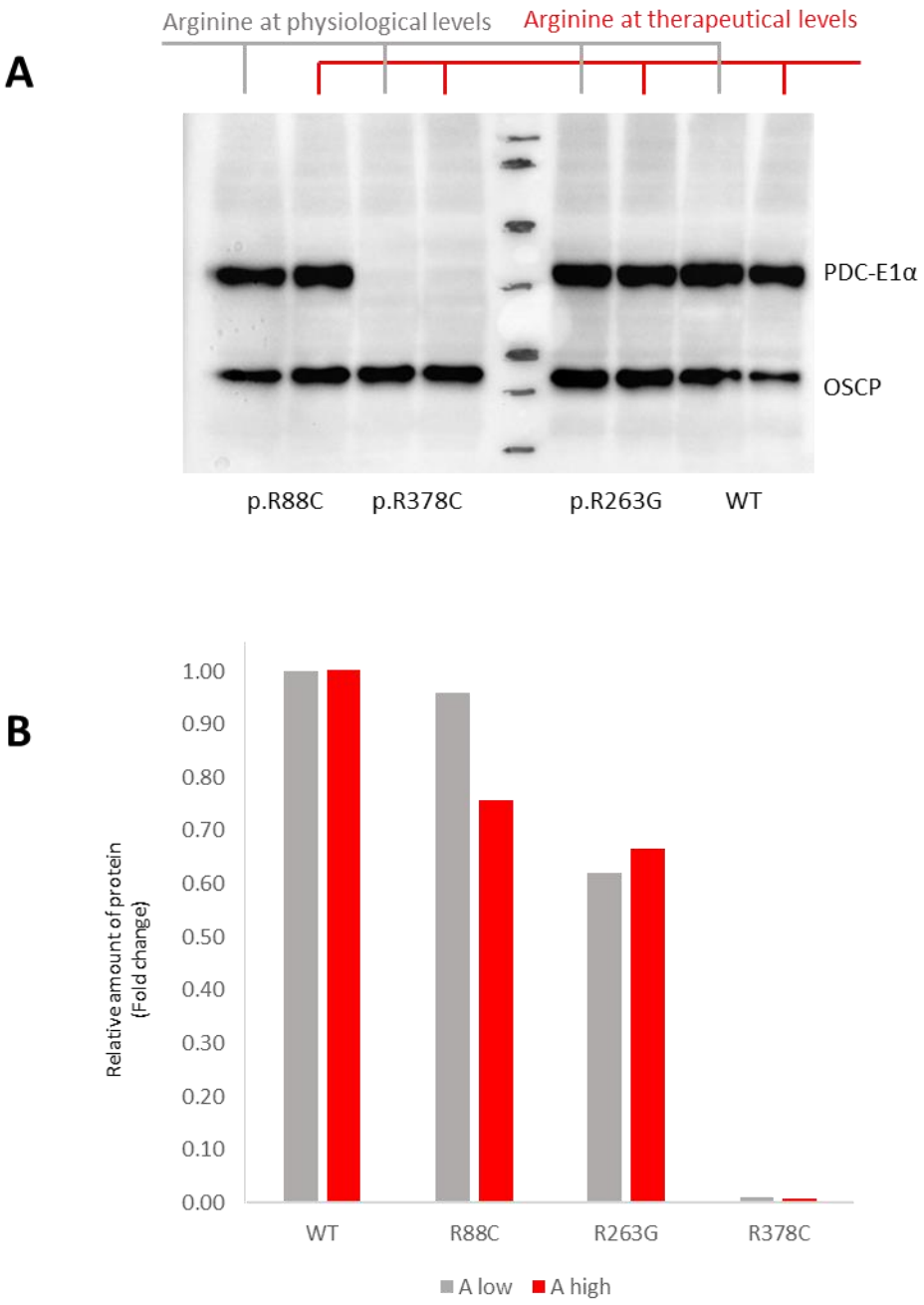

Figure V-3. **PDC-E1α protein levels assessed by western blot,** 48 h after addition of arginine at physiological (low-A) or therapeutic (high-A) levels; Panel A - Immunoelectrophoretic profiles of whole cell extracts derived from PDC-deficient cell lines showing the PDC-E1α subunit and OSCP (subunit of mitochondrial ATP synthase); Panel B - densitometric analysis representing PDC-E1α levels normalized to OSCP. Result of a single analysis performed during the pilot experiment.

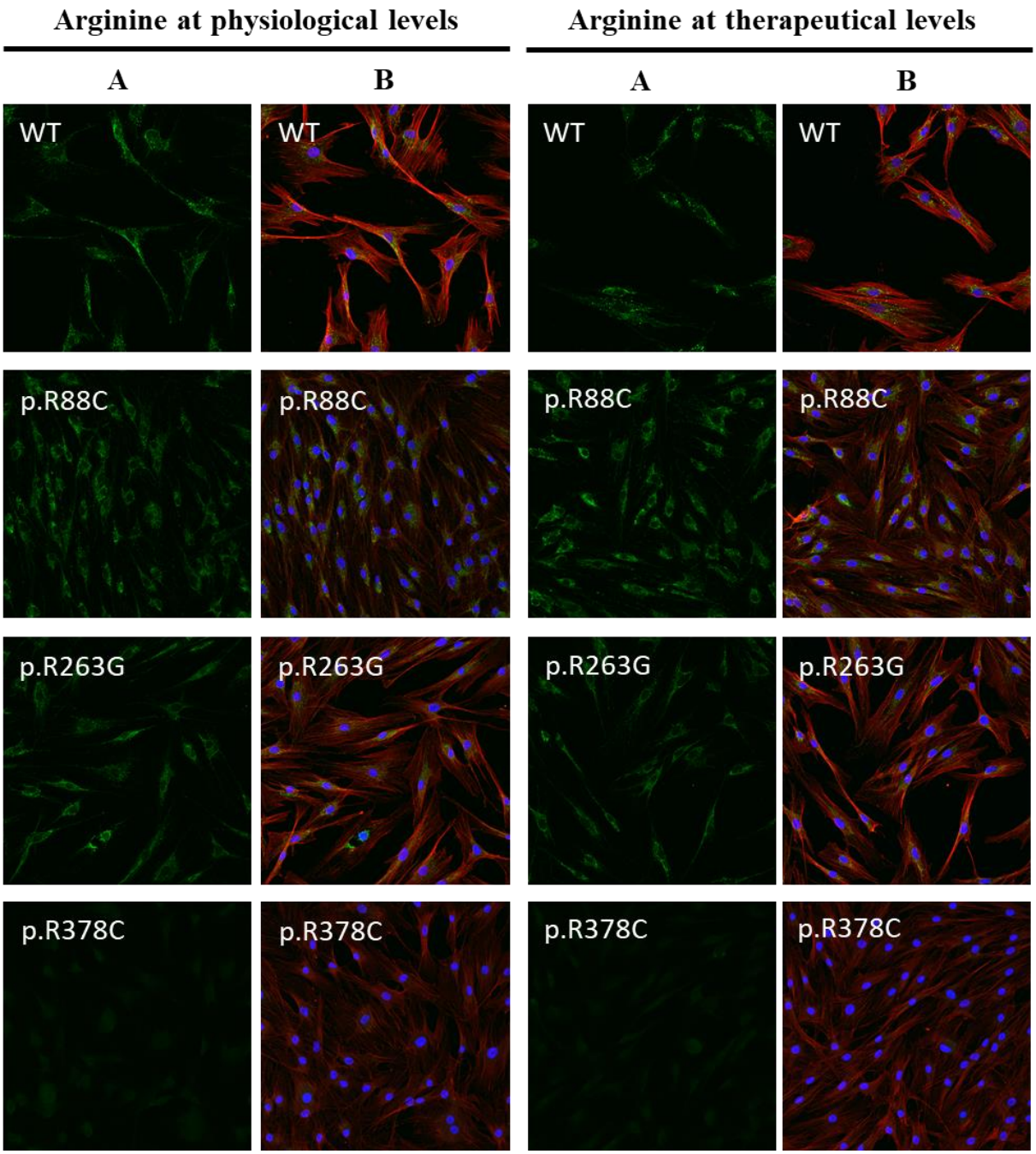

Figure V-4 **Immunohistochemical analyses of PDC-E1α deficient fibroblasts.** Comparative analysis of patient-derived fibroblasts after culture for 48h with arginine at physiological (80 µM) *versus* therapeutical (4 mM) levels. A) Images of staining with anti-PDC-E1α antibody (green); B) Merged images of staining with anti-PDC-E1α (green) and anti-actin (red) antibodies, and DAPI (blue). 20× magnification.

V.3.3. Evaluation of arginine and thiamine effects upon PDC activity and mitochondrial function of patient-derived cell lines

During the course of the pilot experiment, results of the structural and functional analyses of the pathogenic variants found in Portuguese patients were obtained and revealed a marked functional impairment in terms of lower residual PDC-E1 activity, as well as a significantly lower affinity for the thiamine pyrophosphate (TPP) cofactor, in comparison with wild-type PDC-E1 (Pavlu-Pereira et al. 2021). Accordingly, in the second phase of the *ex vivo* studies, the cell culture conditions were modified to accommodate the evaluation of the individual effects of arginine and thiamine, and also a potential synergy between them, upon the improvement of cellular phenotype, namely on enzymatic activity and mitochondrial function. Moreover, to rule out the possibility of 48 h of incubation being too long a period that might not allow the visualization of the anticipated effects, the results of these experiments were evaluated during a shorter time course, 12 and 24 h. Finally, and importantly, it has been possible to analyse the p.R253G fibroblasts derived from the patient presenting a positive response to arginine intake (Silva et al. 2009).

Immunoblotting analysis of whole cell extracts corresponding to the control, the p.R88C, the p.R263G and p.R378C cell lines corroborated the results previously obtained with 48 h of culture with arginine (Figure V-3), since neither arginine nor thiamine, alone or together, at 12 or 24 h, improved their PDC-E1α levels.

However, the p.R253G cell line, and as expected from the *in vivo* experience, revealed an appreciable response to the treatment with both compounds, alone or together. Indeed, at 12 h an increase on PDC-E1α levels induced by thiamine and arginine plus thiamine was observed, while at 24 h an important increase was caused by arginine and also by arginine plus thiamine, although the last one not as expressive (Figure V-5).

Functional studies performed with DCA-activated whole cell extracts from the control and these four patient-derived cell lines allowed to confirm that arginine and thiamine did not significantly influence the activity of most PDC-E1α variants. The basal catalytic activity of the control fibroblasts cultured at physiological levels of arginine and thiamine was 2,715 ± 58 pmol of CO_2 released per minute and per milligram of protein, falling in the normal range of our laboratory's reference values, and was used to express the relative residual activity of all the PDC-E1α deficient cell lines (Table V-3). The treatment with therapeutical levels of

arginine and/or thiamine did not substantially affect the enzymatic activity of the control cell line; the most evident alteration was induced by arginine at 12 h. Figure V-6 depicts the results of the functional tests performed in PDC-E1α deficient fibroblasts cultured for 12 and 24 h at physiological *versus* therapeutical concentrations of arginine and/or thiamine.

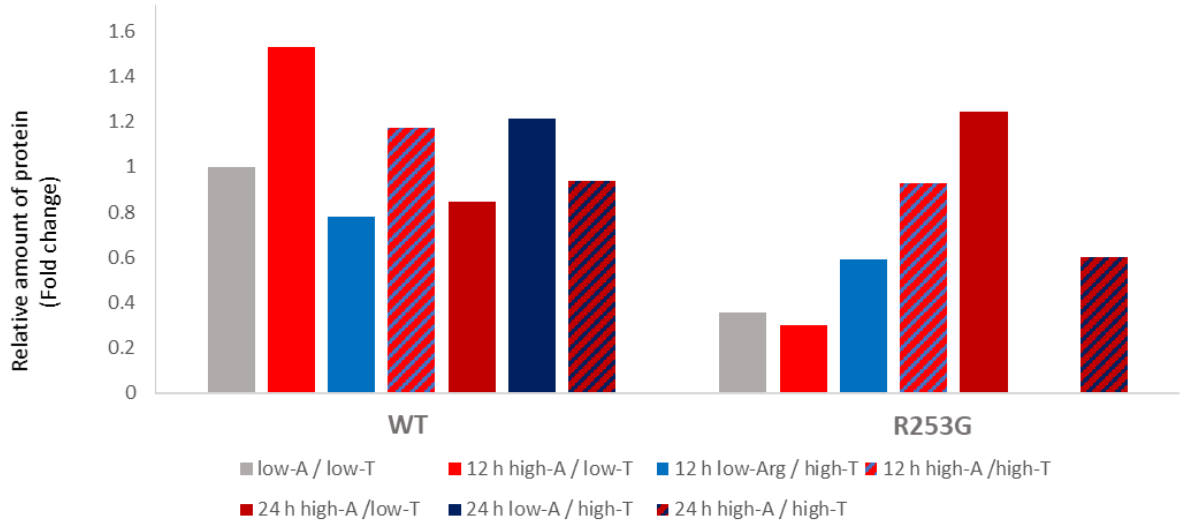

Figure V-5 **PDC-E1α protein levels assessed by western blot.** Cells were cultured for 12 or 24 h after addition of arginine and/or thiamine at physiological (low-A; low-T) or therapeutic (high-A; high-T) levels; densitometric analysis normalized to OSCP. Representative image of two independent experiments of the control cell line and of a single experiment of the p.R253G cell line (the 24 h culture with therapeutical levels of thiamine had not enough protein concentration and had to be discarded).

The p.R88C cell line exhibited 4% of the control enzymatic activity, the lowest result among the studied PDC-deficient cell lines. The R263G and R378C cell lines presented similar low residual PDC activities, 24 and 25% of the control, respectively, and these values were not significantly altered in the presence of any of the tested compounds, either alone or together.

The most interesting results came from the p.R253G cell line which presented the highest basal residual activity at physiological conditions (34%). All the incubation conditions at therapeutical levels of arginine and/or thiamine induced a significant increase in the enzymatic activity of this cell line which reached 81% of the control activity at 12 h of culture with therapeutical levels of arginine. These results fit with the *in vivo* observations which showed that arginine supplementation was truly effective in improving the metabolic, enzymatic and clinical phenotype of the patient carrying this variant.

Table V-3 **Functional studies in PDC-E1α deficient patient-derived fibroblasts.** Basal values of PDC activity related to the basal value of the control cells and their development by 12 and 24 h after addition of arginine and thiamine at physiological (low-A; low-T) or therapeutic (high-A; high-T) levels.

	Activity (% of control basal value)				
	WT	p.R88C	p.R253G	p.R263	p.R378C
low-A / low-T	100	4	34	24	25
12 h high-A / low-T	124*	6	81	28	28
12 h low-A / high-T	117	8	73	25	24
12 h high-A / high-T	109	6	78	30	23
24 h high-A / low-T	100	7	70	23	29
24 h low-A / high-T	111	7	69	31	22
24 h high-A / high-T	93	7	40	25	24

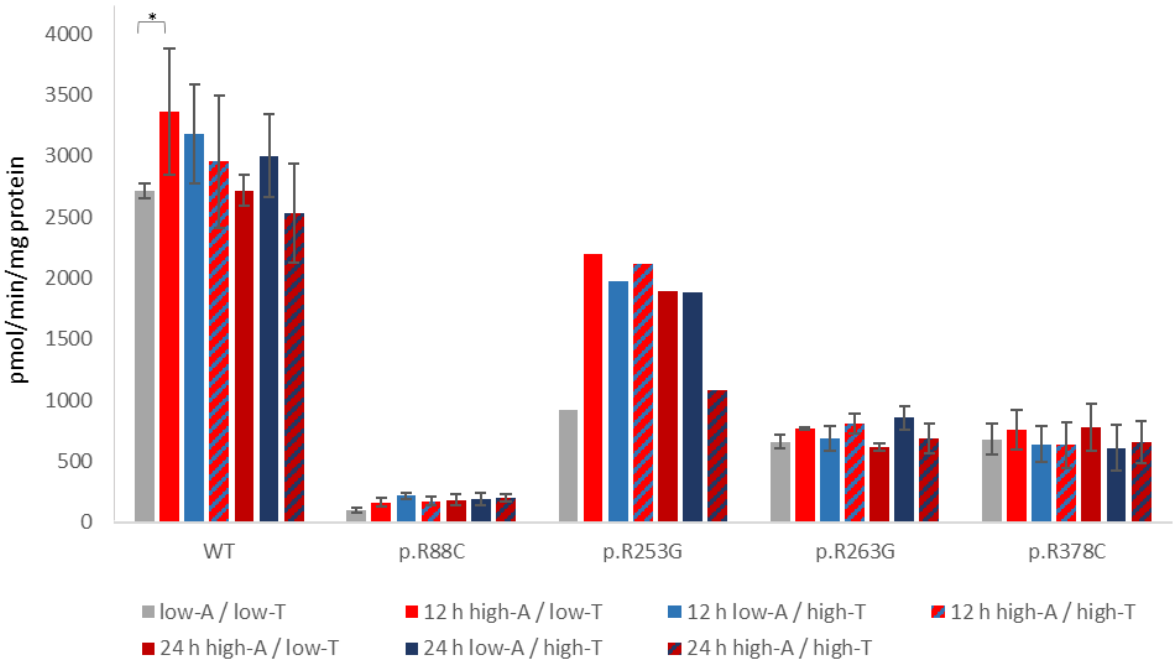

Figure V-6 **Functional studies in PDC-E1α deficient patient-derived fibroblasts.** PDC activity and the impact of arginine and thiamine at physiological (low-A / low-T) or therapeutic (high-A / high-T) levels by 12 and 24 h after supplementation. *Statistically significant difference between the basal value and a 12h exposure to Arg; $p = 0.01$; Statistical significance (p value) was determined using the Student's t test. Triplicates from two independent fibroblast batches, except for the p.R253G cell line from which a single batch was analyzed.

V.3.4. Mitochondrial Oxygen Consumption Rate

The mitochondrial function in the PDC-E1α deficient fibroblasts and the potential effect of arginine and thiamine was evaluated assessing the overall mitochondrial bioenergetics profile using the Seahorse extracellular flux analyzer (Figure V-7). Cell lines were cultured for a 12 h period with arginine and thiamine at physiological levels and with arginine and/or thiamine at therapeutical levels, and the results are presented in Figure V-8. Moreover, it must be emphasized that the results concerning the p.R378C cell line are presented with caution because, due to reduced cell proliferation, only one assay was performed.

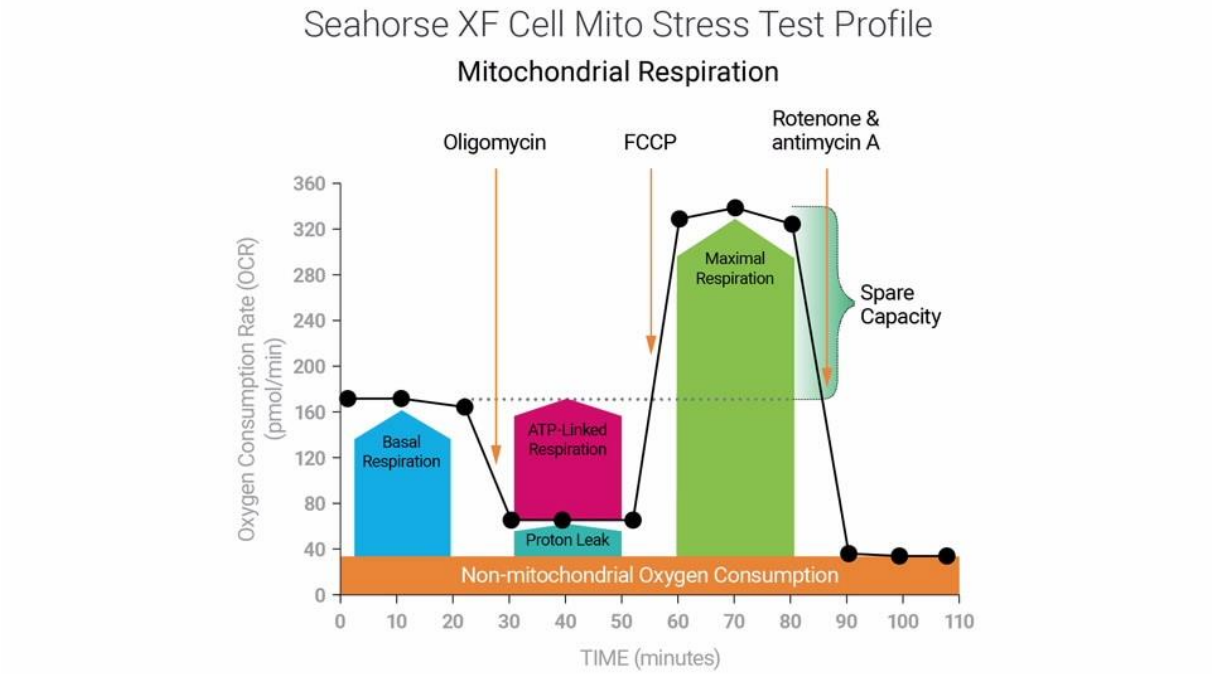

Figure V-7 **Representation of the fundamental parameters of mitochondrial respiration** obtained with these experiments. Basal respiration, ATP-linked respiration, proton leak, maximal respiration, reserve capacity (or spare respiratory capacity) and non-mitochondrial respiration (*www.seahorsebio.com*).

In physiological conditions, the control cells presented standard values for all the parameters evaluating the mitochondrial function, and any significant differences were observed when the cultures were supplemented with therapeutical levels of arginine and/or thiamine.

The results revealed that the treatment of PDC-E1α deficient cell lines with high levels or arginine and/or thiamine mainly affected the following parameters: basal respiration, ATP production, proton leak and non-mitochondrial respiration.

Concerning basal respiration, it was observed that patient-derived cell lines presented decreased levels when compared with the control cell line, showing that cells harboring the PDC-E1α variants consume less oxygen than the wild-type cells in order to meet cellular ATP demand, most probably because substrate supply or proton leak are decreased. However, simultaneous treatment with arginine and thiamine at therapeutical levels increased the basal respiration for values similar to (p.R88C and p.R263G) or higher (p.R378C) than the control cell line.

ATP production, or ATP-linked respiration is measured by the decrease in oxygen consumption rate upon injection of the ATP synthase inhibitor oligomycin and represents the portion of basal respiration that was being used to drive ATP production. The results revealed a significant effect upon the p.R263G cell line when arginine and thiamine were simultaneously added to the culture medium, translated by an increase on oxygen consumption through the respiratory chain leading to ATP production.

Proton leak represents the remaining basal respiration not coupled to ATP production and the results revealed that p.R88C and p.R378C cell lines presented increased values when treated with arginine and thiamine, thus pointing to inefficient OXPHOS.

Finally, the non-mitochondrial respiration indicates that, when OXPHOS response is blocked, cells turn to other non-mitochondrial dependent energy sources. The results showed that p.R263G and p.R378C cell lines, after treatment with arginine and thiamine, presented increased oxygen consumption by enzymes other than those in the respiratory chain, thus relying in cytosolic sources for ATP production, namely glycolysis.

In summary, the overall effect of arginine and thiamine levels on PDC-E1α deficient patient-derived fibroblasts leads to an increase in the basal oxygen consumption rate (OCR), which is attained in the cells prior to injection of mitochondrial inhibitors. Changes in basal OCR indicate that the minimal rate of metabolism required to support basic cellular functions, essential for the overall maintenance and survival of the cell, has shifted; accordingly, mutant cells require a higher metabolic rate to function and to survive. Additionally, ATP-linked OCR (or ATP production) was also increased in these conditions, indicating that an increase in ATP

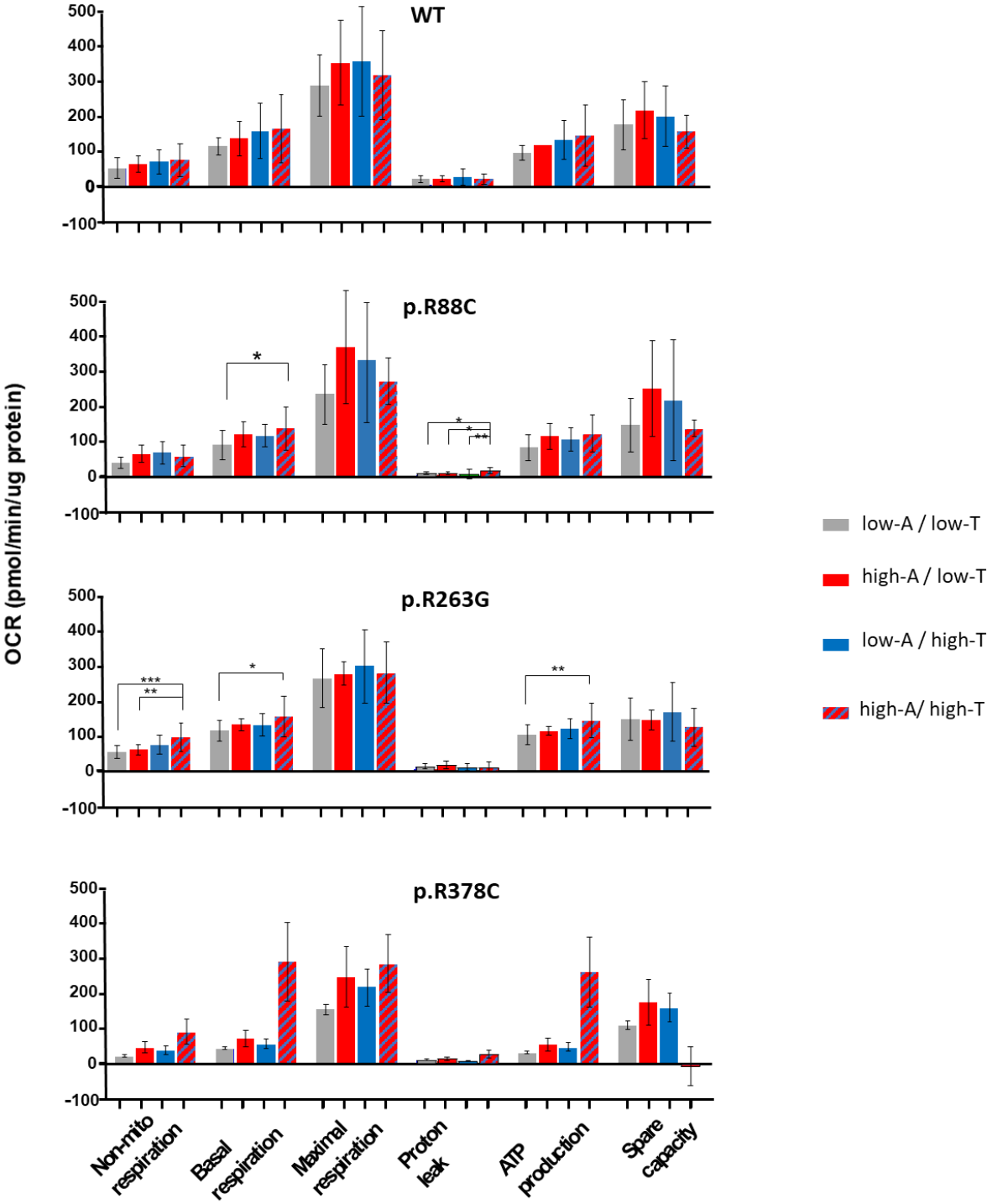

Legend to Figure V-8 on the next page

Figure V-8 **Oxygen consumption rates and bioenergetic profile of PDC-E1α deficient patient-derived fibroblasts.** Oxygen consumption rate was measured in basal conditions and after the addition of oligomycin (5 μM), sequential FCCP at 1.5 μM and 1 μM and Rotenone/Antimycin A at 1 μM each in cells treated with arginine and thiamine at physiological (Arg-/Thiamine-) or therapeutic (Arg+/Thiamine+) levels at 12 h after addition. Data represent average ± SEM of three independent experiments for control, p.R88C and p.R263G, and one experiment for p.R378C. * $p<0.05$; ** $p<0.01$; *** $p<0.001$ in a paired sample Student's t-test (i.e. fifteen replicates from three independent fibroblast batches, except for p.R378C cell line, for which five replicates where from one batch of fibroblasts due to the poor proliferation).

demand occurs when the proton flux of the ATP synthase is inhibited preventing electron transport through Complexes I-IV. ATP-linked respiration is a measure of the capacity of the cell to meet its energetic demands; therefore, this increase reveals a higher electron flow through the respiratory chain, which is coupled to elevated oxidative phosphorylation indicating an overall increased robustness in mitochondrial-related bioenergetics.

These results corroborate the ones previously obtained and concerning the effect of arginine and thiamine upon PDC activity (Figure V-6). Indeed, p.R88C variant is not stabilized by treatment with arginine and thiamine, and so its activity is not increased, which is reflected in the OCR consumption rates observed. However, although the p. R263G cell line presented any statistically significant increase on its activity (24 % at physiological conditions versus 30 % at 12 h at therapeutical levels of arginine and thiamine), the OCR assays revealed an increase ATP production in these same conditions, suggesting that the slight increase in PDC activity may be responsible for the increase in substrate production, namely NADH and $FADH_2$. Effectively, an improvement on PDC activity generates more acetyl-CoA which enters the TCA cycle and originates those substrates needed to the respiratory chain to synthesize ATP, thus increasing overall mitochondrial robustness.

V.4. CONCLUSION

As observed for other inherited metabolic disorders, the rescue efficacy of stabilizing molecules acting as pharmacological chaperones is determined by the mutation *per se.* The patients suffering from PKU are carefully selected by sapropterin dihydrochloride response testing (Muntau et al. 2014). For a peroxisome biogenesis disorder, the biochemical and clinical

improvement upon arginine supplementation in a patient homozygous for the mild p.S320F PEX12 variant (Sorlin et al. 2016) correlated with the data obtained in patient's derived fibroblasts (Berendse et al. 2013). Conversely, for the cytosolic galactose-1-phosphate uridylyltransferase (GALT), the *in vitro* rescuing effect observed in a prokaryotic model of galactose sensitivity for the severe p.Q188R variant (Coelho et al. 2015) did not correlate with arginine aspartate supplementation to patients homozygous for the p.Q188R GALT variant and to the corresponding patient´s derived fibroblasts (Haskovic et al. 2018). These observations also support the requirement of a target protein unstable but still presenting some residual activity, as a rule to observe a rescuing effect of small molecules (Muntau et al. 2014). Concerning the responsivity of the p.R253G variant to arginine and to thiamine, our observations and results are consistent at all the levels. Starting by the improvement of the patient´s clinical state upon the arginine and thiamine intake, through the increase of the PDC-E1α protein expression and PDC enzymatic activity stimulated by arginine and thiamine in the patient-derived cells, to the functional rescue of the p.R253G recombinant protein by arginine. Nevertheless, part of the results presented here are preliminary and require a greater number of independent assays in order to obtain a stronger statistical validation.

ACKNOWLEDGMENTS

We are thankful to René Feichtinger for the help with fluorescence microscopy imaging and to Lídia Gonçalves and Graça Soveral for providing the tissue culture facilities.

SUPPLEMENTARY INFORMATION

Supplementary Table V-S1 **Custom-made culture media formulation**, based on composition of common Dulbecco's Modified Eagle's Medium (DMEM, low glucose, with sodium bicarbonate).

Components	DMEM* Concentration [mmol/L]	c-m DMEM* low-A Concentration [mmol/L]	c-m DMEM* low-A / low-T Concentration [mmol/L]	c-m DMEM Seahorse low-A / low-T Concentration [mmol/L]
Amino Acids				
L-Arginine	0.398	0.08	0.08	0.08
L-Cystine	0.201	equivalent	equivalent	equivalent
Glycine	0.4	equivalent	equivalent	equivalent
L-Histidine	0.2	equivalent	equivalent	equivalent
L-Isoleucine	0.802	equivalent	equivalent	equivalent
L-Leucine	0.802	equivalent	equivalent	equivalent
L-Lysine hydrochloride	0.798	equivalent	equivalent	equivalent
L-Methionine	0.201	equivalent	equivalent	equivalent
L-Phenylalanine	0.4	equivalent	equivalent	equivalent
L-Serine	0.4	equivalent	equivalent	equivalent
L-Threonine	0.798	equivalent	equivalent	equivalent
L-Tryptophan	0.0784	equivalent	equivalent	equivalent
L-Tyrosine	0.398	equivalent	equivalent	equivalent
L-Valine	0.803	equivalent	equivalent	equivalent
Vitamins (2/4)				
Choline chloride	0.0286	equivalent	equivalent	equivalent
Folic Acid	0.00907	equivalent	equivalent	equivalent
i-Inositol	0.04	equivalent	equivalent	equivalent
Niacinamide	0.0328	equivalent	equivalent	equivalent
D-Calcium pantothenate	0.00839	equivalent	equivalent	equivalent
Pyridoxine hydrochloride	0.0196	equivalent	equivalent	equivalent
Riboflavin	0.00106	equivalent	equivalent	equivalent
Thiamine hydrochloride	0.0119	0.0119	0.000015	0.000015
Inorganic Salts (3/4)				
Calcium Chloride ($CaCl_2$)	1.8	equivalent	equivalent	equivalent
Ferric Nitrate ($Fe(NO_3)_3 \cdot 9H_2O$)	0.000248	0.000248	0.000248	0
Magnesium Sulfate ($MgSO_4$-7H2O)	0.813	equivalent	equivalent	equivalent
Potassium Chloride (KCl)	5.33	equivalent	equivalent	equivalent
Sodium Bicarbonate ($NaHCO_3$)	44.05	44.05	44.05	0
Sodium Chloride (NaCl)	110.34	110.34	110.34	143
Sodium Phosphate monobasic (NaH_2PO_4)	0.916	equivalent	equivalent	equivalent
Other Components (4/4)				
D-Glucose (Dextrose)	25	equivalent	equivalent	equivalent
Phenol Red	0.0399	equivalent	equivalent	equivalent
Sodium Pyruvate	1	equivalent	equivalent	equivalent
L-Glutamine	3.97	equivalent	equivalent	equivalent
HEPES	0	0	0	10
adjusted pH to 7.4				

REFERENCES

Berendse K, Ebberink MS, Ijlst L, et al (2013) Arginine improves peroxisome functioning in cells from patients with a mild peroxisome biogenesis disorder. Orphanet J Rare Dis 8:138. https://doi.org/10.1186/1750-1172-8-138

Berg A, Westphal AH, Bosma HJ, De Kok A (1998) Kinetics and specificity of reductive acylation of wild-type and mutated lipoyl domains of 2-oxo-acid dehydrogenase complexes from Azotobacter vinelandii. Eur J Biochem 252:45–50. https://doi.org/10.1046/j.1432-1327.1998.2520045.x

Bradford MM (1976) A rapid and sensitive method for the quantitation of microgram quantities of protein utilizing the principle of protein-dye binding. Anal Biochem 72:248–254. https://doi.org/10.1016/0003-2697(76)90527-3

Brown G (2014) Defects of thiamine transport and metabolism. J Inherit Metab Dis 37:577–585. https://doi.org/10.1007/s10545-014-9712-9

Brown GK, Otero LJ, LeGris M, Brown RM (1994) Pyruvate dehydrogenase deficiency. J Med Genet 31:875–879. https://doi.org/10.1136/jmg.31.11.875

Castiglioni C, Verrigni D, Okuma C, et al (2015) Pyruvate dehydrogenase deficiency presenting as isolated paroxysmal exercise induced dystonia successfully reversed with thiamine supplementation. Case report and mini-review. Eur. J. Paediatr. Neurol. 19:497–503

Cate RL, Roche TE, Davis LC (1980) Rapid intersite transfer of acetyl groups and movement of pyruvate dehydrogenase component in the kidney pyruvate dehydrogenase complex. J Biol Chem 255:7556–62

Ciszak EM, Korotchkina LG, Dominiak PM, et al (2003) Structural basis for flip-flop action of thiamin pyrophosphate-dependent enzymes revealed by human pyruvate dehydrogenase. J Biol Chem 278:21240–21246. https://doi.org/10.1074/jbc.M300339200

Clot JP, Benelli C, Fouque F, et al (1992) Pyruvate dehydrogenase activity is stimulated by growth hormone (GH) in human mononuclear cells: A new tool to measure GH responsiveness in man. J Clin Endocrinol Metab 74:1258–1262. https://doi.org/10.1210/jcem.74.6.1592868

Coelho AI, Trabuco M, Silva MJ, et al (2015) Arginine functionally improves clinically relevant human galactose-1-phosphate uridylyltransferase (GALT) variants expressed in a prokaryotic model. In: JIMD Reports. Wiley-Blackwell, pp 1–6

De Matos MR, Posaioana I, Carvalho FS, et al (2019) A systematic pan-cancer analysis of genetic heterogeneity reveals associations with epigenetic modifiers. Cancers (Basel) 11:. https://doi.org/10.3390/cancers11030391

Di Rocco M, Doria Lamba L, Minniti G, et al (2000) Outcome of thiamine treatment in a child with Leigh disease due to thiamine-responsive pyruvate dehydrogenase deficiency. Eur J Paediatr Neurol 4:115–117. https://doi.org/10.1053/ejpn.2000.0278

El-Gharbawy AH, Boney A, Young SP, Kishnani PS (2011) Follow-up of a child with pyruvate dehydrogenase deficiency on a less restrictive ketogenic diet. Mol Genet Metab 102:214–215. https://doi.org/10.1016/j.ymgme.2010.11.001

Ferriero R, Brunetti-Pierri N (2013) Phenylbutyrate increases activity of pyruvate dehydrogenase complex. Oncotarget 4:804–805

Fouque F, Brivet M, Boutron A, et al (2003) Differential effect of DCA treatment on the pyruvate dehydrogenase complex in patients with severe PDHC deficiency. Pediatr Res 53:793–799. https://doi.org/10.1203/01.PDR.0000057987.46622.64

Guo J, Hezaveh S, Tatur J, et al (2017) Reengineering of the human pyruvate dehydrogenase complex: from disintegration to highly active agglomerates. Biochem J 474:865–875. https://doi.org/10.1042/BCJ20160916

Haskovic M, Derks B, Van der Ploeg L, et al (2018) Arginine does not rescue p.Q188R mutation deleterious effect in classic galactosemia. Orphanet J Rare Dis 13:. https://doi.org/10.1186/s13023-018-0954-8

Head RA, Brown RM, Zolkipli Z, et al (2005) Clinical and genetic spectrum of pyruvate dehydrogenase deficiency: Dihydrolipoamide acetyltransferase (E2) deficiency. Ann Neurol 58:234–241. https://doi.org/10.1002/ana.20550

Imbard A, Boutron A, Vequaud C, et al (2011) Molecular characterization of 82 patients with pyruvate dehydrogenase complex deficiency. Structural implications of novel amino acid substitutions in E1 protein. Mol Genet Metab 104:507–16. https://doi.org/10.1016/j.ymgme.2011.08.008

Jiang J, Baiesc FL, Hiromasa Y, et al (2018) Atomic Structure of the E2 Inner Core of Human Pyruvate Dehydrogenase Complex. Biochemistry 57:2325–2334. https://doi.org/10.1021/acs.biochem.8b00357

Kaplon J, Zheng L, Meissl K, et al (2013) A key role for mitochondrial gatekeeper pyruvate dehydrogenase in oncogene-induced senescence. Nature 498:109–112. https://doi.org/10.1038/nature12154

Korotchkina LG, Patel MS (2001) Probing the Mechanism of Inactivation of Human Pyruvate Dehydrogenase by Phosphorylation of Three Sites. J Biol Chem 276:5731–5738. https://doi.org/10.1074/jbc.M007558200

Linn TC, Pettit FH, Reed LJ (1969) Alpha-keto acid dehydrogenase complexes. X. Regulation of the activity of the pyruvate dehydrogenase complex from beef kidney mitochondria by phosphorylation and dephosphorylation. Proc Natl Acad Sci U S A 62:234–41. https://doi.org/10.1073/pnas.62.1.234

Milne JLS (2002) Molecular architecture and mechanism of an icosahedral pyruvate dehydrogenase complex: a multifunctional catalytic machine. EMBO J 21:5587–5598. https://doi.org/10.1093/emboj/cdf574

Muntau AC, Leandro J, Staudigl M, et al (2014) Innovative strategies to treat protein misfolding in inborn errors of metabolism: pharmacological chaperones and proteostasis regulators. J Inherit Metab Dis. https://doi.org/10.1007/s10545-014-9701-z

Naito E, Ito M, Yokota I, et al (2002) Thiamine-responsive pyruvate dehydrogenase deficiency in two patients caused by a point mutation (F205L and L216F) within the thiamine pyrophosphate binding region. Biochim Biophys Acta - Mol Basis Dis 1588:79–84.

https://doi.org/10.1016/S0925-4439(02)00142-4

Nascimento C, Leandro J, Tavares de Almeida I, Leandro P (2008) Modulation of the activity of newly synthesized human phenylalanine hydroxylase mutant proteins by low-molecular-weight compounds. Protein J 27:392–400. https://doi.org/10.1007/s10930-008-9149-9

Pastoris O, Savasta S, Foppa P, et al (1996) Pyruvate dehydrogenase deficiency in a child responsive to thiamine treatment. Acta Paediatr Int J Paediatr 85:625–628. https://doi.org/10.1111/j.1651-2227.1996.tb14104.x

Patel KP, O'Brien TW, Subramony SH, et al (2012) The spectrum of pyruvate dehydrogenase complex deficiency: Clinical, biochemical and genetic features in 371 patients. Mol Genet Metab 106:385–394. https://doi.org/10.1016/j.ymgme.2012.03.017

Patel MS, Korotchkina LG (2006) Regulation of the pyruvate dehydrogenase complex. In: Biochemical Society Transactions. pp 217–222

Pavlu-Pereira H, Lousa D, Tomé CS, et al (2021) Structural and functional impact of clinically relevant E1α variants causing pyruvate dehydrogenase complex deficiency. Biochimie 183:78–88. https://doi.org/10.1016/j.biochi.2021.02.007

Pavlu-Pereira H, Silva MJ, Florindo C, et al (2020) Pyruvate dehydrogenase complex deficiency: updating the clinical, metabolic and mutational landscapes in a cohort of Portuguese patients. Orphanet J Rare Dis 15:. https://doi.org/10.1186/s13023-020-01586-3

Seifert F, Ciszak E, Korotchkina L, et al (2007) Phosphorylation of serine 264 impedes active site accessibility in the E1 component of the human pyruvate dehydrogenase multienzyme complex. Biochemistry 46:6277–6287. https://doi.org/10.1021/bi700083z

Senisterra GA, Finerty PJ (2009) High throughput methods of assessing protein stability and aggregation. Mol Biosyst 5:217–223. https://doi.org/10.1039/b814377c

Silva MJ, Pinheiro A, Eusébio F, et al (2009) Pyruvate dehydrogenase deficiency: identification of a novel mutation in the PDHA1 gene which responds to amino acid supplementation. Eur J Pediatr 168:17–22. https://doi.org/10.1007/s00431-008-0700-7

Smolle M, Prior AE, Brown AE, et al (2006) A new level of architectural complexity in the human pyruvate dehydrogenase complex. J Biol Chem 281:19772–19780. https://doi.org/10.1074/jbc.M601140200

Sorlin A, Briand G, Cheillan D, et al (2016) Effect of l -Arginine in One Patient with Peroxisome Biogenesis Disorder due to PEX12 Deficiency. Neuropediatrics 47:179–181. https://doi.org/10.1055/s-0036-1578798

Sperl W, Fleuren L, Freisinger P, et al (2015) The spectrum of pyruvate oxidation defects in the diagnosis of mitochondrial disorders. J Inherit Metab Dis 38:391–403. https://doi.org/10.1007/s10545-014-9787-3

Vander Heiden MG, Cantley LC, Thompson CB (2009) Understanding the warburg effect: The metabolic requirements of cell proliferation. Science (80-.). 324:1029–1033

Wexler ID, Hemalatha SG, McConnell J, et al (1997) Outcome of pyruvate dehydrogenase deficiency treated with ketogenic diets. Studies in patients with identical mutations. Neurology 49:1655–61.

https://doi.org/10.1212/wnl.49.6.1655

Yu X, Hiromasa Y, Tsen H, et al (2008) Structures of the Human Pyruvate Dehydrogenase Complex Cores: A Highly Conserved Catalytic Center with Flexible N-Terminal Domains. Structure 16:104–114. https://doi.org/10.1016/j.str.2007.10.024

Yue WW (2016) From structural biology to designing therapy for inborn errors of metabolism. J Inherit Metab Dis 39:489–498. https://doi.org/10.1007/s10545-016-9923-3

Zhou ZH, McCarthy DB, O'Connor CM, et al (2001) The remarkable structural and functional organization of the eukaryotic pyruvate dehydrogenase complexes. Proc Natl Acad Sci U S A 98:14802–7. https://doi.org/10.1073/pnas.011597698

Zimmermann FA, Mayr JA, Neureiter D, et al (2009) Lack of complex i is associated with oncocytic thyroid tumours. Br J Cancer 100:1434–1437. https://doi.org/10.1038/sj.bjc.6605028

Chapter VI

General Discussion and Perspectives

The truly intricated character of the pyruvate dehydrogenase complex (PDC) is fulfilled in numerous aspects, considering among others i) its prominent position in controlling the energetic metabolism, ii) the involvement of a high number of diverse elements in the multifactorial sequential reaction, iii) sophisticated functional mechanisms such as coupled and directed metabolic channeling within multi-step reactions by swinging lipoyl arms and regeneration of co-factors, iv) refined and rapid regulation and, finally yet importantly v) a highly organized assembly of large multidomain proteins.

Hence, any alteration leading to PDC dysfunction originates a deficiency which is categorized among inherited metabolic diseases (IMD), a vast and heterogeneous group of genetic disorders and an important cause of child morbidity and mortality. Individually they are rare but, in total, they represent around 5% of pediatric admissions in hospitals, thus representing an important health problem. The degree of success in the treatment of inherited metabolic disorders depends on early and accurate diagnosis, prompt intervention and intimate understanding of disease pathogenesis. The ideal goal of IMD treatment is to reestablish the balance of physiological processes in the organism, in other words, to restore homeostasis, a term introduced by Walter B. Cannon in 1934 (Cannon 1934; Scriver and Treacy 1999). Even so, most of the currently available therapies meet many limits to reach this aim.

The solely symptomatic treatment at the level of clinical phenotype, such as the use of anticonvulsants in neurodegenerative genetic disorders or surgical interventions in case of malformations, is independent from understanding the pathogenesis and has mainly a palliative effect. In contrast, treatment at the metabolite level is closely related to the knowledge of the pathophysiological processes and involves a reasonable variety of nutritional and pharmacological approaches (Treacy et al. 2001). For example, dietary alterations designed to restrict the intake of a particular substrate allow controlling the major source of a toxic precursor in metabolic disorders like galactosemia or PKU and thus preventing infantile mortality and severe mental retardation. Despite the global improvement, patients on restricted diets frequently present decreased plasma levels of trace elements and vitamins (Acosta 1996; Hanley et al. 1996) or often exhibit long-term serious complications as for example brain impairments and primary ovarian insufficiency in classic galactosemia (Delnoy et al. 2021). Dietary regulation can also be used in IMD to stimulate alternative metabolic pathways. This is the case of the ketogenic diet used in PDC deficiency, which enhances β-oxidation and the

use of ketone bodies for ATP production; nevertheless, the efficacy of this approach is limited by the capacity of the metabolism.

In some disorders, where the accumulation of upstream substrates could be tolerated, inhibiting a prior step in the pathway may reduce the accumulation of the toxic metabolite (Treacy et al. 2001). Substrate reduction therapy (SRT) is often used in lysosomal storage disorders caused by defects in the enzymes involved in glycosphingolipid degradation (Platt et al. 2003; Cox 2007). However, downstream side effects, such as diarrhea and peripheral or even central neuropathy may occur, as a result of inhibition of other glycosidases and to the capacity of the SRT compounds to cross the blood–brain barrier, altering consequently the homeostasis of the more complex glycolipids, gangliosides, and related lipids in the brain (Desnick et al. 2018; Sun et al. 2021).

Overcoming the limitations of the existing therapies for IMD mentioned above, the gap between the theoretical erudition in medical sciences and its applications in practice is becoming increasingly filled. Expanding the knowledge regarding the molecular basis of IMD and advances in analytic and diagnostic technologies permit the use of therapeutic strategies with good prospects to achieve the restoration of homeostasis. Although further progress will depend also on the challenging development of genetic medicines, recent available therapeutic approaches acting at the level of dysfunctional protein, involving protein-replacement and protein-enhancement strategies, are being successfully applied in some IMD. Since the first enzyme replacement therapy for Gaucher disease (Barton et al. 1991), the approval has been lately extended to eleven lysosomal storage disorders and few other IMD, such as PKU (Markham 2018; Bonam et al. 2019; Ploeg 2020). Several concerns about the replenishing recombinant enzymes are still under investigation, such as immunogenicity and limitations in crossing the blood-brain barrier (Marchetti et al. 2021). New targeted delivery systems are being developed in order to improve the efficacy, the enzyme interaction with cell membrane and internalization, the reduction in the immune response, the cost, etc. (Safary et al. 2018; Lino et al. 2021).

Nevertheless, instead of being replaced, the dysfunctional misfolded protein can be recovered using chemical and pharmacological chaperones as stabilizers of protein structure and rescuers of enzymatic function. Chaperone therapy is an appealing therapeutic strategy for conformational disorders. In general, the compelling number of missense mutations responsible

for IMD corroborates the need for structural and functional studies of the variant proteins in order to disclose the molecular changes caused to the defective enzyme and to open avenues for designing therapies based on small molecules able to rescue protein structure and function (Yue 2016, 2021).

From this perspective, we consider the PDCD an eligible candidate for chaperon therapy. Due to the central position of PDC in energy metabolism, the only therapeutic approach at the metabolite level, suitable for PDC deficient patients, is the ketogenic diet, where the ketone bodies produced by β-oxidation offer an alternative energy substrate to glucose. As well, owing to the large multienzyme assembly of PDC, the enzyme replacement strategy is not an option.

Accordingly, to get insights into PDC and related deficiencies, a multifactorial approach is needed, using methodologies from many different experimental areas, namely genetics, cellular and molecular biology, biochemistry and biophysics, and metabolic flux analysis. Indeed, each technique addresses specific aspects of the structure and function of biological molecules and, as such, a plethora of techniques are needed to get an integrated view of the abnormal cellular metabolism.

In the first part of this study, we characterized the profiles of thirteen Portuguese PDC deficient patients. Evaluation of a wide range of phenotypic parameters, as clinical features, brain malformations, biochemical biomarkers and current therapy, together with PDC activity assay, sequencing and *in silico* analysis of PDC mutations granted the composition of a complete information on the associated clinical, biochemical, enzymatic and genotypic spectra. We presented the first comprehensive report on phenotypic and genotypic variability in a cohort of PDC deficient patients diagnosed in Portugal.

Establishing an accurate diagnosis of PDC deficiency (PDCD) is a demanding process due to the phenotypic presentation which can be observed in many other neurodegenerative disorders. Due to variability in a high number of parameters, the adversity in finding a diagnosis is a common challenge in mitochondrial disorders (Parikh et al. 2019; Forny et al. 2021). The wide group of mitochondrial diseases shares not only many clinical symptoms as neurological impairment and muscle hypotonia, but even biochemical markers such as elevated lactate and alanine (Boenzi and Diodato 2018; Parikh et al. 2019). Nevertheless, these analytes may display normal levels even in individuals with genetically confirmed mitochondrial disease, thus giving importance to the evaluation of blood lactate/pyruvate molar ratio for the differential diagnosis

of PDCD (Debray et al. 2007). The precise interpretation of biochemical biomarkers together with sequence analysis is essential to achive the acurate diagnosis in mitochondrial disorders (Forny et al. 2021). Accordingly, in this study we only included the PDC deficient patients whose diagnosis was confirmed at the molecular level.

Taking into consideration our data from the Portuguese subset of patients, the phenotype roughly resembled the genotype. However, up to date, there is no consensus about what degree allows establishing the genotype-phenotype correlation in PDCD. Indeed, its clinical spectrum is, like in other mitochondrial diseases, very broad. According to several authors, the severity of the disease can be generally associated with the mutation type and with the affected subunit (Gray et al. 2014; Sperl et al. 2015). On the other hand, an extensive survey on 371 PDC deficient individuals highlighted the difficulties to distinguish the clinical, neuroimaging or biochemical characteristics of patients bearing the frequently reported mutations in the *PDHA1* gene from those with genetic defects in any of the other PDC components (Patel et al. 2012). The poor correlation between PDC activity and clinical presentation, regardless of the affected subunit, was reported in this work as an outcome of a general PDC impairment, caused by potentially any congenital or acquired defect in any component of the complex.

From our perspective, the clinical presentation of PDCD in the Portuguese group of patients allowed to estimate an approximate division into two categories: one, caused by *PDHA1* and *PDHX* mutations, and the other, caused by *DLD* mutations. The first group, indeed, exhibited a considerable variability in the clinical symptoms, in conformity with the broad phenotypic spectrum reported in these patients (Sperl et al. 2015). However, we were able to observe some differences at the level of enzymatic activity, allowing to distinguish between the *PDHX* deficient patients presenting higher and closer relative PDC activity values (median value 29 ± 3.4 %) and *PDHA1* deficient patients displaying a wider range of activities (median value 23.5 ± 10.7 %), with half of them below 20 %.

The mutational spectrum of E1α deficiency was represented exclusively by missense mutations. From our three male patients carrying the potentially lethal p.R378C mutation (Patel et al. 2012), one deceased at three years of age and the twins, presently aged 8 years, display a severe clinical picture. However, a female patient bearing the p.R378H substitution reached adulthood, probably due to a lyonization effect.

The high incidence of E3BP deficiency is mostly caused by the p.R284X variant in the *PDHX* gene, half the cases originating from the Azores Islands, thus denoting a founder effect. We described this E3BP variant for the first time in 2016 (Pinheiro et al. 2016) and, until now, only another Portuguese patient has been reported to carry this mutation (Nogueira et al. 2019). Besides this nonsense mutation, the genotypes of all our E3BP deficient patients encompass other very severe mutations, leading to null alleles. Nevertheless, our older patients reached adulthood, in accordance with a reportedly high proportion of long-term survival among E3BP deficient patients (Marsac et al. 1993; Brown et al. 2007; Imbard et al. 2011). In general, an overwhelming majority of the mutations hitherto identified in the *PDHX* gene are, as in this work, deletions, nonsense mutations, point mutations at intron-exon boundaries, or even large intra-genic rearrangements, expected to result in a complete absence of E3BP protein (Brown et al. 2007; Imbard et al. 2011; Gray et al. 2014; Byron and Lindsay 2017). Despite this fact, the patients retain considerably significant PDC activity (20 - 30 %). This evidence might represent an unassuming contribution to the debate about the E2 / E3BP stoichiometry and the structure of the basic trimeric unit in the PDC core. The exact organization of the PDC core remains questionable due to the absence of high-resolution information (Zhou et al. 2001; Brautigam et al. 2006; Kyrilis et al. 2021). Thus, even the accurate placing of the E1 and E3 subunits around the core may be intriguing, because their catalytic function depends on the proximity to the swinging lipoyl arm and on their attachment to the flexible peripheral-subunit binding domains of the E2 and E3BP, respectively (Kyrilis et al. 2021).

On one hand, as a structural subunit, E3BP does not directly contribute to the complex enzymatic activity. On the other hand, the significantly truncated E3BP, if present at all in the cell, would likely compromise the structure of the E2/E3BP PDC core and respective binding of the E3 component and ultimately lead to drastic loss of PDC activity. Both the E2 and E3BP components have a similar structure and domain organization, despite only E2 being endowed with catalytic activity (Harris et al. 1997). The hypothesis of the E2 core directly binding to the E3 enzyme may underlie the observed residual PDC activity (Brown et al. 2007; Vijayakrishnan et al. 2011; Gray et al. 2014; Byron and Lindsay 2017). In their recent work, Prajapati and collaborators report a non-uniform stoichiometry of the E2 / E3BP PDC core. The imbalanced distribution of E2 and E3BP constituents of the trimeric units results into structurally dynamic E1 and E3 clusters (Prajapati et al. 2019). Interestingly, in a current publication, Kyrilis and

coworkers (Kyrilis et al. 2021) contested the lately favored “substitution model” comprising 40:20 or eventually 48:12 E2 and E3BP subunits, respectively, to form the PDC core (Hiromasa et al. 2004; Brautigam et al. 2009; Jiang et al. 2018; Prajapati et al. 2019). Based on diverse biochemical and biophysical methods to probe PDC organization in native cell extracts from *Chaetomium thermophilum*, Kyrilis presented an asymmetric reconstruction of the active, native PDC with the stoichiometry 60:12, supporting the original “addition model” of the core organization (60 E2 + 12 E3BP) (Maeng et al. 1996; Sanderson et al. 1996).

Nevertheless, all current works agree in defining the ”division-of-labor” (DOL) system as a mechanism for the higher-order interaction between the components of 2-oxoacid dehydrogenase complexes (Milne et al. 2006; Prajapati et al. 2019; Kyrilis et al. 2021).

The fact that PDC deficient patients lacking the E3BP component retain considerable PDC activity and often reach adulthood might provide the evidence for the DOL mechanism, where the enzyme components form a transient flexible catalytic cluster, including tethering the E3 component.

In general, the phenomenon of reaching adulthood was remarkably common to most of our PDC deficient patients, as opposed to several other reports (Barnerias et al. 2010; Quintana et al. 2010; Patel et al. 2012; DeBrosse et al. 2012). The most notable example is the case of a very mild deficiency in PDC-E3 subunit, which was only diagnosed when the patient was 17 years old. Short time later, after suffering an acute metabolic decompensation originating spastic tetraparesis with gait and language loss, the patient currently exhibits a moderate-to-severe psychomotor handicap. Moreover, although the PDC-E3 subunit is a common component to 2-oxoacid dehydrogenase complexes, this patient did not display the associated biochemical or clinical phenotypes.

Concerning the possible therapies, the ketogenic diet is an adequate measure to stimulate alternative metabolic pathways; nevertheless, the overall effect in our patients is mainly palliative, since all patients but one continue presenting clinical features ranging from moderate to severe forms. Still, the ketogenic diet was effective in controlling childhood-onset epilepsy and paroxysmal dystonia in our patients. Some authors suggest the use of ketogenic diet as a first-line therapy for patients with seizures and consider this treatment as appropriate for pediatric patients selected by clinical trials (Bhandary and Aguan 2015).

In theory, the impaired catalytic activity of PDC can be intervened also by virtue of the regulatory system and, indeed, dichloroacetate (DCA) or phenylbutyrate, as xenobiotic inhibitors of PDKs, are suggested by some authors for treating PDC deficient patients (Fouque et al. 2003; Han et al. 2008; Ferriero et al. 2013). In general, the tight regulation of PDC activity through the control of PDKs is gaining importance as a target for the treatment of oncologic and other diseases (Stacpoole 2017), as it was mentioned in Chapter I. Curiously, the importance of PDC regulation has been demonstrated also in hibernating mammals, where the narrow control of the metabolic flux into the TCA cycle switches via PDC phosphorylation between the aerobic and anaerobic metabolism during times of nutrient deprivation (Wijenayake et al. 2017).

When administered to patients, DCA supposedly increases PDC activity by inhibiting its phosphorylation, maintaining PDC-E1α subunit in the catalytically active state. From my point of view, however, this molecular mechanism can only be operational for the phosphorylation loops which folded properly. According to the results achieved in this work and to recently published data (Whitley et al. 2018), the structure of the PDC-E1α regulatory loop can be affected by the global effect of missense mutations in the *PDHA1* gene and it is questionable whether promoting the permanent dephosphorylation of the disturbed loop may improve the catalytic activity in the case of impaired E1 inactivation.

Most of the patients from our cohort receive long term thiamine supplementation. This treatment can compensate the impaired PDC-E1 affinity to the TPP cofactor and may potentially stabilize the PDC-E1 active site in several variants.

To investigate the molecular mechanisms underlying the pathogenic effects of the *PDHA1* mutations p.F205L, p.R253G, p.R378C and p.R378H, found in the Portuguese population, we employed a set of biochemical and biophysical procedures, namely far-UV circular dichroism, differential scanning fluorimetry, dynamic light scattering, limited proteolysis by trypsin and activity assays, complemented by molecular dynamics (MD) simulations. This methodological strategy enabled a valuable detailed insight into the functional and structural molecular characteristics of the wild-type PDC-E1 and its pathogenic variants. We used a bicistronic expression vector to produce in *Escherichia coli* the PDC-E1α protein integrated in biologically active heterotetrameric PDC-E1 (αα'ββ'). For the same objective regarding biochemical and biophysical analyses of PDC-E1α variants, it has been reported either an analogical expression

method (Whitley et al. 2018) or a system using yeast as an eukaryotic model (Drakulic et al. 2018).

Whitley and coworkers highlighted the role of the disordered regulatory loop in PDC-E1 inactivation, reported affected coenzyme binding and even the absence of phosphorylation due to the p.V138M amino acid substitution. Besides, this work suggested a reduced capacity of PDC-E1 subunit to bind the PDC-E2 lipoyl domain, as a consequence of the disturbed loop structure (Whitley et al. 2018). Likewise, in a yeast model, Drakulic and collaborators present discrete amino acid substitutions causing various global effects not only on PDC-E1 folding and PDC function, but also on the subunit structure and complex assembly (Drakulic et al. 2018).

In accordance with these works, our results suggested that several missense mutations disrupt the possible interactions in unstructured loops and indicate a general relationship between regulatory loop disorder and loss of PDC-E1 catalytic efficiency. In our work, and performing MD simulations, we confirmed the flexible and unstable nature of the phosphorylation loops; indeed, mapping the average root mean square deviation (RMSD) of each residue on the PDC-E1 protein structure revealed that, both in WT and in all variants, the most unstable region corresponded to loop A.

MD simulations together with complementary experimental methods became an important tool for unraveling the functional mechanisms of proteins and elucidating the structural bases of disease (Hollingsworth and Dror 2018). Since the first experiment with simple gasses (Alder and Wainwright 1957), through publications which originated Nobel Prize achievements (Lifson and Waeshel 1968; Levitt and Lifson 1969) and enabled the first protein simulations (McCammon et al. 1977), MD simulations have proven to be increasingly valuable. In recent years, many works have been published in the field of molecular biology, neuroscience and drug discovery, combining experimental and computational data (reviewed by Hollingsworth and Dror 2018).

In this work, we sought to complement the information on stability/flexibility by MD simulations with a zoomed-in view to each amino acid substitution. It was revealed that all amino acid substitutions, even the remote ones, alter the stability of the active site and of the TPP binding region. The effect of the different affected residues seemed to propagate from disparate locations through the protein to the α–β interface channel and to affect the stability of

the TPP binding region. A similar phenomenon was commented recently in a review on biochemical and biophysical data on the impact of missense mutations on the structure and catalytic activity of aldehyde dehydrogenase 7A1 (ALDH7A1) causing pyridoxine-dependent epilepsy (Korasick and Tanner 2021). Curiously, in ALDH7A1, some of the amino acid substitutions located in the active site of the enzyme showed a mild impact on structure and function, whereas the remote missense mutations exhibited profound effects. Some of them, leading to substitution of remote residues in oligomer interfaces, inhibit the formation of the active ALDH7A1 tetramer. Correspondingly, the effect of *PDHA1* mutations on the interaction with other PDC components cannot be excluded. For example, the PDC-E1α C-terminal region (residues Y369-S390) has a putative role in stabilizing the A190-N195 helix holding the K^+ on the PYR domain of the neighboring β' subunit (Ciszak et al. 2003). So, whereas the R378 substitutions clearly impair the α-β interactions within PDC-E1 and affect E1α TPP binding, this structural perturbation may also propagate to the E1-E2 interaction, causing the severe phenotypes observed in patients bearing the corresponding mutations (Patel et al. 2012). Apparently, the function of hypothetical transient flexible catalytic clusters working in the DOL mechanism (Kyrilis et al. 2021), may also suffer a negative impact.

Combining the results from our multi-methodological approach to analyse the pathogenic variants with our observations on a patient carrying the c.757A>G mutation in the *PDHA1* gene, yielding the PDC-E1α p.R253G variant, and who revealed to be remarkably responsive to supplementation with thiamine and arginine aspartate (Silva et al. 2009), we evaluated the potential effect of arginine in rescuing the PDC-E1 enzyme *in vitro*. However, regardless of their specific structural and functional characteristics, most variants did not exhibit any significant improvement when expressed in the medium enriched with arginine. Noteworthy, the enzymatic activity of the p.R253G recombinant variant achieved a statistically significant increase when expressed in the presence of arginine. The improvement of the relative basal activity from 21 to 37 % may be decisive according to the notion that increasing the patients' enzymatic activity to minimal threshold level is sufficient to reverse or at least ameliorate the phenotype (Yue 2016).

To extend the *in vitro* results obtained using the recombinant expression system, we undertook a study to evaluate the ability of arginine and/or thiamine to restore PDC function and mitochondrial bioenergetics in hemizygous patient-derived cell lines. Accordingly, we

designed an *ex vivo* comparative study aiming to evaluate the effect of the two compounds, individually or synergistically, upon culture of PDC patient-derived skin fibroblasts bearing p.R88C, p. R253G, p.R263G and p.R378C variants caused by mutations in the *PDHA1* gene.

The experimental approach included immunochemical and immunohistochemical analyses, PDC activity assays but also evaluation of mitochondrial function by measuring the oxygen consumption rate (OCR) under different conditions.

Traditionally, mitochondrial function was evaluated using the Clark electrode, based on polarography, a method discovered by Jaroslav Heyrovský in Prague in 1922 (Heyrovský 1922; Clark et al. 1953; Li and Graham 2012). Lately, measuring OCR in an automated system brings the advantage of a real time analysis in a multi-well plate, containing living fibroblast cultures, resembling closer the physiological state of the analyzed patient-derived cells. Our results confirmed the importance of evaluating the mitochondrial bioenergetics profile as one of the most valuable contributions to the overall perception of the arginine and thiamine effects. For instance, while the impact of therapeutic levels of thiamine and arginine on the p. R263G cell line, evaluated by the enzymatic assay, was sparse and statistically insignificant, the OCR assays revealed a significant increase on ATP production, suggesting that the slight increase in PDC activity may be responsible for the increase in substrate production, namely NADH and $FADH_2$, thus improving cellular homeostasis.

Regrettably, the generally poor proliferation of PDC deficient cells prevented the mitochondrial OCR assays for the p.R253G cell line. Nevertheless, the cultured p.R253G fibroblasts presented a positive response to thiamine and to arginine supplementation concerning either the PDC-E1α protein levels or the PDC activity, being in consonance both with the clinical improvement observed in this patient upon thiamine and arginine supplementation and with our data concerning the biochemical and biophysical analysis of this recombinant variant.

As observed for other stabilizing molecules acting as pharmacological or chemical chaperones (Muntau et al. 2014), the obtained results highlighted that the arginine and thiamine rescue efficacy is clearly determined by the mutation *per se*. The knowledge about the responsiveness to thiamine is becoming increasingly integrated (Pastoris et al. 1996; Di Rocco et al. 2000; Naito et al. 2002; Brown 2014; Castiglioni et al. 2015; Pavlu-Pereira et al. 2021), and, definitely, thiamine supplementation seems like a viable option to surpass the functional

impairment of many of the studied variants. Yet, the structural and functional rescue by arginine as a chemical chaperone is still to be fully understood. Arginine supplementation has been attempted as a treatment measure in different metabolic diseases (Plecko et al. 1998; Koga et al. 2007; Silva et al. 2009; Mercimek-Mahmutoglu et al. 2014; Coughlin et al. 2015). Nevertheless, in the case of the substrate-reduction therapy in lysine-restricted diet, arginine does not operate as a chemical chaperone, but as competitor for the amino acid transporters (Hägglund et al. 2015). Our data indicate that the putative chemical chaperone nature of arginine may help stabilizing the otherwise disordered domains in PDC-E1 subunit, though the detailed molecular insight and the specifity towards the distinct amino acid substitutions remains to be clarified.

I believe that a correlation among the clinical response to arginine and thiamine observed *in vivo*, the metabolic data obtained *ex vivo*, the experimental results assessed *in vitro* and the data *in silico*, is possible to be achieved. In the near future, we would like to intensify our research using the patients' fibroblasts in order to better understand the molecular mechanism underlying arginine effect and to wider explore the perspective of a hypothetical synergistic operation between arginine and thiamine. To overcome the difficulties with the poor cell proliferation in culture due to lactate accumulation leading to medium acidification, we plan to transform the patients-derived cell lines. Importantly, it is worth mentioning that the energy metabolism in skin fibroblasts might not completely represent the deficient energy production in the skeletal muscle of PDC deficient patients; however, muscle biopsy should be perhaps bypassed, except on clinically urgent situations (Forny et al. 2021).

The custom-made cultivation medium with levels of thiamine and arginine reduced to concentrations analogous to physiological plasmatic levels has proven to be effective in allowing to assess the potential therapeutic effect of both compounds. Concerning the future, we plan a wider adjustment of the amino acid composition in the medium in order to be adequate to a recently published method (Bedoyan et al. 2020). As stated in this report, the combined Ala:Leu ≥4.0 and Pro:Leu ≥3.0 ratios in plasma is an accurate benchmark for the PDCD diagnosis in such a manner that these authors suggested its use as a suitable biomarker for newborn screening. From my perspective, monitoring the levels of those amino acids for evaluating the function of arginine and thiamine supplementation could become an additional tool to follow the potential response in patients' fibroblasts. Ultimately, we intend to provide

the support to our argument about altered PDC-E1 inactivation in disordered regulatory loops, assessing the phosphorylation sites in PDC-E1α protein expressed in fibroblast by western blot with the adequate antibodies.

We hope to improve and to refine the methodologies based on PDC deficient patients-derived cells in order to obtain a solid *ex vivo* system that would allow us to further extend our knowledge on the molecular mechanisms of pyruvate dehydrogenase deficiency.

REFERENCES

Acosta PB (1996) Nutrition studies in treated infants and children with phenylketonuria: Vitamins, minerals, trace elements. In: European Journal of Pediatrics, Supplement. Eur J Pediatr

Alder BJ, Wainwright TE (1957) Phase transition for a hard sphere system. J. Chem. Phys. 27:1208–1209

Barnerias C, Saudubray JM, Touati G, et al (2010) Pyruvate dehydrogenase complex deficiency: Four neurological phenotypes with differing pathogenesis. Dev Med Child Neurol 52:e1–e9. https://doi.org/10.1111/j.1469-8749.2009.03541.x

Barton NW, Brady RO, Dambrosia JM, et al (1991) Replacement Therapy for Inherited Enzyme Deficiency — Macrophage-Targeted Glucocerebrosidase for Gaucher's Disease. N Engl J Med 324:1464–1470. https://doi.org/10.1056/nejm199105233242104

Bedoyan JK, Hage R, Shin HK, et al (2020) Utility of specific amino acid ratios in screening for pyruvate dehydrogenase complex deficiencies and other mitochondrial disorders associated with congenital lactic acidosis and newborn screening prospects. JIMD Rep 56:70–81. https://doi.org/10.1002/jmd2.12153

Bhandary S, Aguan K (2015) Pyruvate dehydrogenase complex deficiency and its relationship with epilepsy frequency--An overview. Epilepsy Res 116:40–52. https://doi.org/10.1016/j.eplepsyres.2015.07.002

Boenzi S, Diodato D (2018) Biomarkers for mitochondrial energy metabolism diseases. Essays Biochem. 62:443–454

Bonam SR, Wang F, Muller S (2019) Lysosomes as a therapeutic target. Nat. Rev. Drug Discov. 18:923–948

Brautigam CA, Wynn RM, Chuang JL, et al (2006) Structural insight into interactions between dihydrolipoamide dehydrogenase (E3) and E3 binding protein of human pyruvate dehydrogenase complex. Structure 14:611–621. https://doi.org/10.1016/j.str.2006.01.001

Brautigam CA, Wynn RM, Chuang JL, Chuang DT (2009) Subunit and catalytic component stoichiometries of an in vitro reconstituted human pyruvate dehydrogenase complex. J Biol Chem 284:13086–98. https://doi.org/10.1074/jbc.M806563200

Brown G (2014) Defects of thiamine transport and metabolism. J Inherit Metab Dis 37:577–585. https://doi.org/10.1007/s10545-014-9712-9

Brown RM, Head RA, M AA, et al (2007) Pyruvate dehydrogenase E3 binding protein (protein X) deficiency. Dev Med Child Neurol 48:756–760. https://doi.org/10.1111/j.1469-8749.2006.tb01362.x

Byron O, Lindsay JG (2017) The pyruvate dehydrogenase complex and related assemblies in health and disease. In: Sub-Cellular Biochemistry. pp 523–550

Cannon WB (1934) The Wisdom of the Body. Nature 133:82–82. https://doi.org/10.1038/133082a0

Castiglioni C, Verrigni D, Okuma C, et al (2015) Pyruvate dehydrogenase deficiency presenting as isolated paroxysmal exercise induced dystonia successfully reversed with thiamine supplementation. Case report and mini-review. Eur. J. Paediatr. Neurol. 19:497–503

Ciszak EM, Korotchkina LG, Dominiak PM, et al (2003) Structural basis for flip-flop action of thiamin pyrophosphate-dependent enzymes revealed by human pyruvate dehydrogenase. J Biol Chem 278:21240–21246. https://doi.org/10.1074/jbc.M300339200

Clark LC, Wolf R, Granger D, Taylor Z (1953) Continuous recording of blood oxygen tensions by polarography. J Appl Physiol 6:189–193. https://doi.org/10.1152/jappl.1953.6.3.189

Coughlin CR, van Karnebeek CDM, Al-Hertani W, et al (2015) Triple therapy with pyridoxine, arginine supplementation and dietary lysine restriction in pyridoxine-dependent epilepsy: Neurodevelopmental outcome. Mol Genet Metab 116:35–43. https://doi.org/10.1016/j.ymgme.2015.05.011

Cox TM (2007) Substrate reduction therapy for lysosomal storage diseases. Acta Paediatr 94:69–75. https://doi.org/10.1111/j.1651-2227.2005.tb02116.x

Debray FG, Mitchell GA, Allard P, et al (2007) Diagnostic accuracy of blood lactate-to-pyruvate molar ratio in the differential diagnosis of congenital lactic acidosis. Clin Chem 53:916–921. https://doi.org/10.1373/clinchem.2006.081166

DeBrosse SD, Okajima K, Zhang S, et al (2012) Spectrum of neurological and survival outcomes in pyruvate dehydrogenase complex (PDC) deficiency: Lack of correlation with genotype. Mol Genet Metab 107:394–402. https://doi.org/10.1016/j.ymgme.2012.09.001

Delnoy B, Coelho AI, Rubio-Gozalbo ME (2021) Current and future treatments for classic galactosemia. J. Pers. Med. 11:1–14

Desnick RJ, Astrin KH, Schuchman EH (2018) Therapies for lysosomal storage diseases. In: Emery and Rimoin's Principles and Practice of Medical Genetics and Genomics: Clinical Principles and Applications. Elsevier, pp 205–227

Di Rocco M, Doria Lamba L, Minniti G, et al (2000) Outcome of thiamine treatment in a child with Leigh disease due to thiamine-responsive pyruvate dehydrogenase deficiency. Eur J Paediatr Neurol 4:115–117. https://doi.org/10.1053/ejpn.2000.0278

Drakulic S, Rai J, Petersen SV, et al (2018) Folding and assembly defects of pyruvate dehydrogenase deficiency-related variants in the E1α subunit of the pyruvate dehydrogenase complex. Cell Mol Life Sci 75:3009–3026. https://doi.org/10.1007/s00018-018-2775-2

Ferriero R, Manco G, Lamantea E, et al (2013) Phenylbutyrate therapy for pyruvate dehydrogenase complex deficiency and lactic acidosis. Sci Transl Med 5:. https://doi.org/10.1126/scitranslmed.3004986

Forny P, Footitt E, Davison JE, et al (2021) Diagnosing Mitochondrial Disorders Remains Challenging in the Omics Era. Neurol Genet 7:e597. https://doi.org/10.1212/NXG.0000000000000597

Fouque F, Brivet M, Boutron A, et al (2003) Differential effect of DCA treatment on the pyruvate dehydrogenase complex in patients with severe PDHC deficiency. Pediatr Res 53:793–799. https://doi.org/10.1203/01.PDR.0000057987.46622.64

Gray LR, Tompkins SC, Taylor EB (2014) Regulation of pyruvate metabolism and human disease. Cell Mol Life Sci 71:2577–2604. https://doi.org/10.1007/s00018-013-1539-2

Hägglund MGA, Hellsten S V., Bagchi S, et al (2015) Transport of l-Glutamine, l-Alanine, l-Arginine and l-Histidine by the Neuron-Specific Slc38a8 (SNAT8) in CNS. J Mol Biol 427:1495–1512. https://doi.org/10.1016/J.JMB.2014.10.016

Han Z, Berendzen K, Zhong L, et al (2008) A combined therapeutic approach for pyruvate dehydrogenase deficiency using self-complementary adeno-associated virus serotype-specific vectors and dichloroacetate. Mol Genet Metab 93:381–387. https://doi.org/10.1016/j.ymgme.2007.10.131

Hanley WB, Feigenbaum ASJ, Clarke VJ, et al (1996) Vitamin B12 deficiency in adolescents and young adults with phenylketonuria. In: European Journal of Pediatrics, Supplement. Springer, pp 145–147

Harris RA, Bowker-Kinley MM, Wu P, et al (1997) Dihydrolipoamide dehydrogenase-binding protein of the human pyruvate dehydrogenase complex. DNA-derived amino acid sequence, expression, and reconstitution of the pyruvate dehydrogenase complex. J Biol Chem 272:19746–19751. https://doi.org/10.1074/jbc.272.32.19746

Heyrovský J (1922) Electrolysis with the dropping mercury electrode. Chem List 16:256–304

Hiromasa Y, Fujisawa T, Aso Y, Roche TE (2004) Organization of the cores of the mammalian pyruvate dehydrogenase complex formed by E2 and E2 plus the E3-binding protein and their capacities to bind the E1 and E3 components. J Biol Chem 279:6921–33. https://doi.org/10.1074/jbc.M308172200

Hollingsworth SA, Dror RO (2018) Molecular Dynamics Simulation for All. Neuron 99:1129–1143

Imbard A, Boutron A, Vequaud C, et al (2011) Molecular characterization of 82 patients with pyruvate dehydrogenase complex deficiency. Structural implications of novel amino acid substitutions in E1 protein. Mol Genet Metab 104:507–16. https://doi.org/10.1016/j.ymgme.2011.08.008

Jiang J, Baiesc FL, Hiromasa Y, et al (2018) Atomic Structure of the E2 Inner Core of Human Pyruvate Dehydrogenase Complex. Biochemistry 57:2325–2334. https://doi.org/10.1021/acs.biochem.8b00357

Koga Y, Akita Y, Nishioka J, et al (2007) MELAS and l-arginine therapy. Mitochondrion 7:133–139. https://doi.org/10.1016/j.mito.2006.11.006

Korasick DA, Tanner JJ (2021) Impact of missense mutations in the ALDH7A1 gene on enzyme structure and catalytic function. Biochimie 183:49–54

Kyrilis FL, Semchonok DA, Skalidis I, et al (2021) Integrative structure of a 10-megadalton eukaryotic pyruvate dehydrogenase complex from native cell extracts. Cell Rep 34:108727. https://doi.org/10.1016/j.celrep.2021.108727

Levitt M, Lifson S (1969) Refinement of protein conformations using a macromolecular energy minimization procedure. J Mol Biol 46:269–279. https://doi.org/10.1016/0022-2836(69)90421-5

Li Z, Graham BH (2012) Measurement of mitochondrial oxygen consumption using a Clark electrode. Methods Mol Biol 837:63–72. https://doi.org/10.1007/978-1-61779-504-6_5

Lifson S, Waeshel A (1968) Consistent force field for calculations of conformations, vibrational spectra, and enthalpies of cycloalkane and n-alkane molecules. J Chem Phys 49:5104–5107. https://doi.org/10.1063/1.1670007

Lino PR, Leandro J, Amaro M, et al (2021) In silico and in vitro tailoring of a chitosan nanoformulation of a human metabolic enzyme. Pharmaceutics 13:1–17. https://doi.org/10.3390/pharmaceutics13030329

Maeng CY, Yazdi MA, Reed LJ (1996) Stoichiometry of binding of mature and truncated forms of the dihydrolipoamide dehydrogenase-binding protein to the dihydrolipoamide acetyltransferase core of the pyruvate dehydrogenase complex from Saccharomyces cerevisiae. Biochemistry 35:5879–5882. https://doi.org/10.1021/BI9600254

Marchetti M, Faggiano S, Mozzarelli A (2021) Enzyme Replacement Therapy for Genetic Disorders Associated with Enzyme Deficiency. Curr Med Chem 28:. https://doi.org/10.2174/0929867328666210526144654

Markham A (2018) Pegvaliase: First Global Approval. BioDrugs 32:391–395. https://doi.org/10.1007/s40259-018-0292-3

Marsac C, Stansbie D, Bonne G, et al (1993) Defect in the lipoyl-bearing protein X subunit of the pyruvate dehydrogenase complex in two patients with encephalomyelopathy. J Pediatr 123:915–920. https://doi.org/10.1016/S0022-3476(05)80387-7

McCammon JA, Gelin BR, Karplus M (1977) Dynamics of folded proteins. Nature 267:585–590. https://doi.org/10.1038/267585a0

Mercimek-Mahmutoglu S, Cordeiro D, Cruz V, et al (2014) Novel therapy for pyridoxine dependent epilepsy due to ALDH7A1 genetic defect: L-arginine supplementation alternative to lysine-restricted diet. Eur J Paediatr Neurol 18:741–746. https://doi.org/10.1016/j.ejpn.2014.07.001

Milne JLS, Wu X, Borgnia MJ, et al (2006) Molecular structure of a 9-MDa icosahedral pyruvate dehydrogenase subcomplex containing the E2 and E3 enzymes using cryoelectron microscopy. J Biol Chem 281:4364–4370. https://doi.org/10.1074/jbc.M504363200

Muntau AC, Leandro J, Staudigl M, et al (2014) Innovative strategies to treat protein misfolding in inborn errors of metabolism: pharmacological chaperones and proteostasis regulators. J Inherit Metab Dis. https://doi.org/10.1007/s10545-014-9701-z

Naito E, Ito M, Yokota I, et al (2002) Thiamine-responsive pyruvate dehydrogenase deficiency in two

patients caused by a point mutation (F205L and L216F) within the thiamine pyrophosphate binding region. Biochim Biophys Acta - Mol Basis Dis 1588:79–84. https://doi.org/10.1016/S0925-4439(02)00142-4

Nogueira C, Silva L, Pereira C, et al (2019) Targeted next generation sequencing identifies novel pathogenic variants and provides molecular diagnoses in a cohort of pediatric and adult patients with unexplained mitochondrial dysfunction. Mitochondrion 47:309–317. https://doi.org/10.1016/j.mito.2019.02.006

Parikh S, Karaa A, Goldstein A, et al (2019) Diagnosis of possible' mitochondrial disease: An existential crisis. J Med Genet 56:123–130. https://doi.org/10.1136/jmedgenet-2018-105800

Pastoris O, Savasta S, Foppa P, et al (1996) Pyruvate dehydrogenase deficiency in a child responsive to thiamine treatment. Acta Paediatr Int J Paediatr 85:625–628. https://doi.org/10.1111/j.1651-2227.1996.tb14104.x

Patel KP, O'Brien TW, Subramony SH, et al (2012) The spectrum of pyruvate dehydrogenase complex deficiency: Clinical, biochemical and genetic features in 371 patients. Mol Genet Metab 106:385–394. https://doi.org/10.1016/j.ymgme.2012.03.017

Pavlu-Pereira H, Lousa D, Tomé CS, et al (2021) Structural and functional impact of clinically relevant E1α variants causing pyruvate dehydrogenase complex deficiency. Biochimie 183:78–88. https://doi.org/10.1016/j.biochi.2021.02.007

Pinheiro A, Silva MJ, Pavlu-Pereira H, et al (2016) Complex genetic findings in a female patient with pyruvate dehydrogenase complex deficiency: Null mutations in the PDHX gene associated with unusual expression of the testis-specific PDHA2 gene in her somatic cells. Gene 591:417–424. https://doi.org/10.1016/j.gene.2016.06.041

Platt FM, Jeyakumar M, Andersson U, et al (2003) Substrate reduction therapy in mouse models of the glycosphingolipidoses. Philos Trans R Soc Lond B Biol Sci 358:947–54. https://doi.org/10.1098/rstb.2003.1279

Plecko B, Erwa W, Wermuth B (1998) Partial N-acetylglutamate synthetase deficiency in a 13-year-old girl: Diagnosis and response to treatment with N-carbamylglutamate. Eur J Pediatr 157:996–998. https://doi.org/10.1007/s004310050985

Ploeg A van der (2020) Future directions in the treatment of lysosomal disorders

Prajapati S, Haselbach D, Wittig S, et al (2019) Structural and Functional Analyses of the Human PDH Complex Suggest a "Division-of-Labor" Mechanism by Local E1 and E3 Clusters. Structure 27:1124-1136.e4. https://doi.org/10.1016/j.str.2019.04.009

Quintana E, Gort L, Busquets C, et al (2010) Mutational study in the PDHA1 gene of 40 patients suspected of pyruvate dehydrogenase complex deficiency. Clin Genet 77:474–482. https://doi.org/10.1111/j.1399-0004.2009.01313.x

Safary A, Khiavi MA, Mousavi R, et al (2018) Enzyme replacement therapies: What is the best option? BioImpacts 8:153–157. https://doi.org/10.15171/bi.2018.17

Sanderson SJ, Miller C, Lindsay JG (1996) Stoichiometry, organisation and catalytic function of protein X of the pyruvate dehydrogenase complex from bovine heart. Eur J Biochem 236:68–77.

https://doi.org/10.1111/j.1432-1033.1996.00068.x

Scriver CR, Treacy EP (1999) Is there treatment for “genetic” disease? Mol Genet Metab 68:93–102. https://doi.org/10.1006/mgme.1999.2907

Silva MJ, Pinheiro A, Eusébio F, et al (2009) Pyruvate dehydrogenase deficiency: identification of a novel mutation in the PDHA1 gene which responds to amino acid supplementation. Eur J Pediatr 168:17–22. https://doi.org/10.1007/s00431-008-0700-7

Sperl W, Fleuren L, Freisinger P, et al (2015) The spectrum of pyruvate oxidation defects in the diagnosis of mitochondrial disorders. J Inherit Metab Dis 38:391–403. https://doi.org/10.1007/s10545-014-9787-3

Stacpoole PW (2017) Therapeutic Targeting of the Pyruvate Dehydrogenase Complex/Pyruvate Dehydrogenase Kinase (PDC/PDK) Axis in Cancer. J Natl Cancer Inst 109:. https://doi.org/10.1093/jnci/djx071

Sun A, Chang IJ, Lam C, Berry GT (2021) Lysosomal Storage Disorders. In: Emery and Rimoin’s Principles and Practice of Medical Genetics and Genomics. Elsevier, pp 563–682

Treacy E, Valle D, Scriver C (2001) Treatment of genetic disease. In: Scriver ChR, Beaudet AL, Valle D, Sly WS, Childs B, Kinzley KW VB (ed) The metabolic and molecular bases of inherited disease, VIII. McGraw-Hill, Inc., New York, pp 175–192

Vijayakrishnan S, Callow P, Nutley MA, et al (2011) Variation in the organization and subunit composition of the mammalian pyruvate dehydrogenase complex E2/E3BP core assembly. Biochem J 437:565–74. https://doi.org/10.1042/BJ20101784

Whitley MJ, Arjunan P, Nemeria NS, et al (2018) Pyruvate dehydrogenase complex deficiency is linked to regulatory loop disorder in the αV138M variant of human pyruvate dehydrogenase. J Biol Chem 293:13204–13213. https://doi.org/10.1074/jbc.RA118.003996

Wijenayake S, Tessier SN, Storey KB (2017) Regulation of pyruvate dehydrogenase (PDH) in the hibernating ground squirrel, (Ictidomys tridecemlineatus). J Therm Biol 69:199–205. https://doi.org/10.1016/j.jtherbio.2017.07.010

Yue WW (2021) Structural biochemistry coming of age in the study of genetic metabolic disorders. Biochimie 183:1–2

Yue WW (2016) From structural biology to designing therapy for inborn errors of metabolism. J Inherit Metab Dis 39:489–498. https://doi.org/10.1007/s10545-016-9923-3

Zhou ZH, McCarthy DB, O’Connor CM, et al (2001) The remarkable structural and functional organization of the eukaryotic pyruvate dehydrogenase complexes. Proc Natl Acad Sci U S A 98:14802–7. https://doi.org/10.1073/pnas.011597698

LIST OF PUBLICATIONS

Structural and functional impact of clinically relevant E1α variants causing pyruvate dehydrogenase complex deficiency.

Pavlu-Pereira H, Lousa D, Tomé CS, Florindo C, Silva MJ, Tavares de Almeida I, Leandro P, Rivera I and Vicente JB

Biochimie 2021; 183:78–88

Pyruvate dehydrogenase complex deficiency: updating the clinical, metabolic and mutational landscapes in a cohort of Portuguese patients.

Pavlu-Pereira H, Silva MJ, Florindo C, Sequeira S, Ferreira AC, Duarte S, Rodrigues AL, Janeiro P, Oliveira A, Gomes D, Bandeira A, Martins E, Gomes R, Soares S, Tavares de Almeida I, Vicente JB and Rivera I

Orphanet J Rare Dis.2020; 15:298

Complex genetic findings in a female patient with pyruvate dehydrogenase complex deficiency: Null mutations in the PDHX gene associated with unusual expression of the testis-specific PDHA2 gene in her somatic cells.

Pinheiro A, Silva MJ, Pavlu-Pereira H, Florindo C, Barroso M, Marques B, Correia H, Oliveira A, Gaspar A, Tavares De Almeida I and Rivera I

Gene 2016; 591: 417-424

Data supporting the co-expression of PDHA1 gene and of its paralogue PDHA2 in somatic cells of a family.

Pinheiro A, Silva MJ, Pavlu-Pereira H, Florindo C, Barroso M, Marques B, Correia H, Oliveira A, Gaspar A, Tavares De Almeida I and Rivera I;

Data Brief 2016; 9:68–77

ACKNOWLEDGMENTS, AGRADECIMENTOS

VERBA MOVENT, EXEMPLA TRAHUNT

Latin proverb

Associate with people who are likely to improve you.

Lucius Annaeus Seneca

I am profoundly grateful for all the words of support and motivation and for all the inspiring examples that I have received all along this journey.

A finalização desta tese representa para mim uma oportunidade para recapitular, reflectir e sentir-me plenamente agradecida. Espero conseguir exprimir este sentimento, desta vez em português, para todos, que tanto me ajudaram e tanto me apoiaram.

Um agradecimento profundo aos meus orientadores.

Isabel, foi o elo que me ligou de volta ao mundo da investigação. Foi com a Isabel que me entusiasmei pelo mundo complexo das vertentes harmónicas (e desarmónicas) da piruvato desidrogenase. Foi com a Isabel e com a sua habilidade de juntar um olhar e raciocínio perspicaz e detalhado com toda objectividade distanciada, que aprendi o mesmo olhar cúmplice tão importante na perspectiva científica. Muito obrigada pela oportunidade de evoluir consigo, obrigada por todo o apoio, compreensão, paciência, confiança e amizade.

João, foste tu, quem me introduziu ao universo da estrutura proteica. Foi graças ao teu entusiasmo incansável pelo comportamento das proteínas, aos nossos debates, ao teu talento na leveza da apreciação e no rigor da concentração, que progredi nesta área. Muito obrigada por este espírito, por todas as ideias, sugestões, motivação, apoio e amizade.

Prof. Isabel Tavares, muito obrigada por me ter trazido de volta para a área das doenças metabólicas, de que sempre gostei tanto, área de procura intensa de tantas respostas na imensidão das vias metabólicas. Agradeço muito toda a sua atenção, e todos os conselhos preciosos que tanto me inspiraram e me ajudaram a levar este trabalho para a frente.

Paula, muito obrigada por ter me acolhido no seu laboratório das proteínas mal-comportadas. Agradeço sinceramente todo o seu intenso interesse e entusiasmo pelo meu

trabalho, as imensas sugestões e esclarecimentos que me deu, as suas preocupações, partilhas e apoio.

Maria João e Margarida, foi graças a vocês, que me senti tão bem por fazer parte do grupo de Metabolismo e Genética, que tanto significou para mim. Obrigada por todas as conversas inspiradoras e pelo espírito de amizade.

Cristina, foste tu, quem me deixou a "pasta" de piruvato desidrogenase tão bem preparada e foste tu quem me ajudou a esclarecer muitas dúvidas. Obrigada, e obrigada pela tua amizade, tua boa disposição, energia, preocupação e alegria.

Agradeço toda a disponibilidade permanente da D. Lurdes e da D. Ana, que sempre se preocuparam com as melhores condições de trabalho com uma dedicação admirável.

A todos os colegas que me acompanharam e, entretanto, partiram para outros destinos, a todos os colegas atuais, simplesmente, a todo o grupo de Met&Gen agradeço por todos os braços abertos com que me receberam, o respeito, a motivação a inspiração, a confiança e o carinho com o qual sempre ouvi o "Hana com H" tão bem pronunciado.

Agradeço também a maneira como fui acolhida pela Vanessa e pela Filipa no IMM e pela oportunidade de ter aberto mais uma janela para a área fascinante do metabolismo mitocondrial.

To all the members of the MX Macromolecular Crystallography Unit in Oeiras. Thank you for sharing all the kindness and all the energy in the team.

My days in Salzburg passed by the light-speed, but in the same way, they were very intensive. Thank you, Johannes for all your kind availability, for the intensive talks we had, for all your precious ideas that have given such a progress to this work.

I would like to express my deep gratitude to whom brought me with an incredible enthusiasm into the field of inherited metabolic diseases. Thank you, Viktor, for believing on me all these long years. I wish to dedicate this work to the memory of Prof. Milan Elleder.

And to the memory of my father, without him and his passion for the classical education and science, I would not be the same person.

My mother, my husband, my children, my family, you all know, what I feel by saying:

DĚKUJI…

OBRIGADA…

Cover: Alien DNA, video artwork by Hugo Lami